Price: 10 EUR

HUNGARIAN GROUP OF *fib*

CONCRETE STRUCTURES

ANNUAL TECHNICAL JOURNAL

2011

Vol. 12

CZECHS AND HUNGARIANS SIDE BY SIDE OVER THE CENTURIES – HISTORY, CULTURE AND CONCRETE


Géza Tassi – György L. Balázs

The Czech Republic and the Republic of Hungary are situated in Central Europe, and their current territory and population is similar (approximating that of Ohio in USA). The similitude and difference between the situation of Czech and Hungarian countrymen changed over the centuries. However, there has always been a close connection between the two people.

It is a great honour for the headquarters and the member countries of fib that the 2011 Symposium will be organized in Prague. Our Czech colleagues have hosted on several occasions various events of fib=CEB+FIP. Their excellence in organization and the high technical-scientific value of previous meetings predicate the success of the symposium. This paper wishes to give an impression of past relations in anticipation of good co-operation in the future.

1. INTRODUCTION

Following the Second *fib* Congress, the journal of the Hungarian Group of *fib called* CONCRETE STRUCTURES starts with a leading article that aims to improve friendship between the member groups of our international federation. We wish to introduce our country emphasizing our respect to other nations as well as showing in our mirror to the host countries.

2. HISTORY

Both nations, Czech and Hungarian have a history spanning more than thousand years. Both countries experienced periods of suppressions, wars, revolutions, and an enduring yearning for freedom and progress. The commotions experienced between these two states were sometimes fluctuating but there has always been good neighbourliness between our people.

In this paper it is impossible to write about all rich areas of links. Due to limited space we have to omit some areas like fields of science, sports and we will deal in more detail with others.

2.1 The Commencement

There are innumerable facts that bind both the Czechs and the Hungarians together. Firstly there is the duality of the names of the two peoples and lands.

The name Čechy is a documented name for people from as early as the 10th century A. D., when they called themselves Češi, a name based on the name of a middle Bohemian tribe. The etymologies of the two names, Češi, and Bohemia, until now have not satisfactorily been explained. Since their settlement in the region during 6th century, their learned contemporaries call them Bohemians. The origin of this name seems to be hidden in the Celtic Boier (Encyclopaedia, 2003).

As for the Hungarians, who call themselves Magyars after the name of one of their tribes, they emerged in the neighbouring area some two hundred years after the Czechs. The Hungarians soon involved themselves in transitory antagonisms with the Czechs, having opposing interests and a long and mutual frontier. The latter is proved also by the place-names Uherské Hradiště, Uherský Ostroh, Uherský Brod and Tlumačov which is the name of the Pecheneg tribe called Talmács in Hungarian. The Talmács people were then Hungarian subjects and they served as border guards of the country (Györffy, 1977).

2.2 In the Middle Ages

In the 10th century, during the reign of the Bohemian Přemyslid prince Boleslav II. and his Hungarian counterpart prince Géza, there was a longer period of peace which facilitated the adoption of Christianity of the then heathen Hungarians aided by the Bohemians. By this time the Bohemians had already converted to Christianity, nevertheless the missionary of the bishop Saint Adalbert and his mostly Benedictine friars were ascribed mainly to the grave hostility between the Přemyslid prince Boleslav II and the Slavnikid family of Adalbert. However, the veneration of the blessed bishop Adalbert proved to be stable and long lasting throughout the whole of Europe, as testified in a wood cutting of the 16th century (*Fig. 1*, Fitz,1956).

The cause of Christianity remained a lasting mutual interest between Hungary and Bohemia into the future. Consequently the Hungarian king, St. Ladislas (Szent László), appointed the Bohemian friar Duch as the head of the newly established episcopate of Zagreb with Latin rite (Hóman, Szekfű, 1935).

Less than two hundred years later the Hungarian king Anjou Louis the Great (Nagy Lajos) presented Bohemia the sword of the first Hungarian king, St. Steven (Szent István), which remains to this day in even now in the treasury of the Sv.

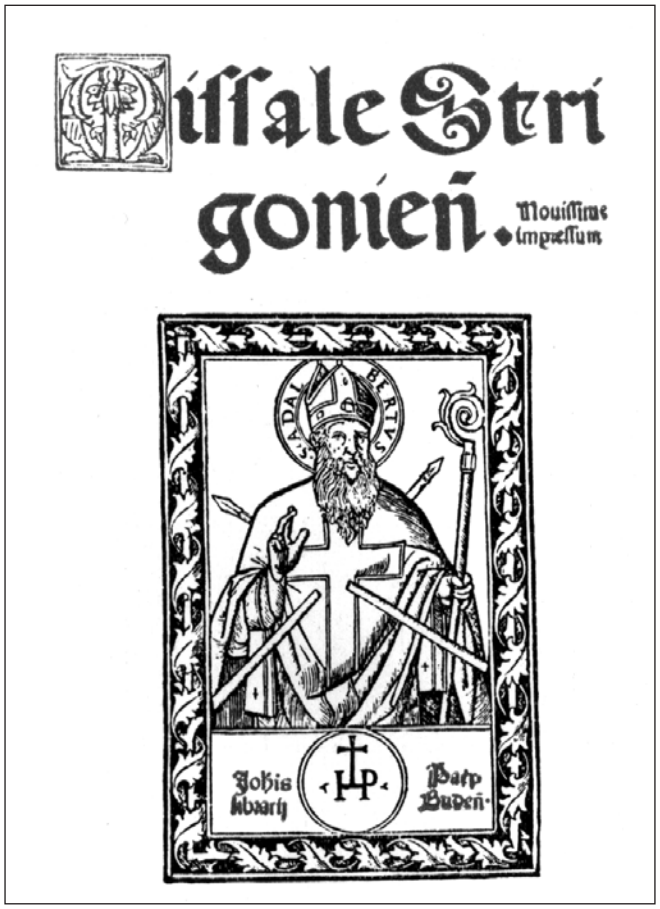

Fig. 1: St. Adalbert from the Missale Strigoniensis

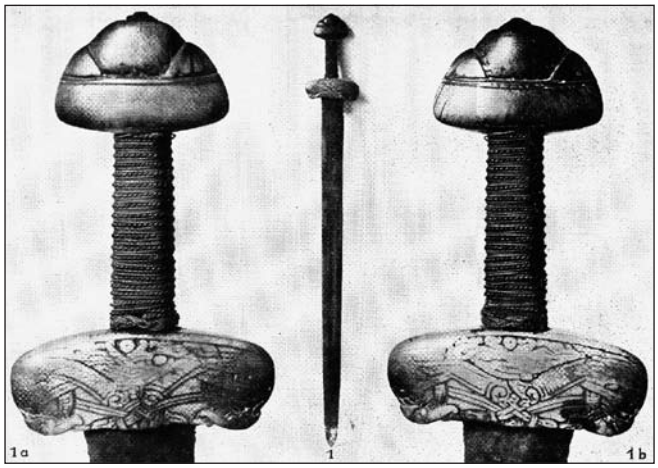

Fig. 2: The sword of the first Hungarian king St. Steven from the Cathedral St. Vid, Prague

Vít (St. Vid) Cathedral Prague (*Fig. 2*, Serédy, 1938). These early links between the two people and their dynasties are amply documented both in the contemporary diplomas and legendaries. As for the latter ones, scientists are of the view that both the legends of St. Steven (Szent István), St. Ladislas (Szent László) and of the Bohemian Kristian.

As previously mentioned some names of communities in early Bohemia refer to the Czech-Hungarian links. During the period of the Hungarian Árpád-dynasty there were new settlements containing in their name the "Czech" word, such as the following: Csehi ("belonging to Czechs" (Vas County), Drávacsehi (Baranya County), Egercsehi (Heves County), furthermore Csehbánya (Veszprém County), Kiscsehi (Zala County), Kálmáncsa, referring that King Kálmán settled Czech people to that village, Ordacsehi and Sümegcsehi (Zala County), all showing arrival of residents of Czech nationality (Kiss, 1980.). It is noted that even in the present telephone directory of Budapest there are 214 family names "Cseh" (=Czech, Čech).

Returning to medieval history: Some decades after the Mongolian invasion of Hungary the Přemyslid king of Bohemia, Otakar II expressed his endeavour to become also the king of Germany. In order to strengthen his power he seized some Hungarian fortresses at the western frontier of the country and collected troops and allies. However, Otakar's new royal endeavour had to face the claim of Rudolph Habsburg, who, with a clever diplomacy succeeded in winning the support of the young Hungarian king, Ladislas IV (IV. László). The hostilities finally came to the battle near to Stillfried and Dürnkrut on 26th August, 1278 in which the substantial support of the Hungarian troops turned to be decisive in favour of Rudolph Habsburg. King Otakar not only lost the battle but also died in action. With this engagement Hungary actually facilitated the dynastic power of the Habsburg family from which family members later became kings both of Hungary and Bohemia (Hóman, Szekfű, 1935) (*Fig. 3*, Cronicon, 1964).

Fig. 3: King Ladislas IV and the name of the king Otakar from the Cronicon Pictum

The first centuries of the second millennium were, however, marked not only by wars between the two nations, but also by significant cultural influences due initially to the activities of the Benedictine and Cistercian orders both in Hungary and Bohemia. A long list of ecclesiastical institutions and buildings were established by the brave friars in both countries.

Nevertheless, mention must be made of the Bohemian cathedrals of St. Margaret in Břevnov, the St. Prokop in Třebič, in Prague, the monasteries in Vysší Brod and in Zlatá Koruna as well as Hungarian ones in Ják and Zsámbék. The monasteries also had significant scholastic activity and influence in both countries.

Among the artistic monuments of these early centuries erected in an outstanding position in Prague is the beautiful bronze statue of St. George (Sv. Jiří), created by the Hungarian brothers Márton and György Kolozsvári in 1373. According to the records of the Bohemian Jesuit friar Bohuslav Balbin from 1677, the date and the name of the sculptor were inscribed on the now missing shield of the saint (*Fig. 4*, Aradi, 1983).

Fig. 4: The statue of St. George from the Hradzin, Prague

After Přemyslid dynasty died out,the Luxembourgian dynasty ascended the throne of Bohemia and somewhat later with Sigismund (Zsigmond) (1387-1437) ascended to the Hungarian throne, as well.

In the first decades of the new dynasty the relations between the church and the kingdom were burdened with certain conflicts, among others due to the reluctance of Svatý Jan Nepomucký (~1340-93) to follow the orders of the king Václav (Wenceslas) IV (1361-1419). The king therefore had him captured, tortured and finally thrown from the Charles Bridge into the river Vltava (Moldau), where he immediately died. Jan Nepomucký soon thereafter canonized and became the patron saint of the bridges, in both countries. The time of this sorrowful event was 20th March 1393.

Some years earlier, however, King Karel (Charles IV (1316-78) of the Luxembourg dynasty greatly contributed to the cultural development of Bohemia when establishing the University of Prague (Universitas Carolina Pragensis) in 1348. It is not only one of the oldest universities of Europe but not long after the establishment, it attracted a great number of students from many other countries of the continent, among them from Hungary as well (*Fig. 5*, Magyary-Kossa, 1929).

Being a renowned place of learning, Prague some decades later became the cradle of a spiritual movement which later

Fig. 5: Students and a professor from the University of Prague (second from right might be a Hungarian)

led to the reformation fuelled by Hassidism founded in the teaching and activity of Jan Hus. Hus was a follower of the Englishman John Wycliffe and based on his teaching and the texts of the gospels, he argued for the communion in both kind („sub utraque specie", hence the name of his followers, the „Utraquists"). Additionally he requested the pope and the bishops to abandon secular power and to exercise apostolic activity instead. Hus urged, furthermore the translation of the Bible into national languages and especially the promotion and preference of the Czech language. Hus thus fell under the

Fig. 6: Jan Hus on the stake in Constance, 1415:

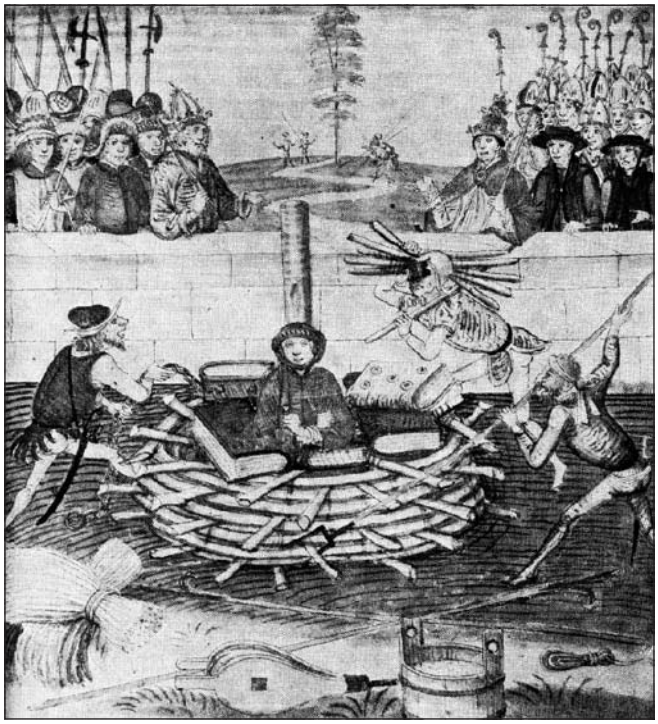

Fig. 7: *A picture from the Hussite War*

suspicion of heresy and in 1414 he was summoned before the Council of Constance, where he finally was committed to the flames, as with his faithful follower, Hieronymus of Prague, one year later (*Fig. 6*, Dürrenmatt, 1963). These miserable events led to the long and painful Hussite War (1419-36). (*Fig. 7*., Pilch, 1933). Nevertheless, the influence of Hussitism became rather widespread and manifold and it did not leave even Hungary untouched. Among others, it resulted in the so called Hussite Bible known only in parts and preserved by certain Hungarian codices. The parts in question are Hungarian translations of the Holy Script due to the work in 1438-39 of two clergymen known by the names Tamás (Thomas Quinqueecclesiensis) (1399) and Bálint (Valentinus de Újlak) (1411). (Horváth, 1957). The successful tactics of the Hussite warriors found way also to the famous Black Army of the Hungarian king Matthias (Mátyás) Corvinus (1443-90), who even took into his services such eminent Czech warriors as Jan (Jan Hus 1369-1415 Jan Giskra (Jiskra) (15th century) and the brothers Zlopna (Tóth, 1925).

2.3 The Renaissance and the Following Centuries

During the reign of Matthias Corvinus the relationship between Hungary and Bohemia was rather intense if not unclouded. Matthias Corvinus married first Catherine (Katalin) Podjebrad (-1464), the daughter of the Bohemian king Jiří Podjebrad (1420-71), but these familiar relations did not exclude hostilities between the two countries, especially after the early death of the young royal wife. Nevertheless, this was also the time of the renaissance, which had left significant marks on the culture of both countries. The famous library of Matthias Corvinus possessed, among others, codices with beautiful pictures painted by Bohemian illuminators (*Fig. 8*, Csapodi – Gárdonyi, 1990).

The richly illuminated Turóczy chronicle prepared during the reign of the Hungarian king Matthias Corvinus was met with great demand for publication of additional copies. Among other places it was once printed in Brno also (*Fig. 9*, Fitz, 1956).

Fig. 8: *The Bohemian king Wenceslas from a Codex Corvinianus with his initial "W" Bohemian illumination*

Fig. 9: *The Hungarian king St. Steven from the Brno edition of the Turóczy Chronicle*

After the death of Matthias Corvinus, Vladislav Jagellonský (Ulászló II 1456-1516) ascended both the Hungarian and the Bohemian throne. His reign was weak, however during his reign, the famous Jagello Hall in the Hradzin (Hradčany), Prague was constructed, the magnificent vaulting of which can even amaze structural engineers of modern times.

Due to the fatal battle of Mohács against the Turks in 1526, Hungary lost its independence for the next 150 years. However, a part of the country remained spared from Turkish devastation and for centuries it came under the realm of the Habsburg dynasty, as Bohemia.

The 16th century was a real golden age for Bohemia under the Habsburg kings, whose seat was then in Prague. Both the culture and the economy of the country came into bloom. The sciences of the time were represented by such intellectual giants as Johannes Kepler (1571-1630) and Tycho Brahe (1546-1601). Mining flourished and the glass products of Nové Hrady (Gratzen) became widespread (Vávra, 1954).

Meanwhile, a large part of Hungary suffered heavily from the Turkish occupation, though the flame of culture did not cease to burn, and the importance of connections with Bohemia were not forgotten. Gábor Pesti (16th century) published his *Nomenclatura sex linguarum* in Vienna, 1538, and among the six languages mentioned in the full title of his book, Czech and Hungarian are indicated, as well. In 1590 Balázs Szikszai-Fabricius (1530-76) had his similar dictionary printed, which in its following editions gave explanations for words also in the Czech language. Accordingly it is no wonder that there exists a deep interest in Prague by such outstanding personalities of Hungarian culture as Albert Szenczi Molnár (1574-1634), Mátyás Nyéki Vörös (1575-1654) and Márton Szepsi Csombor (1594~1623), who all did not fail to pay a visit to this important centre of European culture.

The cause of Bohemian Protestantism suffered a final and crushing defeat in the Battle of the Bílá Hora (White Hill) 1620. After the defeat 24 vanquished Bohemian noblemen were beheaded in Prague. The rector of the University of Prague and private physician of the king, Jan Jessenius (1566-1621) („eques Hungarus") also involved himself in the matter. His tongue was cut out, then beheaded and his head staked out on the old bridge tower of Prague (*Fig. 10*, Magyary-Kossa, 1929).

Fig. 10: The old bridge tower in Prague with the cut head of J. Jessenius staked out

Happier memories are recorded from the year 1655, when the Hungarian Jesuit friar Benedek Szőlősy (1609-56) published a hymn-book with the title *Cantus Catholici, Pýsně Katholické* including 228 texts in Latin and the old-Bohemian language containing 209 different melodies. The Bohemian hymn-book by Jiří Hlohovský (Olomouc, 1622.) seems to be an immediate source from it (*Fig. 11*, Bárdos, 1990).

Along with the counter-reformation, Bohemia became a reliable ground for the education of loyal members of the Habsburg dynasty. Still in his childhood as an offspring of an old Hungarian noble family, the young, Ferenc Rákóczi II (1676-1735) was sent by the Habsburg Court specifically to study in the Bohemian Jesuit monastery of Jindřichův Hradec

CANTVS CATHOLICI.
Pýsne
KATHOLICKE.
Latinské, y Slowenské: Nowé y Starodawné.
Z-kterymi Krestiané w-Pannonygi Na Wýročné Swatky, Slawnosti, pry Službe Boži, a w ginem obwzlasstnem času, z pobožnosti swé Krestianské ožýwagi.
Nasledugý po tem, Pýsne na Katechismus: O Swatostech Nowého zakona.
Letanye rozlične na Wýchodi Cyrkewne, a neb Processyge, a Putowaňy.
Z-mnohú pilnosti, ku potessenj Lidu Krestianskému, z-nowu zebrané, a wšdec widané.

S. Pawel k-Ephesskym Cap. 5. v. 19.
Naplňeňi budte Duchem Swatým, mluwjce sami sob w Zalmých, a w-Chwalach, a w Pýsničkach duchownjch spýwagjce, a chwalu wzdawagjce w srdcých swých Panu.

Cum facultate
ILLUSTRISSIMI ac REVERENDISSIMI
DOMINI. DOMINI
GEORGII LIPPAI
ARCHIEPISCOPI STRIGONIENSIS.
Regni Ungariæ Primatis.
A. M. D. G. B. V. M. & O. SS. H.
A. P. R.
1655.

Fig. 11: Title-page of the Cantus Catholici i. e. Pýsné Katholické

(Neuhaus) and later on at the University of Prague. However, the Imperial Court misjudged the young Rákóczi and had to suffer a bitter disappointment from his plans for the future. After returning home, Rákóczi became prince of the country and leader of a fight for the liberation of Hungary from the Habsburg dynasty. With his address issued in 1703, Rákóczi also tried to gain support to his cause of the Bohemian people and nobility. Details of lasting values about the time and movement of Rákóczi are commemorated by the pictures of the excellent Bohemian painter Jan Kupecký (1667-1740) (*Fig. 12*, Pesti Napló, 1907).

2.4 Enlightenment and its Aftermath

The age of enlightenment resulted in similar achievements in the cultures of both countries. To detail all results of this spiritual movement would be lengthy; nevertheless mention must be made of the new historiography represented by Gelasius Dobner (1719-90) in Bohemia and György Pray (1723-1801) in Hungary. Some decades later the great historian František Palacký (1798-1876) was also elected as an external member of the Hungarian Academy of Sciences. As for the social aspects of the time, the ideas of Josef Dobrovský (1753-1829) are especially worthy of mention. He is considered to have established the Finno-Ugrian science in Bohemia. A very important movement of this time was the language reform pioneers of which were the Hungarian, Ferenc Kazinczy (1759-1831) and the Czech, Josef Jungmann (1773-1847).

Other branches of learning also started to prosper. In botany the common efforts of scientists from each of the two countries resulted in a work not to be equalled. The work in question is „*Descriptiones et icones plantarum rariorum Hungariae*

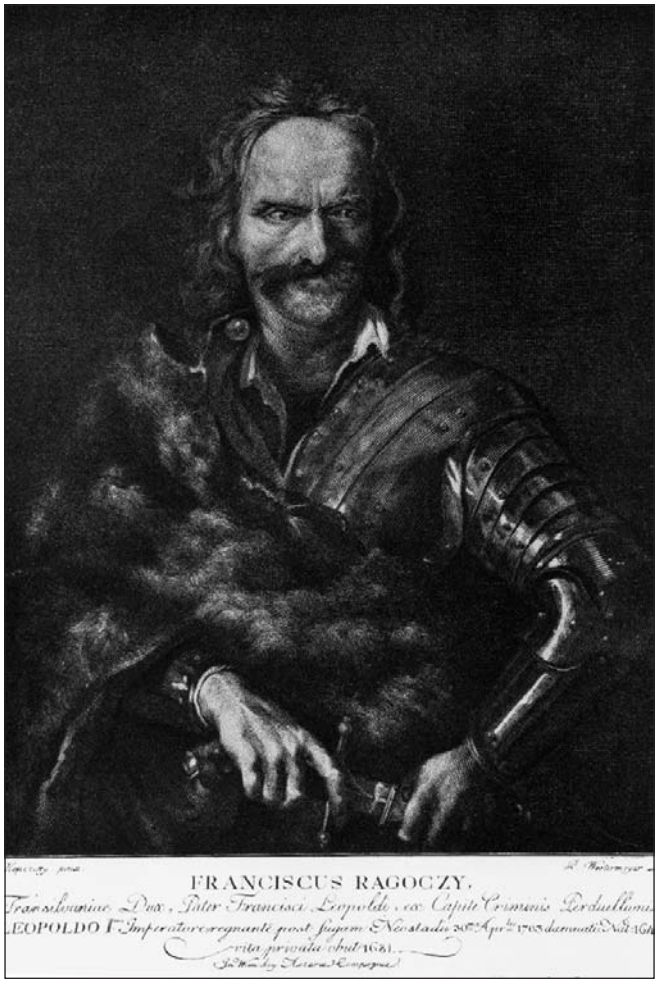

Fig. 12: Portrait of Ferenc Rákóczi I. painted by Jan Kupecký

Fig. 13: Illustration from the Descriptiones et icones plantarum rariorum Hungariae

I-III, Viennae, 1805-1812" by Pál Kitaibel (1757-1817) and count František Valdštejn-Wartenberg (1680-??) a study which aimed to offer a survey of 280 rare plants of Hungary. Half of them were described scientifically by the Hungarian Kitaibel himself. The illustrations of the work are unequalled (*Fig. 13*, Auction, 2010).

2.5 From 1848

February 1848 is significant in Czech history because up to that time there were individuals dealing with politics, but from that time onwards, political life started to develop. In Czech circles – similarly in Hungary – there were two groups. There were Czechs who wanted to improve the situation together with Vienna, whilst other people urged on secession from Austria. It was the latter group who started the uprising in June.

After many centuries of oppression this was the first occasion when Czech people upheld their rights. Unarmed, the people mounted an uprising, but were not successful against the canons of A. C. F. Windischgrätz (1787-1862). The leader of the Czech students and spirit of the fights in the streets was Josef Václav Frič (1829-1890). The other part was represented by František Palacký.

The majority of the Czech people were inspired by the Hungarian revolution and freedom-fighters in 1848-49, while others remained adherents for compromise with Vienna.

Without doubt both nations would have benefited from mutual assistance, and this plan had place in notes of Frič. Finally Frič had to escape after the Prague uprising was beaten and the Slovakian efforts were unsuccessful.

In March 1849, when Austria compelled the constitution to Bohemia, many people realised that if the Hungarian revolution fails, all others fighting for liberty will also fail. During that period more and more notices were posted advocating "Long live Kossuth".

Julius Jakob v. Haynau (1786-1853) in his manifest of 1st September 1849 declared that the Hungarian revolution had failed, and called out all participants to present themselves to the district commandant, or face court martial.

After 6th October 1849 when the 13 generals of the Hungarian army were executed, there were repeated hungarophile manifestations in Prague and also in Vienna.

The period of absolute rule, named the Bach era, had similar depressive effect on both Bohemia and Hungary, and all progressive movements were nipped in the bud (Kovács, 1952). The problems of these nations were pushed to the background.

After the 1850's the perception of political leaders was to see Bohemia as being a separate part within the Habsburg Empire. Anton v. Schmerling (1805-93) was replaced by Richard Belcredi (1823-1902) who was tasked with leading the Austrian-Hungarian Compromise. In 1866 Austria was beaten by Prussia at Hradec Králové (Königgrätz). Following this defeat Austria considered compromise with Hungary to be of highest importance, so the Czech question was fell into the background.

The compromise with Hungary took place in 1867, and cleaves to the name of Ferenc Deák (1803-76). The Austrian-Czech compromise followed later in 1871.

From both compromises to WW I there was solid civil development in both countries. However, the serious problems of multiple nationalities, poverty in segments of the population and the desire for independence were not solved. WW I brought

heavy burdens to both nations. The end of the war brought a different outcome for Czech and Hungarian nations. Hungary lost two third of its territory through the Trianon treaties, and at the same time Czechoslovakia was founded containing the Slovakian part which had previously belonged to Hungary for a thousand years. The only positive result of the Trianon can be said to be that in place of the Habsburg Monarchy the nations formed largely represented a relatively homogeneous people within their new borders.

Naturally, the political links between the truncated Hungarian Kingdom under a governor-admiral and the newly born republic of Czechoslovakia was not advantageous. The same cannot be said about personal connections, commerce, health tourism and other fields. Furthermore, there were many young people who attended Czech universities and colleges due to restrictive regulations in Hungary.

The new Czechoslovak state's population – as mentioned above, was not fully uniform - contained German, Hungarian, Polish and Ruthenian minorities. Hitler took advantage of the discord between these nationalities and introduced first the Munich pact (with consensus from Italy, Great Britain and France) and followed with the Vienna pact in 1938. In 1939 after some re-organization the remaining Czech territory was occupied by the Nazi Germany and created the Bohemian-Moravian Protectorate as a part of Germany.

During WW II a Czechoslovak government and army, on the side of the allied forces, was acting in exile.

On 9th May 1945 Prague was liberated by American and Soviet troops supported by the Prague uprising.

After WW II there were some contradictions between the two countries as Czechoslovakia belonged to the allied forces and Hungary to the Berlin-Rome axis. The problem of Hungarian minorities in Czechoslovakia was not resolved by the exchange of a part of ethnic inhabitants.

The political changes in 1948-49 and the influence of Moscow touched both countries similarly. Both countries had to join to the Warsaw Pact in 1955 and were a part of Comecon already in 1949.

Perhaps the common problems and difficulties brought the Czech and Hungarian people closer to each-other. This was in part aided by their governments as within the so called iron curtain of middle 1950's there was possibility of travel at least to the neighbouring Warsaw Pact member countries, giving rise to the development of cultural, commercial and sport exchanges.

A large part of Czech people turned with sympathy to the 1956 Hungarian Revolution. Similarly the sympathy of the Hungarian people at the time of the Prague Spring in 1968 was with the Czech people. The great majority of Hungarians was squarely behind the trend for changes in Czechoslovakia and was distressed with the forceful suppression of the Soviet government. The greatest part of the Hungarian people was ashamed that the Hungarian army had to participate in an invasion within the circle of the Warsaw Pact. Moscow's political involvement in suppressing Hungarian economic activity and reform (the "new economic mechanism") was also a painful experience for Hungarians.

After 1968 the links between these two countries were positive despite the stranglehold of Moscow over the Hungarian economy and Czech politics.

Until the political changes of 1989 the situation remained as before. In 1989 some Hungarian politicians, mostly young people, participated in demonstrations in Prague demanding parliamentary democratic change. The change came in both countries.

In 2003 the Czech Republic was separated from Slovakia. The Hungarians endeavoured to improve the already good relations and this was achieved in large measure through the organization of the Visegrád Countries founded in 2001 as V3 with participation of Hungary, Poland and Czechoslovakia. V4 when the Czech Republic and Slovakia were separated.

Today the Czech Republic and Hungary are both members of the European Union (both joined in 2004) and of NATO (both becoming members in 1999). There is a sincere hope that this brings a spirit of cooperation and mutual help in all fields of politics and economy (Romsics, 2007).

Certainly in the field of concrete technology there are good traditions which are independent of all other circumstances.

3. CULTURE

There are many close links between Czech and Hungarian cultures. In this paper we can write about literature and music, although in field of arts like painting, sculpture and others there are also many connections between the Czech and Hungarian nations.

An early influence in culture between the two nations was the Czech, Comenius – Jan Amos Komenský (1592-1670). He came to teach in the College of Sárospatak at the invitation of Zsuzsanna Lórántffy (~1600-1660). He wrote pedagogic material on his unique methods in education.

3.1 Music

The Czech-Hungarian links are very rich in many fields of art. However, in this paper we can only speak in detail about music, and even in this field alone this report cannot be complete and comprehensive. But we are convinced that the introduction of the Czech and Hungarian musical life can give a picture about our mutual and common soul and empathy.

Music has a special place in Czech-Hungarian relationship. Because there is a wide range of connections in music this chapter is more a compilation of data than on extensive study, but hopefully, it gives an impression on the very close Czech-Hungarian links.

Around 1790, when the Hungarian crown had been transferred from Vienna to Buda, the Czech composer Pavel Vranický (Paul Wranitzky) (1756-1808) presented his new symphony Op. 2, three String Quartets, therein the "Pleasure of the Hungarian Nation". As for the Hungarian recruiting music (i. e. verbunk) of the early 19th century, the contribution of the Czech Antonín Čermák cannot be left unmentioned. Later, when the Budapest Opera House underwent modernization, the famous Czech Wagnerian tenor Karel Burian (1870-1924) frequently sang there and was always welcome in Hungary.

A century ago two excellent Czech violinists, František Ondříček (1857-1922) and Jan Kubelík (1880-1940) frequently gave concerts in Hungary. Jan Kubelík was the son-in-law of the Hungarian Prime Minister of the time, Kálmán Széll (1843-1915), and the father of the famous conductor and thus "half Hungarian", Rafael Jeroným Kubelik (1914-1996), was at home when in Hungary. Bedřich Smetana's (1824-1884) works (among others The Bartered Bride, My Country) have been from the time of their first performance welcomed on the Hungarian stages, as are the works composed by Antonín Dvořak (1841-1904).

Music is one of the most international arts that connect nations. Covering cultural connections between two independent states after WW I, it is worthwhile mentioning that from the beginning of the 18th century Czech musicians

played throughout the world and including in Hungary. In the Esterházy court at Fertőd (Hungary) following the musical activity of Haydn, a Czech composer and conductor, Pavel Vranický, continued Haydn's work and composed among others a Hungarian Symphony.

When reflecting on the 19th century it is important to mention that the first music teacher of Ferenc Liszt (1811-1886) was Czech. As a consequence of this and the invitation of Viscount Leopold Thun (1811-88), Liszt (*Fig. 14.a*) went to Prague. The Czech music history registers the six concerts given by Liszt as a significant influence on Czech musical life, with particular influence on the work of Bedřich Smetana (*Fig. 14.b*).

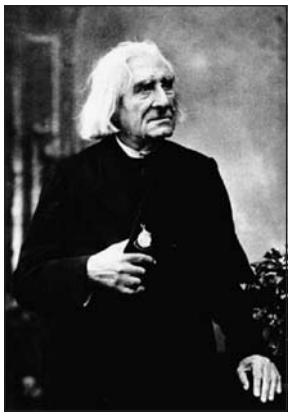

Fig.14.a: Ferenc Liszt

Fig. 14.b: Bedrich Smetana

At the turn of the 20th century the Czech, Vilém (Vilmos) Roubal (1877-1968) came to Budapest and played in the orchestra of the Hungarian State Opera. One of his sons Rezső Roubal (1907-85) played percussion instruments in the Hungarian State Opera, the other son became a well known Hungarian conductor under the name Vilmos Rubányi (1905-72). In the period before WW I the violinist Jan Kubelík came to Hungary and married a Hungarian lady. Their son Rafael Kubelík became a famous conductor. At that time a well known Czech quartet played in Budapest.

After WW I, because of political contradictions, there was no official connection in culture, however, the Hungarian Philharmonic Orchestra played in Prague conducted by Jenő Hubay (1858-1937). The Czech Philharmonic under Václav Talich presented in Budapest Bartók's Dance Suite with great success.

Václav Talich (1883-1961) introduced in Prague Bartók's work Music for Strings, Percussion and Celesta earlier than in Hungary.

Before WW II the Hungarian conductor György Széll (1897-1970) was the leader of the German Opera in Prague from where he left for the USA.

During this time there was little knowledge in both countries about music of each-other. In Hungary only the New World Symphony by Antonín Dvořák and Smetana's Vltava (Moldau) were known. Czech people were aware that Ferenc Liszt was an international success.

Interest in Bartók developed at a later time. It was significant that Zdeněk Nejedlý (1878-1962) asked Juraj Szántó the musicologist living in Prague, whose origins are from Rimavska Subota (Rimaszombat), Slovakia and who understood Hungarian, to lecture on Bartók. Bartók's music was widely known, but not his background and life.

Just after WW II when there was still no diplomatic link between Czechoslovakia and Hungary, there developed a strong interest in each-other's culture. There was already a concept that after the conclusion of peace the official cultural connections should be rebuilt with emphasis on music. In 1949 there was already formal diplomatic connection. Prague despatched a cultural attaché to the Budapest embassy who had a personal contact to the minister of culture in Hungary at that time, Dezső Keresztury (1904-96), and to state secretary, László Bóka (1910-64), who originated from Slovakia.

The first result was a concert in Prague by Géza Böszörményi-Nagy, the violinist György Garay (1909-88), and pianist István Antal (1909-78). The Czech Trio, the conductor Václav Smetáček (1906-86), the cellist Bohuš Heran (1907-1968) were sent to perform in Hungary. The latter learned the Solo Sonata for violoncello of Zoltán Kodály (1882-1967) and played it in many other countries.

There was a Liszt-Bartók festival in Hungary in 1949 to which a five member delegation came from Czechoslovakia, the members were Evžen Suchoň, a Slovak composer who had been learning in Prague; Alois Hába, a famous composer; scientist Václav Holzknecht; the director of the Music Academy, Štěpán Lucký; a young composer and Juraj Szántó.

During this period the two countries became acquainted with the music of each-other. The Hungarian radio orchestra presented the Symphony in D Major of František Adam Míča and in the Budapest Károlyi Garden the Hungarian State Concert Orchestra (ÁHZ) presented Forests and Fields parts from the Ma Vlást (Homeland) cycle of Smetana and the violin concerto of Dvořák that was previously unknown in Hungary.

Following the signing of the peace treaty in May 1949, Bartók's Concerto for Orchestra was performed at the Prague

Fig. 15.a: János Ferencsik

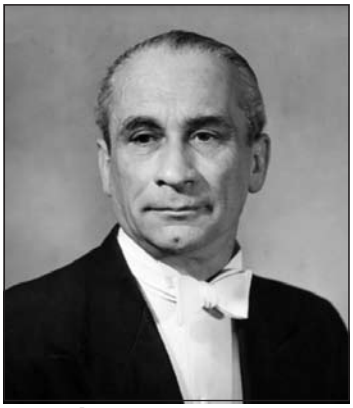

Fig.15.b: Karel Ancerl

Music Festival by the Hungarian State Orchestra, conducted by János Ferencsik (1907-84) (*Fig.15.a*).

The first tour abroad of the newly founded Hungarian State Folk Ensemble was to Czechoslovakia. The performing ensemble of the ČS Army had its first performance in Hungary.

Previously unknown to the Czech public, the opera in Prague presented the Ban Bánk written by the famous Hungarian composer Ferenc Erkel (1810-93).

The Czech participants in cultural exchange were the Czech Philharmonia, Prague Symphony Orchestra, the Prague Chamber Orchestra without conductor, and later the Prague Chamber Philharmonia and the Brno Philharmonia.

The exchange of major ensembles commenced with the staging of cultural festivals. Such famous Hungarian singers as Mihály Székely (1901-63), Sándor Svéd (1906-79), Mária Mátyás, (1924-1999), Mária Gyurkovics (1913-73), Paula Takács (1913-2003), György Melis (1923-2009), József Gregor (1940-2006), József Simándy (1916-1997), József Réthy (1925-1973), Erzsébet Házy (1929-82), Éva Marton,

Sándor Sólyom-Nagy, Ilona Tokody and others participated in this exchange. The ballet ensemble of the Hungarian State Opera, the ballet ensembles of Győr and Pécs were also guests in Czech cities. The ballet "Handkerchief" (Keszkenő) by Jenő Kenessey; the "The Transylvanian Spinning Room" by Kodály; the three one act plays of Bartók etc. were all performed. Solo evenings of ballet dancers Gabriella Lakatos (1927-89) and Viktor Fülöp (1927-97) were staged in Prague.

The Czechs sent such notable performers to Hungary as Marie Tauberová (1911-2003), Věra Soukupová and Milada Šubrtová. Czech productions were innovative and modern.

Several works of Smetana were performed in Budapest and several other Hungarian cities. The opera Jenufa and the Fox by Leoš Janáček (1854-1928) was performed in Hungary.

Hungarian conductors were active in ČSR namely János Ferencsik, Vilmos Komor (1895-1971), András Kóródi (1922-86), György Lehel (1926-89), Iván Fischer, Ádám Fischer, Zoltán Kocsis and many pianists frequently performed before the Czech public.

Karel Ančerl (1908-73) (*Fig.15.b*) must be mentioned. He was a very well known Czech conductor in Hungary and his name was very frequently heard on Hungarian radio. Among many others he was highly regarded for his performances of contemporary music. For example he conducted the Czech Philharmonic Orchestra's performance of the Concerto of Béla Bartók in the Dvořák Hall in Prague. He was made popular in Hungary by his recordings of the Sinfonietta by Janaček. Czech music lovers could enjoy the Psalmus Hungaricus by Zoltán Kodály.

Visiting musicians were: the pianists Zoltán Kocsis, Annie Fischer (1914-95), István Antal, Mihály Bächer (1924-93), Dezső Ránki, András Schiff; the violinists, Ede Zathureczky (1903-59), Eliz Cserfalvy, Dénes Kovács (1930-2005), Miklós Perényi, Csaba Onczay. Pál Lukács (1894-1971), cellist, presented the last work of Bartók in Prague, being the Concerto for Violoncello and Orchestra. He also presented the concerto for violoncello of the baroque classic Czech composer Míča Stamíc.

There was a special evening held in Prague on the works of György Kurtág. Hungarians frequently visited Prague, among them the Hungarian composers Ferenc Farkas (1905-2000), András Mihály (1917-93), Ferenc Szabó (1902-69), Emil Petrovics, Pál Kadosa (1903-83).

From the Czech side, the conductors Václav Neumann (1920-95) and Zdeněk Košler (1928-95) presented in Hungary the Slavic Mass by Janaček.

Also playing in Hungary were the famous Czech artists Jaroslav Krombholc (1918-83), Leoš Svarovský, the conductor Jiří Bělohlávek, the violinist Josef Šuk, harpsichordist Zuzana Růžičková, the famous Czech Smetana String Quartet, the Prague Quartet, the Pro Arte Antiqua Quartet. The Panoha Quartet performed regularly at the concert halls of Hungary.

On the Hungarian side the Bartók Quartet, Éder Quartet, and the Tátray Quartet played in different Czech cities. From the late 1950's the Hungarian Interkoncert and the Czech Pragokoncert organized exchanges between Hungarian and Czech music world.

There were competitions for young musicians during the season of the Prague Spring; in Hungary there were competitions for conductors and pianists with mutual participation. Jury members represented both countries.

Czech composers composed pieces for Hungarian artists, such as Lubomír Železný who wrote a violin concerto for Dénes Kovács and Oldřich Flosman who composed for Endre Gertler.

In the field of musicology, Jaroslav Volek (1923-89) published an analysis of Bartók's Orchestral Concerts; in Hungary a volume was published on the works of Nejedlý. Musicologists and music critics held conferences. Two examples, György Kroó (1926-97) and József Újfalussy (1920-2010), participated at such meetings in Prague.

A few words about light music:

In 1970-78 the Hungarian Cultural Institute in Prague was famous for recordings of LGT conducted by Gábor Presser. The LGT played in Prague to a crowded auditorium.

Following political changes in both Hungary and Czechoslovakia, music festivals spread throughout both countries. This provided an opportunity for sponsorship and the states also added financial support. These additional sources of funding facilitated the many exchanges.

We hope that the connection of both nations in musical life will be strong in the future and improve the links between the countries.

3.2 Literature

Last but not least is the theme of love and in this context mention must be made of the literary connections between our two nations. The list is so lengthy that only fractions and hints can be cited: poems by Sándor Petőfi (1823-1849) and Mihály Vörösmarty (1800-1855); novels by Mór Jókai (1825-1904) were translated into Czech and were warmly welcomed.

A great supporter of contemporary Hungarian literature was Jan Neruda (1834-1891) who not only revered the poems of Petőfi, but he considered the Hungarian poet to be a symbol of freedom. Some decades later Jan Neruda's poetry was masterfully interpreted for Hungarian readers.

The Tragedy of Man by Imre Madách (1823-64) was performed in Prague in 1894 so successfully that, during the scene of the French Revolution, a real demonstration against the Habsburgs broke out in the theatre. This inspired translation was made by the excellent Czech novelist, František Brábek (1848-1926). Later, the novels by Karel Čapek (1890-1938), Ivan Olbracht (1882-1952), Bohumil Hrabal (1914-97) and Franz Kafka (1883-1924) became enduring successes among Hungarian readers with numerous editions and the printing of a great number of copies demonstrating the deep interconnection and literary appreciation between the people of both countries (Király, 1984).

Returning to earlier times, after the fall of the movements for freedom, many Hungarians, along with their Czech comrades in misfortune, were imprisoned. Friendships were born, such as in the prison of Olomouc, where the Hungarians János Földesi, József Barsi-Naumann (1810-93), János Földy (1811-96), József Szlávy (1818-1900), Pál Szontágh (1820-1904), Anna Boér-Kenderessy (the only female prisoner) were interred.

The comrade-in-prison of Barsi-Naumann was the Czech Karel Sladkovský (1823-80) politician, Karel Sabina (1813-77) writer and Karel Tuček.

Barsi-Naumann and Tuček collaborated on translations of poems of Petőfi.

There were Czech prisoners in prisons in Hungary, in such places as Munkács and Komárom (today Mukachevo and Komárno). The best known Czech prisoner was Frič (See Chapter 2.5), who was later imprisoned in Dés (today Dej).

Péter Rákos (1935-2002) was a genius of literature who added enormously to the intersection of Czech and Hungarian culture. He was author of the Hungarian encyclopaedia of literature in the Czech language and did much to introduce Hungarian writers to the Czech public. He became professor

of the Charles University in Prague and head of department teaching Hungarian language and literature. Rákos did his work with much enthusiasm and energy. Today the head of the Department of Hungarian is Jenő Gaál who does his best to continue the work of Péter Rákos.

Regrettably the literature of each other was not taught in secondary schools. Perhaps this was due to rapid development of a new trend in style of literature and cinema during the 1980's (e. g. the works of Hrabal and Kundera), and the Hungarian school syllabus was not updated rapidly enough to include this new generation of artists. Petra Hulova, Joachim Topol, Miloš Urban were all contemporaries of the Hungarian Péter Esterházy. These writers were in time translated into Hungarian. On the other hand, contemporary Hungarian authors, such as Péter Nádas and Nobel laureat Imre Kertész were relatively well known in the Czech Republic.

The dramas of Lajos Parti Nagy were published and played in the theatres of Prague. The works of György Konrád are known in Czech circles as well as that of Sándor Márai (1900-89) whose works were published in Czechoslovakia prior to political changes. The writings of Antal Szerb (1901-45) were also published in Czech.

There is an interesting parallel between the Hungarian Petőfi and the Czech, Karel Hynek Macha (1810-1836). Macha, who had the reputation of a romantic, also died at a very young age. Petőfi translated Macha into Hungarian, as did Attila József (1905-37) at a later time.

Jaroslav Hašek (1883-1923) was best known in Hungary for his series entitled "Dobrý voják Švejk". The novels of Karel Čapek are also well known.

Hungarians had greater exposure to Czech culture preceding Hrabal. Jaroslav Seifert (1901-86) was awarded the Nobel Prize in 1984. His poems were published in Hungary.

Between 1980 and 2006 the Bohemia Festival was a regular cultural event in Hungary delivering diverse aspects of the Czech culture. There was literature, music, discussions and also gastronomy. There was always Czech beer and waiters.

Hungarian movies are screened weekly at the Hungarian Cultural Institute in Prague. There were literary evenings and expositions.

Enikő Eszenyi produced plays such as the Tóts by István Örkény (1919-79) as well as Shakespearean plays in the Prague National Theatre on many occasions. The Czech stage manager, Ivo Krobot frequently travelled to Hungary working on the stage of the New Theatre in Budapest.

During the past decades a prestigious Hungarian monthly journal called the "Nagyvilág" published translations of Czech authors. E. g. Edgar Dutka, Ivan Jergl, Emil Hakl, Petra Hůlová were translated by Ottilia Barna. Some Czech writers were introduced to the Hungarian public through condensed versions of their stories. Bohumil Hrabal was already popular in Hungary when this periodical presented sections of his new novels. The novels of Ladislav Fuks were first accessible in Nagyvilág and the same can be said for Eduard Petiska. One could find among the new authors names such as Vilém Zavad, Vladimír Holan, Miroslav Holub, Ludmila Pomportová and others.

It is to be emphasized that interest was mutual. Kamil Bednar and Ladislav Hradský were respected translators and prepared translations of classical Hungarian lyric poetry.

The above are only examples over a very long period of cultural connection between these two nations.

4. CONCRETE

4.1 Traditional techniques in industry and transportation

There has been a wide range of Czech-Hungarian connections in technology. The Czech Republic was instructed to become the heart of industry in the Habsburg Empire. In this paper we will only mention a few examples of Czech achievements from which Hungary had benefit. Much heavy machinery was exported to Hungary for manufacture in the textile and electronics industries.

One of the most important fields of Czech export to Hungary after WW I was that of automobiles and motorcycles. The Škoda 110 cars could be seen on Hungarian roads as early as 1925. Taxicabs were also imported. Tatra trucks and equipment were very popular. Export to Hungary after WW II expanded. The Tatra-148 trucks were running on Hungarian roads in relatively large numbers. The Jawa 350 motorcycle was the dream of young Hungarians in the 1950's and 60's. Later different types of Škoda cars were widely used.

Even now in currently use there are more than 200 Czech manufactured BZ motorised trains on the Hungarian railway lines as well as many Tatra trams in Budapest and other cities.

4.2 Activity in concrete works

In this paper we will concentrate on concrete technology. Collaboration in construction works was extensive and flourishes even today. The links are multifaceted, so we can only show some examples.

4.21 Bridges

In connection with railway and highway bridges, there were a number of agreements between Hungary and Czechoslovakia. In 1954, post WW II, the first important step was the exchange of trade delegations. Common works in concrete bridge construction utilised Czech experience (Dénes, 1955).

Towards the end of March 1945 the railway bridge across the Danube between Komárom and Komárno was destroyed by Hitler's troops as they withdrew. Reconstruction was started in 1952 and the new structure was inaugurated in late 1954. The concrete substructure was completed by Hungarian authorities and firms, while the elements of the steel superstructure were manufactured in the Czech part of the former Czechoslovakia and transported to the construction site in Slovakia and Hungary (Kmoskó, 1956). The highway bridge was reconstructed already in 1945, also by Czech engineers.

There was a close cooperation between the Czech, Slovakian and Hungarian engineers under the framework of UIC (International Railway Union) and OSZhD (Organization for cooperation of railways). On the Czech side, under the chairmanship of Petr Štěpanek (Brno), jointly developed instructions were published on maintenance and reconstruction of bridges (Nemeskéri-Kiss, 1986).

Bridge experts were welcomed at the Technical University of Budapest by László Szerémi, where the Czech guests were Milan Petr, Karel Chobot, Antonín Jílek, Milan Holický, Richard Bareš, and Zdeněk Kleisner.

There were many study tours organized by the Hungarian Scientific Society for Transport (KTE). E.g. in 1973 there was a technical visit to the Nusle-bridge and the metro construction in Prague. In the same year there was a meeting in Prague

Fig. 16: Berettyó River Bridge

on concrete structures and the delegates had the opportunity to visit notable examples of Czech concrete highway bridge construction (Tassi, 1973).

There was co-operation in concrete bridge construction. The first Czech cable-stayed bridge was constructed under the leadership of Hynek Hlasivec in Tábor during the late 1980's by the firm SSŽ (Road and Railway Constructions, Prague). The fatigue test of the cable vibration damping devices and the cable splicing appliance was carried out in the experimental research station of the Institute of Building Science (ÉTI) at Szentendre near Budapest. The tests were managed by Ferenc Gyökös.

The first concrete bridge constructed in Hungary by incremental launching, the highway bridge across the Berettyó River at Berettyóújfalu (*Fig.16*) had significant technical input in 1988 from Hynek Hlasivec, SSŽ, Prague. The equipment for this system was also delivered by a Czech firm. The Hungarian partner was the Hídépítő Co., and among the Hungarians involved we should mention József Vörös.

It belongs to the essence of this review that the firm SSŽ – known today as Eurovia – employs a colleague who has been, over many decades, responsible for collaborative projects between this enterprise and other foreign companies, among them Hungarian partners of the first order, Hídépítő Co.

Petr Somló (*Fig.17.a*) was born in Hungary, started his studies at the Technical University of Budapest. He then continued his career in Prague and entered SSŽ in early 1950's where he is still active. It is noteworthy that he is now one of the coordinators of the joint Hungarian-Slovak-Czech bridge construction at Nitra (Slovakia).

4.22 Buildings and other structures

There have been a number of concrete technologies that were designed in Hungary and constructed in the Czech Republic of today and vice versa. Some notable examples in this field follow.

The LIFT-FORM technology was initiated at the Hungarian ÉTI in cooperation with the Czech Research Institute of Ostrava. Hungarian partners were István Nagy, Ferenc Nagy, Andor Gábori, István Pozsgai, and from the Czech part Ladislav Majoroš, Ladislav Vižda, Jiří Hudečka, Ivan Kašpar.

The method was worked out in the1980's for the factory construction of multi storey concrete skeleton buildings.

For the production of the floor slabs of the building, formwork and its supports are mounted at ground level (Nagy,

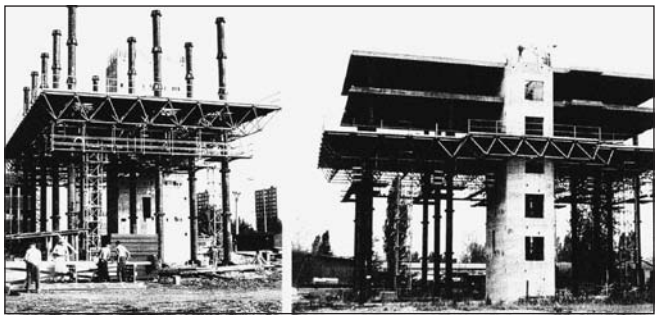

Fig. 18: LIFT-FORM method

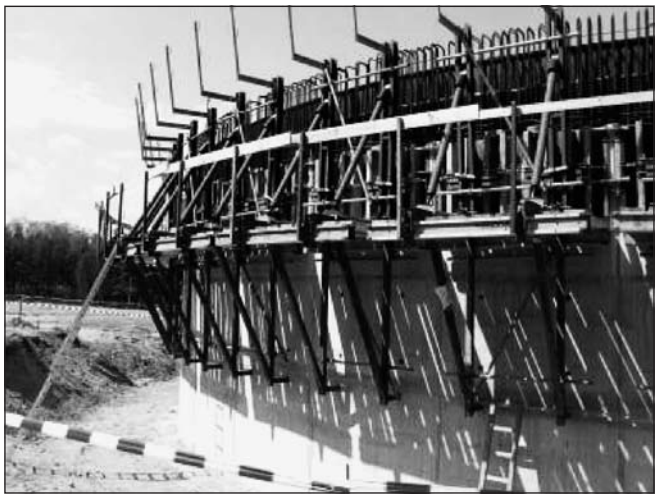

Fig. 19: Roudnice NATO base

1984ab, 87). Using specialised equipment this is moved vertically upwards along the previously assembled steel tube columns which are subsequently concrete filled. The formwork is lifted to the top floor, reinforcement is put into place and concrete is cast there (*Fig.18*). After concrete hardening, the formwork is lowered to the next level down from the top. We may therefore say that the building is constructed from the top to bottom.

The ground area of the buildings measured 1000 to 2000 m^2. The equipment can be reused many times. No scaffold is needed and manpower is minimized.

The first building that was constructed by the LIFT-FORM method was the institute for Geology in Ostrava in 1987. A structure in downtown Budapest, erected by the same procedure, was shown at the construction site to the participants of the FIP Symposium in 1992.

Fig. 17.a: Petr Somló **Fig. 17.b:** Márta Doležová **Fig. 17.c:** Ludevít Végh

In the Czech Republic the Roudnice NATO base was constructed by the Hungarian Hídépítő Co. The head of management was Ferenc Szalai. Large steel and concrete reservoirs (*Fig.19*) and a large concrete industrial space were constructed.

We would draw your attention here to a type of hall structure which has a special though indirect Czech-Hungarian link. The properties of the Oikos system are such that space structures can be produced by beam elements crossing each-other according a given rule (Soltész, Varga 1962). The method of construction was known previously, e. g. Pier Luigi Nervi and Rudolf v. Halász designed noteworthy halls using this principle. Omitting other antecedents we will only reflect here on those with Czech collaboration. In 1956 Hungarian engineers visited an Oikos hall in Brno. Not long after, in the early 1960's other large-span concrete bus garages, designed by Árpád Varga, were built in Budapest and Szombathely.

In Hungary mass production of concrete railway sleepers was developed (Beluzsár, 1990). From the early 1960's Hungarian experience in this field was shared with Czech specialists. A great number of LM type prestressed concrete sleepers produced by the Hungarian Concrete and Reinforced Concrete Works (BVM) were exported. Additionally the IPARTERV bureau in Budapest designed railway sleeper factories using the Hungarian BVM technology for installation in the Czech localities of Uherský Ostroh, Nové Hrady, Čerčany and Doloplazy.

Reflecting on links in field of civil engineering works, a particular lady, who travelled from Budapest to Prague, must be mentioned. Being an excellent specialist in foundation and earth structures she has indirect, though definite, connection to the construction of concrete structures. Márta Doležová (*Fig. 17.b*) was born in Hungary and completed elementary and secondary school there. She continued studies in civil engineering abroad, and after graduation she chose Prague as her home.

She has a PhD degree and has been Professor at the University of Arizona and at Charles University, Prague. The Dolexpert firm in Prague was founded by her and is active in a wide range of civil engineering works, principally in geotechnics and hydraulic structures. Among numerous high level works Márta Doležová contributed to the construction of the Prague metro network and she was invited as an expert to Hungary. She works closely with Hungarian institutions, especially with the University of Pécs.

4.3 Education: contact between universities

4.31 Hungarian students in Czech institutions

Between 1920 and the Nazi occupation of Bohemia many young people in Hungary who were denied entry to universities in their homeland found a haven in Prague, Brno and other Czech cities where they could attend institutions of higher education.

During the late 1940's both in Czechoslovakia and Hungary there was much interest in sending Hungarian students to Czech institutions of learning and to firms. The main purpose was to educate specialists to know the language of the allied country. In technical science there was another aim: to study those fields that were not fully covered in the curriculum of institutions of the other country.

In the field of building science the first noteworthy steps were made in 1949. To Hungarian students who finished one academic year in their homeland a scholarship was offered to continue studies mainly in Prague or Brno. After a very intensive summer course in Czech, continuing studies in a foreign language was not easy, but by the second semester at a Czech university, the new language became quite familiar. The majority of Hungarian students have achieved very good results. Some of them after graduation and practice in Hungary continued studies in Bohemia aiming at PhD (CSc) degrees.

Two examples of outstanding Hungarian specialists who graduated from the Czech Technical University in Prague (ČVUT) and received scientific degree there:

István Kürti after his return from Prague worked in Hungary in the field of research and construction and then started teaching at the Technical University of Budapest (BME). Later he was appointed as Head of Department of Building Management and Organization.

A similar career was followed by Ottó László who was also a former student of ČVUT. After working for a time in Hungarian building firms he came to teach at BME. He became professor and director of the Institute of Building Constructions and Equipment. He also was, for a period, dean of the Faculty of Architecture.

4.32 Exchange of staff members and students

There were several other types of mutual educational activities between Czech and Hungarian universities and colleges. Students' practical exercises, study tours, exchange of university staff members and common research work were regularly scheduled. Following are some examples.

The Author[1] was fortunate as a student to have summer practice placement in Havlíčkův Brod during 1948. The task was interesting: the structural control of the scaffold for the concrete arch railway bridge between Havlíčkův Brod and Pohled, under the supervision of the experienced Czech engineer Vilém Možiš. (It was a pleasant surprise to meet him much later at the headquarters of SSŽ in Národní Třída, Prague.) The other work was the surveying of the concrete dewatering system of the neighbouring tunnel. Weekends offered a possibility to visit Prague, Brno and other places of Bohemia.

Unfortunately after 1949 there was a partial isolation between the two countries. In this period there was no significant contact between Czech and Hungarian specialists in the building industry, or in education and the sciences.

During the summer of 1956, prior to the Hungarian Revolution in October, the separation between these two countries eased a little. The first exchange served as a basis for further fruitful connections between the Prague ČVUT and Budapest BME technical universities.

A study tour, including staff members of Departments of Bridge Construction No. I and II of BME and their counterparts

from the Department of Steel structures and Department of Concrete Structures of ČVUT, took place in the summer of 1956.

Czech colleagues visited the BME as well as significant steel and concrete structures in the Hungarian capital. Additionally they made a study tour of industrial construction works in North-East Hungary.

The Czech delegation was headed by Professor František Faltus and organized by Zdeněk Budinka and Ludevít Végh.

Ludevít Végh (*Fig.17.c*) originated from Košice, Slovakia and was fluent in the Hungarian language. He graduated from ČVUT Prague, and after working in the Czech building industry he became staff member of his alma mater. To this day he represents a worthy connection between Czech and Hungarian experts in concrete construction. He became professor of ČVUT and among others tasks, chairman of IASS WG 18. He contributed much to the Czech concrete industry and to science (Balázs, 2008).

Shortly after the study tour of Czech colleagues came the trip of the Hungarian expert group, headed by Professor Imre Korányi and organized by Antal Szittner and Bertalan Juhász. Professor František Faltus and colleagues, from the Department of Steel Structures joined by Professor Stanislav Bechyně and his staff from the Department of Concrete Structures of ČVUT in Prague, assisted Hungarian visitors to learn more about Czech engineering works and education. In focus were the major achievements of the Czech bridge engineering and experimental works in the Klockner Research Institute and other workshops of science and technology.

In 1958 the Author[1] and Jenő Megyeri led a group of BME students to Prague. The host institution was the railway university (VSŽ), represented by Professor František Klimeš and his colleagues Karel Slach and Bohumil Kubát. The Hungarian student group had the possibility to study concrete railway bridges and other structures at various locations throughout the country.

It is difficult to enumerate all links in the field of education. We will mention only a few examples. At the laboratory exercises of students of BME, post-tensioning procedure and measurements were learned using the hydraulic jack developed by the Czech engineer Jiří Horel. Postgraduate students made use of the book of Vladimír Křístek (1979). The Author[1] was in close professional contact with Karel Zůda and used his book (Zůda, 1958) as a teaching resource.

Czech universities frequently invited Hungarian colleagues to visit laboratories and other facilities. Czech colleagues were invited to study Hungarian methods and equipment. Among others Jaroslav Procházka, Jiří Krátký and Ladislav Hrdoušek came from Prague. There were mutual invitations to conferences. E. g. lectures at conferences in Prague were published in the periodical of the ČVUT (Tassi, 1983) and vice versa, at BME (Végh, 2009).

Indeed, all this has been only a brief sample, and restricted mainly to concrete, but hope that this gives an impression of the wide and substantial connections that exist.

4.4 Professional organisations

There were many international professional organisations where productive cooperation between Czech and Hungarian engineers could be developed. The history in this territory is so rich that we can only mention some special events and data.

4.41 *fib* = CEB + FIP

From the early 1970's Czech and Hungarian specialists cooperated in the framework of CEB. A good example is the Task Group VI/1 "Anchorage Zones". The reporter was Ralejs Tepfers (Sweden) and one of the most active members was Vladimír Urban from Prague. On the Hungarian side both Authors of this paper, as well as Andor Windisch, László Erdélyi collaborated. There were task group meetings – between other countries – in Prague and in Budapest. The result of the collective work was a CEB Bulletin (Tepfers, 1987).

Among others the Plenary Session of CEB, which was held in 1980 in Budapest, included several Czech participants providing an opportunity to strengthen the cooperation between specialists from both nations.

Before the foundation of the Hungarian Group of FIP, there were already events where Hungarian delegates could build good connections with Czech colleagues, e. g. with Jiří Krchov at the FIP Congress 1962 held in Rome-Naples. This continued at the FIP Congress 1966 in Paris, where a close friendship to Karel Zůda (Brno), among others, was initiated.

The FIP Congress of 1970 in Prague was a milestone in the life of the Hungarian Group of FIP. A Hungarian delegation of 16 members were present as registered participants, and 52 Hungarian engineers, organized by the Hungarian Scientific Society for Building (ÉTE), visited the exhibition and construction sites. This was the first significant event after the foundation of the Hungarian Group of FIP. The President of the Hungarian FIP Group, Lajos Garay chaired a plenary session. He and György Balázs Sr. were present at the general assembly. Hungarian speakers presented on all topics of outstanding structures and seven papers were published for section meetings. Additionally, a special issue of the periodical "Magyar Építőipar" was published on the occasion of the Prague Congress.

Authors of this paper attended 13 FIP/*fib* congresses, and many symposia, and it may be said that the Prague 1970 Congress was one of the best organized, of highest scientific calibre, with the most splendid social program meetings.

All other FIP events provided opportunities for good contact between Czech and Hungarian colleagues.

There were several FIP commissions where Czech and Hungarian engineers were in close cooperation, nevertheless, the strongest contacts were built up at congresses and Symposia. Jiří Klimeš, FIP medallist, was one of the most active specialists in developing professional contacts. Lubor Janda initiated relationships between Czech and Hungarian colleagues, in large part under the flag of FIP. It was rather regrettable that in 1988 due to political reasons on the Czechoslovak side, Lubor Janda was denied the FIP medal at the Symposium. The president of FIP later handed him the award in Prague at a scientific session that was also attended by Hungarian delegates.

The FIP Council Meeting took place in Prague in 1989. As well as the very good atmosphere the Author[1] enjoyed the excursion to the cable-stayed bridge that was designed by Jiří Stráský. This structure won the FIP award.

There was a significant event for the Hungarian FIP Group at the FIP 1992 Symposium in Budapest with notable participation and presentations from Czech delegates.

The 1999 *fib* Symposium in Prague had the very impressive title "Structural Concrete – The Bridge between People". Sixteen Hungarian engineers were pleased to participate at the symposium reinforcing the bridge between the two countries. Five Hungarian presentations were given in Prague on Hungarian projects and research results.

We were delighted to celebrate at the ***fib*** Congress 2010 held in Washington the presentation of the ***fib*** Freyssinet Medal to Jiří Stráský for his outstanding contribution to the field of

structural concrete. An important collaboration since 2010 in the *fib* TG 4.1 "Serviceability Models" is for the convenorship by Jan L. Vítek, successor to György L. Balázs,

We take also this opportunity to congratulate Vladimír Červenka who receives the *fib* Medal of Merit for his outstanding contributions to structural concrete and to *fib* during the *fib* Symposium 2011 in Prague for which this Journal is prepared.

4.42 RILEM (International Union of Laboratories and Experts in Construction Materials, Systems and Structures)

In 1961 a meeting of the union was organized in Prague. At the scientific sessions the presentation of György Balázs Sr. was delivered. The Author[1], among other Hungarian engineers, attended the conference.

The symposium of this organisation had its venue in Budapest in 1977. Many Czech experts in long-term observation of structures were present. These people played a significant role in the work of RILEM and involved Hungarian engineers in their activities.

4.43 CCC (Central European Congress on Concrete Engineering)

This international organisation was founded by Austria, Croatia, the Czech Republic and Hungary in 2004, and there have been annual congresses held in different cities of the member countries.

In 2006 Czech colleagues hosted the very successful congress in Hradec Kralové. The topic of the Congress was "Concrete Structures for Traffic Network". The 2007 Congress took place in Visegrád, Hungary. The Topic of the Congress was "Innovative Materials and Technologies for Concrete Structures". The 2010 CCC Congress was held in Marianské Lazně, Czech Republic. The topic of the congress was "Concrete Structures for Challenging Times".

The Hungarian organizers look ahead to the 2011 CCC Congress to be held in Balatonfüred, Hungary. Czech colleagues are welcomed in the committees as well as experts interested in these topics.

4.44 IASS (International Association for Shell and Space Structures)

Among many fields there was a special topic, being the problem of environmentally compatible structures and structural materials (ECS), that was discussed by a working group, WG18, acting in the name of the Prague Technical University under the chairmanship of Ludevít Végh. The work started in early 2000's and resulted in a book published in 2010 (Végh, 2010). The majority of seminars took place in Prague but some sessions were held in Budapest. Represented among numerous contributors were Czech and other European and overseas countries. Many Hungarian task group members also participated in the work, publishing their papers in the Proceedings of the seminars and were authors of several chapters in the book.

4.45 Other organizations

There are other professional organizations dealing with concrete. Among them we mention IABSE, CIB, ACI, UIC, ISO and others. Czech and Hungarian engineers meet frequently at various points around the globe to carry out many collaborative studies.

5. CONCLUSION

In this paper it was our aim to show the close connection between the countries of *fib* Groups, in this case focusing particularly on Hungary and the host country of this year's *fib* Symposium, the Czech Republic. We are convinced that knowing better the history and culture of our nations helps to build better cooperation generally but also in the field of structural technology.

It is our pleasure to have had the opportunity to present on collaborations between the Czechs and Hungarians in diverse fields of life, among them concrete technology. The above examples give only a narrow fragment of links between governments, businesses and diverse institutions. To show the depth and frequency of joint activity we offer the following list of Czech colleagues with whom a single Hungarian (in particular Author[1]) was in contact during his professional life. The list cannot be complete and there are names of colleagues with whom there has been a long and lasting friendship and cooperation and many others who have become known by a single or infrequent meeting. The list below includes internationally recognised scientists and honoured colleagues of different firms and institutions:

StanislavBechyně, Petr Bouška, Zdeněk Budinka, Jaroslav Čermák, Vladimír Červenka, Karel Dahinter, Jiří Dohnálek, Jaroslav Feigerle, Adolf Fiala, Bedřich Hacar, Jaroslav Hájek, Jiří Hejnic, Rudolf Hela, Hynek Hlasivec, Jaroslav Hlavač, Leoš Hobst, Milan Holický, Ladislav Hrdoušek, Ivo Hruban, Konrad Hruban, Ilja Hustý, Lubor Janda, Milan Kalný, Eugenia Kiselýová, Zdeněk Kleisner, František Klimeš, Jiří Klimeš, Alena Kohoutková, Miroslav Koreněk, Jiří Krátký, Ludvik Kratochvíl, Vladimír Křístek, Vladislav Křížek, Bohumil Kubát, Rudolf Landa, Ferdinand Lederer, Vladimír Meloun, Jiří Meřička, Vilém Možiš, Ladislav Novaček, Jaroslav Novák, Jiří Pechar, Jaroslav Procházka, Zdeněk Radkovský, Jiři Rojan, František Šimaček, Karel Slach, Bohuslav Slanský, Petr Somló, Zdeněk Špetla, Josef Špůrek, Anton Štefanek, Jiří Stráský, Josef Švajcr, Bratislav Teplý, Milík Tichý, Jiří Tomek, Karel Urban, Vladimír Urban, Jan Valentin, Ludevít Végh, Jan Vodička, Jan Vítek, Jan L. Vítek, Bohumil Voves, Karel Zůda.

Author[2] has the honour, due to the confidence of *fib* member groups, to be the current president of our international association. Beside our duty to improve technical development and to increase scientific knowledge and technology, it is our noble aim to bring the member groups closer to each other and to facilitate closer relationships with each other in diverse areas of our lives. In this context we wish to serve friendship and cooperation within the members of *fib*.

Finally we express our hope that the *fib* Symposium in Prague brings much success to our Czech colleagues, to the benefit of all participants, and to all engineers in the world of concrete.

6. ACKNOWLEDGEMENT

The authors express their gratitude to Eng. Dr. L. Bajzik (Kecskemét), Mr. J. Szántó (Prague), Mrs. O. Barna (Budapest-Prague) for the contribution to this paper. Our deep gratitude is due to Mrs. K. Haworth-Litvai (Sydney, Australia) for the revision of the text.

7. REFERENCES

Aradi, N. et al. (1983). "*History of art in Hungary*" (In Hungarian), Gondolat, Budapest.

Auction Catalogue Nr. 117 of the Central Second-Hand Bookshop (2010) (In Hungarian), Budapest.

Balázs, Gy. (2008)*: "Concrete and reinforced concrete VII, What did create Hungarians abroad"* (In Hungarian), Akadémiai Kiadó, Budapest.

Bárdos, K. (1990): "*History of music in Hungary*" (In Hungarian), Akadémiai Kiadó, Budapest

"*Cronicon Pictum*" (facsimile), (1964), Magyar Helikon, Budapest.

Beluzsár, J. (1990): „Railway sleepers", *Achievements in Prestressed Concrete in Hungary. Special issue of Magyar Építőipar,* pp. 27-29.

Csapodi, Cs., Gárdonyi, K. (1990) "*Bibliotheca Corviniana*" (In Hungarian), Helikon Kiadó, Budapest.

Dénes, O. (1955):"Design and construction of concrete railway bridges in Czechoslovakia" (In Hungarian), *Mélyépítéstudományi Szemle* 10.

Dürrenmatt, P. (1963) "*History of Switzerland*" (In German), Schweizer Druck- und Verlagshaus AG, Zürich.

"*Encyclopaedia of the Middle Ages*" (2003) (In German), Deutscher Taschenbuch Verlag, Munich, 2003.

Fitz, J. (1956): "*History of typography, Publishing and Booktrade in Hungary*" (In Hungarian), Akadémiai Kiadó, Budapest.

Györffy, Gy. (1977): „*King Steven and his work*" (In Hungarian), Gondolat Kiadó, Budapest.

Hóman, B., Szekfű, Gy. (1935): "*History of Hungary*" (In Hungarian), Királyi Magyar Egyetemi Nyomda, Budapest.

Horváth, J. (1957): "*In the spirit of the Reformation*" (In Hungarian), Gondolat Kiadó, Budapest.

Király, I. (editor in chief) (1984): "*Encyclopaedia of the world literature"* (In Hungarian), Akadémiai Kiadó, Budapest.

Kiss, L (1980): *"Etymology dictionary of geographic names"* (In Hungarian), Akadémiai Kiadó

Kmoskó, K. (1956): "The railway bridge at Komárom"*,* (In Hungarian) *Mélyépítéstudományi Szemle*, 5.

Kovács, E. (1952): „*Hungarian-Czech historical links"* (In Hungarian), Közoktatásügyi Kiadóvállalat, Budapest.

Křístek, V. (1979): "*Theory of box girders*" John Wiley & Sons, Chichester-New York-Brisbane-Toronto.

Magyary-Kossa, Gy. (1929): "*Hungarian medical memories*" (In Hungarian), Magyar Orvosi Könyvkiadó Társulat, Budapest.

Nagy, I. (1984a): "LIFT-FORM building method", *CIB International Symposium, Mechanisation of concrete technologies,* Prague.

Nagy, I. (1984b): "Erecting load-bearing structures with the LIFT-FORM system", *High-rise construction techniques & management for the 1990s, Proc. International CIB building conference,* Singapore.

Nagy, I. (1987): "The LIFT-FORM method", *The Journal of CIB,* 1-2.

Nemeskéri-Kiss, G. (1986): "Activity of bridge expert group of OSZhD" (In Hungarian), *Mélyépítéstudományi Szemle*

Pilch, J. (editor) (1933) „*One thousand year from the heroism of the Hungarian soldier*" (In Hungarian), Franklin Társulat, Budapest.

"Rákóczi Album" (1907) (In Hungarian), Pesti Napló

Romsics, I. (2007): "*History of Hungary*" (In Hungarian); Akadémiai Kiadó, Budapest.

Serédy, J. (editor) (1938): "*A memorial volume on the 900th anniversary of the death of King Saint Steven*" (In Hungarian), A Magyar Tudományos Akadémia Kiadása, Budapest.

Soltész, B., Varga, Á. (1962): "*Evaluation of experiments on Oikos structures"* (In Hungarian). UVATERV Report, Budapest.

Tassi G. (1973): "Review-muster of prestressed concrete structures in Czechoslovakia*"* (In Hungarian) *A Jövő Mérnöke,* XX. p.2.

Tassi, G. (1983): „Behaviour of prestressed concrete beams under repeated load", (In Russian) *Acta Polytechnica. Práce ČVUT Series 1. Civil Engineering. (*Prague*),* 1. pp. 109-117.

Tassi, G., Lenkei, P. (2003): „FIP and CEB, the two antecedents of *fib* were founded fifty years ago", (In Hungarian) *Vasbetonépítés,* 4, pp. 94-97.

Tassi, G. (2003): "History of the Hungarian FIP Group from the beginning to 1998." (In Hungarian), *Vasbetonépítés,* Special issue.

Tepfers, R. (reporter), Tassi, G., Balázs, L. G., Urban, V. et al. (1987): „*Anchorage zones of prestressed concrete members*". Bulletin d'Information No. 181. CEB, Paris.

Tóth, Z. (1925): "*The foreign mercenary army of King Matthias Corvinus, called Black Army*" (In Hungarian), "Stádium" Sajtóvállalat, Budapest.

Vávra, J. R. (1954) "*The Glass and the Ages*" (In German), Artia, Prague.

Végh, L. (2009): "Analysis and application of the hexagonal patterns to environmentally compatible concrete structures and brick wall systems" *Scientific Publications of the Department of Structural Engineering, Faculty of Civil Engineering, Budapest University of Technology and Economics.* pp. 141-152.

Végh, L. (editor-in-chief) (2010): "*Concept of the theory of environmentally compatible structures and structural materials (ECS)",* IASS WG18. Technical University Prague, Faculty of Civil Engineering,

Zůda, K. (1958): "*Calculation of prestressed concrete structures*", (In Czech), Štatní Nakladatelství Technické Literatury, Prague.

Prof. Géza Tassi (1925), Civil Engineer, PhD, D.Sc., FIP medallist, lifetime honorary president of Hungarian Group of ***fib,*** awarded at the first congress of ***fib,*** holder of Palotás László award of the Hungarian Group of ***fib***. He is active (semi retired) at the Department of Structural Engineering, Budapest University of Technology and Economics. Main field of interest: prestressed concrete, bridges and other structures.

Prof. György L. Balázs (1958), Civil Engineer, PhD, Dr.-habil., professor of structural engineering, head of Department of Construction Materials and Engineering Geology at the Budapest University of Technology and Economics. His main fields of activities are experimental investigation and modelling of RC, PC, FRC structures, HSC, fire resistance of concrete. He is chairman of several commissions and task groups of ***fib***. He is president of Hungarian Group of ***fib,*** editor-in-chief of the journal Concrete Structures. From 1st January, 2011 he is president of ***fib.***

DESIGN OF REINFORCED CONCRETE COLUMNS UNDER CENTRIC LOAD ACCORDING TO EUROCODE 2


Bernát Csuka - László P. Kollár

The paper presents a very simple method for the design and analysis of centric loaded, symmetrically reinforced concrete columns with rectangular or circular cross-sections. The concept of the "capacity reduction factor" (or "instability factor", "buckling coefficient") is introduced, which was applied for steel, timber and masonry columns in Eurocode 3, 5 and 6, respectively. The "capacity reduction factor" is determined on the basis of Eurocode 2. It is shown numerically that the method is always conservative and reasonably accurate. The usage of the method is demonstrated through numerical examples.

Keywords: Reinforced concrete column, concentric compression, capacity reduction factor, simplified design, parametric calculation, Eurocode 2.

1. INTRODUCTION

Concentricly loaded RC columns are common structural elements of braced building structures. In Eurocode 2 (2004) – unlike the previous Hungarian code MSZ – these columns must be designed the same way as eccentricly loaded columns, with the only difference that the eccentricity of the load is set equal to zero. In EC 2 there are two methods of calculation: (1) Nominal Stiffness, (2) Nominal Curvature. The National Annex (NA) has to decide which method must be used in a country. In Hungary both methods are accepted.

There are several articles in the literature which deal with the design procedures of columns according to Eurocode 2 (Bonet et al. (2007), Bonet et al. (2004), Mirza and Lacroix (2002), Aschheim et al. (2007)), however none of these treats the centric loaded columns separately. Other parts of Eurocode contain simple methods, which can be used for the calculation of centric loaded columns. For example, the "buckling coefficient", χ, the "instability factor", $k_{c,y}$ or $k_{c,z}$ or the "capacity reduction factor", $\Phi_{m,s}$ are introduced for steel- (EC 3, 2004), timber- (EC 5, 2004) and masonry structures (EC 6, 2006), respectively.

Our aim in this paper is to derive a similarly simple design method for centric loaded RC columns. We wish to use the following expression:

$$N_{Rd} = \Phi N'_u \tag{1}$$

where N_{Rd} is the ultimate load of a column, Φ is the capacity reduction factor, and N'_u is the plastic ultimate load of the cross-section:

$$N'_u = f_{cd} A_c + A_s f_{yd} \tag{2}$$

where A_c is the cross-sectional area of concrete, A_s is the total cross-sectional area of the reinforcement, f_{cd} is the design compressive strength of concrete, and f_{yd} is the design yield strength of steel. The concrete cross-section and the arrangement of the reinforcing bars is doubly symmetric and hence the center of gravity of the reinforcement and the concrete are at the same point.

In a previous paper Kollár (2004) presented a solution for this problem – applying an approximate interaction diagram –, however the presented method has the following shortcomings: it is valid only for rectangular columns and according to the applied approximations the accuracy is not satisfactory.

2. THE PROCEDURE OF EUROCODE 2

Here we present briefly the method of the Eurocode for calculating the design value of eccentricities for concentric loading applying the method of "Nominal Curvature". These eccentricities are used in the cross-sectional design of columns.

In the analysis the original eccentricity of the normal force on the undeformed column ($e_e = 0$), the eccentricities due to the imperfections (e_i) and the (second order) eccentricities due to the deformations of the column (e_2) must be taken into account (*Fig. 1*).

When the first order bending moment along the column is uniform, the cross-section of the column must be designed for the eccentricity e_{tot}:

$$e_{tot} = \max \begin{cases} e_e + e_i + e_2 & \text{sum of eccentricities} \\ e_0 & \text{minimal value of eccentricities} \end{cases} \tag{3}$$

where $e_e = M_{0e} / N_{Ed}$ is the first order eccentricity (for uniform bending moment), e_i is due to the imperfections and e_2 is the second order imperfection. The expression for e_i is as follows:

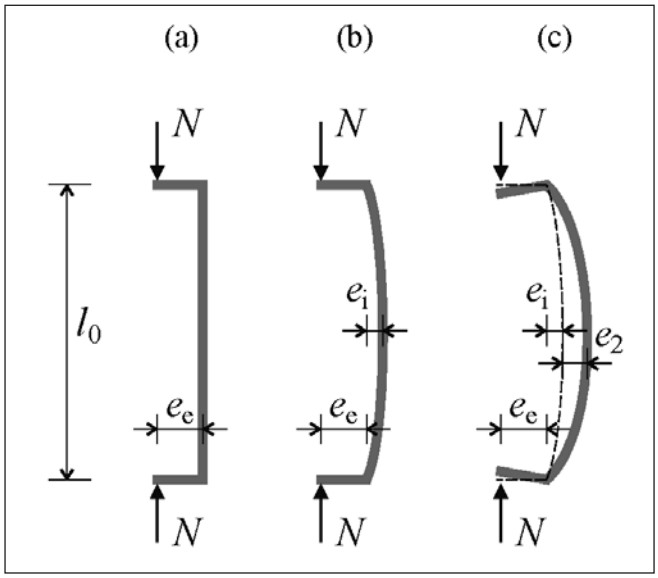

Fig. 1: Eccentricities of a RC column subjected to a normal force: due to the load (a), due to the load and the imperfection (b), and due to the load, imperfection and second order effects (c)

$$e_i = \begin{cases} \dfrac{l_0}{400}, & \text{if } l \le 4 \text{ m} \\ \dfrac{2}{\sqrt{l}}\dfrac{l_0}{400}, & \text{if } 4 \text{ m} < l < 9 \text{ m}, \\ \dfrac{2}{3}\dfrac{l_0}{400}, & \text{if } l \ge 9 \text{ m} \end{cases} \tag{4}$$

where l_0 is the effective length of the column (in m), which depends on the length, l, and on the boundary conditions of the column.

The second order eccentricity is calculated as:

$$e_2 = \frac{1}{r}\frac{l_0^2}{\pi^2} \approx \frac{1}{r}\frac{l_0^2}{10}, \tag{5}$$

where the curvature is

$$\frac{1}{r} = K_r K_\varphi \frac{1}{r_0}, \tag{6}$$

the basic value of the curvature is

$$\frac{1}{r_0} = \frac{f_{yd} / E_s}{0.45\ d'}, \tag{7}$$

and a parameter

$$K_\varphi = \max\{1 + \beta\varphi_{ef}; 1\}, \tag{8}$$

which depends on the effective creep coefficient, φ_{ef}

$$\beta = 0,35 + \frac{f_{ck}}{200} - \frac{\lambda}{150}. \tag{9}$$

In Eq. (7) E_s is the elastic modulus of steel, in Eq. (9) λ is the slenderness ratio of the homogeneous bar (according to EC 2 a cross-section without cracks should be taken into consideration; for a rectangular cross-section bent about the y-axis $\lambda = \frac{l_0}{h}\sqrt{12}$), and f_{ck} is the characteristic compressive trength of concrete in N/mm^2.

$$K_r = \min\left\{\frac{N'_u - N_{Ed}}{N'_u - N_{bal}}; 1\right\}, \tag{10}$$

depends on the applied normal force N_{Ed}. In Eq. (10) N'_u is given by Eq. (2), N_{bal} is the value of the normal force at maximum moment resistance, as shown in *Fig. 2*.

In Fig. 2 N_u is the ultimate load of the centric loaded cross-section according to EC 2 ($N_u \le N'_u$), which is calculated as:

$$N_u = f_{cd} A_c + \min\{400;\ f_{yd}\} A_s. \tag{11}$$

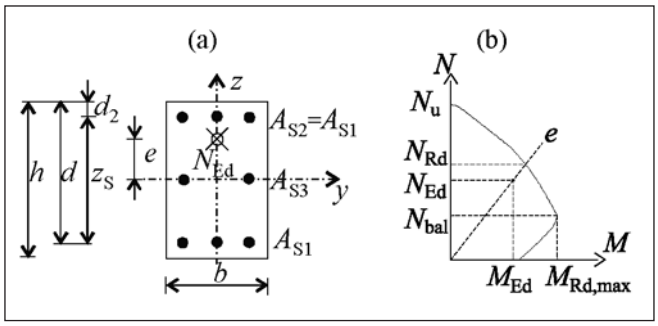

Fig. 2: Doubly symmetric cross-section (a) and the interaction diagram with eccentricity in direction z (b) (For the load $N_{Ed} \le N_{Rd}$ with the eccentricity e, the cross-section is safe)

The value of d' (Eq. 7) is defined as:

$$d' = h/2 + i_s, \tag{12}$$

where h is the height of the cross-section and i_s is the radius of gyration of reinforcing bars (rebars) about the center of gravity of the reinforcement.

The minimum value of the eccentricity (Eq.3) is:

$$e_0 = \begin{cases} 20 \text{ mm}, & \text{if } h \le 600 \text{ mm} \\ h/30, & \text{if } h > 600 \text{ mm} \end{cases}. \tag{13}$$

We may observe that the eccentricity of the normal force depends on

- the effective length of the column,
- the amount and arrangement of the rebars,
- the value of the axial load, N_{Ed},
- the concrete class (through the creep effect).

3. PROBLEM STATEMENT

We consider reinforced concrete columns with concrete class up to C50/67, and effective length to depth ratio (l_0 / h) up to 22. The cross-section is either rectangular with doubly symmetric reinforcement, or circular, where at least six rebars are placed uniformly around the circumference. The column is subjected to an axial load at the center of the cross-section.

Our aim is to determine the ultimate load N_{Rd} of the column following Eurocode 2. If the parameters of the column and the load (N_{Ed}) are given, we can determine with the above expressions (section 2), whether $N_{Rd} < N_{Ed}$ or $N_{Rd} \ge N_{Ed}$. In this paper we wish to derive the "capacity design factor", Φ, with the aid of which, N_{Rd} can be calculated in a very simple way (see Eq.(1)).

4. METHOD OF SOLUTION

To fulfill our goal we performed several thousand calculations of different reinforced concrete columns. Here we discuss the procedure and the parameters used in the calculations.

According to the method presented in section 2 the amount and arrangement of the rebars affect the additional

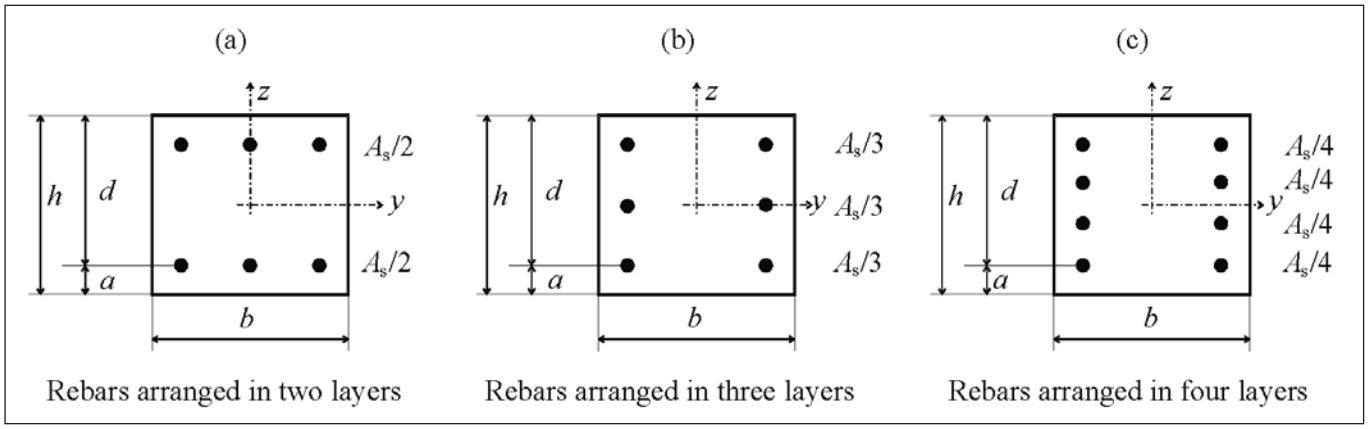

Fig. 3: Rectangular RC cross-sections with uniform rebar arrangements along the height (Bending is around the y-axis)

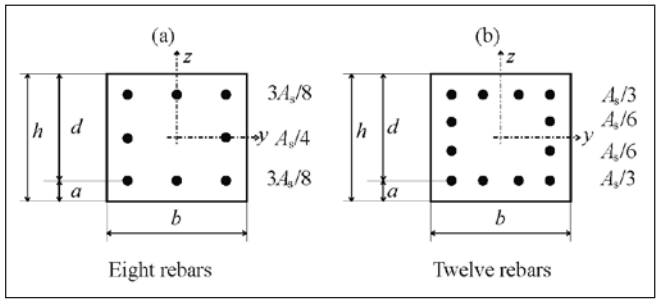

Fig. 4: Rectangular RC cross-sections with uniform rebar arrangements along the circumference (Bending is around the y-axis)

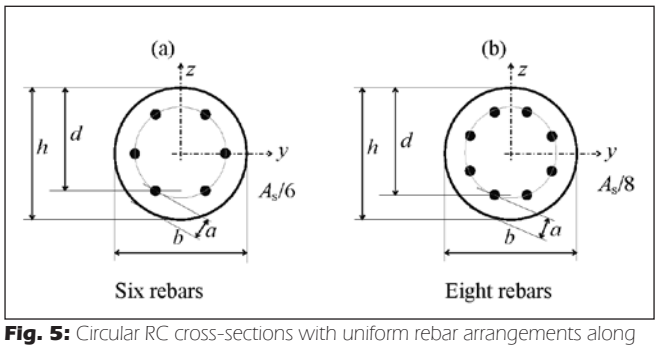

Fig. 5: Circular RC cross-sections with uniform rebar arrangements along the circumference (Bending is around the y-axis)

eccentricities significantly. In our calculations we consider the rebar arrangements shown in *Figs. 3, 4 and 5*.

The strength class of the concrete was varied between C20/25 and C50/67. The creep coefficients used in the calculations are given in *Table 1*.

The following values of a / h (*Figs. 3, 4 and 5*) were considered: $a / h = 0.2, 0.15, 0.1, 0.05$, where a is the distance between the center of gravity of the rebars and the edge of the cross-section and h is the height of the cross-section. The slenderness (l_0 / h) was varied between 0 and 22, and the amount of reinforcement was changed from zero to infinity, knowing however, that the minimum and maximum reinforcement will give the actual limits. The minimum reinforcement according to EC 2 is:

$$A_{s,min} = \max \begin{cases} 0.1 N_{Ed} / f_{yd} \\ 0.002 A_c \end{cases}, \qquad (14)$$

and the maximum is $A_{s,max} = 4\%$. (Note that the Hungarian NA gives a minimum reinforcement ratio as 3‰ which is higher than the value in Eq. (14). In our calculations we will use the original value (2‰).)

Reinforcing steel B500 was applied in the calculation, lower yield stress (which is rarely used nowadays) results in higher Φ value.

In the calculation the following steps were performed:

- for a given cross-section the *M(N)* interaction diagram was determined, following the rules of Eurocode. (An example is shown in *Fig. 6*)
- for a given l_0 / h value, N_{Rd} was determined with the aid of iteration. (The iteration was needed because the eccentricity e_2 depends on the – unknown – load (N_{Rd})).
- the Φ parameter was calculated as (Eq. 1): $\Phi = N_{Rd} / N'_u$

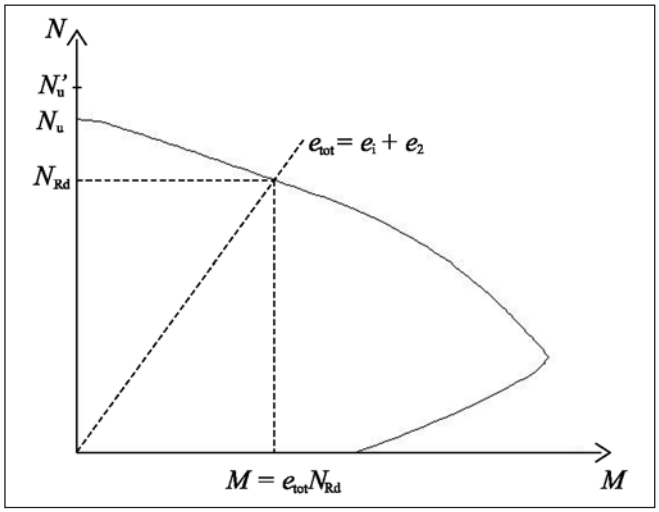

Fig. 6: Interaction diagram

The total eccentricity is calculated as $e_{tot} = \max\{e_i + e_2; h/30\}$ (see Eqs. (3) and (13)), applying Eqs.(4-10) and (12). (According to Eq. (13) this formula can only be used for cross-sections bigger than 600 mm. We will discuss this matter in section 7.) As we stated above, e_2 depends on the yet unknown $N_{Ed} = N_{Rd}$, and hence an iteration is needed for the calculation. The starting value of the eccentricity is calculated from the normal force value at maximum moment resistance ($N_{bal} = N_{(0)}$). The value of e_1 is calculated and the value of N_1 can be determined using the interaction diagram. Now considering $N_{Ed(i)} = N_{Rd(i-1)}$, the eccentricity of the next step can be calculated. This method is convergent because of the monotony of the functions, and the result is always obtained in a few steps (*Fig.*

Table 1: Creep coefficient

Strength class	C16/20	C20/25	C25/30	C30/37	C35/45	C40/50	C45/55	C50/60
$\varphi(\infty,28)$	2.76	2.55	2.35	2.13	1.92	1.76	1.63	1.53

Note: 70% relative humidity, 28 days strength, plastic consistency at manufacturing and 100 mm effective thickness of the member

7). In bending (and compression with high eccentricity) the limit strain of concrete is ε_{cu} = 3.5‰, while in pure compression

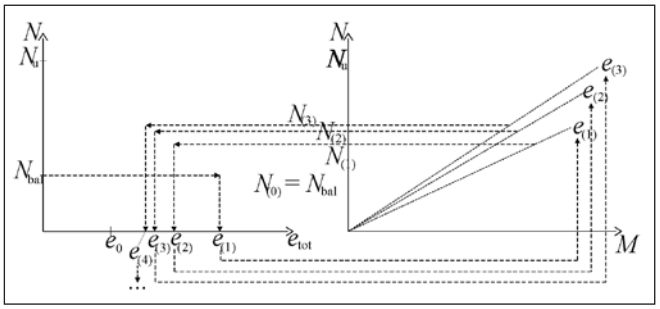

Fig. 7: Steps of iteration to determine $N_{Ed} = N_{Rd}$

it is ε_{cu} = 2‰ (In case of compression with small eccentricity two conditions must be fulfilled: the compression at the side of the cross-section can not be higher than 3.5‰ and at 3/7 of the cross-section 2‰). This latter constraint causes a small reduction in the interaction diagram, when the eccentricity is small as shown in *Fig. 8*. (See also Eqs. (2) and (11).)

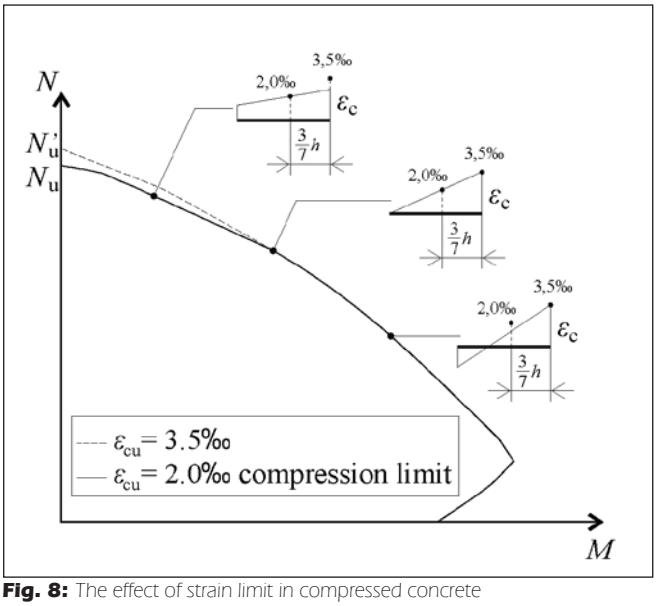

Fig. 8: The effect of strain limit in compressed concrete

5. CALCULATION OF THE CAPACITY REDUCTION FACTOR

The capacity reduction factor, Φ depends on the effective length (l_0), the height of the cross-section (h), the concrete class, the amount of reinforcement and the rebar arrangement. The key to the applicability of the calculated results is the proper choice of the parameters. After several unsuccessful experiments the following governing parameters were chosen:

$$\alpha = \frac{l_0}{h}, \tag{15}$$

$$\beta = \frac{\mu}{0{,}5 + \mu}, \tag{16}$$

where

$$\mu = \frac{A_s f_{yd}}{bhf_{cd}}. \tag{17}$$

The value of β is between 0 and 1 depending on the reinforcement ratio. If β = 0 there is no reinforcement in the cross-section and, in theory, if β = 1 the amount of reinforcement in the cross-section is infinite. In reality there is a lower and an upper limit for β: its value varies between 0.08 and 0.72.

5.1 Solution for a reference cross-section

First a rectangular cross section with the simplest rebar arrangement (two layers, *Fig. 3(a)*) was considered with a / h = 0.15 (approximately 300-350 mm column size) and concrete class C30/37. The results ($\Phi = \Phi_2$) are shown in *Fig. 9* as a function of parameters β and α. The dots on the curves belong to the cases, where the amount of reinforcement is equal to the minimum given by Eq. (14).

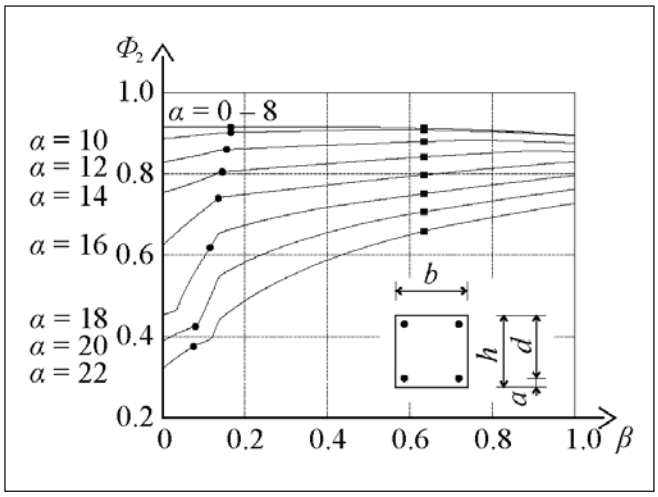

Fig. 9: Results of calculations for the reference cross-section. The dots on the curves belong to the cases, where the amount of reinforcement is equal to the minimum given by Eq. (14), the squares belong to 4% maximum reinforcement

The results are also given in *Table 2*. As a rule, the higher the reinforcement ratio the higher the capacity reduction factor. We may observe, however (*Fig. 9*) that for short columns (with small slenderness ratio, $l_0 / h < 10$) Φ_2 slightly increases with β. In *Table 2* this increment was neglected, and Φ_2 is a monotonic function of both β and α.

Table 2: The value of Φ_2 as a function of β (Eq. 16) and α

β	$\alpha = l_0 / h$						
	≤10	12	14	16	18	20	22
0.00	0.88	0.82	0.75	0.62	0.45	0.38	0.32
0.08	0.89	0.84	0.77	0.69	0.56	0.42	0.37
0.10	0.89	0.84	0.78	0.71	0.59	0.45	0.38
0.12	0.89	0.85	0.79	0.72	0.62	0.50	0.39
0.14	0.89	0.85	0.80	0.74	0.65	0.54	0.44
0.16	0.89	0.86	0.80	0.74	0.66	0.56	0.45
0.18	0.89	0.86	0.80	0.74	0.66	0.57	0.47
0.20	0.89	0.86	0.80	0.74	0.67	0.58	0.48
0.25	0.89	0.86	0.81	0.75	0.68	0.60	0.51
0.30	0.89	0.86	0.81	0.76	0.69	0.62	0.54
0.60	0.89	0.87	0.83	0.79	0.74	0.70	0.65
0.90	0.89	0.87	0.85	0.82	0.78	0.74	0.71

Note: Φ can not be higher than Φ_{max} given in *Table 4*.

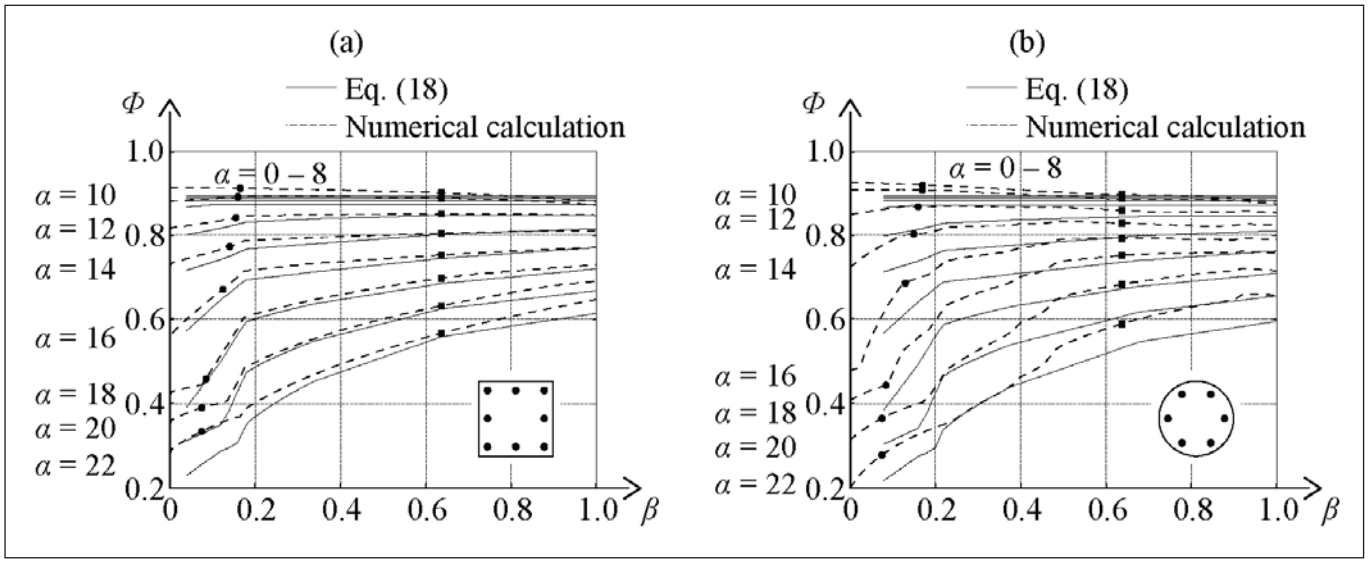

Fig. 10: *Effect of rebar arrangement and cross-sectional shape. Rectangular cross-section with eight bars arranged uniformly along the circumference (a) and circular cross-section with six bars arranged uniformly along the circumference (b) (a = 0.15h, concrete class C30/36 for both cases.) The dots on the curves belong to the cases, where the amount of reinforcement is equal to the minimum given by Eq. (14), the squares belong to 4% maximum reinforcement*

5.2 Effect of rebar arrangement and cross-sectional shape

We have calculated the capacity reduction factor for the cross sections shown in *Figs 3, 4 and 5*. Two illustrative examples are shown in *Figs. 10(a) and (b)*, where the results of the numerical calculations are given by dashed lines. It may be observed that the shape of these curves are similar to those given in *Fig 9*.

We propose to approximate these curves with the aid of the values given in *Table 2*, however the parameter β and the resulting Φ are shifted with the following expressions:

$$\beta = \frac{\mu}{0.5+\mu} - \Delta\beta\,, \quad \Phi = \Phi_2 - \Delta\Phi_1\left(\frac{l_0/h}{22}\right)^2, \tag{18}$$

where μ is given by Eq (17), parameter $\Delta\beta$ is 0.04 or 0.08 and Φ_2 is given in *Table 2* as a function of β, while $\Delta\Phi_1$ is 0.09 or 0.10 for the cases shown in *Fig 4(a) or 5(a)*, respectively. The results of the approximation are shown by solid lines in *Figs. 10(a) and (b)*. We may conclude that for realistic β values the results are conservative, and reasonably accurate.

The approximate curves were calculated for all the cross-sections shown in *Figs. 3, 4 and 5*. The results showed similar tendencies; differences are only found in the values of $\Delta\beta$ and $\Delta\Phi_1$.

The recommended values for these parameters can be found in *Table 3*.

5.3 Effect of concrete strength class

The effect of different concrete classes was investigated numerically. It can be observed that the lower the concrete class, the higher the Φ value, and the difference increases with higher slenderness ratios l_0 / h. Two illustrative examples are shown in Figs. 11(a) and (b) for the simplest cross-section (see Fig. 3(a)). The calculated Φ values are given by dashed lines. We may observe again the similarity with the curves given in Fig. 9. We again suggest to approximate the dashed lines by the values given in Table 2, with the following modification in parameter α:

$$\alpha = \frac{l_0}{h} + \Delta\alpha\left(\frac{l_0/h}{22}\right)^3, \ \Phi = \Phi_2\,, \tag{19}$$

where for concrete strength class above C30/37 ($f_{ck} > 30$)

$$\Delta\alpha = 0{,}14\left(f_{ck} - 30\right), \tag{20}$$

and for $f_{ck} \le 30$, $\Delta\alpha = 0$.

The results are shown by solid lines in *Fig 11*. (Note that the formulas expressions are empirical, they are results of fitting different curves on each other and have no real physical content.)

5.4 Effect of effective depth to total depth ratio

If the effective depth, $d > 0.85h$ (or $a < 0.15h$), the results given in Table 2 are conservative. A better approximation can

Table 3: *Value of parameters $\Delta\beta$ and $\Delta\Phi_1$ depending on cross-sectional shape and rebar arrangement*

Cross-section		$\Delta\beta$	$\Delta\Phi_1$
Rectangular, uniform reinforcement along the height	2 layers of rebars (*Fig. 3(a)*)	0	0
	3 layers of rebars (*Fig. 3(b)*)	0.05	0.13
	4 layers of rebars (*Fig. 3(c)*)	0.08	0.19
	5 or more layers of rebars	0.14	0.30
Rectangular, uniform reinforcement along the circumferencre	8 rebars (*Fig. 4(a)*)	0.04	0.09
	12 rebars (*Fig. 4(b)*)	0.05	0.10
	16 or more rebars	0.06	0.11
Circular	6 or more rebars (*Fig. 5*)	0.08	0.10

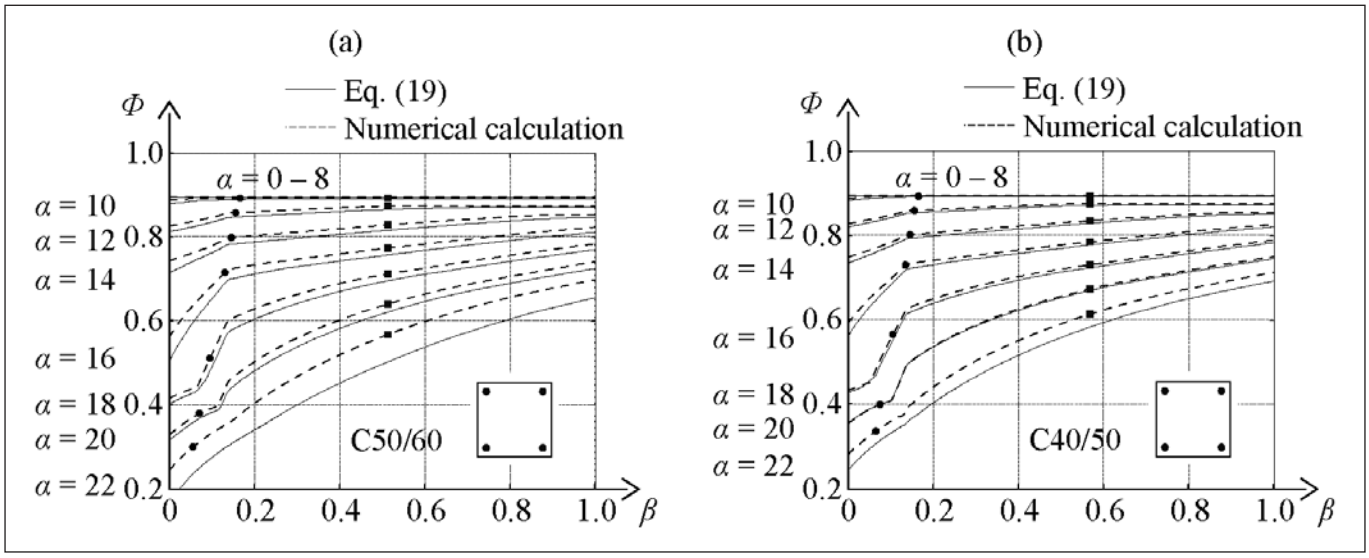

Fig. 11: Effect of concrete strength class. Rectangular cross-section with four bars arranged at the corners with concrete class C50/60 (a) and concrete class C40/50 (b) ($a = 0.15h$)

be obtained, if the following modification is performed:

$$\Phi = \Phi_2 + \Delta\Phi_2 \left(\frac{l_0 / h}{22} \right)^2, \quad \Delta\Phi_2 = 0.37 \left(0.15 - \frac{a}{h} \right), \tag{21}$$

where again Φ_2 is given in *Table 2*. (If $a > 0.15h$ we recommend the calculation of a reduced cross-section with total height: $h = z_s / 0.7$ as shown in *Fig. 12*.)

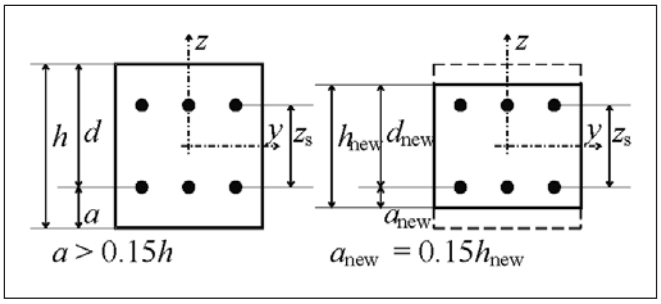

Fig. 12: Reduction of cross-section if $a > 0.15h$

An illustrative example is shown in *Fig. 13*, where the dashed lines are obtained by the accurate calculation, while the solid lines are calculated by *Table 2* and Eq. (21).

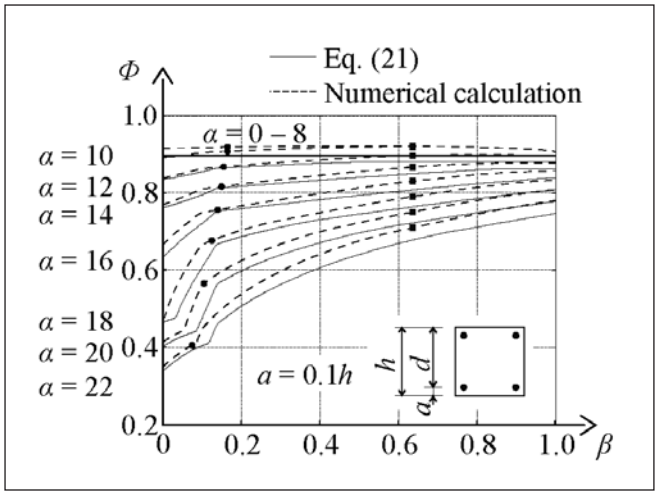

Fig. 13: Effect of effective depth to depth ratio. Rectangular cross-section with four bars arranged at the edges, with $a = 0.1h$ and concrete class C30/37

5.5 Summary of calculation of capacity reduction factor

In summary the capacity reduction factor can be calculated with the following expression:

$$\Phi = \Phi_2 - \Delta\Phi_1 \left(\frac{l_0 / h}{22} \right)^2 + \Delta\Phi_2 \left(\frac{l_0 / h}{22} \right)^2. \tag{22}$$

here Φ_2 is obtained from *Table 2* with the following parameters:

$$\alpha = \frac{l_0}{h} + \Delta\alpha \left(\frac{l_0 / h}{22} \right)^3, \quad \beta = \frac{\mu}{0.5 + \mu} - \Delta\beta. \tag{23}$$

The parameters $\Delta\Phi_1$ and $\Delta\beta$ are listed in Table 3. The values of $\Delta\Phi_2$, μ and $\Delta\alpha$ are given by Eqs. (21), (17) and (20), and reiterated below, for convenience:

$$\Delta\Phi_2 = \begin{cases} 0.37\left(0.15 - \dfrac{a}{h}\right), & \text{if } a \le 0.15h \\ 0, & \text{if } a > 0.15h \end{cases}, \quad \mu = \frac{A_s f_{yd}}{bhf_{cd}},$$

$$\Delta\alpha = \begin{cases} 0.14(f_{ck} - 30), & \text{if } f_{ck} \ge 30 \\ 0, & \text{if } f_{ck} < 30 \end{cases}. \tag{24}$$

6. LINEAR APPROXIMATION

If someone needs a really quick answer, the middle part of curves in *Fig. 9* can be replaced by straight lines, and we obtain an explicit expression for the capacity reduction factor Φ_2. We write:

$$\Phi_2 = 0.88 - (1.2 - \beta)\frac{l_0 / h - 12}{24} \le 0.85, \quad \textit{if } 0.15 < \beta < 0.7 \tag{25}$$

Note that $\beta = 0.7$ belongs roughly to $A_s / A_c = 4 - 5\%$ (strongly depending on the strength of the materials). The results are shown in *Fig. 14*.

The modification factors developed in subsections 5.2 to 5.4 (see Eqs. (22-24)) can also be used with Eq. (25).

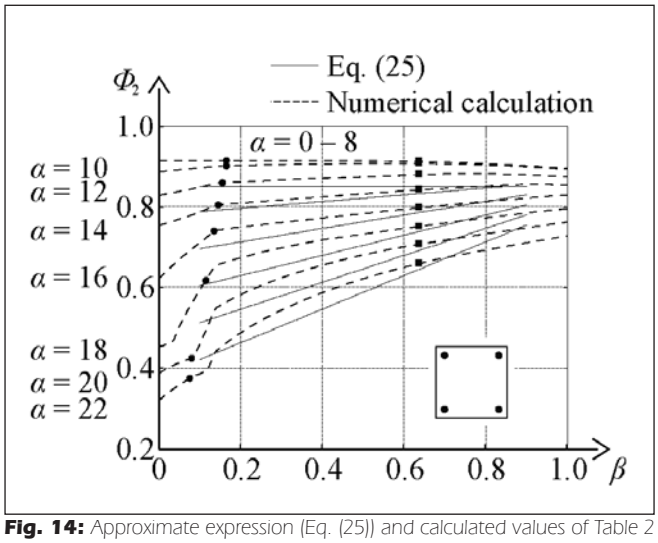

Fig. 14: Approximate expression (Eq. (25)) and calculated values of Table 2 for rectangular cross-section with four bars arranged at the edges, concrete class C30/37, $a = 0.15h$

7. EFFECT OF THE SIZE OF THE CROSS-SECTION

In the previous three sections the eccentricity was calculated as $e_{tot} = \max\{e_i + e_2; h/30\}$, and Φ was the function of the relative sizes, such as l_0/h and μ. However, for cross-sections with height (or diameter) smaller than 600 mm ($h < 600$ mm) the size may have a direct effect. The reason is, that for these cross-sections the minimum value of eccentricity is calculated according to Eq. (13) as:

$$e_0 = 20 \text{ mm}. \qquad (26)$$

We calculated the parameter Φ with this $e_{tot} = 20$ mm value, instead of $\max\{e_i + e_2; h/30\}$ (see Eq. (3)). For simplicity – as the most conservative case – only the minimum reinforcement was taken into account. For rectangular and circular cross-sections the reinforcement arrangements shown in *Figs. 3, 4 and 5* were considered and the smallest Φ was selected. The conservative Φ_{max} values, which are independent of the concrete class, rebar arrangement, reinforcement ratio and a / h value are given in *Table 4*. The value of Φ can not be higher than these.

Table 4: values of Φ_{max}

h[mm]	150	200	300	400	500	≥600
Φ_{max}	0.60	0.68	0.77	0.81	0.84	0.87

8. THE SIMPLIFIED METHOD

The more parameters are taken into account, the more accurate (approximate) results can be obtained. The simplest solution can be obtained if only the minimum reinforcement is considered, and the capacity reduction factor is determined accordingly. We performed this calculation for rectangular cross sections with four rebars in the edges, rebars arranged in three rows and a circular cross section with 6 rebars. The results are given in *Table 5*.

9. NUMERICAL EXAMPLE

A braced office building contains RC columns with the length $l = 6$ m, which are simply supported at both ends. The columns are subjected to concentric loads, $N_{Ed} = 1600$ kN. The dimensions of the cross-section are given in *Fig. 15*, the area of the cross-section is 300 × 300 mm, the reinforcement is 8ø20 ($A_s = 2513$ mm^2), the stirrup is ø8 and the concrete cover is 20 mm. The concrete class is C35/45 ($f_{ck} = 35$ N/mm^2, $f_{cd} = 23.3$ N/mm^2), the reinforcing steel is B500 ($f_{yd} = 435$ N/mm^2). The load bearing capacity of the column is investigated.

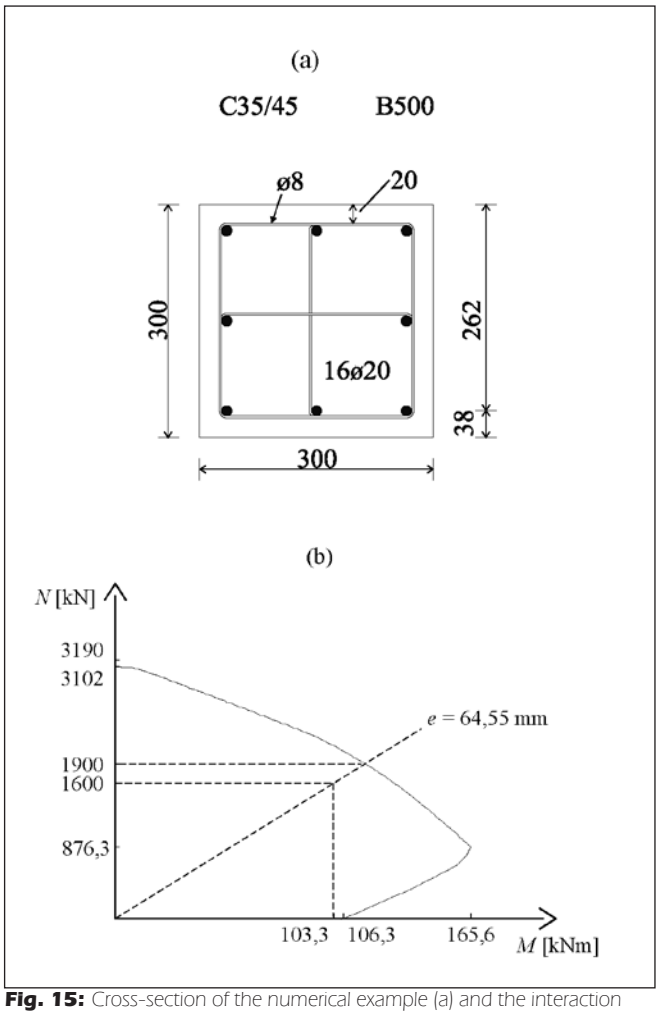

Fig. 15: Cross-section of the numerical example (a) and the interaction diagram (b).

The effective length of the column is $l_0 = 6$ m, $h = 300$ mm, the effective depth is $d = 262$ mm, $a = 38$ mm. From Eq. (2) we have:

$$N_u' = (23.3 \times 300^2 + 2513 \times 435) \times 10^{-3} = 3190 \text{ kN}.$$

9.1 Checking with the simplified (Sec. 5) method

As a rough approximation, we can use *Table 5*. $\alpha = 6000 / 300 = 20$, so the third row gives $\Phi = 0.36$, this is smaller than Φ_{max} ($\Phi_{max(h=300)} = 0.77$, see *Table 4*).
Hence (according to Eq. (1)):

$N_{Rd} = 0.36 \times 3190 = 1148 \text{ kN} < N_{Ed}$, the column is UNSAFE.

9.2 Checking with the recommended expressions (Sec. 5.5)

We may take into account the effect of reinforcement to improve the calculation. From Eq (24) we obtain:

Table 5: Φ for minimum reinforcement, as a function of concrete class and α Note that Φ can not be higher than the values given in *Table 4*.

Concrete class	rectangular cross-section, reinforcement in two rows						rectangular cross-section, reinforcement in three rows							circular cross-section					
	$\alpha = l_0 / h$						$\alpha = l_0 / h$							$\alpha = l_0 / h$					
	≤12	14	16	18	20	22	≤10	12	14	16	18	20	22	≤12	14	16	18	20	22
C20/25	0.86	0.81	0.75	0.68	0.56	0.39	0.88	0.83	0.77	0.68	0.54	0.41	0.33	0.87	0.82	0.75	0.55	0.38	0.30
C25/30	0.86	0.80	0.74	0.65	0.49	0.38	0.88	0.83	0.76	0.65	0.46	0.40	0.32	0.87	0.82	0.72	0.51	0.37	0.29
C30/37	0.85	0.80	0.74	0.62	0.42	0.37	0.88	0.83	0.76	0.64	0.43	0.37	0.32	0.87	0.81	0.69	0.44	0.36	0.28
C35/45	0.85	0.80	0.73	0.59	0.41	0.35	0.88	0.83	0.76	0.62	0.42	0.36	0.30	0.87	0.81	0.66	0.42	0.36	0.27
C40/50	0.85	0.80	0.73	0.56	0.39	0.33	0.88	0.83	0.75	0.61	0.41	0.34	0.28	0.87	0.80	0.63	0.41	0.34	0.26
C45/55	0.85	0.80	0.72	0.54	0.39	0.31	0.88	0.83	0.75	0.59	0.40	0.33	0.26	0.87	0.80	0.61	0.40	0.33	0.26
C50/60	0.85	0.79	0.71	0.51	0.38	0.30	0.88	0.83	0.75	0.58	0.40	0.32	0.24	0.86	0.79	0.58	0.39	0.31	0.24

Table 5 is recommended to be used for the preliminary design of centric loaded RC columns.

$$\Delta\Phi_2 = 0.37 \times \left(0.15 - \frac{38}{300}\right) = 0.0086,$$

$$\mu = \frac{2513 \times 435}{300^2 \times 23.3} = 0.5213, \qquad \Delta\alpha = 0.14\left(35 - 30\right) = 0.70.$$

$\Delta\Phi_1$ and $\Delta\beta$ from Table 3 are:

$\Delta\Phi_1 = 0.09, \quad \Delta\beta = 0.04.$

According to Eq. (23) we have:

$$\alpha = \frac{6000}{300} + 0.70 \times \left(\frac{6000/300}{22}\right)^3 = 20.53$$

$$\beta = \frac{0.5213}{0.5 + 0.5213} - 0.04 = 0.470$$

.

From *Table 2* – with linear interpolation – we obtain $\Phi_2 = 0.644$ and the final value observed from Eq. (22) is ($l_0 / h = 20$):

$$\Phi = 0.644 - 0.09 \times \left(\frac{20}{22}\right)^2 + 0.0086\left(\frac{20}{22}\right)^2 = 0.577,$$

which results in (Eq. (1)):

$N_{Rd} = 0.577 \times 3190 = 1841$ kN > N_{Ed} the column is SAFE.

9.3 Checking using linear approximation

The value of Φ_2 can be found quickly if we use the approximate equation (Eq. (25)):

$$\Phi_2 = 0.88 - (1.2 - 0.470) \times \frac{20 - 12}{24} = 0.637$$

value of Φ according to Eq. (22):

$$\Phi = 0.637 - 0.09 \times \left(\frac{20}{22}\right)^2 + 0.0086 \times \left(\frac{20}{22}\right)^2 = 0.569,$$

which results in (Eq. (1)):

$N_{Rd} = \Phi N_u' = 0.569 \times 3190 = 1815$ kN > N_{Ed} the column is SAFE.

9.4 „Accurate" calculations according to Eurocode 2

The „accurate" calculations according to Eurocode 2 are as follows. The calculated eccentricities are (Eqs. (3) and (4)):

$e_e = 0$ mm (concentric loading), $e_i = \frac{2}{\sqrt{6}} \frac{6000}{400} = 12.25$ mm,

without giving the details, from Eqs. (5-13) we have

$e_2 = 52.30$ mm.

The total eccentricity is

$e_{tot} = 12.25 + 52.30 = 64.55\ mm > e_0 =$

$\max\left\{\frac{300}{30}; 20\right\} = 20$ mm.

Using the accurate interaction diagram (see *Fig. 15(b)*),

$N_{Rd} = 1900$ kN > N_{Ed}, the column is SAFE.

9.5 Evaluation of results

In summary, the ultimate loads according to the different calculations are as follows:

- Eurocode 2 ("accurate") 1900 kN,
- capacity reduction factor (Eq. 22) 1841 kN,
- linear approximation (Eq. 25) 1815 kN,
- minimal reinforcement (*Table 5*) 1148 kN.

Note that all the calculations are conservative. Finally we state that Eurocode also allows the usage of a second order numerical calculation, which – as a rule – results in higher load bearing capacity than the methods above.

10. DISCUSSION

In this paper a table and expressions were developed which enable the designer to determine the load bearing capacity of centric loaded RC columns by Eq.(1), using a simple method based on the capacity reduction factor and the nominal (plastic) resistance of the cross-section. The capacity reduction factor, Φ depends on the shape of the cross-section (rectangular or circular); on the amount and arrangement of the reinforcement and the concrete class.

The values of *Table 5* were calculated assuming minimal reinforcement. Taking the effect of the reinforcement and the concrete class into account (using *Table 2* and the modification

factors) gives a good approximation for the resistance of the structural element. This indicates that *Table 5* should be used for preliminary design – finding the needed cross-sectional area of the concrete – while *Table 2* (or the linear approximation of Eq. (25)) and the modification expressions can be used for checking the centric loaded columns.

In the calculation conservative values were assumed for the creep coefficient (*Table 1*), if the creep coefficient is lower, the capacity reduction factor is higher, and the presented results can be used as conservative solutions. The imperfection was calculated assuming a total height of l = 4m (or shorter), for longer columns, Φ may be higher, and the presented values may be used. All the calculations are based on steel strength class, B500. It was found, that for lower steel classes the Φ-s are higher, and again, the presented results can be used as conservative solutions. For higher steel classes the presented values should not be used.

11. LIST OF NOTATION

a	the distance between the center of gravity of the lower rebars and the lower edge of the cross-section
A_c	the cross-sectional area of concrete
$A_s = \Sigma A_{si}$	the total cross-sectional area of the reinforcement
$A_{s,min}$	minimum amount of reinforcement
$A_{s,max}$	maximum amount of reinforcement
b	the width of the cross-section
d	effective depth
d'	reduced effective depth
E_s	=200 kN/mm^2, elastic modulus of steel
e_0	minimal eccentricity
e_2	second order eccentricity (from the deformation of the column)
e_e	the original eccentricity of the normal force
e_i	the eccentricity due to the imperfection
e_{tot}	total eccentricity (sum of eccentricities)
$f_{cd} = f_{ck} / 1{,}5$	the design compressive strength of concrete
f_{ck}	the characteristic compressive strength of concrete
$f_{yd} = f_{yk} / 1{,}15$	the design yield strength of steel
f_{yk}	the characteristic yield strength of steel
h	the height of the cross-section
i_s	the radius of gyration of steel about the center of gravity of the reinforcement
$M_{Rd,max}$	the maximal moment resistance of the cross-section (under compressive force)
N_{bal}	the value of the normal force at maximum moment resistance
N_{Ed}	(design) value of the axial load
N_{Rd}	(design) value of the axial load bearing capacity of the compressed column
N_u	the ultimate load of the cross-section under concentric compression
N'_u	the plastic ultimate load of the cross-section (Eq. 11)
l	the length of the column
l_0	the effective length of the column
α	parameter depending on the slenderness of the column (Eq. 15)
β	parameter depending on the reinforcement ratio (Eq. 16)
ε_c	compressive strain of concrete
ε_{cu}	maximal compressive strain of concrete
μ	parameter depending on the reinforcement ratio (Eq. 17)
Φ	capacity reduction factor
Φ_2	capacity reduction factor for the reference cross-section
φ_{ef}	effective creep coefficient

12. ACKNOWLEDGEMENT

The authors are grateful for the helpful remarks and advises of Prof. György Visnovitz.

13. REFERENCES

Aschheim, M., Hernández-Montes, E., Gil-Martín, L.M., (2007), „Optimal domains for design of rectangular sections for axial load and moment according to Eurocode 2", *Engineering Structures*, 29 pp. 1752-1760.

Bonet, J.L., Miguel, P.F., Fernandez, M.A., Romero, M.L., (2004), „Biaxial bending moment magnifier method", *Engineering Structures*, 26 pp. 2007-2019.

Bonet, J.L., Romero, M.L., Fernandez, M.A., Miguel, P.F., (2007), „Design method for slender columns subjected to biaxial bending based on second-order eccentricity", *Magazine of Concrete Research*, 59 pp. 3-19.

Eurocode 2 (2004), „Design of concrete structures – Part 1-1: General rules and rules for buildings", EN 1992-1-1

Eurocode 3 (2004), „Design of steel structures – Part 1-1: General rules and rules for buildings", EN 1993-1-1

Eurocode 5 (2004), „Design of timber structures – Part 1-1: General – Common rules and rules for buildings", EN 1995-1-1

Eurocode 6 (2006), „Design of masonry structures – Part 3: Simplified calculation methods for unreinforced masonry structures", EN 1996-3

Kollár, L.P., (2004), „Simplified analysis of reinforced concrete columns according to Eurocode 2", *Concrete Structures Journal of the Hungarian Group of fib*, 5 pp. 11-16

Mirza, S.A., Lacroix, E.A., (2002), „Comparative study of strength-computation methods for rectangular reinforced concrete columns", *ACI Structural Journal*, 99 pp. 399-410

CONSTRUCTION OF METRO LINE 4 IN BUDAPEST
GENERAL DESIGN OF KELENFÖLD METRO STATION

Gábor Pál

Design and construction of Kelenföld metro station was a real challenge for all participants: for designers and contractors alike. Working on an operational railway station demanded stern procedural and technological discipline. Application of the Milanese method made it possible to disturb the surface facilities only temporarily, and to organise the finishing works outside of the railway territories in operation. Application of these technologies in Hungary was quite unknown before this project, it provided the participants valuable experiences.

Keywords: metro, civil engineering, railway bridge, underpass, D-wall, tunnel

1. LOCATION

Kelenföld Station of Budapest Metro Line 4 is constructed under 28 tracks of Kelenföld railway station. Besides serving as an underground – railway junction, the station is connecting Kelenföld and Őrmező urban districts as a pedestrian underpass as well; forming a hub with the existing and under construction transport lines. Design and construction of the structure was heavily influenced by the operational railway station, safe operating of which had to be maintained throughout the works.

Fig. 2: General cross-section beneath the railway bridge

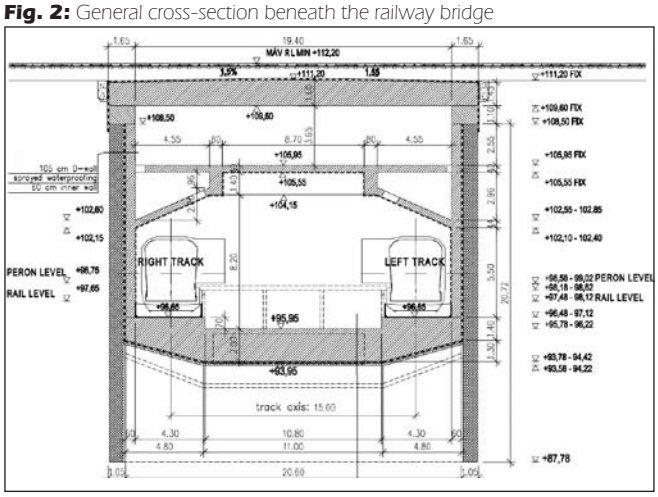

2. ANTECEDENTS

Permission design as well as the tender drawings were prepared by Főmterv Zrt. based on the architectural guidelines by Palatium Stúdió. The FIDIC yellow book tender called on the basis of these drawings was awarded to Hídépítő Ltd. in 2007. General constructional design was made by Speciálterv Ltd. on the awarded company's commission. The assignment contained

Fig. 1: Longitudinal section of the station

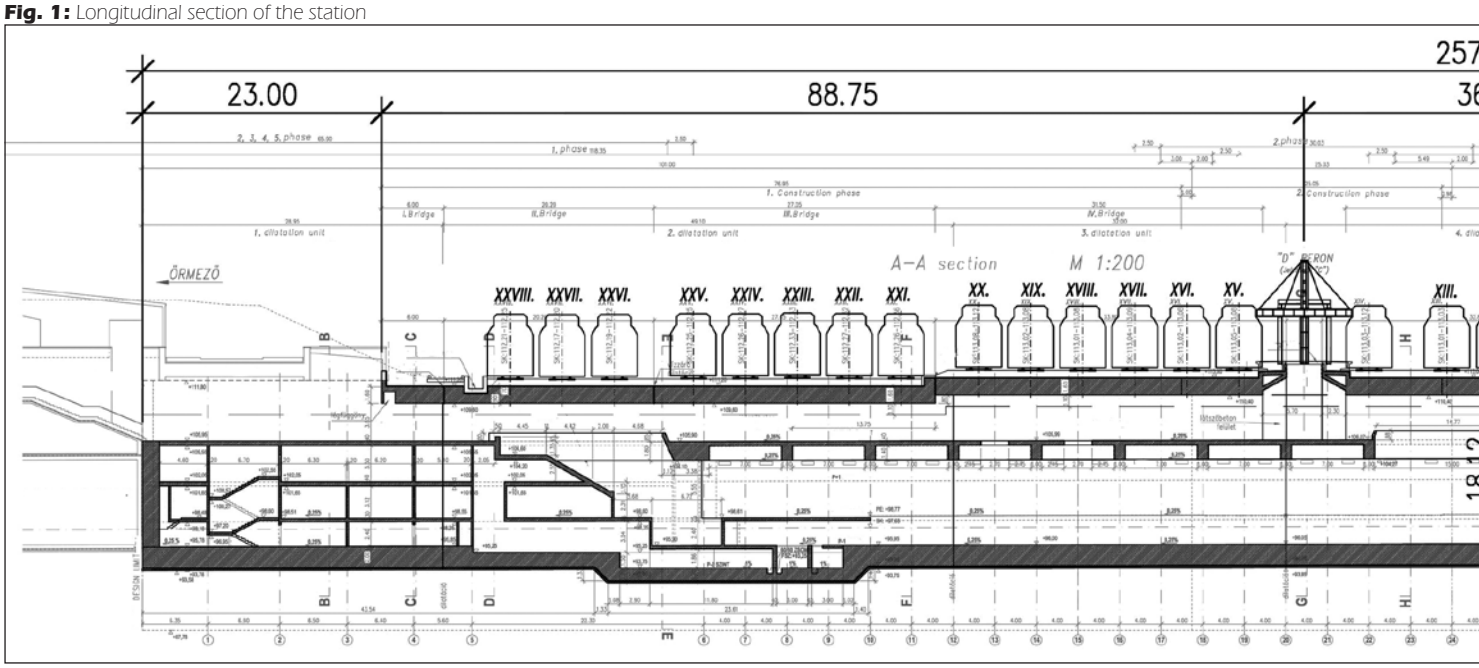

the structural design of the load-bearing structures of the station as well as the design to transform the railway station in order to adopt it for the works. Based on the permission design and the tender drawings the structure beneath the railway was constructed by the Milanese method, which means, that after completion of the top slabs the surface – the railway tracks in this case - can be reset, while excavation and further construction of the shaft is carried on beneath the top slabs.

3. GENERAL EXPOSITION, CONSTRUCTION

On the Etele tér side the structure under the railway station is connected to the previously constructed TBM launching shaft. The pedestrian underpass and station shaft is 260 m long; making it 340 m together with the adjoining train reversing structure on the Őrmező side. A 90 m long SCL (Shotcrete Lining) tunnel is connencted to the D-walled train reversing structure, so the entire length of the designed civil engineering section is 430 m; which means, that Kelenföld Station is the longest station in Underground Line 4. (*Fig. 1)*.

1.00 m thick and 22-23 m deep parallel D-walls were lowered at the section of the shaft located beneath the rails, distance between their axis is 21.60 m. The top slab, which is a ballasted railway bridge by function, is connected to the capping beam of the D-walls by flexible joints (*Fig*. 2*)*.

Waterproofing, dewatering system, ballast and railway tracks were constructed on the upper surface of the top slab. Beneath the top slab excavation was carried out between the D-walls while the railway tracks were reinstalled on the surface.

Excavation between the D-walls was done in one go down to the lower level of the base slab, which is approximately 18 m below surface. During this temporary construction stage, in order to avoid the D-walls to be exposed to water pressure the occasional waters found in the cohesive, watertight soil were „let in" by temporarily piercing the panels. The base slab joins the D-wall by moment bearing connection. The force transmitting connection was carried out by applying „Lenton" couplers (*Fig. 3)*. „Lenton" couplers are bolted reinforcement bars used for splicing. The ordinary reinforcement steel bars are lathe-turned to a coned shape, onto which the splicer shuck is bolted. The shucks – prepared in advance in the reinforcement

Fig. 3: Coupler connection joint of D-wall and base-slab

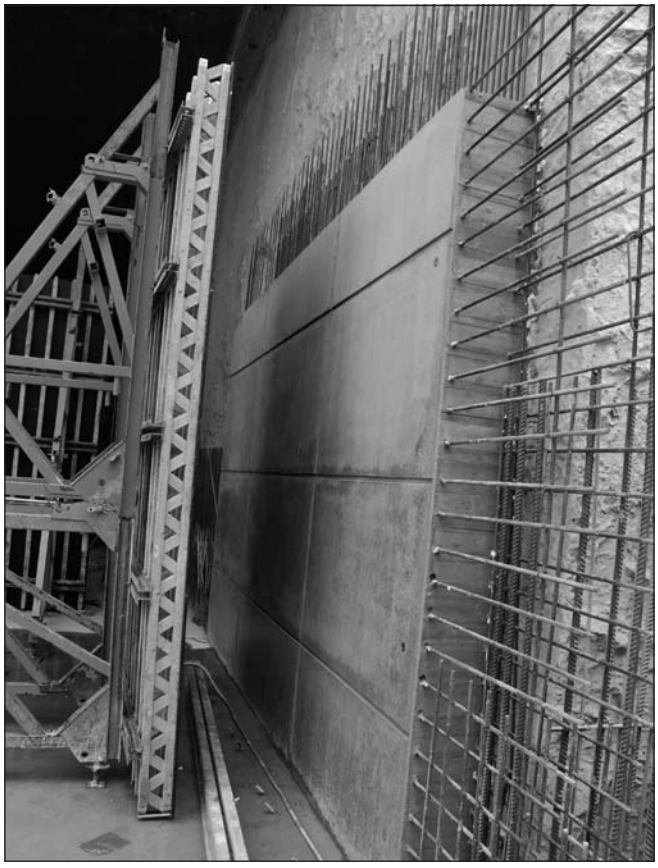

Fig. 4: Construction of visible concrete surface structure

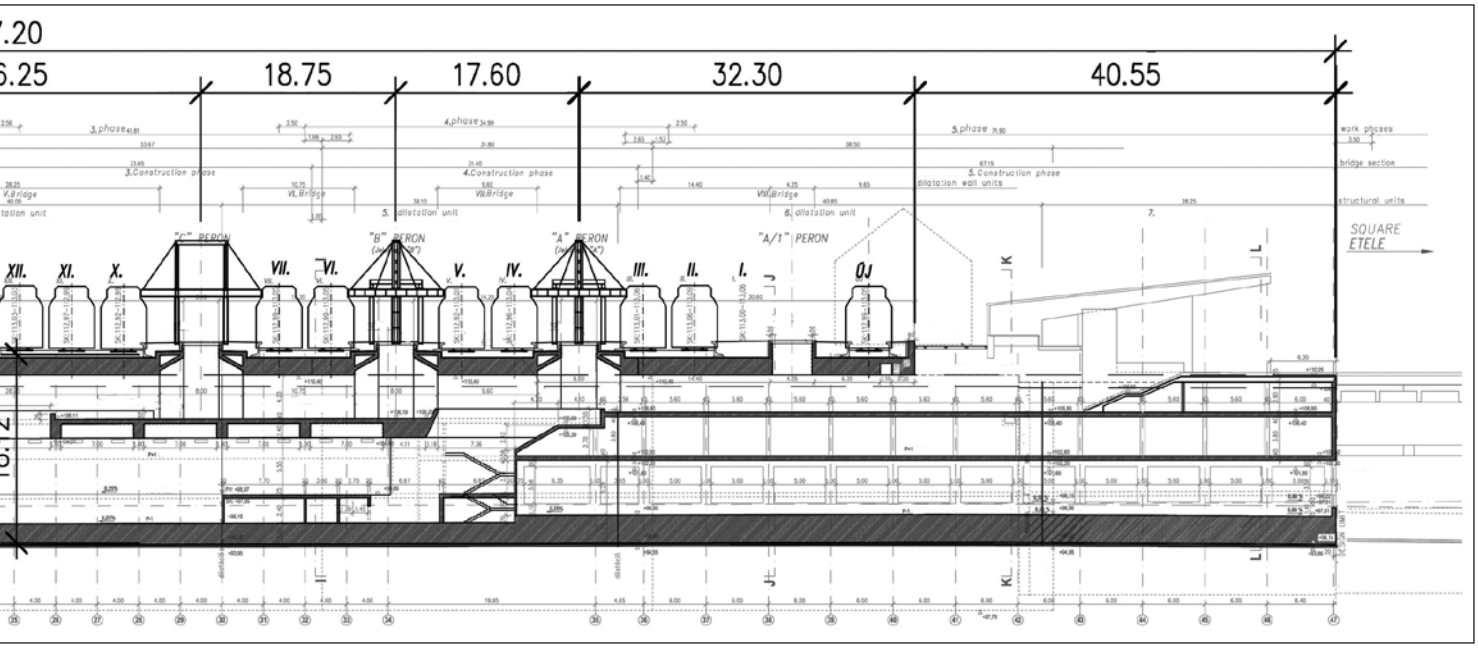

of the diaphragm wall and protected by temporary plastic caps – are to be found on the diaphragm wall surface already stripped, and the force conducting steel reinforcement will be joined into these.

Installation of the reinforcement and shutters of inner walls took place following casting the base slab. A significant proportion of these walls are visible concrete surfaces, for the fine implementation of which the application of specially surfaced formworks, special concreting technology and stern procedural discipline are necessary (*Fig*. 4*)*.

The top slab at most parts of the shaft under the station's platforms is supported by a frame structure (*Fig*. 5*)*.

Connection between the upper pedestrian underpass level and the platforms between the undergruond rails is provided by elevators, stairways and escalators. Concurrently to the underground shaft construction, the surface platform roofs were also transformed. Owing to minimalization of the construction program durations, the new roofs segments harmonizing with the forms of the existing platform roofs are applied.

The shaft construction works crossed the entire service system of the station on the sides of the tracks; therefore, appropriate substitution and diversion in different construction phases had to be designed for the entire overhead cable network, signals and security system elements. Conditions of safe operation had to be maintained for each phase of the works, design for each phase had to be prepared.

Construction works crossing the station were carried out in five main construction phases. D-walling and reinforced concrete structure construction works had to be organized on the „islands" bordered by operating railway tracks. Construction works amid tracks raised severe technological problems. High voltage cables running alongside the site area made the craneage, D-walling and servicing activities

Fig. 5: *Frame section of the inner slab after removal of shutter*

Fig. 6: *Completed primary lining of SCL tunnel*

even more difficult. Concrete is supplied through the existing pedestrian underpass, restricting the passenger area, applying concreting tubes. Materials were transported on railway in and out of site using the tracks being reinstated.

The train reversing structure joining in to the shaft on the Őrmező side consists of two structural units: an 80 m long reinforced concrete structure built between diaphragm walls and a 90 m long SCL tunnel. The reinforced concrete structure, similarly to the section under the railway, is constructed by Milanese method, however, in this case, not the roof slab but an intermediate slab directly above the clearance envelope of the underground provides the supporting functions. The SCL tunnel, which temporarily functions as a terminal, receives underground vehicles of the station in a unified cross-section. For further perspectives, the metro line can be extended through this tunnel in the direction of Budaörs (*Fig*. 6*)*.

4. STRUCTURAL ELEMENTS, METHODS OF ANALYSIS

4.1 Diaphragm walls (D-walls)

In the area affected by the underground construction middle Oligocene Kiscell clay can be found under the made ground layer. Calculations for the permanent structural state of the diaphragm walls were carried out considering surface loads, at-rest soil pressure and water pressure on the whole surface of the side walls, while for calculations of temporary state, groundwater was only taken into account in the upper weathered medium and fat clay and less weathered medium and fat clay layers. Considering the deeper intact medium and fat clay as watertight, water pressure during construction was not taken into account in this layer; which made it possible to excavate from below the top slab down to the lower level of the base slab (close to 16 m) in one go.

To make sure that this condition be valid, water-conducting steel tubes were installed in the watertight layer behind the 100 cm thick diaphragm wall, so as to eliminate any incidental water pressure. Two tubes were installed for each reinforcement D-wall segments.

Excavation was carried out under regular control measurement surveys and inclinometer readings.

In permanent stage D-walls are carrying the loads imposed on them jointly with the inner walls and supported by the base slab and internal reinforced concrete structures. The D-walls and inner walls are not connected structurally, which means that they are carrying loads proportionally to their stiffness. Nominal thickness of the watertight D-walls is 60 cm at the adjoining platform stairs, and 100 cm at the pedestrian underpass section.

4.2 Top slab functioning as railway bridge

The roof slab of the underground station is a monolithic reinforced concrete slab which also functions as a railway bridge. Considering its structural system, it bears the weight of the slab and of the railway as a single span bridge with two supports. The thickness of the monolithic reinforced concrete slabs concreted on the ground varies between 1.45 and 1.60 m; the upper surfaces incline towards their supports by 1.5%.

Permission design was prepared initially showing bridges' slabs with welded steel main girders embedded into reinforced

Fig. 7: Installation of the reinforcement of a cast in situ reinforced concrete slab-bridge, formwork for visible surface concrete

Fig. 8: Construction of the „U" shaped eigth slab-bridge supporting three railway tracks

concrete. As first phase of the constructional design, economical comparison analysis were carried out assessing the application of a traditional as well as an improved embedded steel girder structure scheme against the monolithic reinforced concrete slab concept with the thickness proposed in the original design. Economical advantages were considered on the basis of structural calculations prepared for each model.

As an improved embedded steel girder concept we proposed the application of steel beams halved longitudinally along the axis of the web. The method commonly used in Germany improves in great deal the load distributional parameters of the joint between steel and concrete by cutting longitudinally the web of the girders in a specific way.

Compared to the traditional embedded steel girder beam solution, considerable thrift in structural steel appropriation can be achieved with the structure constructed along these lines. On the other hand though in temporary (under construction) stage the structure is less rigid, which implies more dense support propping. We were be able to exploit the benefits of this improved structural scheme by considering the construction of the slabs on ground-supported shuttering system.

At the end these slabs were constructed as simple cast-in-situ reinforced concrete slab-bridges due to enormous method-related complications which arose when lifting the steel girders in place amongst several high voltage cables was considered. Reinforcement of the compact slabs casted on ground-supported shuttering system consists of 40 mm diameter reinforcement bars installed in two layers (*Fig*. 7).

Top slab of the pedestrian subway is articulated with work joints and expansion joints bridged watertightly, in accordance with the constructional phases. The expansion joints created eight structurally independent reinforced concrete slabs, the equivalents of eight separate railway upper-decks lying side by side. The slab bridges lead across two to five tracks each, which makes it 28 in total.

On the platform edge of the slab bridges, cantilevers are made with visible concrete surface. The inner voids of these provide ventilation. According to the architects intention, glass slabs between the slab bridges are to provide natural daylight in the subway.

Slab bridge No. 8 is U-shaped layout. The gap in its middle provides connection between the subway and the new „A1" platform (*Fig*. 8*)*.

4.3 Internally reinforced concrte structures

Between the diaphragm walls and under the roof slab, inner reinforced concrete structures are made. These are: the base slab, the platform level and a slab labelled „P_1" at pedestrian underpass level and mechanical engineering areas.

Thickness of the base slab varies between 1.40 and 2.70 m in cross direction, it's connected to D-walls by moment bearing joints. Applying „Lenton" shucked steel splicers for these joints made it possible to distribute the moment between base-slab and D-wall.

The structure as a whole as well as the base slab on its own, are both calculated for uplift in its permanent state. Considering the fact, that the structure is embedded into a hard, watertight layer of soil, uplift-related forces are foreseen to come in effect years and decades after the construction is completed.

The subway level above the passenger traffic section of the platform level is a beam supported reinforced concrete slab (*Fig*. 9). Its thickness is 40 cm, supported by a 1.80 m high beams at every 7.0 m, which are joined into a 1.80 × 0.80 m longitudinal girder. The inner walls, the angled and

Fig. 9: Downward cross-supported reinforced concrete roof slab

the horizontal slabs are forming a frame. At the calculation several aspects had to be taken into account. Forces acting in the structure are massively affected by the horizontal supporting rigidity of the frame, which contains uncertainties for some degree due to the fact, that it's the soil which is supported by the frame on the outside. Calculation for one of the extreme limit states of the structure was made neglecting the soil, while calculation for the other one was done supposing infinitely rigid horizontal support. Reality lays somewhere in between. Signs of moment are opposite for the two extreme limit cases for a considerable section of the slab. Finally, we took into account the elastic support of the soil, and created the graphs of overall moments for the calculation by iterating between the two extreme limit cases. Above the mechanical engineering areas

of the structure, top slabs are 40 cm thick cast in situ reinforced concrete plates supported by reinforced concrete pillars.

4.4 Temporary access ramp

The removal and transportation of the approximately 120 000 m^3 spoil from an 18 m depth below surface was made possible by a temporary access ramp built in the south-western corner of the shaft, which joined in to the service road of the railway station. This ramp was constructed with pile wall supporting at the deeper parts in the side of the Őrmező hill, and with stabilized ground slope at shallower parts. There are gaps in the pile walls. The diameter of the applied CFA piles is 80 cm; their length is adapted to the depth of the cutting. The applied reinforcement is correlating with the actual strain. At sections where it was allowed by the depth of the cutting and size of the clearance envelope, the pile walls facing each other were countersupported with steel props. The props were made of HEB 300 steel segments. The laminated beams recline on the reinforced concrete support beams distributing the loads of the beams. (*Fig. 10*).

Fig. 10: Construction of temporary access ramp sheltered by anchored piled walls

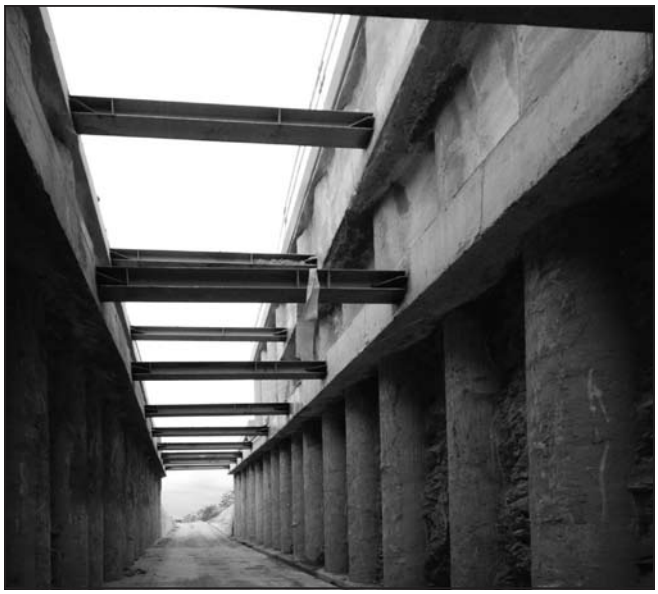

Fig. 11: Cross-section of the reversing structure

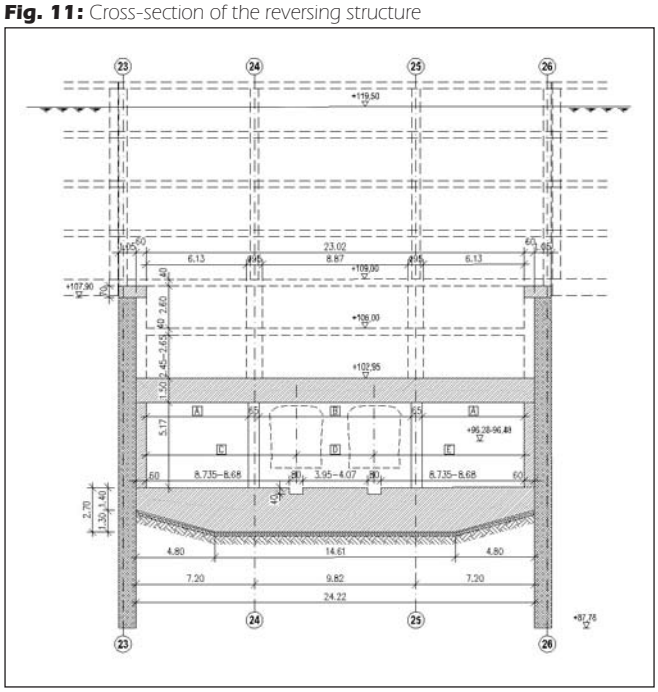

4.5 Train reversing structure

The train reversing structure on Őrmező side is constituted by two structural units: an 80 m long reinforced concrete structure constructed between D-walls, and a 90 metres long SCL tunnel. The cut renforced concrete shaft was built by Milanese method similarly to the section beneath the railway tracks. The difference between them is that the reversing structure's supporting slab is not the top slab located at surface level, but a 140 cm thick intermediate level slab right above the permanent underground rolling stock clearance envelope. Capping beam was built on top of the D-walls, inner walls were constructed next to the inner surface of the D-walls, the base slab is connected to the D-walls by moment conducting „Lenton" joints.

The intermediate level supporting slab was constructed as a two-legged structure for the first phase, but it was supported by pillars erected from the base slab below for permanent stage (*Fig. 11*).

The SCL tunnel joining the cut and cover reinforced concrete shaft bears a cross-section suitable for two underground vehicles. Bottom line of the SCL technology is that a primary lining is formed for the consecutive excavation phases by placing lattice girders configured by steel reinforcing bars and reinforcement meshes and then covering them with shotcrete. The primary lining acts as a load bearing tunnel walling in temporary stage. The completed primary lining is sealed off by watertight membrane. It's followed by the construction of a loadbearing reinforced concrete secondary lining, which supports the loads in permanent stage.

The entire surface of excavation for the reversing structure's SCL tunnel is 100 m^2. Excavation is carried out with one-side gallery and enlargement. The thickness of the closed circular lining is 0.30 m as well as the thickness of the temporary sidewall (*Fig.* 12). Distance between the tracks in the completed tunnel is 4.75 m.

Fig. 12: Construction of SCL tunnel, second phase excavation is ongoing, while the plum kernel shape internal shotcrete lining of the first phase was not yet torn down.

Concurrently with the tunnel construction, continuous monitoring system was operated. Dislocation of the tunnel linings and of the surface was controlled by survey methods, movements of the adjoining D-walls and of the soil was controlled by inclinometers and extensometers; parameters of the ground- and layer-waters were followed with piezometers.

5. CONCLUSIONS

Complexity and dimensions of the construction of the underground station structure beneath Kelenföld railway station made it a real challenge for all participants. As for the structural designer, the most impressive novelty was the process of design updated to and corrected by the regular measurements on site, which is a fairly common practice in the mining industry, but rarely applied for civil engineering design tasks.

Structural assumptions (such as neglecting the water pressure in hard soil), which made the construction economical, were tested against measurements on site. On the basis of these measurements, design assumptions could be verified and, if necessary, the designs could be amended adding or removing specific temporary supporting structures. This feed-back driven practice helps to design enormous structures with extreme complexity and unforeseeable difficulties in an economical way; and it's adopted throughout the industry.

6. REFERENCES

Pál, G. (2009): „Design of metro station beneath Kelenföld railway station", (In Hungarian) *Sínek Világa* - VII. Vasúti Hidász Találkozó Különszám, pp. 74-79.

Schulek, J. (2008): „Construction of Metro Line 4, the forth metro line of Budapest", (In Hungarian) *Vasbetonépítés* 4. pp. 102-108.

SpeciálTerv Kft. (2007-2010): „*Budapest metro line 4 Section I (Between Kelenföld railway station – Keleti railway station). "Tunnel line and connected structures"* project Nr. 03. Designs for contract for construction of "Kelenföld railway – and metro station" (In Hungarian)

CONSTRUCTION OF BUDAPEST METRO LINE 4
Detail design of the „KELENFÖLD" metro station
Gábor Pál

The metro station called "Kelenföld railroad station" is the head point of the 4th metro line of Budapest, it's located beneath the 28 tracks of Kelenföld railway station. After its finalization, as a south-west gate of Budapest it creates an intermodal connection between the metro line and the railway system. The structure under construction is the first in Hungary built underneath a railroad station with a separate level junction. The design and construction of this metro station imposed a serious challenge on the designers and contractors. To work on a railroad station in operation requires very strict technological concentration. Applying the top-down excavation method ensured a restricted disturbance of the surface, finishing works can be carried out with an installation not affecting the railway areas.

Gábor Pál (1970) MSC civil engineer (Budapest Technical University, 1994) 1994-1999 designer (FŐMTERV Co.) 1999 onwards executive of SpeciálTerv Ltd. His scope is to manage the 30 employees organisation of designers, and to control and expertly lead the civil engineering design works of the company. General designer of the underground station Kelenföld, which is part of the DBR 4 metro project. Member of Hungarian Group of ***fib***.

CONCRETE TECHNOLOGY OF EXTRADOSED TISZA BRIDGE OF M43 MOTORWAY IN HUNGARY

Zsuzsanna Török

River Tisza crossed by the M43 Motorway is one of the greatest rivers of Hungary. The prevailing ground conditions characteristic of the riverbank justified the building of a bridge with a relatively lightweight superstructure – and this is the finally realized Móra Ferenc Bridge that connects the two banks of the river. This special bridge structure neccesitates the application of such a concrete mix that ensures a perfect connection between the lower and upper monolithic reinforced concrete slabs on the one part, and corrugated steel web plates on the other.

Keywords: concrete technology, bridge construction, special bridge construction technology

1. INTRODUCTION

The M43 motorway forks off from M5 motorway at northwest from the city of Szeged; the motorway crosses No.5 main road, from where it starts heading east. After a few kilometres it reaches No.47 main road; it runs through the crude-oil fields of Algyő, and crosses River Tisza through the new bridge. The motorway passes by the settlements Maroslele and Makó at north, heading towards Romania. The construction works of the entire motorway section are carried out in four phases.

From the bridge-construction points of view, the greatest challenge is represented by Phase 2. The construction works of this phase are carried out by Tisza M43 Consortium, in which the technical leadership is performed by Hídépítő Zrt. Among the bridge-construction structures the greatest attention is paid to the Tisza Bridge *(Fig. 1)* that crosses the river at 182.970 river-kilometres.

2. DESCRIPTION OF THE BRIDGE

The bridge is made from three bridge-parts, which are separated from one another by expansion-joint structures. These three parts are: flood-basin bridge at the right bank, bridge over the riverbed, and flood-basin bridge at the left bank. The riverbed-bridge is made of a single structure, while each of the flood-basin bridges are made of two separate structures for the left and the right motorway tracks. The length of the flood-basin bridge at the right bank (with four spans) is 232.00 m; the length of the riverbed bridge (with three spans) is 370.00 m, while the span of the flood-basin bridge at the left bank (with one span) is 52.00 m. The total width of the bridge is 29.94 m. The speciality of the bridge –both from the engineering and the concreting technology points of view - lies in the design of the riverbed-bridge superstructure. The cross-section is a three-cell box girder with steel transverse girder at every 5 meter. The deck and the bottom slabs are prestressed concrete slabs, interconnected by webs made of corrugated steel plate. In order to ensure an increased moment bearing capacity for the girder bridge, stay cables are led outside the structure, which are anchored at the steel transverse girders under the deck. On the top of pylons saddle structure is crossed over. The pylons have a reinforced concrete structure and the steel saddle structures are installed in the solid pylon head. Internal cables are installed in the reinforced concrete deck slab, while external cables are located outside the reinforced concrete bottom slab, parallel with that. In selecting the appropriate bridge structure, the most important aspect was to take local circumstances into consideration. As the foundation conditions were very unfavourable due to the specific properties of River Tisza (an arched bed section prone to deformation, large and intensive water-level fluctuations, and weak and sandy ground conditions), the bridge structure to be built had to have a relatively small dead load, but at the same time it had to have a large span, which can bridge the river without a pier in the riverbed. One of the favourable properties of extradosed structures is the relatively lower structural height in contrast with traditional girder bridges, which entails a lower dead weight, and this can be even further decreased by the use of corrugated steel plate webs. As regards, the Tisza Bridge in question, this way was possible to ensure that its superstructure crosses the river with a 180 m long middle span, without piers in the riverbed. This solution ensures undisturbed navigation, while the piers do not influence the evolvement of the riverbed, and a safe support for the structure could be ensured in spite of difficult foundation circumstances.

The concrete volumes built in:

- piles: ~ 10 000 m^3
- pile-caps: ~ 5 500 m^3
- support structures and curls: ~ 6 500 m^3
- superstructure, pylons and bearing tables: ~ 10 000 m^3
- auxiliary structures: ~ 2 000 m^3

Total volume: ~ 34 000 m^3.

3. DEFINITION OF REQUIREMENTS

As any other bridge building project, this one also started with a coordination process with the Client in order to avoid unnecessary labour and lavish spending. In this phase a clarification was needed as regards the (often contradictory) chapters and norms and standards references of the Tender

Fig.1: *Tisza Bridge of M43 motorway*

Technical Specifications in connection with the concrete types to be used, and the design of concrete and concrete qualification issues.

In Hungary, the concrete design requirements for the construction of motorway bridges are jointly defined by Tender Technical Specifications and the standards and norms referred to therein. The most important parameters were the following:

- concretes, markings and ratings: e.g.: C45/55-16/K-f50-vz5

  Explanation of markings:

  Compressive strength of the concrete: C45/55. Requirement: the rating value should be R_{bk}=60 N/mm^2, in the case of a series of trial slumps (1 series is made from 5 trial slumps of 150 mm x 150 mm), stored under variable conditions (at 20°C in water for 7 days, then at 20°C in laboratory air until the age of 28 days) (ÚT 2-3. 414:2004). This means that the rating value (R_{bk}) of the various trial-slump series must be 60 N/mm^2 as a minimum. The rating value is the characteristic value of compressive strength, calculated in accordance with Hungarian Standard MSZ 4720/2: $R_{bk}=R_m-k\cdot t\cdot s$, where k is the inclination factor, t is the Student factor, and s is the calculated dispersion.

  D_{max}: 16 mm.

  Consistency: plastic, measured with a 43-50 cm spread.

  Frost resistance: f50. Relevant standards: MSZ 4715/3-1972, MSZ 4719-1982.

  Requirement: the ratio by which the compressive strength of the trial slumps under test decreases after freezing should not be more than 25% in comparison with the standard cubes. The loss of mass of the investigated trial slumps shall be max. 5%.

  Water-tightness: vz5. Relevant standards: MSZ 4715/3-1972 and MSZ 4719-1982.

  Requirement: the highest permissible water-penetration value is 40 mm if the following water pressures are applied: 1 bar for 48 hours, then 2 bars for 24 hours, then 5 bars for another 24 hours.
- applicable cement types: for piles, pilecabs beams, and the upgoing walls of piers No. 5, 6, 7, 8: CEM II/B-S 32.5 R slag cement; for the rest of structures: CEM I 42.5 N pure Portland cement.
- cement dosage: piles: min 400 kg/m^3 and max. 450 kg/m^3, for the rest of the structures: min. 350 kg/m^3 and max. 450 kg/m^3
- water-cement ratio: maximum 0.4

The 0.4 water-cement ratio, which should have been applicable for all structures, is very low in this case. According to our former experience, it is almost impossible to use e.g. Soil-Mec pile types or for high-mass pile-caps. Concretes with very high superplasticiser admixtures (to ensure proper consistency) are difficult to preserve, it is impossible to vibrate the various layers together perfectly, the concrete is similar to honey: viscous and sticky. These circumstances together make it impossible to lower an armature in the concrete subsequently, or to produce a solid structure in case of large-surface concreting. In the end, thanks to long-winded coordination and professional reasoning, the values of the water-cement ratio were the following: piles, pile-caps: 0.45; upgoing structures: 0.42, and the superstructure of the bridge over the riverbed: 0.4.

After having agreed upon all the debated questions, we compiled the concrete formulas required for the implementation of the project, taking into consideration the engineering, the process, the transport and the concrete- workability needs as well.

4. TRIAL MIXINGS

The trial mixing procedures started on 9th September 2008, with making the trial mix of pile concrete (Soil-Mec formula C20/25-24/F, R_{bk}=27 N/mm^2, consistency: fluid) in the primary mixing facility. This was followed, on 17th September 2008, by the formula of pile-caps (under the name Alaptest (f*oundation body*) - C20/25-24/K, R_{bk}=27 N/mm^2) and the concrete formula of high-mass piers (under the name CEM II. Pillér (*pier*) – C35/45-16/K-f50-vz5, R_{bk}=49 N/mm^2). After that, on 7th October 2009, concrete was tested for up-going walls of the rest of structures (*up-going structure* – C35/45-16/K-f50-vz5, R_{bk}=49 N/mm^2). *Table 1* shows the properties, base materials and their place of origin for the various concrete formulas

Each of our mixes were successful for the first time, thanks to the consciousness of design, the clarification of requirements, the preparedness of the concrete casting plants, and as a result of former professional experience. The charts in *Fig. 2* show the average compressive-strength values of trial slumps made in the trial mixing procedure (the tests were made on series of 3 pieces each for the pilot tests, and on series of 10 pieces each in the frame of the 28-day concrete rating tests).

Table 1: Concrete formulas, their properties, base materials and places of origin thereof

Components and properties	*Soil-Mec C20/25*	*Foundation body C20/25*	*CEM II. Pier C35/45*	*Up-going structure C35/45*
Cement - DDC Ltd. CEM II/B-S 32.5 R CEM I 42.5 N	400 kg/m^3	350 kg/m^3	390 kg/m^3	390 kg/m^3
Aggregates – DK Ltd. D max	24 mm	24 mm	16 mm	16 mm
v/c	0.45	0.45	0.42	0.42
Superplasticiser – Sika Ltd. Decelerator – Sika Ltd.	VC 1050 VZ2	VC 1050 VZ2	VC 1050 VZ2	VC 1050 VZ2

4.1 Special structures

As for this Tisza Bridge, the concrete formulas of the pile-caps and the superstructure had to have specific properties. The size of the largest foundation bodies was ~ 1 600 m^3, the upper part had a 12° and a 16° angle of elevation, with a truncated pyramid shape *(Fig. 3)*.

The surface to be concreted was ~ 500 m^2, which required a very intensive work. In our opinion the proper working-rate was ensured between 120 - 130 m^3/h concreting capacity which could be met by the joint servicing of three concrete factories.

After the casting of the pile-caps had been completed, the support-building work went on by the construction of the piers. The concreting works of the up-going structures took place according to the schedule. It was the very first time in Hungary that CEM II/B-S 32,5 R type of cement was used for a motorway construction project. We used this particular cement type (defined in the Tender Technical Specifications) for the larger-mass piers (~ 500 m^3) *(Fig. 4)*. (Until now CEM I type of cement could only be used for motorway-bridge structures built in Hungary.) As this is not a pure Portland-cement, there is a lower risk that cracks develop due to heat generated in the process. Of course, we paid special attention to after-treatment in order to avoid other cracks.

From the concrete method aspective, the most difficult and at the same time the most interesting task was compiling the formula for the superstructure of the riverbed-bridge, where we had to take into consideration the concrete working

Fig. 3: Concreting of the pile-cap of pier No.6 at Tisza Bridge (May 2009).

difficulties due to a complex design of the bottom slab, at the joint between the steel boom plate *(Fig. 5)* and the reinforced concrete slab.

4.2 Trial mixings preparations

4.2.1 Design and method requirements for the concrete

- low (0.4) water-cement ratio
- concrete strength: C45/55 (R_{bk}=60 N/mm^2)
- use of CEM I 42.5 N Portland cement
- high strength at an early stage – 35 N/mm^2 at the age of 36 hours – for prestressability in the case of the upper slab

Fig. 2: Average compressive strength values in trial mixings for the various concrete formulas

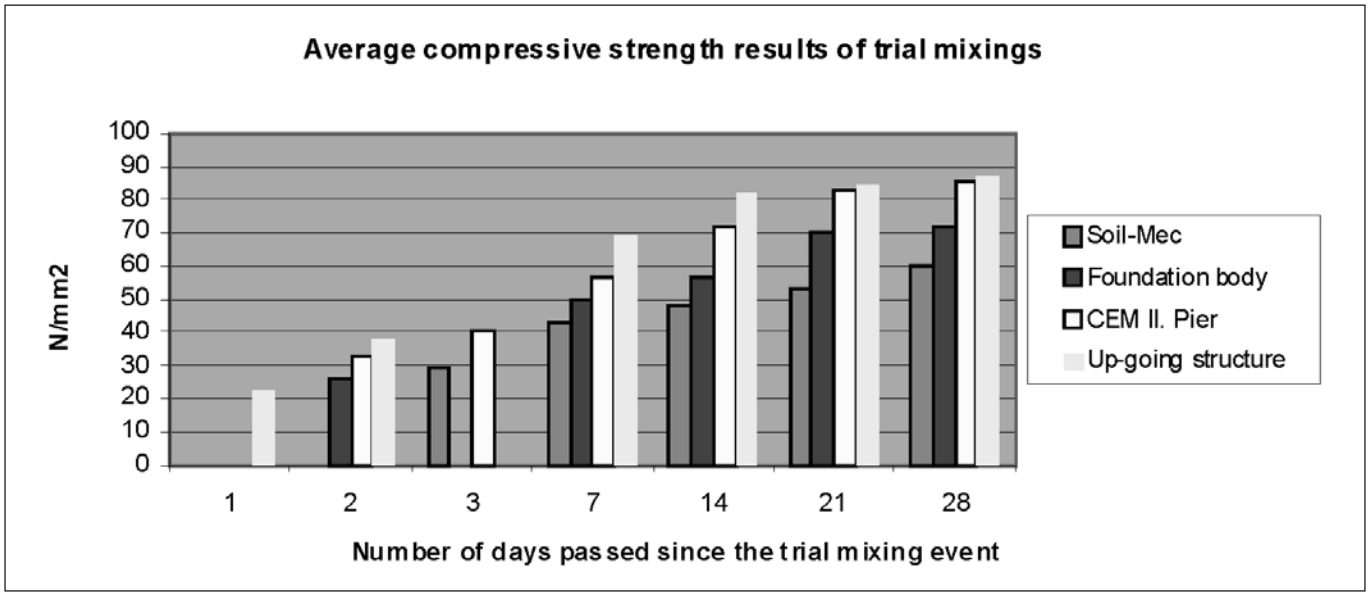

Fig. 4: Tisza Bridge, support No. 5, upgoing wall, Phase I. – concreting works (April 2009)

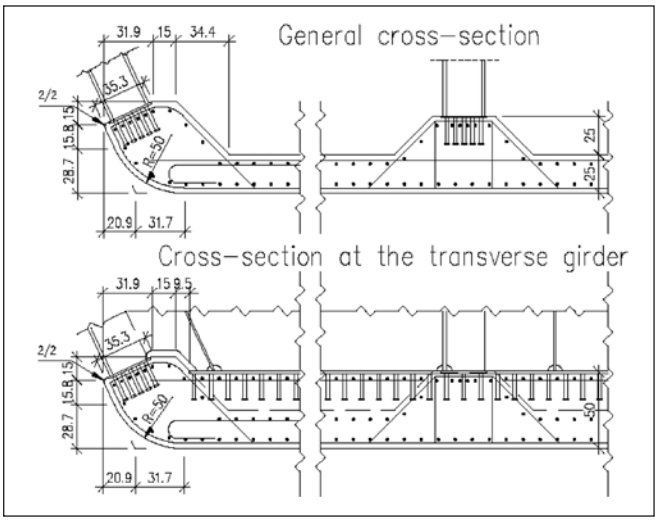

Fig. 5: Cross-sections

- good preservability, mobility, workability, good filling out of the formwork.
- special formwork-making and working-in circumstances (difficulties in introducing the concrete in, and in vibration)
- good-looking concrete surface

4.2.2. Construction of the trial formworks:

During the trial mixing procedure, we tested not only the "usual" concrete properties in this case, but also tried to create the actual working circumstances by modelling the formwork of the lower slab of the superstructure. The footprint dimensions of formworks: 3.0 m x 2.5 m. Volume: 3 m^3. At the upper part of the formworks, a plexi plate was used at the pin-connected part of the steel plate in order to ensure the visibility of fill-out and wooden cylinders were used as modelling of pins. The reinforcement was also installed within the formwork in order to ensure a real model for the introduction of concrete.

The formwork of the reinforced concrete structure of the bottom slab was made in two different ways:

Type 1 *(Fig. 6)*:

This type was made according to the original construction work plans, so that the concrete is connected with the steel structure with a slope of 1:1 gradient at both sides of the lower belt plate.

Type 2 *(Fig. 7)*:

The design according to the original construction works plans is kept at one side, while at the other side concreting is done vertically from the lower point of wedging.

4.3 Trial mixing, trial installation

During the trial mixing procedure, the same formula was made by various doses of flux. The reason for different dosage was

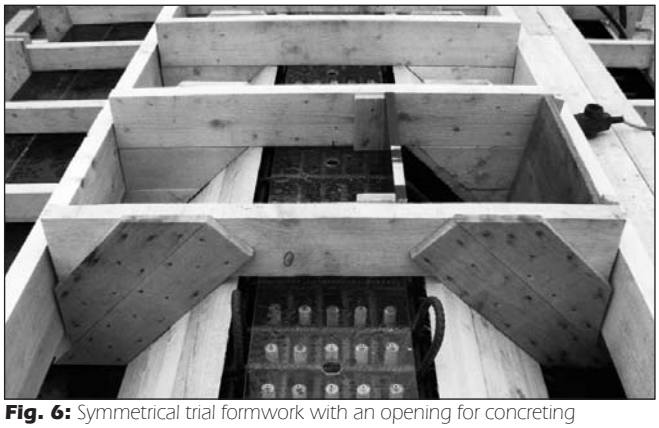

Fig. 6: Symmetrical trial formwork with an opening for concreting

Fig. 7: Asymmetrical trial formwork

that the formwork also had two different types. (As for the filling out of the formwork, which has a slope at both sides [where concrete is introduced through concreting openings], a higher-consistency mix is required, while the concrete has to move here in longitudinal direction too, in parallel with the ridge of the steel structure, in between the pins and the reinforcement cage.)

In the first mixing process *(Fig. 8)*, we made the lower-consistency mix first, that is, the concrete for formwork type 2. The spread of this mixture at installation was 56/54 cm. Experience has shown that the concrete of this consistency filled out the formwork uniformly and completely when the vibration took place along the "concreting lane". It was possible to vibrate the layers well together.

After the removal of the formwork, there were no unfilled parts in the structure. The concrete was well-compacted with this uniform texture. There were no cracks or pockets anywhere on it.

In the second mixing process *(Fig. 9)*, we produced the higher-consistency mix, which is the concrete for formwork type 1. The spread of this mixture at installation was 57/55 cm. The installation experience has shown, with this consistency, that the introduction of concrete through the concreting openings and the vibration of concrete have not yielded an appropriate structure.

Upon the effect of vibrating the concrete at only one place (at the concreting openings placed in defined distances), and upon the effect of high chemicals' doses, the concrete became foamy and did not fill out the complete cross-section of the formwork. A continued vibration could have helped the concrete to spread further, but (in addition to foaming), the concrete started to fall apart into fractures at the limited number of vibration points. Thus we stopped the vibration. In the completed structure there were unfilled places, but no cracks were visible on the concrete. Beneath the plate that was the model of the lower belt plate, fill-out was complete just only around the concreting

Fig. 8: Asymmetrical trial formwork with a concreting belt

Fig. 9: Symmetrical formwork with an opening for concreting

opening. In a distance of not more than 30 - 40 centimetres from the opening, a gap of variable size developed between the steel plate and the concrete. Vibration applied via the hole of the lower plate did not yield satisfactory results, as the fine-aggregate and the liquid part got separated.

4.4 Evaluation of the trial installation; concreting

On the basis of the model experiment, we have established the following:

- There is a high risk in connection with using the lower slab to steel structure connection according to the original plan (with sloping surfaces at both sides – wedged).

Fig. 10: Concreting of the lower slab (April 2010)

- At the working-in phase, the consistency of concrete must be kept between 50 and 55.
- In order to ensure proper concrete fill-out, it is beneficial to use a vertical formwork (instead of wedging) at one side.
- The vertical design at one side must be used both under the trapezoid-plate ribs and the lower belt of transverse beams (always at the higher side in the case of transverse beams).
- During the execution of works, special attention must be paid to control the consistency of concrete, and during the vibration process used in the working of the concrete in.
- Concreting should be done at one side, while the proper appearance of the counter-side concrete must be continually checked.
- The holes made on the lower belt should be used for controlling the adequacy of concreting. These holes are not suitable for vibration.

On the basis of the experience gained through the trial mixing, and in order to make a higher quality structure, the lower slab of the superstructure was redesigned in accordance with "formwork type 2" we had recommended. The lower-consistency concrete formula, tried out in the trial mixing process, carried out on 28th May 2009, was used for the building of the lower and upper slab of the superstructure of the bridge over the riverbed (*superstructure*- C45/55-16/K-f50-vz5 – 400 kg/m^3 CEM I 42.5 N, v/c=0.4, Sika VC1050, VZ2). *(Fig. 10).*

Due to the continuously controlled base materials and produce, the concrete could have continually met all of our requirements during the construction works. *Fig. 11* shows the

Fig. 11: Superstructure, compressive strength measurements

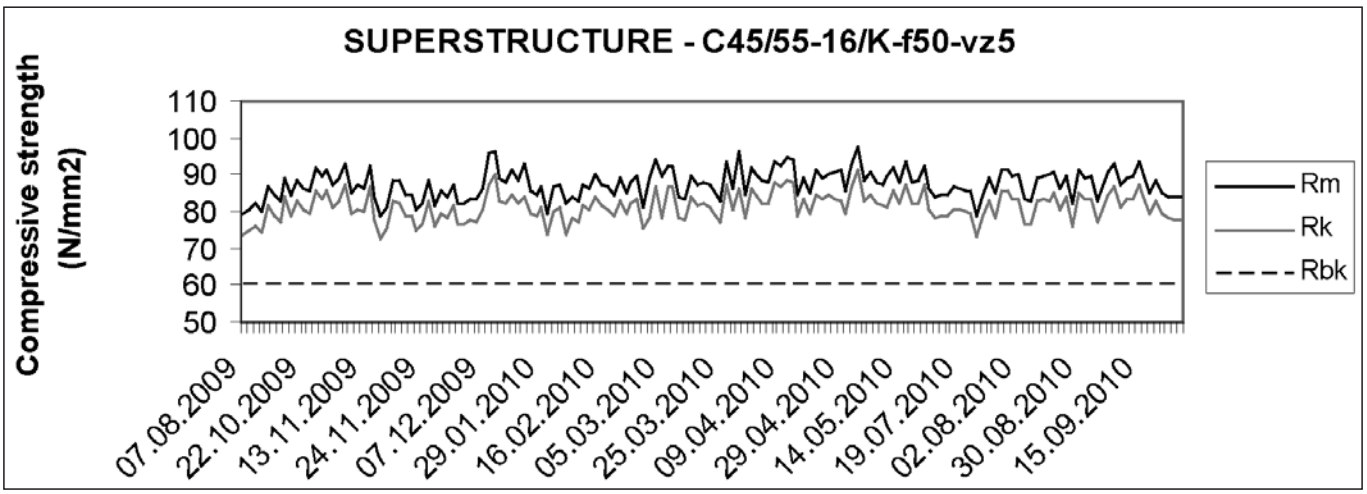

results of compressive strength tests carried out on the concrete test cubes of the reinforced concrete superstructures made by using the SUPERSTRUCTURE formula.

5. CLOSING THOUGHTS

The construction works of Móra Ferenc Bridge completed as part of the M43 Motorway started in August 2008. The extradosed superstructure type represented a challenge for us both from the engineering and the concrete-technology points of view. However, as a result of trial mixtures and model experiments on the basis of a conscious design work and a carefully compiled concrete mixture, the concrete has fulfilled the expected parameters, with special view to the structural design elements. In my opinion, in the construction of a bridge, it is definitely important on what basis, from what kinds of base materials and how it is built, but I reckon that it is (at least) equally important by whom that particular bridge is built. Now I can proudly say that we were those who built this bridge, who conceived the smallest details of the implementation of this absolutely new technology, furthermore who coordinated the subcontractors' activities in the working site, and finally who contributed by their jobs and professional knowledge to the construction of this special and attractive structure.

6. REFERENCES

ÚT 2-3.414:2004 „Design of concrete, reinforced concrete and stretched reinforced concrete bridges for public roads"

MSZ 4715-3:1972 „Testing of cured concrete. Hydrotechnical properties" Hungarian Standardisation Body

MSZ 4719:1982 „Concretes", Hungarian Standardisation Body

Mátyássy László. „Construction of the Tisza-Bridge spanning the river on the motor road M43", Concrete Structures, 2010. vol. 11. pp. 29-31.

Török Zsuzsanna: „Az új Tisza-híd fontosabb építőanyagai és szerkezetei elemei" („The most important building materials and structural elements of the new Tisza-Bridge"), Hídépítők lapja, XXXIX. évf. 1 szám, 2011/1, pp. 8-10.

Török Zsuzsanna: „Különleges hídépítési és betontechnológiák az M43 autópálya új Tisza-hídján" („Special bridge-construction and concrete technologies for the new Tisza-bridge of M43 Motorway"), Beton szakmai havilap, XVIII. évf. 6 szám, 2010/6, pp. 3-6.

Török, Zsuzsanna: graduated as an engineer specialized in construction works at the University of Pécs (JPTE), Pollack Mihály Department of Engineering, in 1998. She passed a Construction Technical Inspector examination in 2004, in the special field of Bridge Construction, while, in 2007, she graduated as specialized engineer in the field of Concrete Technology at the University BME, Construction Engineering Department. From 1998 on, she has been employed by Hídépítő Zrt. Her most important bridge-construction projects are the following: Duna-bridge at Baja, Tisza-bridge at Tiszaug, railroad bridge at Kunszentmárton, M7 Motorway: 50 motorway bridges and the Viaduct at Köröshegy. At present she is engaged with Phase 2 of M43 Motorway, working as a Senior Engineer of Quality Assurance.

CHILDREN'S DREAM POURED IN ORGANIC RC FORM – ELEMENTARY SCHOOL IN PÉCEL, HUNGARY


Zoltán Klopka - Péter Szász

It does not come so often that the structural engineer is involved in the design of such an interesting but yet in such a demanding building complex as the Szemere Pál elementary school in Pécel. Fortunately, from the first sketches in the process of planning and design the structural requirements were absolutely accepted and implemented by the team of architects who were not afraid to modify and change the conceptual design when the structural aspects showed that the initial design path proved to be a one-way street.

Keywords: organic architecture, cast in situ reinforced concrete, elementary school, cantilever

1. SAYING GOODBYE TO THE PAST - TE BEGINNINGS

The children attending the state elementary school in Pécel were educated in very unfavourable conditions for years. The school itself, though very close to the historic Ráday castle and Calvinist church, contained of an old multi-storey masonry house and of a lightweight barrack building. Fortunately, the government of the city with state aided financial support enabled a large-scaled renewal and enlargement of the school premises.

The design was entrusted to Dezső Ekler DLA, a well-known contemporary Hungarian architect who used well this exceptional opportunity and came out with an outstanding design of his own. Due to economical stipulation and the fact that the old masonry building was still safe and sound, he incorporated this building into the new layout consisting of a new wing, a spacious hall area, both containing classrooms, the wing with kitchen and dining area and finally the library and school management section *(Fig. 1)*.

In architect's concept the school building was not only there to house the classrooms and accommodate the pupils and lecturers; it reacts and counteracts with the children who spend a significant portion of their time inside, therefore it has to offer functional and visual excitement and make the time spent inside more playful and enjoyable.

Fig. 1: The lay-out of the school complex

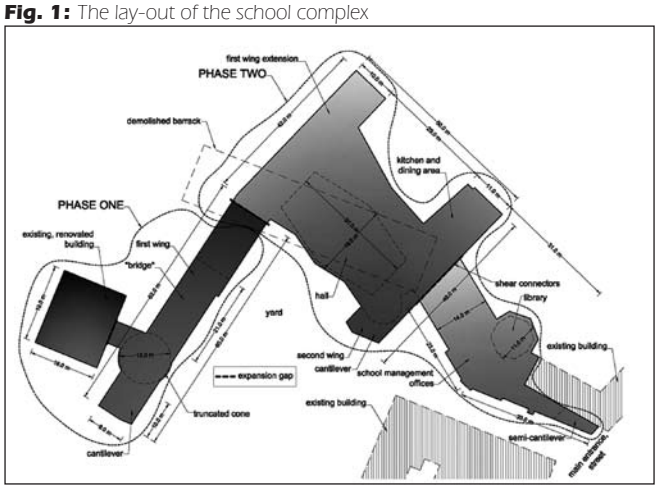

At first view the architect's unusual shapes, curved forms and non-parallel surfaces were hard to fit in the structural designer's point of view, but at the end of the day everything seemed to match in a perfectly sensible manner.

The material of the new buildings is reinforced concrete. This material was chosen not only because it is the most widely used structural material for this type of structures, but because only it could cost-effectively solidify the exciting and non-conventional forms of the new school.

2. THE LAUNCH – PHASE ONE

To maintain the minimum space requirements for education a two-phase construction was carried out, where an expansion gap provided the boundary between the two phases. In the first phase the existing masonry building was renovated and the first wing was erected *(Fig. 2)*.

In the second phase the barrack was demolished giving way to the execution of the larger portion of the new school.

Phase two consists of two units divided by an expansion gap.

After detailed soil investigation and foundation supervision, the masonry building was found to be suitable for minor internal structural modification and capable of housing another solid RC slab with a light steel roof over attic. The existing classrooms were renewed and in the new attic HVAC (heating, ventilation, air condition) equipment was installed. The existing building has been separated by means of an expansion joint from the new construction.

Despite appearances, the new wing of phase one has a very simple structural system which is a two-storey "bridge" cantilevering on one side. The middle support is a truncated-cone shaped staircase and foyer, and from this support are the music and art classrooms cantilevering on one side, on an average of 11 m *(Fig. 3)*. Although significant effort was made by the contractor to use the conventional formwork system,

Fig. 2: *The first phase of school complex to the left, as seen from the yard*

for some of the structural parts with significant curvatures the formwork had to be custom tailored.

The soil investigations found under topsoil fine to medium sand expanding underneath the whole school complex, so strip foundations and spread footings at appropriate depth were used. Ground water was neither expected, nor found. Where it was applicable, the RC floor was connected to the strip foundations. The deeper placed spread footings were interconnected by means of downstand beams.

The load-bearing elements on both side of the truncated cone

Fig. 3: *The cantilever of phase one*

form a spatial interconnected system of RC walls, columns, floors and beams. Due to the fact that it was acoustically favourable not to have a flat soffit in the music classroom, a structurally advantageous small-scaled folded plate system restrained into the truncated cone was used to increase the rigidity of the upper zone under tension. A detailed plan of propping removal and monitoring vertical deflections vs. age of concrete was issued.

The load-bearing elements of the bridge itself, spanning 21 m, are mirroring those of the cantilever: on one side a solid RC wall of 20 cm thickness is spanning the distance, while on the other, a system of parapet beams and wide columns of 30 cm thickness provide the necessary rigidity in vertical direction. Due to the significant classroom and corridor width and relatively thin slabs of 22 cm, an internal row of columns measuring 30x30 cm was used to maintain the allowable deformations; to support these columns a system of downstand beams was placed perpendicular to the "bridge" span. Here the propping removal was also detailed and monitored.

3. THE FULFILMENT – PHASE TWO

The second phase of execution meant the erection of the extension of the first wing, a hall and classrooms between the first and second wing, the second wing housing classrooms, kitchen and dining area and finally the terminating section of the complex containing information technology rooms, library and offices for the management and staff.

After the demolition of the barrack on the construction site first the form of the hall started to emerge from the ground. The hall consists of two broken and inclined walls on the yard side and a system of ramps, corridors and stairs on the opposite side *(Fig. 4)*.

In the hall inclined columns support two deep beams

Fig. 4: *The broken and inclined walls of hall as seen from yard side*

mirror the shape of the yard side to form the support structure for the nailed wooden truss system of the hall roof. The inexpensive simply supported trusses are positioned at every 2 m and spanning up to 19 m. At bottom of the trusses a fire resisting ceiling is mounted, so thus the covering and the wall

geometry with the ramps and pathways provide a very vivid and appealing common space for the hall *(Fig. 5)*.

To enlighten the cantilevering portions of the walls at yard-side, the relatively thick walls at their restrains were executed with an internal layer of hard heat insulation material at their top.

As all stairs in the complex, the stairs of the hall were executed as RC slabs with load-bearing RC balustrades.

The structural system of the wing extension from the

Fig. 5: *The hall*

first phase and the classrooms neighbouring the hall consist of 30x30 cm RC columns, 22 cm thick flat slabs and edge beams.

The arrangement of structural elements in the wing hosting the kitchen and the dining area deviates from the regular due to functionality requirements. The larger floor spans are stiffened by means of downstand inner and edge beams, while the higher loads from HVAC located in the attic are taken by upstand beams. A cantilever of more modest measurements can be found at the yard side. This cantilever is supported by two 25 cm thick external and one 20 cm thick internal RC wall, which are led over the supporting curved RC wall at ground level *(Fig. 6)*. An expansion joint is located along one of the edge walls.

As from the architectural point of view it was found to be unfavourable to duplicate the load bearing elements along the expansion joint, the neighbouring structure to this expansion joint is supported by means of shear bolt connectors. The shear bolts are arranged at calculated distance along the perimeter of the connecting RC walls at first floor.

From structural point of view the covering of the library section is worth noting. The lay-out of the library forms a regular octagon with an overall span of 11 m, and the visible soffit called for a more exciting covering solution. The inclination of the roof was relatively shallow and due to functionality reasons the supporting system was far from ideal for membrane shell action. To accommodate these boundary conditions a 15 cm thick RC folded plate system resting on a solid ring beam, subjected both to bending and in-plane action was implemented. The non-parallel plate portions were also favourable from acoustical point of view.

Fig. 6: *The cantilever of the second wing supported by a curved wall*

Finally, a narrowing end section of the school building was designed to blend in with the neighbouring existing building on the main entrance side. As the school complex hosted several cantilevers, it was almost straightforward to form a similarly designed section at this area also. The load bearing elements of this cantilever are the 25 cm thick RC walls and, here, inclined flat slabs of 22 cm.

Along this narrowing section the strip foundation of the neighbouring building had to be deepened to accommodate to the depth of the strip foundation of the new building.

4. PARTING THOUGHTS

Such non-conventional buildings as the Szemere Pál elementary school complex require an increased effort from the whole design team. The calculations and result evaluations are difficult to cope with, only a complex spatial model provides the appropriate data for design. The drawings of the formwork and reinforcement are more labour-intensive, surplus energy has to be added to provide a clear and understandable execution documentation. Regrettably, it proves to be hard for any developer to accept the extra effort involved from the design parties, while on the other hand, he is more than pleased with the aesthetical impact such a structure may pose to the society and urban environmental surrounding. Undoubtedly the construction itself is more complex and pricier than that of a conventional structure. At this point one may pose a question whether such extraordinary design, engineering and constructional achievements are worth dealing with. Fortunately this question lingers only until one hears the happy chatter of satisfied and dazzled children of the school. It was surely worth taking part in this adventure.

5. ACKNOWLEDGEMENT

The authors express their thanks to Ms. Angéla Kalló for the photos.

Zoltán Klopka (1967) civil engineer (BME 1993, MSc), from 2007 one of the managing directors of E+H Ltd. Main fields of interest: numerical simulation and FEM analysis of reinforced concrete structures, seismic design. Member of the Hungarian Group of *fib*.

Péter Szász (1983) civil engineer (BME 2006, MSc). Structural designer of E+H Ltd. His main field of interest is the static and dynamic FEM analysis of non-conventional reinforced concrete structures.

ROOF STRUCTURES IN MOTION –
ON RETRACTABLE AND DEPLOYABLE ROOF STRUCTURES ENABLING QUICK CONSTRUCTION OR ADAPTION TO EXTERNAL EXCITATIONS


Noémi Friedman – György Farkas

This paper focuses on roof structures that are movable either for enabling quick and/or safe construction or in order to adapt the structure to external excitations. Roof designs coming from both motives will be discussed in this article. After a short review on historical background an extensive overview will be given on different types of transformable roof structures. Namely retractable roofs with rigidly moving parts, retractable/deployable pantograph structures, the pantadome erection, deployable tensegrity structures, retractable/deployable membrane structures, pneumatic structures and constructional methods of concrete shell structures will be shortly presented. In case of need for a more profound understanding of the different types of transformable systems an extensive reference is given.

Keywords: deployable roof structures, retractable roof structures, pantograph structures, scissor-like structures, adaptive structures, responsive architecture, tensile structures, tensegrity, pneumatic formwork.

1. INTRODUCTION

The history of transformable roof structures goes back to centuries before. Though possibly everybody is familiar with the light deployable nomad Indian tepees (*Fig. 1a*) that could be transported by animals, only very few know that a part of the auditorium of the Roman Colosseum (Amfiteatro Flavio) (*Fig. 1b-c*) built in the first century had a convertible textile roof (Ishii, 2000). The structure of the umbrella is an ancient structure as well, but its principle is used in modern adaptive architecture.

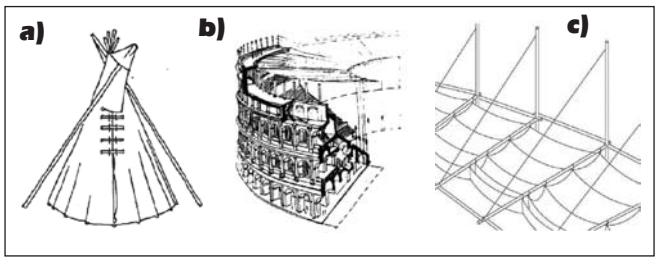

Fig. 1: Early movable roof constructions: a) Tepee tent from the Sioux Indians (Otto et al, 1971; cited by Walter, 2006); b) Roman Colosseum (Escrig and Brebbia, 1996) and c) the reconstruction of its convertible roofing system (Gengnagel, 2001; cited by Walter, 2006)

Evidently higher scale transformable roof structures appeared only in the last century. With the growing demand of hosting sport venues, starting from the 1930s an increasing trend toward building retractable roofs can be observed. As cranes were already common at that time and standards were available for transport tracks, control and drive, the first constructions stem from the principles of crane technology (Ishii, 2000). Thus early designs mainly run on rails. The first retractable big span roof is said to be the Pittsburgh Civic Arena (*Fig. 4*) that was opened in 1961.

After the World War II — parallel to the appearing of retractable roofs opened with rigid body movements — significant pioneer works have to mentioned regarding deployable/ratractable lightweight structures. B. Fuller's reinvention of the geodesic dome (*Fig. 2a*) and his lectures on 3D geometrical forms for architecture, space frames and structural efficiency (Fuller and Applewhite, 1975) inspired several researchers to further elaborate his ideas. The invention of the tensegrity system by K. Snelson (Snelson, 2009) and B. Fuller in 1949 is still the main topic of several ongoing research work that try to widen the application possibilities of these systems and to adapt them to deployable structures (Motro et al, 2001). Furthermore the works of F. Otto in the field of tensile and membrane structures (Otto, 1973) and his systematic research work on deployable and retractable structures (Otto et al, 1971) in the 1960s led to a big variety of retractable membrane roof structure designs in the second half of the century (e.g. retractable roofs of Montreal Olympic Stadium, bullfighting ring in Zaragoza). Membrane structures can be combined with scissor-like deployable structures. E. P. Pinero's movable theatre (*Fig. 2b*) presented in 1961 can be mentioned as pioneer work of this type (Pinero, 1961). Though his deployable trellis design had major structural drawbacks, he motivated further pantographic deployable designs like Escrig's deployable swimming pool (Escrig et al, 1996) and Zeigler's pop-up dome (Zeigler, 1976).

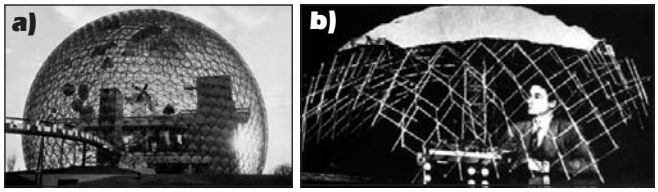

Fig. 2: a) The US Pavilion for the 1967 World's Fair, Montreal by B. Fuller (Hienstorfer, 2007); b) Pinero with his movable theatre (Robbin, 1996)

Transformability can be used not just for lightweight structures. In the last decades promising experiments were made with constructions using transformable systems to combat the main problem of concrete shell structures, namely the expensive, difficult and time-consuming production of them.

In the second half of the 20th century, regarding deployable and inflatable structures developments were in first place achieved in spatial engineering (Pellegrino, 2001; Gantes, 2001) for booms, solar arrays, antennas, reflectors, as the volume and the weight of a structure to be transported there is crucial. Current trends show a re-increasing interest in kinetic architecture due to the growing demand on provisory architecture (Kronenburg, 2008) and the need for sustainable technologies (Kibert, 2007, Friedman et al, 2011). Aiming sustainable architecture there is a remarkable tendency towards adapting seminal ideas of the 60s and 70s (Sadler, 2005; Zuk, 1970) to create an undeterminate architecture that can conform to uncertainty and emergent situations, changing in occupant demand and energetic considerations (Fox and Yeh; Rosenberg, 2010).

As it has been shown above, involving motion systems to structural design is not a novel idea. Nevertheless it seems to be a currently improving segment of civil engineering thanks to the available technologies that are just catching up with these ideas of the 1960s and 70s. More precisely the recent research actuality of transformable structures is due to the continuously improving computer, robotic and nanotechnologies, the ameliorated numerical methods (Ibrahimbegovic, 2009) and the progressive properties of novel and conventional building materials. Though the main research topic of the authors within this theme is just a small slice of the mentioned topics (namely the engineering application and dynamic analysis of snap-through type deployable lattice structures), for the recently started research work an extensive study was carried out to explore earlier and current researches and technologies to approve the actual interest in developing these systems. Herein the reader can see a generalized and shortened version of this demonstrative study, which reflects well that transformable architecture has not just a past but may also have a future.

This article tries to give a general overview on transformable roof structures built from both motivations: 1.: enabling a quick/safe construction and 2.: providing an adaptive design. The most commonly used systems for roofing sport venues, namely the ones that can be opened by *rigidly moving panels* (*2nd chapter*) is presented first. Scissor-like structures or *pantograph structures* are also presented in this article (*3rd chapter*). These structures are preliminary used for smaller span provisory buildings, however they can be applied for a specific structural system enabling a quick and safe construction for large span domes (pantadome erection), as well as for retractable roof structures. Afterwards a different deployable lattice system will be presented, namely the deployable *tensegrity structures* (*4th chapter*) that are still rather in an experimental phase. The *deployable and pneumatic membrane structures* are explained in the *5th chapter*. Pneumatic systems can be used for the erection of *double curved and irregular curved concrete shells*. Construction methods of concrete shells using transformational systems will be discussed in a separate chapter (*6th chapter*).

2. RETRACTABILITY WITH RIGID BODY MOVEMENT

As mentioned in the introduction, first designs for retractable covering of sport stadiums stem from the crane technology. F. Otto classified these convertible roofs by a movement matrix (*Fig. 3*).

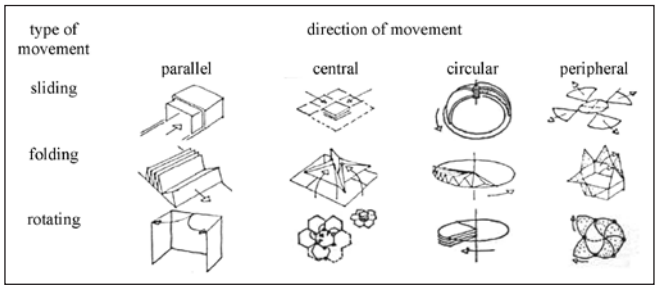

Fig. 3: Classification of rigid retractable constructions: the movement matrix (Otto et al, 1971)

Fig. 3 shows that the retraction can be obtained by sliding, folding or rotating the panels in different directions. The panels can overlap while retracting or move independently. The first retractable dome structure is said to be the circularly sliding retractable roof of the Pittsburgh Civic Arena (*Fig. 4*) opened in 1961 and closed in 2010 summer. The 127 m span roof consists of eight, 300 ton sections, six of which are able to rotate by five motors per panel. All panels are fixed on the top to a gigantic, 80 m tall steel truss cantilever. The roof could be opened in about two minutes (Ishii, 2000).

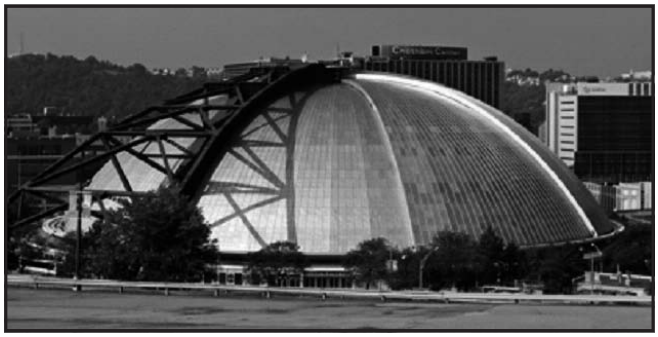

Fig. 4: Photo of the Pittsburgh Civic Arena (architect: Mitchell and Ritchey) (Lorentz, 2008)

The structural form of the civic arena is initially optimal as bending moments are minimal due to geometry. Unfortunately for retractability this optimal shape had to be sliced in parts, thus the cost was the huge cantilever that supports the panels, and the bigger structural height. A similar geometry was achieved by a more recent construction that did not apply an external structure to hold the panels. The Fukuoka stadium in Japan (*Fig. 5.*) opened in 1993 spans 222 m. The three parts of the roof — two of which is rotatable — are independent frameworks, with remarkable bending moments. Though careful shape correction was performed for the geometry of individual parts (*Fig. 6a*) to avoid singularities in reaction forces at the inclination lines (Ishii, 2000), the structural height is still gigantic. Each panel is four meters thick, and the total roof weighs 12 000 tons. The sliding rotation of the two panels is enabled by 24 bogie wheel assemblies (*Fig. 6b*). It takes approximately 20 minutes to open the roof.

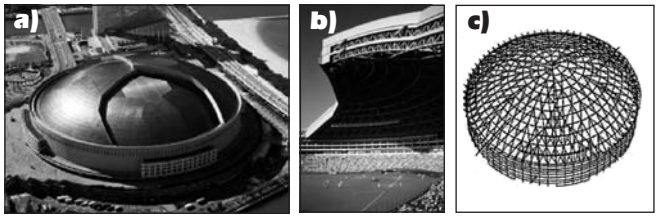

Fig. 5: Fukuoka stadium (architect: Takenaka Corp.) a) photo with closed (Yahoo, 2010) and b) with opened roof (Japan Atlas) c) structure (Ishii, 2000)

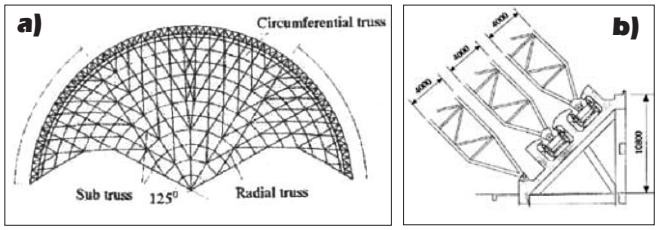

Fig. 6: Fukuoka stadium a.) geometry of a roof panel b.) roadbed section (Ishii, 2000)

Much more slender retractable structure was constructed in Oita, Japan, in 2001 called the Oita Stadium or more commonly the "Big Eye" (*Fig. 7*). A large part of the 274 m diameter spherical roof is fix *(Fig. 8b)*, only the top two panels are retractable, that slide parallel on seven rails to the periphery of the dome. The sliding panels are covered with a special membrane containing a Teflon film that provides better transparency, thus even on rainy days natural lighting is provided. (Ishii, 2000)

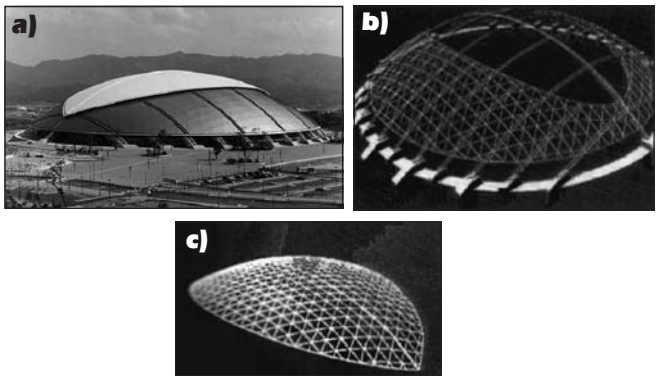

Fig. 7: Oita Stadium (architect: Kisho Kurokawa) a) photo (Ezinemark, 2010); b) fix structural part (Ishii, 2000) and c) retractable top section (Ishii, 2000)

To mention other motion systems for rigid retractable construction just briefly three different examples are shown. A parallel overlapping system was used for the 40 m span retractable roof of the Komjádi swimming pool in Budapest, built in 1976. A more complex system of rigid systems is the roof of the Qi Zhong stadium in Shanghai that opened in 2005. Resembling a flower opening its petals the eight panels rotate towards the perimeter in 8 minutes. Of course not every retractable roof can be clearly classified by the categories of the motions matrix shown in *Fig. 3*. For example the roof of the Toronto Skydome (*Fig. 9*) is a nice example of a mixed system. The 213 m diameter roof is made up of 4 sections, one remains stationary while the two panels slide parallel and one circularly to achieve a high rate of retractability.

Fig. 8: a) Retractable roof of the Komjádi swimming pool (Komjádi); b) Qi Zhong stadium (architect: Mitsuru Senda), (Ezinemark, 2010)

More and more recent architectural designs try to apply transformable systems only for achieving the variability of a shell or an envelope of the permanent structure. Though the motion of the building might not be as spellbound as the ones where whole massive structural parts are in motion, but can offer a nice solution for integrating structural efficiency and

Fig. 9: Toronto Skydome (architect: Rod Robbie) a) photo of closed and b) opened roof c) The structure (Ishii, 2000)

the adaption to external excitation. This was the case with the adaptive sun shading system of the Audencia Provincial, Madrid (*Fig. 10*) designed by Hoberman. The hexagonal shading cells can completely cover the roof, but disappears when retracted into the structural profiles of the structure. The algorithm that controls the movement combines historic solar gain data with real-time sensing of light levels (Hoberman, 2010). Hoberman designed several adaptive shading systems in accordance to his new patented technology (Hoberman and Davis, 2009) to enhance the architectural design of Foster + Partner's buildings.

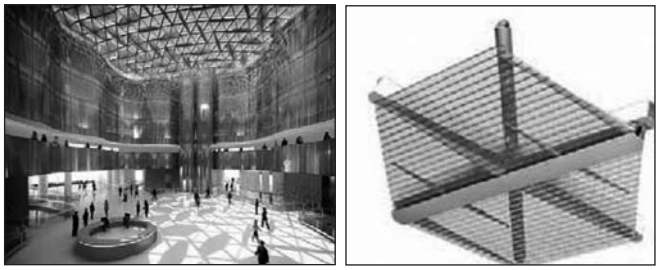

Fig. 10: Adaptive shading system of the Audencia Provincial, Madrid (Hoberman and Fox+Partners) and the model of a hexagonal retractable panel (Hoberman, 2010)

3. PANTOGRAPH STRUCTURES

A large number of structures that can be opened and closed are based on the well known concept of the lazy tong system. The minimum component of this system is the so called scissor like element (furthermore SLE). The SLE consists of two bars connected to each other with a revolute joint. By the parallel connection of SLEs the simplest 2D deployable structure, the lazy tong is constructed. Connecting at least three of SLEs through complete pin joints a ring is formed, providing a secondary unit of this frame structure (*Fig 11a-d*). By the further connection of secondary units almost all kind of 3D-shapes can be formed folding into bundle. Adding tension components like wire or membrane to its developed form, it becomes 3D-truss and gets effective strength, thus towers, bridges, domes and space structures can be rapidly constructed. (Atake, 1995)

3.1 Deployable structures folding into a bundle

Using scissor-like deployable structures for architecture was pioneered by the Spanish engineer, E. P. Pinero. He presented a foldable theatre (*Fig. 2b*) in 1961 (Pinero, 1961), and elaborated several other deployable designs. The biggest drawbacks of his designs were the relatively heavy and big joints due to eccentric connections and necessary temporary support as the structure was stiffened by intermediate bars or tension elements that were added after the structure was deployed in the desired configuration (Gantes, 2010). Despite of all the disadvantages of his structures Pinero inspired several

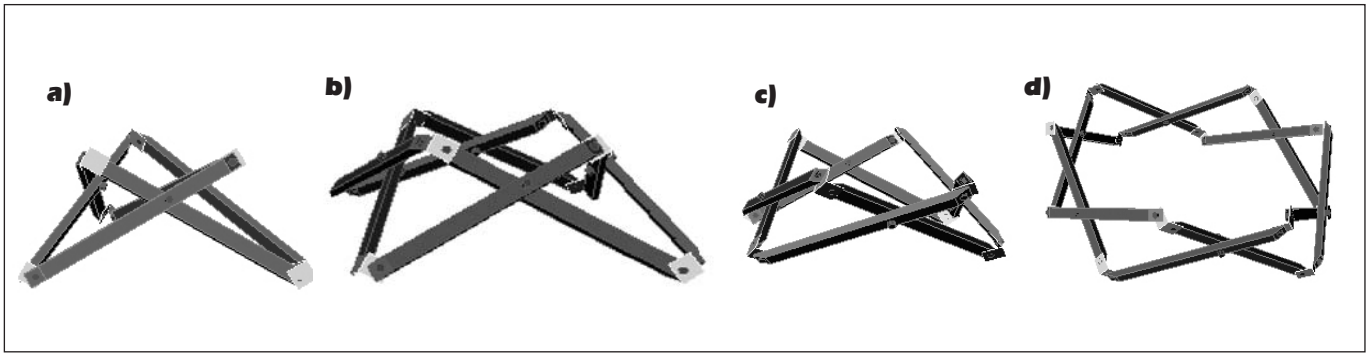

Fig. 11: Some secondary units of scissor like deployable structures (a-d), (Atake, 1995)

researchers. This was the case with Professor F. Escrig, who designed the 30 m×60 m deployable roof for a swimming pool in Seville (Escrig, 1996; *Fig 12)*.

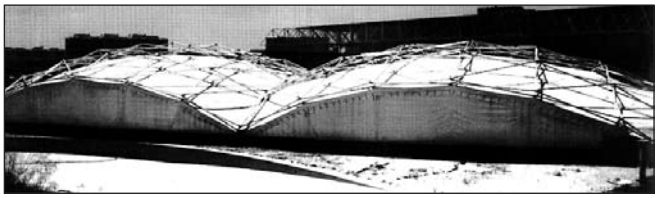

Fig. 12: Deployable swimming pool (architect: Prof. Felix Escrig) (Escrig et al, 1996)

While pantograph structures discussed above need additional stabilizing elements like cables or other locking devices, it is possible to design deployable structures that are self-stable in the erected configuration without any additional member with the application of a special geometric configuration. This can be achieved by adding inner SLEs to the initial secondary units. These inner SLEs deform while unfolding due to geometric incompatibilities thus resulting a self-locking, self-stabilizing mechanism that locks the structure in its opened configuration (Clarke, 1984; Gantes, 2001). The first dome structure of this type was introduced by T. Zeigler in 1974 (Zeigler, 1976; *Fig. 13*). Several pop-up displays and pavilions are constructed in accordance with his patents. About self-stable structures a practical and detailed design guide was published, written by C. J. Gantes (Gantes, 2001), where design examples like airship cover and the adaption of self-locking systems to scaffolding systems are presented.

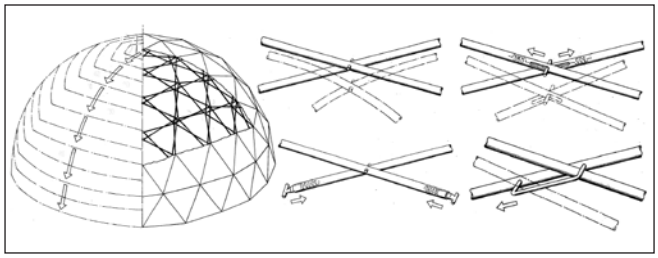

Fig. 13: Zeigler's patent for collapsible self-supporting structure (Zeigler, 1976)

3.2 Retractable pantograph structures

The application of structures that can fold into bundle when continuous transformability needed could be difficult to get. The American engineer, C. Hoberman made a considerable advance in the design of retractable roof structures by the discovery of the simple angulated element (Hoberman, 1990, 1991). By the refraction of the two straight rods of a single SLE the angulated element is formed (*Fig. 14b*). This element is able to open and close while maintaining the end nodes on radial lines that subtend a constant angle (Pellegrino, 2001; Friedman et al, 2011).

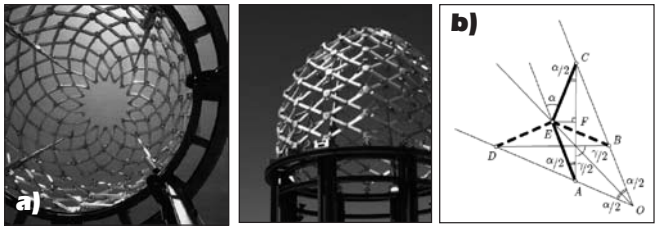

Fig.14: a) Iris dome by Hoberman, EXPO 2000 (Whitehead, 2000); b) angulated element (Jensen, Pellegrino, 2004)

Using angulated elements Hoberman created the retractable roof of the Iris Dome, shown in *Fig. 14a* at the EXPO 2000. Powered by four computer-controlled hydraulic cylinders, the 6,2 m diameter and 10,2 m high retractable dome smoothly retracts toward its parameter and unfolds (Hoberman, 2010). One of the drawbacks of this design is that the structure does not maintain a constant perimeter, thus to connect it to a permanent foundation is quite a challenge especially in case of a bigger scale structure. On the other hand, for the construction of the relatively small span structure required more than 11 400 machined pieces (Whitehead, 2000) which can cause potential problems with reliability and a laborious and expensive manufacturing. Further developments were made by Z. You and S. Pellegrino (You and Pelligrino, 1997) by generalizing these elements to a large family of foldable building blocks and by introducing a new type of pantographic structure based on the so called multi-angulated elements. With multi-angulated elements the number and complexity of elements and joints of retractable trellis structures can be reduced.

P. E. Kassabian succeeded to change the geometry of the structure by rigid body rotation, so that the motion of each angulated element is a pure rotation about a fixed point, and thus allows the application of fixed support points (Kassabian et al, 1999).

An enclosure can be created by covering angulated elements with elastic/folding membrane or rigid plates which are allowed to overlap in the retracted position. Other designs use rigid panel avoiding overlapping of the panels (Jensen and Pellgrino, 2004). Several different designs have been proposed by Hoberman (Hoberman, 1991, 2004). One example is the central part of the responsive dome (*Fig. 15*) that covers a major central courtyard of Abu Dhabi's international airport. The large operable oculus is covered by panels sliding towards the perimeter. The dome's permanent structural part has an envelope that is also transformable varying its permeability. The system performs environmentally both to control light levels and air flows in the space (Hoberman, 2010).

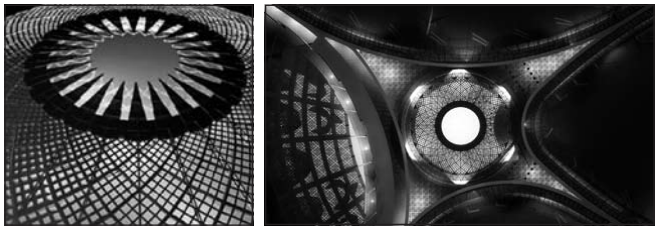

Fig. 15: Development of transformable dome by Hoberman for the dome of Abu Dhabi's international airport, United Arab Emirates, 2006 (Kohn Pedersen Fox Architects) (Hoberman, 2010)

3.3 Pantadome erection

3D spatial structures are extremely efficient ones completed. However the difficulties with installation (big amount of scaffolding, labour and time) often highly decrease this efficiency. This drawback can be significantly reduced with the unique structural system called the Pantadome System invented by M. Kawaguchi and will be herein explained in accordance with (Kawaguchi and Abe, 2002).

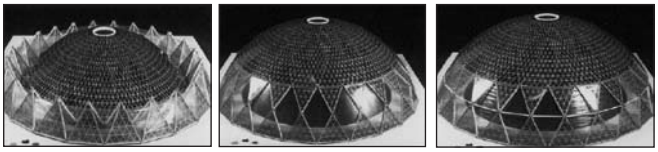

Fig. 16: Schema of the pantadome erection (Kawaguchi and Abe, 2002)

The principle of this structural system is to make a dome or a conical space frame cinematically unstable for a period of construction so that it is "foldable" during its erection. This can be done by temporarily taking out the members lying on a hoop circle (*Fig. 16*) then the dome is given a "mechanism", like a 3-D version of a parallel crank or a "pantograph".

Since such a dome is assembled in a folded shape near the ground level and the entire height of the dome during assembly work is very low compared with that after completion, thus the assembly work can be done safely and economically, and the quality of work can be assured more easily than in conventional erection systems. Not only the structural frame but also the exterior and interior finishings, electricity and mechanical facilities can be fixed and installed at this stage. The dome is then lifted up. Lifting can be achieved either by blowing inside the dome to raise the internal air pressure or by pushing up the periphery of the upper dome by means of hydraulic jacks. The major advantage of this system comparing with different lifting solutions is that no guying cables or bracing elements are necessary for lateral stability. This can be because the mechanism of the system is such that can be controlled with only one freedom of movement in the vertical direction. When the dome has taken the final shape, the hoop members which have been temporarily taken away during the erection are fixed to their proper positions to complete the dome structure. Several designs have been realized in accordance to the pantadome principle. One is the Namihaya Dome with diameter of 127m and 111m, whose erection and its lifting schema can be seen on *Figs. 17* and *18*.

4. TENSEGRITY STRUCTURES

Most of the deployable lattice systems are formed by scissor like structures. However there is a trend to apply also tensegrity systems when deployability needed. This experimental system was born at the end of the 1940s from the artistic exploration of K. Snelson and Fuller's goal of creating maximal efficiency structures (Snelson, 2009). Snelson called his tensegrity sculptures the "floating compression" system. It is worthwhile to mention though that at the same time exactly the same system was patented by D. G. Emmerich, called the "self-tensioning system" (Emmerich, 1964). This spatial truss system's elements can be separated to purely compressed and purely tensile components. With this separation the tensioned members can be as light weight as current material technology allows, resulting extremely light, economical and less visually intrusive structures. Just as the authorship of the invention, the exact definition of tensegrity is still disputed (Motro, 2006). Maybe the first clear definition of this kind of structure is the one that A. Pugh clarified: "A tensegrity system is established when a set of discontinuous compressive components interacts with a set of continuous tensile components to define a stable volume in space" (Pugh, 1976). Clear definition is further investigated and refined by R. Motro (Motro, 2006).

Fig. 17: Erection of Namihaya Dome (Showa Sekkei Corp), Osaka, 1997 (Kawaguchi and Abe, 2002)

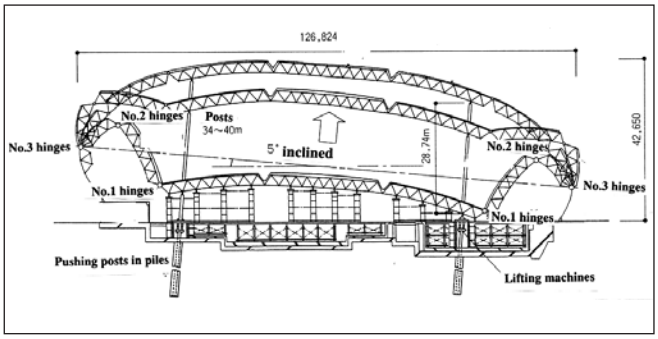

Fig. 18: Erection of Namihaya Dome (Kawaguchi and Abe, 2002)

The simplest tensegrity unit is the tensegrity tripod (Burkhardt, 2008) (*Fig. 19a*) and other tensegrity networks can be derived from geodesic polyhedra (Hugh, 1976, *Fig. 19b-c*). By the assemblage of these units planar and spherical structures can be created, thus it can be used for walls, floors and roofs. *Fig. 20* shows the spherical assembly of tripods designed by B.R. Fuller and a recent design for a tensegrity roof.

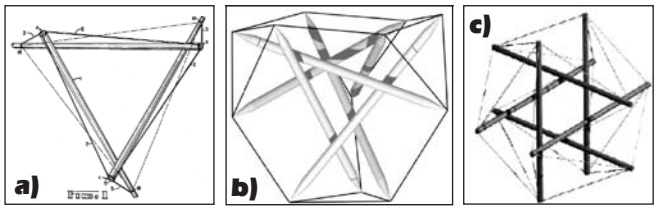

Fig. 19: *Some tensegrity system: a) the tensegrity tripod (Fuller, 1962) b) truncated tetrahedron (Burkhardt, 2008) c) expanded octahedron (Jáuregui, 2010).*

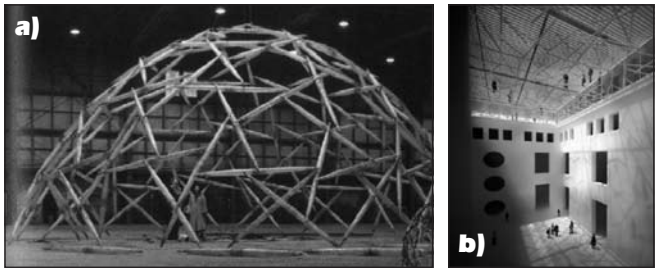

Fig. 20: *Architectural applications: a) Geodesic tensegrity dome by Fuller, 1953 (Gengnagel, 2002) b) tensegrity roof design of ABDR Arch. Association (ABDR)*

The idea to have only tendons connected to struts is probably the most innovative concept of this type of structures resulting extremely simple joints. Beyond the difficulty of form finding (Motro, 2006) the main problem of this type of non-conventional structure is the difficulty of fabrication as the geometry of spherical and domical structures are pretty complex. Other big disadvantage, similarly to all tensile systems, is the poor load response (relatively high deflections and low material efficiency (Hanaor, 1987) as compared with conventional, geometrically rigid structures and the lack of resistance to concentrated loads.

Another big disadvantage is that conventional architectural structures cannot be applied for connecting structural elements, and for cladding. Thus it requires a complete innovation of complementary technologies. A big advance when comparing with other tension systems is that this tensegrity structures can encompass very large areas with minimal support at their perimeters, obviating the "heavy anchorage devices" needed for support with some cable based technologies, or extensive support structures needed by some composite structures, mixing tensegrity systems and non-tensegrity technologies (Motro, 1987). Deviating slightly from the canonical definition R. Motro explored and tested many different tensegrity systems for architectural application (Motro, 2006).

A new type of deployable structure can be created due to the intrinsic property of tensegrity structures. Foldability can be easily obtained by changing the element lengths. This can be either the changing of strut length by using telescopic bars or the folding can be enriched by changing the length of the cable. The main difficulty of the former method is that in the folded configuration the cable often creates an inextricable tangle, thus unfolding the system is often opposed. The later rather proved to be a usable method concerning assemblies. (Motro et al, 2001)

The trend to design adaptive/responsive architectural applications turns the kinematic indeterminacy of tensegrity structures an advantage (Tibert, 2002). This is due to the fact that only small quantity of energy is needed to change the configuration and thus the shape of the structure.

5. MEMBRANE STRUCTURES

5.1 Classification

Similar to the rigid constructions, F. Otto classified also the membrane convertible constructions in a movement matrix (*Fig. 21-22*). He distinguished two different types; the one with stationary supporting structure and the one with movable supporting structure. Pneumatic structures can be also classified as deployable membrane structures. As mentioned in the introduction these types of structures were already in practice in the very past history. However it was just the end of the second half of the last century when engineers began to apply textile as building material for large-span constructions. The pioneering works of F. Otto motivated plenty of membrane designs throughout the world.

type of movement	direction of movement			
	parallel	central	circular	peripheral
bunching				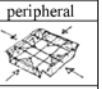
rolling	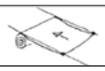			

Fig. 21: *Classification of membrane convertible constructions: the movement matrix of structures with stationary supporting structure (Otto et al, 1971)*

type of movement	direction of movement			
	parallel	central	circular	peripheral
sliding	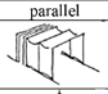		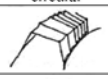	
folding				
rotating				

Fig. 22: *Classification of membrane convertible constructions: the movement matrix of structures with movable supporting structure (Otto et al, 1971)*

5.2 Foldable membrane structures

The main difficulty concerning deployable membrane structures is the stabilization of the membrane in all the possible configurations (folded, during deployment, opened configuration). In the extended position the membrane can be secured with pretensioning, that can be achieved either with the drive system itself or by special tensioning devices at the edge of the roof. The flapping wind effect during deployment resulting quite large deformations with small forces is one of the main difficulties (Walter, 2006).

This difficulty occurred in the case of the Olympic Stadium in Montreal, Canada (*Fig. 23*). The stadium was to open for the 1976 Olympic Game, but the retractable roof was finished only in 1988. The 20 000 m^2 PVC/Kevlar folding membrane roof which was to be opened and closed by the 175 m inclined tower, was repeatedly damaged by local failures due to aero-elastic instability. The structure was replaced with a non-retractable spatial steel roof structure.

Fig. 23: Olympic Stadium in Montreal (architect: Roger Taillibert) (Olympic) an its original retractable membrane roof (Barnes, 2000)

A similar, but more successful design was evolved in 1988, Zaragoza, Spain for the roofing of the bullfighting Arena (*Fig. 24-25*). The roof was separated to a 83 m diameter fixed and a 23 m diameter central convertible membrane roof. For both parts a double spoked wheel system was used. The prestressed outer spokes span between an outer compression ring and two sets of inner tension rings held apart from each other by struts. The membrane of the permanent roof is draped over the lower set of radial cables. The retractable inner roof has similarly two sets of spokes between the inner tension rings and a central hub above the centre of the bullring. The two sets of spokes are connected by an electric spindle. The membrane is suspended to the lower layer of spokes by slides that can be moved by a stationary drive system. When the roof is open, it hangs bunched up in the centre, when is to be closed, 16 electric motors draw the bottom edge of the membrane out to the lower tension rim. Once the edge is secured to the rim, prestress is applied by rotating the top spinder (*Fig. 26*) at the central point, thus the retracted membrane is stabilized (Holgate, 1997; Walter, 2006). Even a 63 m diameter retractable roof was constructed in accordance with this principle over the centrecourt in Hamburg Rothenbaum (Walter, 2006).

Fig. 24: The retractable part of the Bullfighting Arena roof in Zaragoza (architect: J. Schlaich) (Sobek, 1999; cited by Walter, 2006)

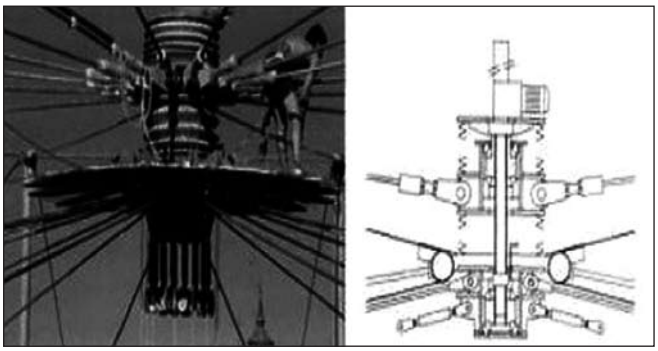

Fig. 25: Central spinder for prestressing the cables (Holgate, 1997)

Different membrane folding can be evolved by the umbrella principle. A nice example is the convertible cover of the two courtyards of the Prophet's holy Mosque in Madinah (*Fig. 26a*). The twelve large umbrellas (17 m x 18 m in the open configuration) are stem from the developed system of F. Otto (Otto and Rasch, 1995). These umbrellas ensure the shading during the day and the ventilation and cooling during the night. The openable roof installed in 2000 in the courtyard of the Rathaus, Vienna (*Fig. 26b*) is an example of a different convertible system where the membrane is retracted with sliding the cross-girders (Walter, 2006; Tillner, 2003).

Fig. 26: a) Architectural umbrellas in the courtyard of Mosque in Madinah (Otto, 1995 cited by Walter, 2006), b) Foldable roof in the Rathaus, Vienna (Tillner, 2003; cited by Walter, 2006)

The ability to provide numerical simulations for increasingly complex membrane is advancing rapidly due to computer hardware development and the improved computational procedures of nonlinear structural systems. This sweepingly advanced development with the inventions in textile technologies is exploring the further architectural and technical potentials of these structures.

5.3 Pneumatic structures

The supporting medium of pneumatic structures is compressed air or gas that creates tension forces on the elastic membrane, thus ensures the strength and the stability of the structure. Probably the balloon is the most well-known classical pneumatic structure. In construction the first inflatable structures appeared in the 1950's. These were mainly shelters with single wall inflatable "bubbles", called air-supported structures constructed from a single layer of pliable material that is supported by the internal pressurized air. This internal air pressure has to slightly exceed the external pressure. Thus this system requires an air lock, a continuous pressurization system that balances the air leakage, and an anchorage that fixes the structure to the ground or to the substructure.

Other inflatable designs use double-layer inflatable configurations. These air-inflated structures use tubular (air-beam structure) or cellular (air-cell building) shaped membrane skin with an internal pressurization that form together structural elements similar to the conventional ones. The skin takes the tension forces whereas the air is responsible for compression forces in a manner like the reinforced concrete. This new generation of inflatable structures has in general no steel, no aluminium, and no traditional supports and yet can handle large structural loads.

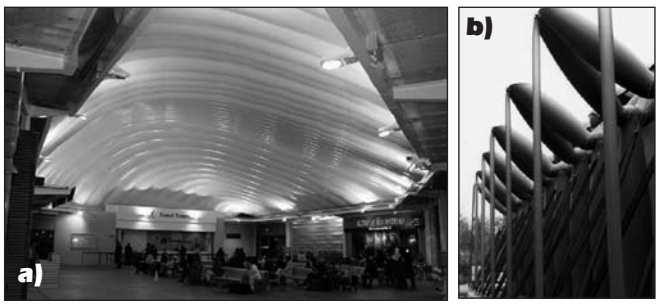

Fig. 27: a) Inflatable roof for Heathrow airport central bus station (architect: D5) (Lindstrand, 2006); b) 19.5 m x 40 m Exhibition Hall with air-inflated elements (architect: Festo AG & Co) in Germany (Festo)

Now that fabric and computer technology are catching up with this concept, the possibilities of inflatable structures in commercial, military and special events applications seem limitless. Even cubic interior building can be constructed with the air-beam technology (*Fig. 27b*). While more expensive than comparable aluminum structures, inflatable beams save money on transportation and installation because of their light weight and small packing size. Proving these facilities the inflatable roof designed for covering the central bus station

of the Heathrow airport (*Fig. 278a*) is an instructive example. The installation of the roof was effectuated in one only night in 2006. Pneumatic design was chosen because the realization of the foundation of a conventional roof would have been run into obstacles as one of the airport's Tube stations is just underneath the site. (Lindstrand, 2006)

6. CONSTRUCTION OF CONCRETE SHELL STRUCTURES

6.1 Pneumatic formwork for thin concrete shell structures

Concrete shells are extremely material efficient structures as for uniformly distributed loads mainly normal forces appear in the cross sections and moments are insignificant. Moreover these structures are also very popular for their attractive architectural appearance. Nevertheless the time-consuming and expensive production with a conventional formwork is an important drawback of these structures. Similarly to the pantadome system used for lightweight 3D spatial structures, transformability can serve for combating this major problem of concrete shell designs.

Three different pneumatic formwork methods are used for monolithic concrete shell structures (van Hennik and Houtman, 2008). If the membrane is inflated first, *(Fig. 28a)* the concrete can be sprayed on the inside or the outside of the membrane. Evidently the reinforcement has to be placed before spraying the concrete. In case of the shotcrete on the inside *(Fig. 28b)* a special layer of polyurethane foam has to be sprayed on the membrane to hold the reinforcement. The membrane can be either taken off/out for reuse after the hardening of the concrete or can be left as a waterproof layer.

Fig. 28: *a) Inflation of formwork; b) shotcreteing on the inside of the membrane; c) irregular shape structure constructed with pneumatic formwork (Pirs SA.)*

The principle of the third method, invented by D.N. Bini, is to do all the constructional work on the ground in plane and then inflating the structure into 3D shape. The pneumatic lifting of the reinforcement and the freshly placed concrete can be effectuated with a special sliding reinforcement system *(Fig. 29a-c)* consisting of conventional steel bars and extensible spirals. As the structure lifts and takes its shape, the spirals stretch and the reinforcing bars slide inside them to reach their final position in the structure (Roessler and Bini, 1986). For Binishells two layers of membrane are used. The inner layer is attached to the ring beam being part of the foundation and the outer layer is placed after putting the reinforcement and the concrete on the inner layer. The concrete is vibrated after lifting the structure via an equipment that is attached to the centre of the outer membrane *(Fig. 29c)*. After lifting the outer membrane can be removed and after hardening the inner layer can be deflated and reused for the next construction.

Fig. 29: *The binishell system: a) expandable reinforcement (Bini, 1972); b) erection of the dome (Binishell System); c) vibration of concrete after erection (Bini, 1972)*

Though pneumatic systems has been already applied for concrete shell structures since the 1960s, these systems seem to regain their popularity due to their aesthetic appearance, improved technological background and renewed structural concepts. Even irregular shell shapes *(Fig. 28c)* are constructed with pneumatic formwork (van Hennik, 2008).

6.2 Erection of segmented concrete or ice domes

Two new and very efficient construction methods for hemispherical concrete shells have been developed at the Institute for Structural Engineering at Vienna University of Technology by J. Kollegger. The novel concepts were tested not just on large scale concrete but as well on ice domes. Both methods start with an initial plain plate that is subsequently transformed into a shell structure (Dallinger and Kollegger, 2009) *(Fig. 30-31)*.

The principal of the first method is to fragment the shell structure into a polyhedron enabling the use of planar precasted parts that can be easily produced at the factory, transported to the site and then quickly assembled. The elements kept together by radial and circumferential steel tendons *(Fig. 30)*. The circumferential tendoms are tightened through winches and are instrumental for the assembly of the elements. The erection is effectuated with a pneumatic formwork that lifts the structure into the desired position. (Dallinger and Kollegger, 2009)

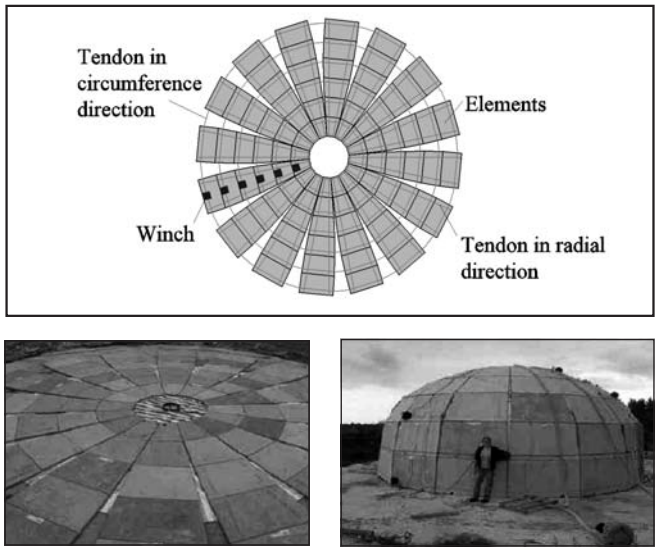

Fig. 30: *Transformation of precast divided planar segments into a hemispherical dome (Dallinger and Kollegger, 2009)*

In case of the second method the flat plate is divided into segments which are distorted uni-axially and lifted into the final position (Dallinger and Kollegger, 2009). The transformation is controlled by one or more active cable(s) and by either a crane positioned in the centre or a pneumatic formwork placed under the structure (Kollegger et al., 2005). *(Fig. 31)*

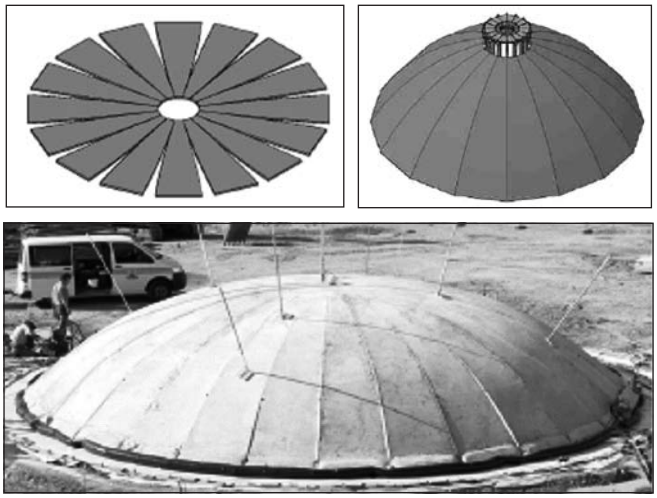

Fig. 31: Segment lift method (Dallinger and Kollegger, 2009)

7. SUMMARY

After shortly summarising the historical background an overview on movable roof structures have been presented. The feature of transformability in case of a roof structure can arouse from two different motivations. The first motivation is to create a fast and/or safe construction method and in some cases it can be also the need for a quick demounting process and the possibility of reusability. The second motivation is to adapt the structure to external excitations like weather conditions. This can either come from energy-saving consideration or from the aim to ameliorate occupant comfort, raise the attraction of the building.

The former motivation resulted in exotic inventions of some *pantographic systems*, like the collapsible movable theatre of Pinero, the quickly retractable swimming pool cover of Escrig, even the pop-up dome of Zeigler and its further developments. The minimal material use *tensegrity systems* also offer the possibility of foldability. Ongoing research works try to find a greater variety of possible architectural applications. Some *soft membrane systems* like cable-stiffened textile structures and pneumatic structure can be quickly installed too. F. Otto remarkable systematic study on foldable membrane structures with the recent available material and calculation technologies led to a wide variety of architectural membrane designs even used for big span permanent structures. Pneumatic systems can also serve as a supplementary system for the erection of 3D structures making the installation easier, faster and safer. The "*pantadome" structural system* invented by Momoru Kawaguchi, and some earlier and novel *pneumatic formwork methods for* constructing monolithic and precasted *concrete domes* can be mentioned among these systems.

Though these structures mentioned above still attract the military and provisory events in first place a trend can be observed to apply them for permanent buildings where translucent or extremely light construction is needed.

With membrane structures roofs that can move while in use can be designed too. The goal to design dynamic structures that are able to change morphological/mechanical/physical properties and behaviour as a response to external excitations and requirements was first addressed in the 1960s and 1970s. Early transformable designs appeared in first place for housing sport venues. With the currently growing media focus on sport events the demand for *retractable structures* seems to be steadily increasing. Most of these designs use *rigidly moving parts* to retract the roof structure. In most of the cases the slicing of an ideal roof shape results in gigantic structural height, and mechanical instruments enabling retraction further increase the costs of these structures. With new generation roofs like the *retractable pantograph* structure of Hoberman and Pellegrino and the application of a *retractable skin* fixed to the permanent structure can rather count with economical aspects. Several research topics focus on adapting *tensegrity and pantographic structures* to adaptive architecture. Combining transformable structures with a highly distributed control system which is already available in today's technology an intelligent responsive architecture is born. This possibility does not only prospect indoor environmental quality enhancement and better occupant comfort but a better use of natural energy resources and thus a rather sustainable design.

8. ACKNOWLEDGEMENTS

This work is connected to the scientific program of the 'Development of quality-oriented and harmonized R+D+I strategy and functional model at BME' project. This project is supported by the New Hungary Development Plan (Project ID: TÁMOP-4.2.1/B-09/1/KMR-2010-0002).

9. REFERENCES

ABDR: *Design of a tensegrity flat*, source: http://complexitys.com/wp-content/uploads/2010/03/v3-535x800.jpg;

Atake, K. (1995): *Diagonal and Variable Frame Structures*, Symmetry Culture and Science Extended Abstracts 1, ISIS Symmetry, pp. 53-56, vol1;

Barnes, M., Dickson, M. (2000): *Widespan Roof Structures*, First ed., Thomas Telford Publishing, London;

Bini, D. (1972): *Expandible reinforcement structure for inflatable domes*, US Patent No 3,686,818;

Binishell System: *Image of the erection of a Binishell Dome*, courtesy of Binishell System, source : http://www.binisystems.com/slide/image/b_3.jpg;

Burkhardt, R. W. (2008): *A Practical Guide to Tensegrity Design*, Cambridge, Massachusetts: Software Services;

Clarke, R.C. (1984): *The kinematics of a novel deployable space structure system*, Noshin, H.: Proceedings of the 3rd International Conference on Space Structures, University of Surrey, Guilford, UK, London, pp. 820-822;

Dallinger, S., Kollegger, J. (2009): *Pneumatic formwork for concrete and ice shells*, Proceeding of the Int. Conf. on Textile Composites and Iflatable Structures, Structural Membranes, CIMNE, Barcelona;

Emmerich, D.G. (1964), *Construction de réseaux autotendants*, French Patent No. 1,377,290;

Escrig, F., Valcarcel, J.P., Sanchez, J. S. (1996): *Las Cubiertas Desplogables de Malla Cuadrangular*, Boletín Academico de Universidad de Coruña, Escuela Téchnica Superior de Arquitectura, Nº20;

Escrig, F., Brebbia, C. (1996) *Mobile and Rapidly Assembled Structures*, II, First ed., Computational Mechanics, Southhampton, UK;

Ezinemark (2010): *Photo of the Oita Stadium*, *and the Qi Zhong Stadium* sources: http://img.ezinemark.com/imagemanager2/files/30002496/2010/08/2010-08-31-17-09-42-9-oita-stadium.jpeg, http://img.ezinemark.com/imagemanager2/files/30002496/2010/08/2010-08-31-17-09-42-7-qi-zhong-stadium.jpeg;

Festo: *Photo of the Airtecture Exhibition Hall,* courtesy of Festo, source:http://www.tensinet.com/project_files/3753/AIRTEC_ESSLIN_FESTO__EXHIBI_PD01.jpg;

Fox, M., Yeh, P.: *Intelligent kinetic system*, http://kdg.mit.edu/Pdf/iksov.pdf;

Friedman, N., Farkas, Gy., Ibrahimbegovic, A. (2011): *Deployable/retractable structures towards sustainable development*, Pollack Periodica, Akadémiai Kiadó, under publication;

Fuller, B. R. (1962): *Tensile integrity structures*, US Patent No 3063521;

Fuller, B.R., Applewhite, E. J. (1975): Synergetics: *Explorations in the Geometry of Thinking, Scribner;*

Gantes, C. J. (2001): *Deployable Structures: Analysis and Design*, WIT Press, Southampton, Boston;

Gengnagel, Ch., Barthel, R. (2001): *Bewegliche Dächer,* Detail 5/2001, pp 841-854;

Gengnagel, Ch. (2002): *Arbeitsblätter Tensegrity*, München, Technische Universität, Fakultät für Architektur;

Hanaor, A. (1987): *Preliminary Investigation of Double-Layer Tensegrities*, H.V. Topping: Proceedings of International Conference on the Design

and Construction of Non-conventional Structures, Vol. 2, Edinburgh, Scotland: Civil-Comp Press;
Van Hennik, P. C., Houtman R. (2008): *Pneumatic Formwork for Irregular Curved Thin Shells.* Textile Composites and Inflatable Stuctures II, Computational Methods in Applied Sciences, Vol. 8, pp 99-116;
Hienstorfer, Ph. (2007), *Photo of the Biosphere, Montreal*, source: http://en.wikipedia.org/wiki/File:Biosphere_montreal.JPG;
Hoberman, C. (1990): *Reversibly expandable doubly-curved truss structure*, US Patent Nº 4,942,700;
Hoberman, C. (1991): *Radial expansion/retraction truss structures*, US Patent No 5,024,031;
Hoberman, C. (2004): *Retractable structures comprised of interlinked panels*, US Patent No 6,739,098;
Hoberman, C., Davis, M. (2009): *Panel assemblies for variable shading and ventilation*, Patent No 7,584,777;
Hoberman, C. (2010): *Portfolio of Hoberman Associates* http://www.hoberman.com/portfolio.php, http://www.hoberman.com/HobermanPortfolio.pdf;
Holgate, A. (1997): *The Art of Structural Engineering - The work of Jörg Schlaich and his Team*, Axel Menges, Stuttgart/London;
Hugh, A. (1976): *An Introduction to Tensegrity*, Berkeley, California: University of California Press;
Ibrahimbegovic, A. (2009): *Nonlinear Solid Mechanics: Theoretical formulations and Finite Element Solution Methods*, Series Solid Mechanics and its application, vol.160, Springer;
Ishii, K. (2000): *Structural Design of Retractatble Roof Structures*, WIT Press, Southampton, Boston;
Japan Atlas: *Photo of the opened Fukuoka dome* by Japan Atlas Architecture, source: http://web-japan.org/atlas/architecture/photo/fuku02.jpg;
Jáuregui, G. (2010): *Tensegrity Structures and their Application to Architecture,* Santander: Servicio de Publicaciones de la Universidad de Cantabria;
Jensen F., Pellegrino S. (2004): *Expandable "blob" structures*, Extended proceeding of the IASS Symposium From Models to Realization, Montpellier;
Kassabian P. E., You Z., Pellegrino S. (1999): *Retractable roof structures.* Proceedings of Institution of Civil Engineers - Structures and Buildings, vol. 134(1), 45-56;
Kawaguchi, M., Abe, M. (2002): *On some characteristics of pantadome system,* IASS 2002: Lightweight Structures in Civil Engineering, proceedings of the international symposium, Warsaw, Poland, 24-28 June, Micro-Publisher Jan B. Obrebski, pp. 50-57;
Kibert, Ch. (2007): *Sustainable Construction: Green Building Design and Delivery,* Wiley;
Kollegger, J., Nemes, R., Preisinger, C., Kratochvill, A., Torghele, H. (2005): *Reinforced concrete shells without formwork – a new approach to the construction of RC – shells* Proceeding of fib Symposium Keep Concrete Attractive. Budapest, Hungary;
Komjádi: photo of the Komjádi swimming pool source: http://www.futas.net/hungary/Budapest/photo/budapest-csaszar-komjadi-uszoda.jpg;
Kronenburg, R. (2008): *Portable Architecture: Design and Technology*, Birkhäuser Architecture;
Lindstrand (2006): *Heathrow airport*, courtesy of Lindstrand Technologies, http://www.lindstrandtech.com/pop_ heathrow_roofs.html; photo source: http://www.lindstrandtech.com/images/pic_popup_heathrow2.jpg;
Lorentz, W. (2008): *Photo of the Mellon Arena Photograph*, Wayne Lorentz/Artefaqs Corp, source:http://www.glasssteelandstone.com/Images/US/PA/Pittsburgh/200801/MellonArena-Jul08-010a.jpg;
Motro, R. (1987): *Tensegrity Systems for Double-Layer Space Structures*, H.V. Topping, ed., Proceedings of International Conference on the Design and Construction of Non-conventional Structures, Vol. 2, Edinburgh, Scotland: Civil-Comp Press;
Motro, R., Bouderbala M., Lesaux C., Cévaer F. (2001): *Foldable tensegrities*, Deployable Structures, Springer-Verlag Wien, New York, pp 199-238;
Motro, R. (2006): *Tensegrity: Structural Systems for the future*, Butterworth-Heinemann;
Olympic: *Photo of the Olympic Stadium in Montreal*, source: http://en.wikipedia.org/wiki/File:Le_Stade_Olympique_3.jpg;
Otto, F et al (1971): *Convertible Roofs,* Institut for Leightweight Structures, Univ. Stuttgart, IL5;
Otto, F. (1973): *Tensile structures*, Vol. 1: *Pneumatic structures* and Vol.2: *Cables, nets and membranes*, The MIT Press, Cambridge, Massachusetts;
Otto, F., Rasch, B. (1995): *Finding form,* Deutscher Werkbund Bayern;
Pellegrino, S. (2001): *Deployable Structures*, Springer-Verlag Wien, New York;
Pinero, E. P. (1961): *Project for a mobile theatre*, Architectural Design, vol. 12, pp. 154-155;
Pirs SA.: *Images of inflatable formwork concrete construction and structure,* courtesy of PIRS SA:,sources:http://www.domepirs.com/img_gonflage2.jpg;http://www.domepirs.com/img_ferrailbeton.jpg;http://www.domepirs.com/img_poisson3.jpg;
Pugh, A. (1976): *An Introduction to Tensegrity*, Berkeley, California: University of California Press;
Robbin, T. (1996) *Engineering a New Architecture,* Yale University Press, London;
Roessler, S.R., Bini, D. (1986): *The Binishell system - Thin Shell Concrete Domes*, Concrete International, Vol January;
Rosenberg, D. (2010): *Designing for Uncertainty: Novel Shapes and Behaviors using Scissor Pair Transformable Structures*, MSC dissertation at the MIT Computation Group;
Sadler, S. (2005): *Archigram Architecture without Architecture,* Cambridge, MIT Press;
Snelson, K. (2009): *Forces made visible*, Hudson Hills Press LLC;
Sobek, W. (1999): *Art of Engineering*, Bales, Boston, 1999;
Tibert, G. (2002): *Deployable Tensegrity Structures for Space Applications*, Doctoral Thesis for the Royal Institute of Techn. Dpt. of Mechanics
Tillner, S. (2003): *Mobile Hofüberdachung in Wien,* Deutsche Bauzeitschrift, Wien, 4/2003, S. pp 48-53;
Walter, M. (2006): *Convertible Roofs*, Kurs 4:Numerische Optimierung und Formfindung – Realisierung an einem Membrantragwerk, Ferienakademie;
Whitehead, I. (2000): *Steel mesh and engineering wizardry unfold into a dome*, Architectural Record, 2000.oct. pp. 79-80;
Yahoo (2010): *Photo of the Fukuoka Dome* source: http://www.sswnews.com/images/dykt/yahoo 20Dome.jpg;
You, Z., Pellegrino, S. (1997): *Foldable bar structures*, Int J. Solids Struct, vol. 34(15), pp. 1825-1847;
Zeigler, T. R. (1976): *Collapsable self-supporting structures*. Us Patent No.3,968,808.

Noémi Friedman (1976) civil engineer, MSc, researcher assistant fellow at the Department of Structural Engineering, Budapest University of Technology and Economics. After her master studies in Budapest, she was enrolled in a master program (DEA MaiSE) at ENS de Cachan, France. Recently she is working on her PhD degree parallel at ENS de Cachan and Budapest University of Technology and Economics. Her research field of interest is the architectural application of deployable and retractable structures and its non-linear numerical modelling. Her main research topic is the numerical modelling problems of self-locking and pop-up systems.

Prof. György Farkas (1947) civil engineer, post-graduated in engineering mathematics, PhD, professor, co-head of the Department of Structural Engineering at the Budapest University of Technology and Economics. Research fields: modelling and strengthening of reinforced and prestressed concrete structures, post-tensioned floor slabs, structural dynamics, HSC/HPC structures. Member of the Hungarian Group of ***fib***.

SURFACE HARDNESS AND RELATED PROPERTIES OF CONCRETE



Katalin Szilágyi – Adorján Borosnyói – István Zsigovics

The theoretical hardness research was initialized by the pioneering work of Heinrich Hertz in the 1880s and the research on hardness of materials has been very dynamic from the beginning up to present day. Hardness testing practice of concrete exclusively applies nowadays the dynamic rebound surface hardness testing devices (e.g. the Schmidt rebound hammers that are appeared in the 1950s). During dynamic hardness measurements the inelastic properties of concrete may be as important as the elastic properties due to the softening fashion of the material response. Objectives of present experimental studies were to thoroughly investigate normal-weight hardened concrete specimens by dynamic and static hardness testing devices on a wide range of compressive strength and age of concrete at testing; and to compare the measured hardness results with Young's modulus and compressive strength values of the same concretes to be able to support the better understanding of hardness of porous solid materials. Results demonstrated that the rebound hammers provide hardness information connected to both elastic and inelastic properties of the surface layer of concrete that can not always be related directly to the compressive strength of concrete. The impact energy of the rebound hammers can result an inelastic response in the case of high water-cement ratios and a mostly elastic material response in the case of low water-cement ratios. Therefore, the rebound hammers provide a hardness value for high strength concretes connected to the Young's modulus of concrete rather than the compressive strength.

Keywords: concrete, surface hardness, rebound, indentation, strength, Young's modulus

1. INTRODUCTION

Concrete is a structural material used most widely and in the highest amount for building, bridge and road construction. The most important material property of hardened concrete is the compressive strength for the civil engineer. Several different non-destructive testing (NDT) methods were developed to estimate the strength of concrete in structures. The NDT methods and the operation of the testing devices are remarkably varied, but the common characteristic of them is that the structures can be directly tested and the strength of concrete can be estimated from the measured results with limited reliability.

Hardness testing was the first material testing practice from the 1600s in geology and engineering through the scratching hardness testing methods (Barba, 1640; Réaumur, 1722; Mohs, 1812); appearing much earlier than the systematic material testing that is considered to be started in 1857 when David *Kirkaldy*, Scottish engineer set up the first material testing laboratory in London, Southwark (Timoshenko, 1951; Szymanski, 1989). The theoretical hardness research was initialized by the pioneering work of Heinrich *Hertz* in the 1880s (Hertz, 1881). Hertz's proposal formed also the basis of the indentation hardness testing methods by Brinell, 1900; Rockwell, 1920; Vickers, 1924 and Knoop, 1934 (Fisher-Cripps, 2000).

Hardness testing practice of cementitious materials – such as concrete – exclusively applies nowadays the dynamic rebound surface hardness testing devices (e.g. the Schmidt rebound hammers that are appeared in the 1950s), rather than devices of plastic indentation hardness testing methods. Rebound hammers can be used very easily and the measure of hardness (i.e. the rebound index) can be read directly on the display of the testing devices. The rebound hammers give information about the elastic and damping properties of the surface layer of concrete that can not be necessarily related directly to the strength of concrete. It was demonstrated recently that the analysis of rebound hammer test data and strength estimation need special considerations for which purpose no general theory was available until now (Szilágyi et al, 2011b).

2. THEORETICAL CONSIDERATIONS

The scientific definition of hardness has been of considerable interest from the very beginning of hardness testing, however, still today – more than 100 years after Hertz's original proposal – no absolute definition of hardness is available in material sciences. According to Hertz, hardness is the least value of pressure beneath a spherical indenter necessary to produce a permanent set at the centre of the area of contact. As Hertz's criterion has some practical difficulties, the hardness values defined by the practical methods usually indicate various different relationships between the indenter load and the tested specimen's resistance to penetration or permanent

deformation. The intention to understand and explain hardness or determine a material property that can be estimated from hardness measurements induces even philosophical questions sometimes: Is hardness a material property at all? Does compressive strength exist?

If one accepts the practical conclusion that a *hard* material is one that is unyielding to the touch, it can be evident that steel is *harder* than rubber (O'Neill, 1967). If, however, hardness is considered as the resistance of a material against *permanent* deformation then a material such as rubber would appear to be 'harder' than most of the metals: the range over which rubber can deform elastically is very much larger than that of metals. If one focuses on hardness testing, it can be realized that elastic properties play a very important part in the assessment of hardness for rubber-like materials, however, for metals the deformation is predominantly outside the elastic range and involves mostly plastic properties (although the elastic moduli are large, but the range over which metals deform elastically is relatively small).

Plastic deformation is normally associated with ductile materials (e.g. metals). Brittle materials (e.g. concrete) generally exhibit elastic behaviour, and fracture occurs at high loads rather than plastic yielding. Pseudo-plastic deformation is observed in brittle materials beneath the point of an indenter, but it is a result of densification, where the material undergoes a phase change as a result of the high value of compressive stress in a restrained deformation field beneath the indenter. The softening fashion of the pseudo-plastic material response with increasing volume of the material is considerably different from that can happen to metals during plastic deformation (where the *volume* of the material is *unchanged* during yielding).

In some cases, particularly on dynamic hardness measurements, the elastic properties may be as important as the inelastic properties of the material.

3. METHODS

Present paper summarizes experimental results mostly concentrated on dynamic hardness testing of concrete as well as compressive strength and Young's modulus measurements. Dynamic hardness tests were carried out by Original Schmidt rebound hammers of L-type and N-type, Silver Schmidt hammer of N-type as well as with a Wolpert Leeb hardness tester with D-type impact device.

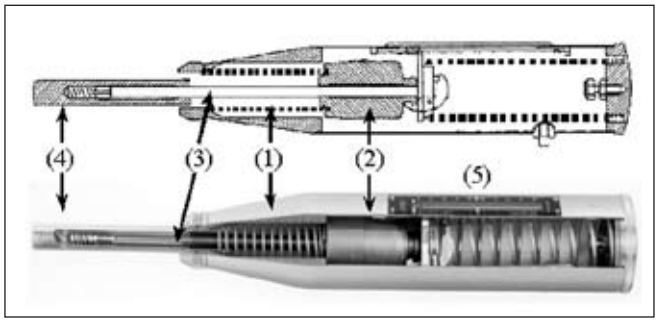

Fig. 1: Parts of the Schmidt rebound hammer.
(See notation in the text)

In the Schmidt rebound hammer (as can be studied in *Fig. 1*) a spring (1) accelerated mass (2) is sliding along a guide bar (3) and impacts one end of a steel plunger (4) of which far end is compressed against the concrete surface. The impact energy is constant (0.735 Nm, 0.883 Nm, 2.207 Nm and 29.43 Nm for L-, P-, N- and M-type rebound hammers, respectively; Proceq, 2003) and independent from the operator, since the tensioning of the spring during operation is automatically released at a maximum position causing the hammer mass to impinge with the stored elastic energy of the tensioned spring. The hammer mass rebounds from the plunger and moves an index rider (5) before returning to zero position. Original Schmidt rebound hammers record the rebound index (R): the ratio of paths driven by the hammer mass before impact and during rebound; see Eq. (1). Silver Schmidt hammers can record also the square of the coefficient of restitution (referred as Q-value): the ratio of kinetic energies of the hammer mass just before and right after the impact (E_0 and E_r, respectively); see Eq. (2).

$$R = \frac{x_r}{x_0} \cdot 100 \tag{1}$$

$$Q = \frac{E_r}{E_0} \cdot 100 = \frac{v_r^2}{v_0^2} \cdot 100 = C_R^2 \cdot 100 \tag{2}$$

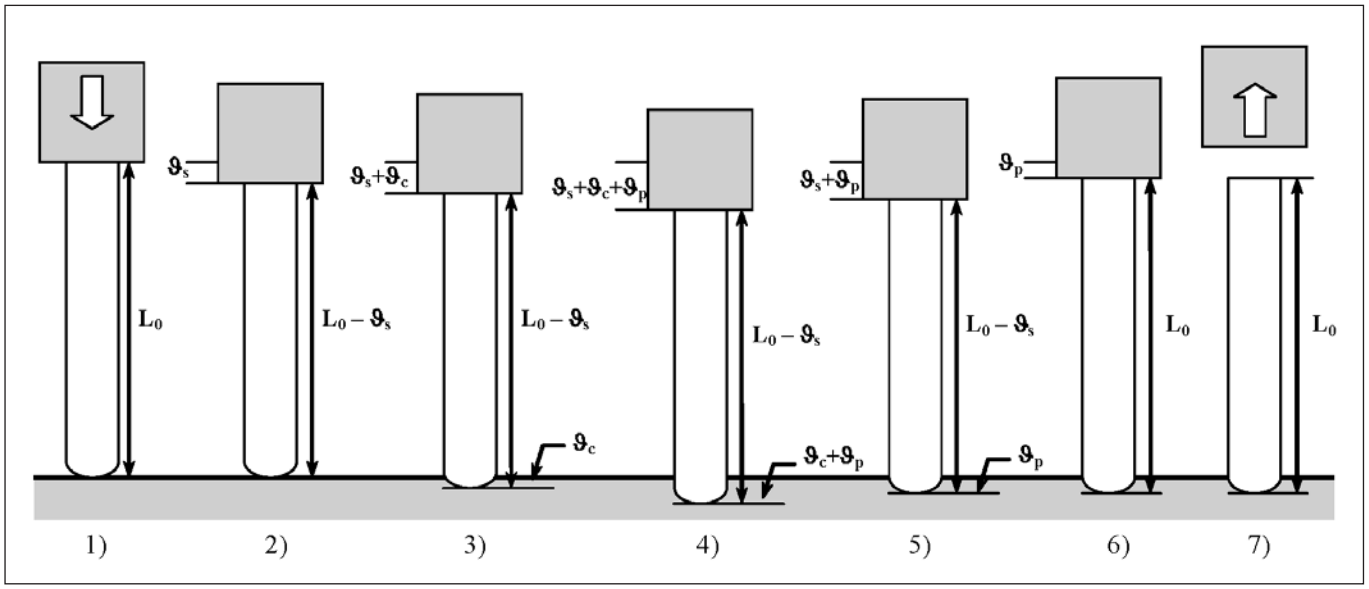

Fig. 2: Phases of the Schmidt rebound hammer test.
1) Collision of the hammer mass to the plunger 2) Elastic deformation of the plunger 3) Elastic deformation of concrete 4) Local crushing of concrete 5) Release of elastic deformation of concrete 6) Release of elastic deformation of the plunger 7) Rebound of the hammer mass (Notations: L_0 – initial length of the plunger, ϑ_s – elastic deformation of the plunger, ϑ_c – elastic deformation of concrete, ϑ_p – local crushing (pseudo-plastic deformation) of concrete).

In Eqs. (1) and (2) x_0 and v_0 indicate the path driven and the velocity reached by hammer mass *before impact*, while x_r and v_r indicate the path driven and the velocity reached by hammer mass *after impact*, respectively.

The phases of the Schmidt rebound hammer test can be seen in *Fig. 2*. When the hammer mass impinges on the plunger, a compression stress wave starts to propagate toward the concrete within the plunger. The plunger deforms elastically during the stress wave propagation. When the compression stress wave reaches the fixed end of the plunger (i.e. the concrete), part of the energy is absorbed in the concrete and the rest of the stress wave is reflected back in the plunger. The reflected compression wave returns to the free end of the plunger and accelerates the hammer mass to rebound. The absorbed energy at the fixed end results both elastic and pseudo-plastic deformations (local crushing) of the concrete. When the acceleration of the plunger is brought to rest the elastic deformation of the concrete recovers, however, a residual set is formed in the concrete under the tip of the plunger.

It can be demonstrated by an elastic numerical analysis that the compression stress wave is reflected up and down within the plunger several times before the hammer mass is brought to rest. *Fig. 3* summarizes the compressive stresses at the free end (i.e. at the collision of the hammer mass) and at the fixed end (i.e. at the concrete) of the plunger of an N-type Schmidt rebound hammer based on the assumptions made by *de Saint-Venant* (Timoshenko, 1951). In the calculations the following input data were used: mass of the striker $m_1 = 0.38$ kg; mass of the plunger $m_2 = 0.099$ kg; velocity of the striker at the moment of the impact $v_0 = 2.4$ m/s (Granzer, 1970; Proceq, 2003). The initial peak of the compression stress wave is calculated to be $\sigma_0 = 95.1$ N/mm^2, therefore the maximum peak of the compression stress wave at the fixed end of the plunger becomes $\sigma_{max} = 3.188 \times 95.1 = 303.2$ N/mm^2. If the transmission coefficient at the steel-concrete interface is assumed to be $C_t \approx 0.4$ then the compressive stress in the concrete is assumed to be $\sigma_c = 121.3$ N/mm^2. It can be also found in *Fig. 3* that the time of the impact (i.e. the time needed for the hammer mass to be brought to rest and rebound back) is $t_r = 106.4$ μs (based on the calculated value of stress wave propagation time through the plunger in one direction being $t_0 = 36.8$ μs).

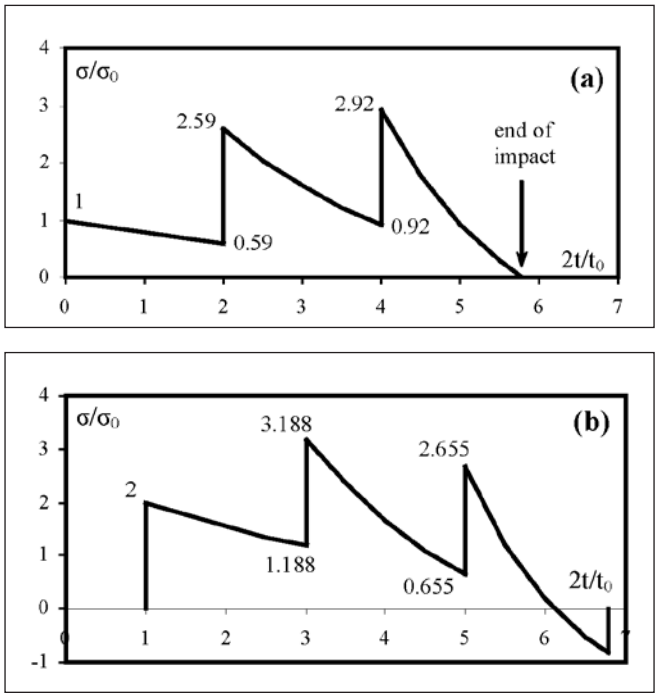

Fig. 3: *Theoretical compressive stresses in time for the free end (a) and the fixed end (b) of the plunger of an N-type Schmidt rebound hammer based on elastic numerical analysis (Remark: $t_0 = 36.8\ \mu s$ is the calculated value of stress wave propagation time through the plunger in one direction).*

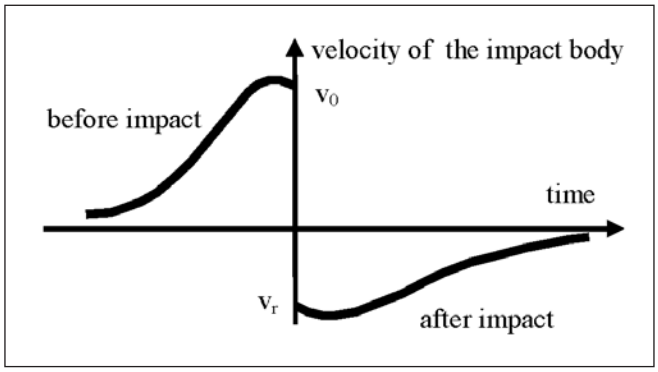

Fig. 4: *The definition of Leeb Hardness, HL.*

It can be also realized that no plastic deformation occurs within the plunger during the impact as the velocity of the hammer mass at the moment of the impact $v_0 = 2.4$ m/s is much lower than the velocity would be needed to initiate plastic stress waves being $v_{crit} = f_y/\rho c_0 = 12.2$ m/s (where the yield stress of the steel plunger is $f_y = 500$ N/mm^2; density of steel is $\rho = 7850$ kg/m^3; velocity of wave propagation is $c_0 = 5200$ m/s) (Johnson, 1985).

The measurement mechanism of the Wolpert Leeb hardness tester used is much simpler than that of the concrete rebound hammers (Wolpert, 2006). A mass is accelerated by a spring toward the surface of a test object and impinges on it at a defined velocity, i.e. kinetic energy. The measurement is implemented by means of an impact body which has a spherical tungsten-carbide tip. The velocities before and after the impact are both measured in a non-contact mode by a small permanent magnet within the impact body which generates an induction voltage during its passage through a coil. The voltage recorded is proportional to the velocity of the impact body (*Fig. 4*). The Leeb Hardness, HL is defined as the multiple of the coefficient of restitution, Eq. (3):

$$HL = C_R \cdot 1000 = \frac{v_r}{v_0} \cdot 1000 \qquad (3)$$

In Eq. (3) v_0 indicates the velocity reached by the impact body *before impact*, while v_r indicates the velocity reached by the impact body *after impact*, respectively.

The within test variation for the Leeb Hardness, HL values is generally expected to be lower than that of the concrete rebound hammer devices (for which the within test standard deviation of rebound index, $s_R = 1.5$ to 5.5 and the within test coefficient of variation $V_R = 5$ to 20% can be assumed by ACI 228.1R-03, 2003). On the other hand, the D-type impact device of the Wolpert Leeb hardness tester has much smaller weight ($m = 5.5$ g) compared to the hammer mass of the concrete rebound hammers as well as the tip of the device ($\varnothing = 3$ mm) provides much smaller contact area during impact, therefore, the within test variation of the measured values may be increased by the inhomogeneity of the concrete surface tested.

It can be also highlighted that the coefficient of restitution is a material property of which value strongly depends on the severity of the impact itself. At sufficiently low impact velocities (when no plastic or pseudo-plastic deformation of the tested surface occurs during the impact) the deformation is elastic and the coefficient of restitution is very nearly equal to unity. However, it is clear that most impacts involve some plastic deformation also in the case of metals (e.g. for

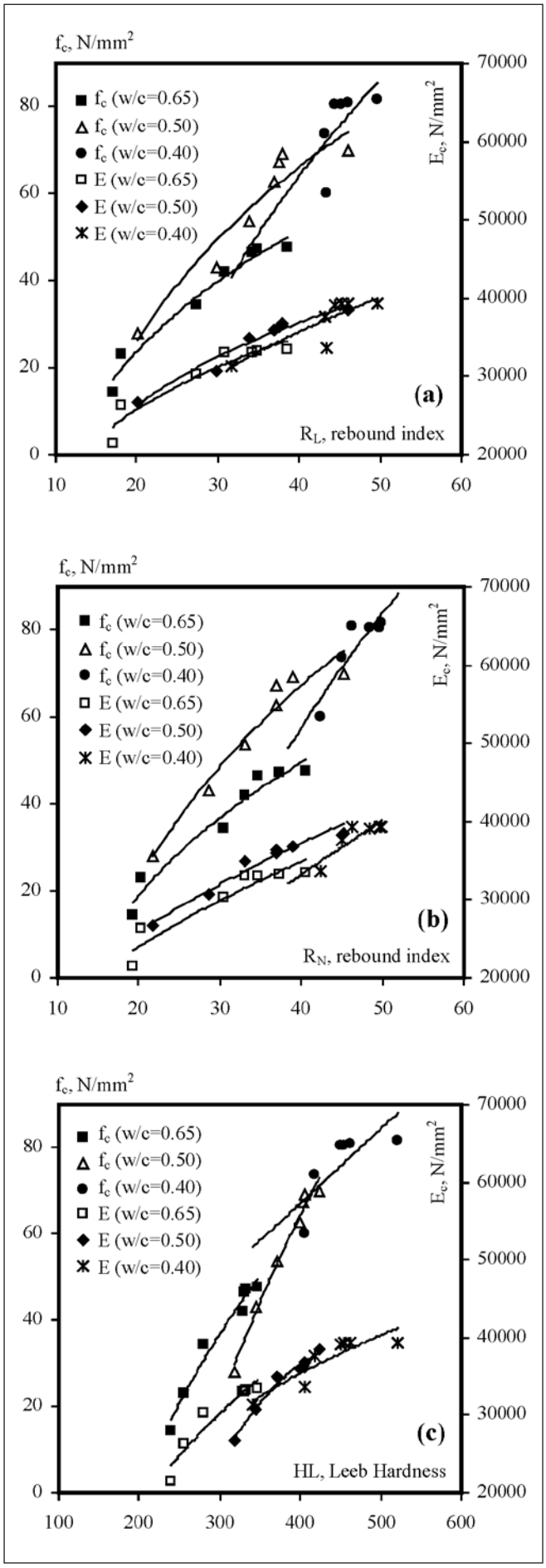

Fig. 5: *Relationships between dynamic hardness and compressive strength as well as Young's modulus of concrete.*

a) L-type Schmidt rebound hammer
b) N-type Schmidt rebound hammer
c) Wolper Leeb hardness tester

a medium of hard steel with f_y = 1000 N/mm² the impact velocity needed for a residual set is $v_y \approx 0.14$ m/s; Johnson, 1985). The coefficient of restitution gradually decreases with increasing impact velocity. The theory suggests that the coefficient of restitution is proportional to $v^{-1/4}$ when a fully plastic indentation is obtained (Johnson, 1985).

Static hardness tests were also carried out in present experimental programme as a comparison to the dynamic hardness tests. Static indentation tests were performed by a Brinell testing device with ball diameter of 10 mm. Testing loads of 1.875 kN to 30 kN were applied for 30 seconds on the concrete surfaces.

4. SIGNIFICANCE AND OBJECTIVES OF PRESENT STUDIES

The development of the surface hardness of concrete in time due to the development of the concrete compressive strength as well as the surface carbonation of concrete have promoted an extensive theoretical and laboratory research with the purpose of development and possible simplification of the theory and testing of surface hardness of concrete. Objectives of present experimental studies were on one hand to thoroughly investigate normal weight hardened concrete specimens by dynamic and static hardness testing devices on a wide range of compressive strength and age of concrete at testing; and on the other hand, to compare the measured hardness results with Young's modulus and compressive strength values of the same concretes. The main purpose of the studies is to provide experimental evidence – if any – between the relationship of dynamic and static hardness values for concretes as well as with compressive strength and elastic properties of concrete to be able to support the better understanding of hardness of porous solid materials.

5. EXPERIMENTS

An experimental programme was completed on a wide range of compressive strength of normal weight concretes in the Budapest University of Technology and Economics (BME), Department of Construction Materials and Engineering Geology, to study the hardness behaviour.

Concrete was mixed from Danube sand and gravel using CEM I 42.5 N cement with w/c ratios of 0.40, 0.50 and 0.65. Consistency of the tested concrete mixes was 500±20 mm flow. Design air content of the compacted fresh concretes was 1.0 V%.

The specimens were cast into steel formworks and the compaction of concrete was carried out by a vibrating table. The specimens were stored under water for 7 days as curing. After 7 days the specimens were stored at laboratory condition (i.e. 20±3°C temperature and 65±5% relative humidity). Tests were performed at the age of 3, 7, 14, 28, 56, 90 and 240 days. 150 mm cube specimens and 120×120×360 mm prism specimens were prepared for the experiments.

The measurement methods were introduced in the foregoing chapters.

Altogether twenty individual rebound hammer test teadings were recorded with every type of Schmidt hammer just before the compressive strength test.

The measurements were carried out in horizontal direction on two parallel vertical sides of the 150 mm cube specimens

restrained into a hydraulic copressive strength tester. Leeb scleroscope tests were carried out on the 120×120×360 mm prism specimens just after the completion of the Young's modulus measurements. Altogether 120 readings were taken on the moulded side surfaces of each specimen.

For the static hardness measurements five individual tests were carried out and five residual impressions were prepared by the Brinell testing device at each load level. Tests were carried out on the 120×120×360 mm prism specimens. Diameters of the residual impressions were measured by a hand microscope of 8× magnification.

6. EXPERIMENTAL RESULTS

6.1 Dynamic hardness

Due to the adequate restraining action on the 150 mm cube specimens that were tested in present experiments with the Schmidt rebound hammers, the within test standard deviation and the within test coefficient of variation became s_R = 2.3 and V_R = 6.3%, respectively, so the measurements can be considered to be rather accurate. Due to the unusually high number of the Leeb Hardness, HL measurement repetitions in present experiments the Leeb Hardness, HL values can be also considered to be available rather accurately.

Concrete compressive strength is represented as a function of the rebound index as well as the Leeb Hardness, HL for the applied water-cement ratios (w/c = 0.40, 0.50 and 0.65, respectively) in *Fig. 5*. The fashion of the regression curves confirms the existence and the validity of the SBZ-model (Szilágyi et al, 2011b). *Fig. 5* also represents the Young's modulus of concrete as a function of the rebound index as well as the Leeb Hardness, HL to study the relationship of the surface hardness and elastic properties. Results seem to indicate that the relationship between rebound index and Young's modulus of concrete is independent from the water-cement ratio, however, in the case of the Leeb Hardness, HL dependency on the water-cement ratio is visible.

6.2 Static indentation hardness

In the representation of the static indentation test results the power functions between the indenter load (F) and the residual impression diameter (d) are formulated in *Fig. 6* for w/c = 0.50 as an example. The proposed functions have the form of $F = a \times d^n$, where the empirical parameters *a* and *n* are material properties as it was demonstrated for metals (Meyer, 1908). Further details of the static hardness results can be found elsewhere (Szilágyi et al, 2011a).

6.3 Time dependency of results

In *Fig. 7* the relative values (referring to the values obtained at the age of 7 days) of all tested parameters are represented in time. The time dependency of the hardness properties, compressive strength and Young's modulus can promote to discover new relationships that can help to understand the material behaviour during surface hardness testing.
Results demonstrated that all the properties represented in time depend on the water-cement ratio.

7. DISCUSSION OF RESULTS

A close correlation can be supposed to exits between two material properties if the development of their relative values in time is identical or very similar.

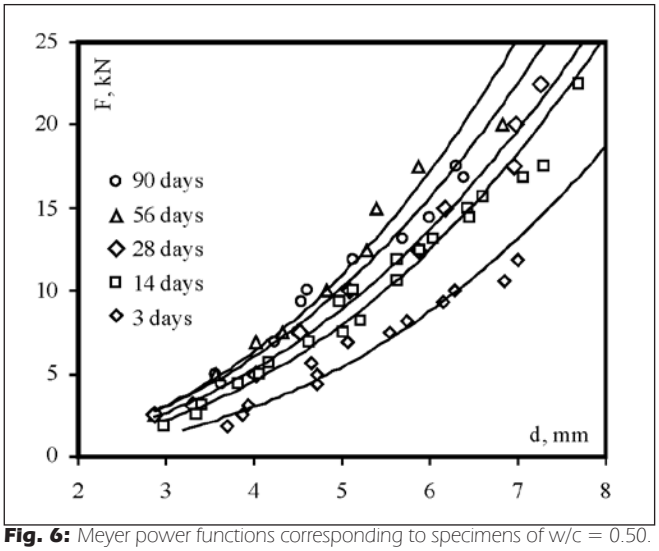

Fig. 6: Meyer power functions corresponding to specimens of w/c = 0.50.

Fig. 7 clearly shows that the different surface hardness methods result different material responses, therefore, different material properties can be estimated by the surface hardness values. In the case of the Leeb Hardness, HL measurements very low impact energy is introduced to the tested surface and the material response is mostly governed by the elastic properties of the tested material. Indeed, it can be realized in the graphical representation that the Leeb Hardness, HL values in time coincides exactly with the Young's modulus of concrete in time, on a wide range of compressive strength, and independently of the applied water-cement ratio or age at testing.

The static indentation response can be considered as the other boundary in the surface hardness behaviour. During testing always considerable residual deformation takes place under the ball indenter and not only local densification occurs in the concrete but also cone cracks are formed under very high testing loads. The material response is mostly governed by the inelastic properties of the material. Indeed, it can be realized in the graphical representation that the Brinell Hardness, HB values in time coincides rather with the compressive strength of concrete in time, on a wide range of compressive strength, and independently of the applied water-cement ratio or age at testing.

The Schmidt rebound hammers apply much higher impact energy (both the L-type and the N-type devices) than the Wolpert Leeb hardness tester, therefore, the material response can be inelastic in a much more pronounced way; strongly depending on the actual strength and stiffness of the concrete. Present results clearly demonstrated that the impact energy of the Schmidt rebound hammers can result a pseudo-plastic response in the case of high water-cement ratio (i.e. low concrete compressive strength). One can realize in *Fig. 7.a* that the represented R_L and R_N rebound index values in time both coincide exactly with the compressive strength of concrete in time, independently of the age at testing. Present results also revealed that the impact energy of the Schmidt rebound hammers can result a mostly elastic material response in the case of low water-cement ratio (i.e. high concrete compressive strength). It can be realized in *Fig. 7.c* that the represented R_L and R_N rebound index values in time both coincide rather well with the Young's modulus of concrete in time, independently of the age at testing. For the medium strength concretes an intermediate behaviour can be studied in *Fig. 7.b*.

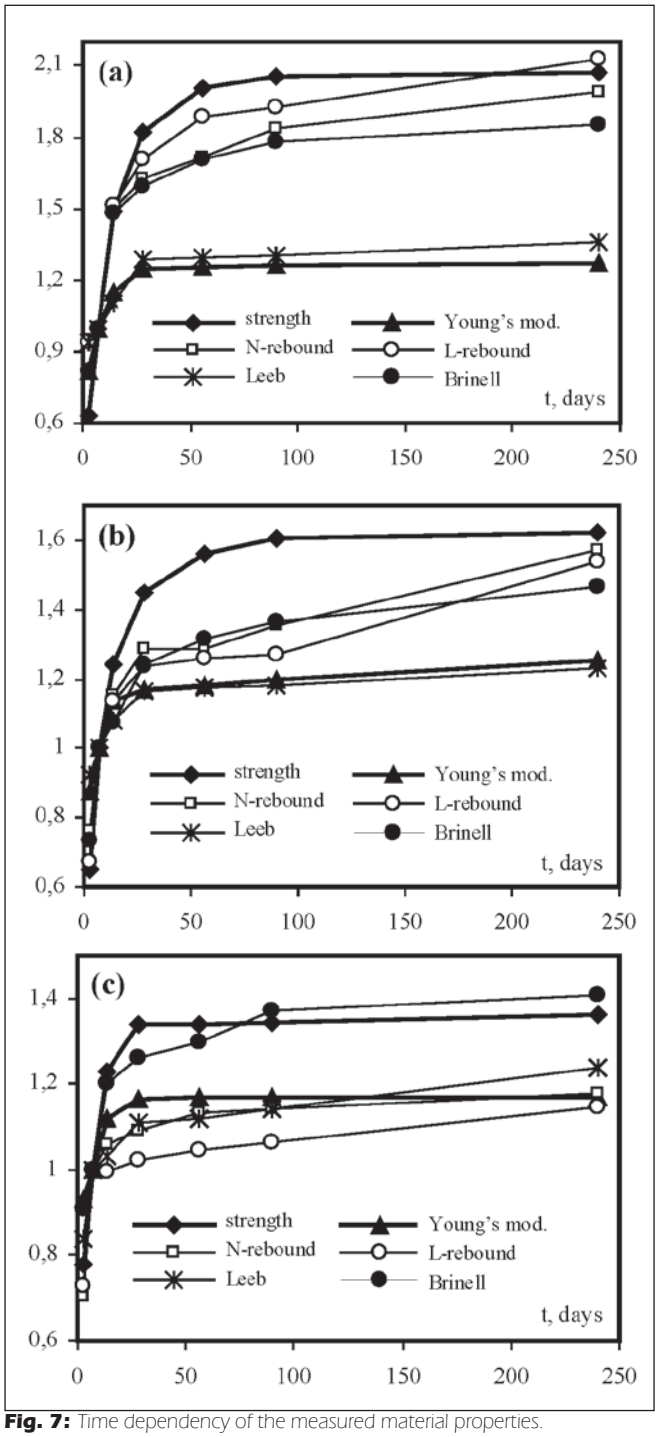

Fig. 7: *Time dependency of the measured material properties.*

a) w/c = 0.65
b) w/c = 0.50
c) w/c = 0.40

8. OUTCOME OF RESULTS

Hardness testing of concrete exclusively applies nowadays the Schmidt rebound hammers that can be used very easily and the rebound index can be read directly on the display of the testing devices. Present experimental studies demonstrated that the rebound hammers provide hardness information connected to both elastic and inelastic properties of the surface layer of concrete that cannot always be related directly to the compressive strength of concrete.

For relatively low strength concretes the devices could provide a hardness value that can be correlated to the compressive strength of concrete, thus the strength estimation is theoretically possible. This conclusion is also a tribute before the genius of *Ernst Schmidt*, the inventor of the concrete rebound hammers, who has fit the impact energy of the hammers to the purpose of concrete strength estimation through inelastic energy absorption under the tip of the testing device suitable for concrete compressive strengths available in the 1950s.

On the other hand, the concrete construction technology nowadays uses concretes of higher and higher compressive strengths (just as one example: a sufficiently performing self compacting concrete provides automatically higher compressive strength than a conventional concrete of the same water-cement ratio). For high strength concretes the Schmidt rebound hammers could not provide a hardness value that can be correlated to the compressive strength of concrete, thus the strength estimation is impossible. Recent theoretical and experimental studies confirmed this conclusion that can be also demonstrated by the very steep rebound index vs. compressive strength response available from the SBZ-model for high strength concretes (Szilágyi et al, 2011b).

Practitioners should take into consideration that for high strength concretes the Schmidt rebound hammers provide a hardness value connected to the Young's modulus of concrete rather than the compressive strength of the concrete and, therefore, the strength estimation is questionable. Let us refer here to the Young's modulus development in time that is considerably different from that of the compressive strength. *Fig. 8.* indicates the functions suggested by the CEB-FIP Model Code 1990. One can realize that the Young's modulus of concrete could not predict compressive strength for mature concrete.

9. CONCLUSIONS

Hardness testing was the first material testing practice in engineering; appearing much earlier than any systematic material testing. Hardness testing practice of concrete exclusively applies nowadays the dynamic rebound surface hardness testing devices for strength estimation: e.g. the Schmidt rebound hammers that are appeared in the 1950s. Rebound hammers can be used very easily and the measure of hardness (i.e. the rebound index) can be read directly on the display of the testing devices. By their original design, the Schmidt rebound hammers targeted to estimate the compressive strength of concrete through inelastic energy absorption during in-situ impact testing. The spring accelerated hammer mass of the devices was fit to provide adequate impact energy to result inelastic deformation in the tested concrete (of which expected compressive strength was much lower at that time than the compressive strength of concretes nowadays used in

Fig. 8: *Time dependency of compressive strength and Young's modulus of concrete according to the CEB-FIP Model Code 1990.*

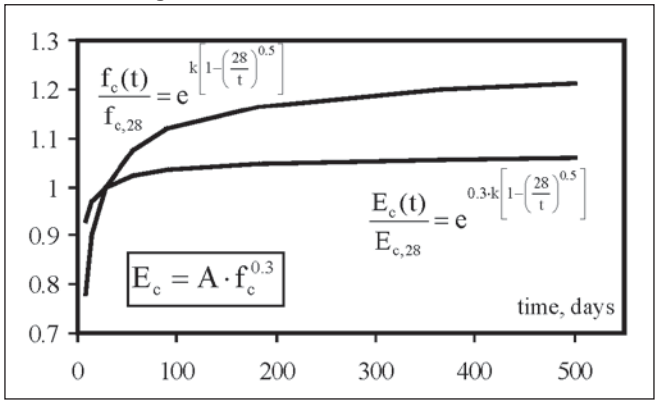

concrete construction). A rigorous experimental analysis was carried out in the Budapest University of Technology and Economics (BME), Department of Construction Materials and Engineering Geology, to examine the hardness behaviour of concrete. Several dynamic and static hardness testing methods were studied on a wide range of compressive strengths and the results were compared to Young's modulus and compressive strength measurements. Results clearly demonstrated that the Schmidt rebound hammers could provide a hardness value that can be correlated to the compressive strength of concrete only if the compressive strength is relatively low. It was confirmed for high strength concretes that the Schmidt rebound hammers provide a hardness value that can be correlated to the Young's modulus of concrete rather than the compressive strength, thus the strength estimation of high strength concretes is impossible with the Schmidt rebound hammers.

10. ACKNOWLEDGEMENTS

The authors appreciate the help of Mr. Kristóf *Dobó* during laboratory measurements and evaluations. Special thanks to Mr. Gábor *Kovács* for his valuable help during the laboratory tests.

11. REFERENCES

ACI (2003) "In-Place Methods to Estimate Concrete Strength", ACI 228.1R-03, American Concrete Institute, Farmington Hills, Michigan

Barba, A. A. (1640) "Arte de los metales", Reprint, Lima, 1817

CEB (1993) "CEB-FIP Model Code 1990 – Design Code", Comité Euro-International du Béton, Thomas Telford, London, 1993 (CEB Bulletin d'Information No. 213/214.)

Fischer-Cripps, A. C. (2000) "Introduction to Contact Mechanics", Springer, New York, 2000, 243 p.

Granzer, H. (1970) „Über die dynamische Härteprüfung von Beton mit dichtem Gefüge", Dissertationen der Technischen Hochschule Wien, No. 14, Verlag Notring, Wien, 1970, p. 103.

Hertz, H. (1881) „Über die Berührung fester elastischer Körper". *J Reine Angew Math* 1881;5:12-23.

Johnson, K. L. (1985) "Contact mechanics", Cambridge University Press, 1985, 452 p.

Meyer, E. (1908) „Untersuchungen über Härteprüfung und Härte", *Zeitschrift des Vereines Deutscher Ingenieure*, Vol. 52, No. 17, April 1908, pp. 645-654, 740-748, 835-844.

Mohs, F. (1812) „Versuch einer Elementar-Methode zur Naturhistorischen Bestimmung und Erkennung von Fossilien", Österreich Lexikon

O'Neill, H. V. (1967) "Hardness measurement of metals and alloys", Chapman & Hall, London, 1967, 238. p.

Proceq SA (2003) "Concrete Test Hammer N/NR,L/LR and DIGI SCHMIDT ND/LD – Rebound Measurement and Carbonation", Info sheet

Réaumur, R. A. F. (1722) "L'art de convertir le fer forgé en acier", French Academy of Sciences, Paris, 1722

Szilágyi, K., Borosnyói, A., Dobó, K., (2011a) „Static indentation hardness testing of concrete: A long established method revived", *Építőanyag*, Vol. 63. No. 1., 2011/1

Szilágyi, K., Borosnyói, A., Zsigovics, I. (2011b) „Rebound surface hardness of concrete: Introduction of an empirical constitutive model", *Construction and Building Materials*, Vol. 25, Issue 5, May 2011, pp. 2480-2487.

Szymanski, A., Szymanski, J. M. (1989) "Hardness estimation of minerals, rocks and ceramic materials", Elsevier, Amsterdam, 1989, 330 p.

Timoshenko, S. P. (1951) "History of strength of materials", McGraw-Hill, New York, 1951, 452 p.

Wolpert Wilson Instruments (2006) "WHL-380 Masster Testor", Info sheet

Katalin Szilágyi (1981) civil engineer (MSc), PhD candidate at the Department of Construction Materials and Engineering Geology, Budapest University of Technology and Economics. *Main fields of interest:* diagnostics of concrete structures, non-destructive testing of concrete, concrete technology, shrinkage compensation of concretes. Member of the Hungarian Group of *fib*.

Dr. Adorján Borosnyói (1974) civil engineer (MSc), PhD, associate professor at the Department of Construction Materials and Engineering Geology, Budapest University of Technology and Economics. *Main fields of interest:* application of non-metallic (FRP) reinforcements for concrete structures, bond in concrete, non-destructive testing of concrete. Member of the Hungarian Group of *fib* and of *fib* TG 4.1 „Serviceability Models".

Dr. István Zsigovics (1949) civil engineer (MSc), PhD, senior lecturer at the Department of Construction Materials and Engineering Geology, Budapest University of Technology and Economics. *Main fields of interest:* concrete technology, self-compacting concretes, diagnostics of concrete structures, non-destructive testing of concrete. Member of the Hungarian Group of *fib*.

VERIFICATION OF THE ULTIMATE LIMIT STATE REQUIREMENTS FOR CONCRETE MEMBERS BY THE USE OF THE GLOBAL SAFETY FACTOR FORMAT


Kálmán Szalai - Tamás Kovács

One half century of Hungarian and almost two decades of European Union experience in the application of the partial safety factor method in structural design led to the conclusion that, in particular cases for recently designed structures and especially for laboratory and on-site investigations of existing structures, the use of the global safety factor format is more advantageous for reliability verification than the recently applied partial safety factor format.

Keywords: reliability, safety, safety factor, action, effect, resistance, reliability index, coefficient of variation, design value, sensitivity factor

1. INTRODUCTION

This paper introduces and then compares two safety formats, which are used for reliability verification of load carrying structures.

One of them is the well-known partial safety factor format, which was implemented in the Hungarian design codes in the early fifties and later adopted by the Eurocode (EC). In complex load cases, particularly when an action simultaneously affects both the action and the resistance-side of the relevant design requirement (e.g. the self-weight of earth for the design of cantilever-type (retaining) walls), the application of the partial safety factor format becomes very complicated and difficult. Another problem arises for the supervision of existing structures. In this latter case, the partial safety factors, which are recommended for newly-built structures and fixed by the relevant design codes, may be lowered because the majority of uncertainties related to the geometrical, strength and, sometimes, loading parameters (design variables) are eliminated owing to the on-site measurability of their statistical properties. However, the specified reliability level covers not only the uncertainties of design variables but also the uncertainties related to the applied calculation model. Therefore, in order to determine the reasonable degree of reduction in partial safety factors for existing structures, the uncertainties included in the partial factors have to be separated.

In the above cases, if modifying the partial safety factor format by expressing the required reliability level by only one global safety factor and then verifying the ultimate limit state requirements by the corresponding global safety factor format, the design procedure becomes more practical and transparent. A limited application of this format, in which the partial risk of only the structural resistance was expressed by one γ_R safety factor, was proposed as "global resistance format" by the recently published *fib* Model Code 2010 (*fib*, 2010).

2. RELIABILITY BACKGROUND OF THE PARTIAL SAFETY FACTOR FORMAT

Reliability analyses of load carrying structures based on minimum life-cycle cost found the optimum risk against ultimate failure as $p_{RE} \approx 10^{-4}$, to which a reliability index of $\beta=3.719$ belongs (Kármán, 1965; Mistéth, 2001). The value-pair of sensitivity factors α_E and α_R associated with equality in the basic design requirement for ultimate limit state (ULS) $R_d(t) = E_d(t)$ may generally be approximated as $\alpha_E = -0.6$ and $\alpha_R = 0.8$ (thus $\alpha_E^2+\alpha_R^2=0.36+0.64=1.0$). (See notations in *Fig. 1* where s_R, s_E and s_{RE} are standard deviations (SD) characterizing the distribution of resistance $R(t)$, action $E(t)$ and their difference $R(t)$-$E(t)$, respectively. Henceforth, for simplification, time t will not be indicated.)

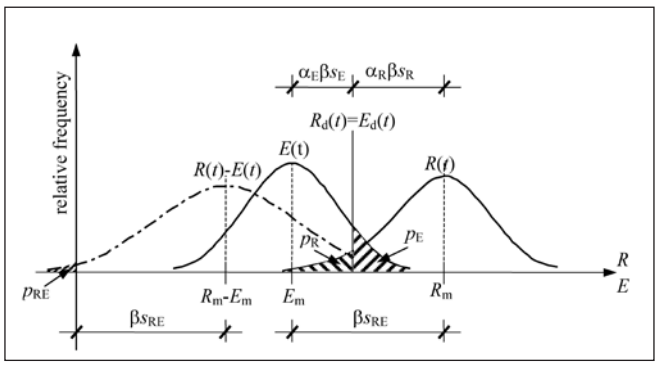

Fig. 1: Interpretation of the reliability index β

In providing background behind the applied partial safety factor format, the EC (EN, 2002) sets a minimum value of $\beta=3.8$ associated with RC2 class structures and 50 years of reference period, and recommends to take the values of sensitivity factors as $\alpha_E = -0.7$ and $\alpha_R = 0.8$. These latter values, which do not fulfil the $\alpha_E^2+\alpha_R^2=1.0$ condition, can be considered as safe-side

approximations of the above ones. The study in this paper is based on the reliability level set by the EC (β=3.8) and focuses on the calculation of the global safety factor together with the associated values of sensitivity factors.

2.1 Reliability interpretation of design values

Taking the assumption that the distribution function of both the action-side (E) and the resistance-side (R) of the basic ULS requirement follows the normal distribution and applying α_E= -0.6 and α_R=0.8 values of sensitivity factors, the partial risks belonging to the action-side and the resistance-side are resulted in $p_E \approx 1\%$ ($-\alpha_E\beta=0.6\times3.8=2.28 \rightarrow p_E=1.13\%$) and $p_R \approx 1‰$ ($\alpha_R\beta=0.8\times3.8=3.04 \rightarrow p_R=1.18‰$) according to the EC. By the use of a logarithmic transformation on the resistance-side for numerical reasons, the design values in the

$$R_d \geq E_d \tag{1}$$

basic ULS requirement can be formulated as follows:
the design value of resistance:

$$R_d = R_m \exp\left(\beta\alpha_R^{(+)}\nu_R\right) \tag{2a}$$

the design value of action:

$$E_d = E_m\left(1-\beta\alpha_E^{(-)}\nu_E\right). \tag{2b}$$

The global safety factor can be deduced from *Eq.(2a)* and *Eq.(2b)* as follows:

$$\gamma_{RE} = \exp\left(\beta\alpha_R^{(+)}\nu_R\right)\left(1-\beta\alpha_E^{(-)}\nu_E\right) \tag{2}$$

where ν_R and ν_E are the resulting coefficients of variation (COV) of the resistance-side and the action-side in *Eq.(1)*, respectively. When using the γ_{RE} global safety factor, *Eq.(1)* changes to

$$R_m \geq \gamma_{RE} E_m, \tag{3}$$

in which γ_{RE} makes direct relation between the *mean* value of resistance (R_m) and action (E_m).
Before demonstrating the practical application of *Eq.(3)*, the standardized procedure of the EC for the calculation of R_d and E_d will be introduced then the relationships between the partial safety factors and the respective COV values will be discussed in detail.

2.2 Calculation of design values according to the partial safety factor format applied by the EC

According to the combination rules of the EC, the design values in *Eq.(1)* in case of a prestressed concrete structural member are calculated as follows:

$$R_d = R\left(\frac{f_{ck}}{\gamma_c};\frac{f_{yk}}{\gamma_s};\frac{f_{pk}}{\gamma_p};L_d\right)\gamma_{Rd} \geq E_d = \cdots$$

$$= \gamma_{Sd}\max\begin{cases}\sum_{j\geq1}\gamma_G G_{kj} + \gamma_P P_k + \gamma_{Q1}\psi_{01}Q_{k1} + \sum_{i>1}\gamma_{Qi}\psi_{0i}Q_{ki} \\ \sum_{j\geq1}\xi\gamma_G G_{kj} + \gamma_P P_k + \gamma_{Q1}Q_{k1} + \sum_{i>1}\gamma_{Qi}\psi_{0i}Q_{ki}\end{cases} \tag{4}$$

where:

E_d – the design value of action(-side);
R_d – the design value of resistance(-side);
f_{ck}, f_{yk}, f_{pk} – characteristic value of concrete compression strength as well as of reinforcing and prestressing steel tensile strength, respectively, all defined as 5%-quantile values;
γ_c, γ_s, γ_p – partial (safety) factor for concrete, reinforcing and prestressing steel, respectively;
G_k, P_k Q_k – characteristic value of permanent action, prestressing and variable action, respectively, all assumed to be defined as mean values;
γ_G, γ_P, γ_Q – partial (safety) factor for permanent action, prestressing and variable action, respectively;
γ_{Rd}, γ_{Sd} – partial (safety) factor associated with the uncertainty of the applied resistance and action (and/or action effect) model;
L_d – design value of geometry defined as either nominal value or nominal value + imperfection depending on the significance of geometrical data on reliability;
ψ_0 – combination factor for variable action;
ξ=0.85 – reduction factor for unfavourable permanent actions.

2.3 Partial factors for resistance and their respective COV values

2.3.1 Background of partial factors for resistance

The probabilistic approach of the partial safety factor method is based on the assumption that the design value of resistance R_d, which, in the majority of cases, is typically a strength parameter, can generally be calculated as

$$R_d = R(f, m, G) \tag{5}$$

where f is the related strength, m means the uncertainty associated with the applied calculation model and G is the uncertainty associated with geometry[1]. The reliability-based design procedures further assume that all three variables (f, m and G) are independent random variables, and that at least f follows the normal distribution. The partial risk p_R set for resistance-side is fully covered by the γ_R partial safety factor, which transforms the related characteristic value R_k into the corresponding design value R_d. According to the EC, the characteristic value R_k is determined solely in statistical way as 5%-quantile value, and does not include any component in association with geometry- or model-related uncertainty.
For civil engineering structures, the resistance-side of *Eq.(4)* is usually governed by only one dominant resistance parameter. It means that the other non-dominant resistance parameters have only slight, thus, from probabilistic point of view, negligible

[1] The Hungarian standards did not account for uncertainties associated with calculation model and geometry therefore the corresponding partial safety factors for resistance were smaller than that in the EC.

effect on the whole resistance-side. Consequently, the design value of this dominant resistance parameter R_d has to cover the full partial risk p_R set for the resistance-side of *Eq.(4)*.
Taking the partial risk p_R=1.18‰ given in *Sec. 2.1* and assuming that the dominant resistance parameter (e.g. a material strength) R follows the normal distribution, the partial factor of R derives as

$$\gamma_R = \frac{1-1.645\,\nu_{Rf}}{1-3.04\,\nu_R}. \qquad (6)$$

Here

$$\nu_R = \sqrt{\nu_{Rf}^2 + \nu_{Rm}^2 + \nu_{RG}^2} \qquad (7)$$

where ν_{Rf} is the COV associated with strength (f) only, moreover ν_{Rm} and ν_{RG} are appropriately chosen (sometimes estimated) COV values covering the uncertainty of the applied calculation model (m) and geometry (G), respectively.

2.3.2 Components of the partial factor for concrete

According to (Soukov and Jungwirt, 1997), the partial factor for concrete compressive strength, which is set to γ_c=1.5 in the EC2 (EN, 2004) for usual permanent and transient design situations, is based on ν_{cf}=0.15, ν_{cm}=0.05 and ν_{cG}=0.05 COV values. Using *Eq.(7)*, the resulting COV for concrete is calculated as

$$\nu_c = \sqrt{\nu_{cf}^2 + \nu_{cm}^2 + \nu_{cG}^2} = \sqrt{0.15^2 + 0.05^2 + 0.05^2} = 0.166\,. \qquad (7a)$$

Furthermore, γ_c may be decomposed into two parts as follows

$$\gamma_c = \gamma_{cM1}\,\gamma_{cM2} \qquad (8)$$

where γ_{cM1} is related to strength and geometry and γ_{cM2} accounts for the uncertainty of the calculation model. By the use of a logarithmic transformation similar to that in *Eq(2a)*, the γ_{cM1} partial factor can be expressed as

$$\gamma_{cM1} = \exp(\alpha_R \beta \nu_c - 1.645\nu_{cf}) = 1.29\,. \qquad (9)$$

The γ_{cM1} may be further decomposed into γ_{cf} (strictly related to the statistical parameters of the distribution of strength) and γ_{cG} (related to geometry) as follows:

$$\gamma_{cM1} = \gamma_{cf}\,\gamma_{cG} \qquad (10)$$

where

$$\gamma_{cf} = \exp(\alpha_R \beta \nu_{cf} - 1.645\nu_{cf}) = 1.23 \qquad (11)$$

and

$$\gamma_{cG} = 1.29/1.23 = 1.05\,. \qquad (12)$$

Using the applied notations in *Eq.(7)*, γ_{cM2} accounting for the uncertainty of the applied calculation model is replaced by γ_{cm} and calculated as

$$\gamma_{cM2} = \gamma_{cm} = \gamma_c/\gamma_{cM1} = 1.5/1.29 = 1.16\,. \qquad (13)$$

As a conclusion of the above, the partial factor for concrete (γ_c) has obtained as

$$\gamma_c = \gamma_{cf}\,\gamma_{cG}\,\gamma_{cm} = 1.23\times1.05\times1.16 = 1.5\,. \qquad (14)$$

Out of the above three components, only γ_{cf} is related to statistical parameters of concrete strength, whose COV is assumed as ν_{cf} = 0.15 (see *Eq.(11)*). When ν_{cf}, which is determined from statistical analysis of strength data measured, for example on existing structures, deviates from 0.15 then both *Eq.(11)* and, consequently, γ_c changes. Assuming $\gamma_{cG}\times\gamma_{cm}$=1.05×1.16 as constant, the following relations between ν_{cf}, γ_{cf} and γ_c exist:

- if ν_{cf} = 0.20 then γ_{cf} = 1.32 and γ_c = 1.61,
- if ν_{cf} = 0.10 then γ_{cf} = 1.15 and γ_c = 1.40,
- if ν_{cf} = 0.05 then γ_{cf} = 1.07 and γ_c = 1.31 .

According to the EC2 (and to the Hungarian standard since the bauxite concrete "era"), when evaluating an *existing* concrete member, the γ_{cm} partial factor component (associated with the uncertainty of the calculation model) may be omitted (e.g. set to 1.0) thus

$$\gamma_c = \gamma_{cf}\,\gamma_{cG} = 1.29\,. \qquad (15)$$

When using *geometrically controlled test specimens* bored from an existing concrete member, the effect of geometry (and the associated partial factor component γ_{cG}) may be divided into two components. One component (γ_{cG1}) belongs strictly to geometrical sizes of the bored specimens which may be omitted if these sizes are controlled and considered accordingly during strength determination. Second component (γ_{cG2}) accounts for the deformation restraints of concrete unit being close to failure. The latter may significantly be different for a specimen bored out of a larger concrete block and then loaded uniaxially as well as for a concrete unit as part of a confined structural concrete member. In the above procedure, both parts are covered by ν_{cG} and the associated γ_{cG}. Their ratio should be the topic of other studies. To sum up the above, in case of strength determination carried out on geometrically controlled, bored test specimens, ν_c (γ_c) should include ν_{cf} (γ_{cf}) and the above second component of ν_{cG} (γ_{cG2}) (i.e. ν_{cf}=0.05 results in γ_{cf}=1,07, and $\gamma_c=\gamma_{cf}\,\gamma_{cG2}$). Nevertheless, the EC2 sets a minimum value equal to 1.3 for γ_c.

2.3.3 Components of the partial factor for reinforcing and prestressing steel

Although (Soukov and Jungwirt, 1997) does not address steel, a procedure similar to that in *Sec. 2.3.2* for γ_c can be conducted for the partial factor γ_s of (both reinforcing and prestressing) steel. The γ_s is set to $\gamma_s=(\gamma_p=)1.15$ in the EC2 for usual permanent and transient design situations, while the COV associated with steel strength is taken as ν_{sf}=0.05 in the relevant literature. Accounting for the corresponding COV values set for concrete in *Sec. 2.3.2*, the other two COV values for steel may be assumed as $\nu_{sm}=\nu_{sG}$=0.03. Thus, the resulting COV for steel is calculated as:

$$\nu_s = \sqrt{\nu_{sf}^2 + \nu_{sm}^2 + \nu_{sG}^2} = \sqrt{0.05^2 + 0.03^2 + 0.03^2} = 0.066\,. \qquad (7b)$$

The decomposition of γ_s is expressed as

$$\gamma_s = \gamma_{sM1}\,\gamma_{sM2} \qquad (16)$$

where γ_{sM1} covers the uncertainty associated with strength and geometry and is formulated as

$$\gamma_{sM1} = \exp(\alpha_R \beta v_s - 1.645 v_{sf}) = 1.124 . \quad (17)$$

The further decomposition of γ_{sM1} is expressed as

$$\gamma_{sM1} = \gamma_{sf}\, \gamma_{sG} \quad (18)$$

where γ_{sf} is related to statistical properties of the distribution of strength and calculated as

$$\gamma_{sf} = \exp(\alpha_R \beta v_{sf} - 1.645 v_{sf}) = 1.072 \quad (19)$$

and γ_{sG} is related to uncertainty of geometry as

$$\gamma_{sG} = 1.124/1.072 = 1.048 . \quad (20)$$

The γ_{sM2}, which accounts for the uncertainty of the applied calculation model, is replaced by γ_{sm} and results in

$$\gamma_{sM2} = \gamma_{sm} = \gamma_s/\gamma_{sM1} = 1.15/1.124 = 1.023 . \quad (21)$$

As a conclusion, the partial factor for steel (γ_s) is composed as

$$\gamma_s = \gamma_{sf}\, \gamma_{sm}\, \gamma_{sG} = 1.072 \times 1.023 \times 1.048 = 1.15 . \quad (22)$$

When *existing* reinforced (or prestressed) concrete members are evaluated with the omission of the γ_{sm} partial factor component (i.e. γ_{sm}=1.0), the γ_s partial factor results in

$$\gamma_s = \gamma_{sf}\, \gamma_{sG} = 1.124 . \quad (23)$$

Analogously to γ_c, γ_s may be further adjusted by determining v_{sf} statistically from strength data measured on geometrically controlled test specimens cut out of an existing concrete member. However, the ratio of γ_{sG1} and γ_{sG2} may significantly be different compared to that for concrete.

2.4 Partial factors for action and their respective COV values

According to the interpretation of the EC, the γ_E partial factor of an action (i.e. γ_g, γ_P or γ_q in *Eq.(4)*) is the quotient of the design value (defined as 95%-quantile value) and the characteristic value (generally considered as mean value) of this action, which can be expressed as

$$\gamma_E = 1 + 1.645\, v_E . \quad (24)$$

Similar to *Eq.(7)*, v_E is interpreted as

$$v_E = \sqrt{v_{Ef}^2 + v_{Em}^2 + v_{EG}^2} \quad (25)$$

where the respective COV value associated with

- the statistical properties characterizing the distribution of action-intensities is v_{Ef};
- the uncertainty of the calculation model is v_{Em};
- the uncertainty of geometry is v_{EG}.

2.5 Summary of the partial factors and the respective COV values

Tab. 1 summarizes the partial factors to be applied for usual permanent and variable actions as well as for usual structural materials (concrete, reinforcing, prestressing) in permanent and transient design situations according to the EC together with their respective COV values. The COV values "based on partial factors" (3rd column) correspond to *Eq.(7)* (for resistances) and to *Eq.(25)* (for actions) and were deduced from the given partial factors (2nd column) by *Eq.(6)* and *Eq.(24)*, respectively.

3. APPLICATION OF THE GLOBAL SAFETY FACTOR FORMAT

3.1 Basic relationships

Referring to *Eq.(3)*, the ultimate limit state requirement is verified by the global safety factor format if the

$$R_m \geq \gamma_{RE} E_m$$

condition is met, where

$$E_m = \sum_{j\geq 1} G_{kj} + P_k + Q_{k1} + \sum_{i>1} \psi_{0i} Q_{ki} \quad (26)$$

is the mean value of actions and γ_{RE} is the global safety factor according to *Eq.(2)*. Numerical values of γ_{RE} associated with reliability index of β=3.8 as well as sensitivity factors of α_R=0.8 and α_E= -0.7 according to the EC can be found in *Tab. 2*.

Table 2: Numerical values of the global safety factor γ_{RE} (accounting for reliability index β=3.8 as well as sensitivity factors α_R=0.8 and α_E=-0.7)

γ_{RE}		v_R						
		0.05	0.10	0.15	0.2	0.25	0.3	0.35
v_E	0.050	1.319	1.536	1.788	2.081	2.423	2.820	3.283
	0.100	1.474	1.716	1.997	2.325	2.707	3.151	3.669
	0.125	1.551	1.806	2.102	2.447	2.849	3.317	3.862
	0.150	1.629	1.896	2.207	2.570	2.991	3.483	4.054
	0.175	1.706	1.986	2.312	2.692	3.134	3.648	4.247
	0.200	1.783	2.076	2.417	2.814	3.276	3.814	4.440
	0.250	1.938	2.257	2.627	3.058	3.560	4.145	4.825
	0.300	2.093	2.437	2.837	3.302	3.845	4.476	5.210

3.2 Example for the application of the global safety factor format

The practical application of the global safety factor format will be demonstrated on the following fictitious simply-supported beam with constant cross-section as shown in *Fig. 2*.

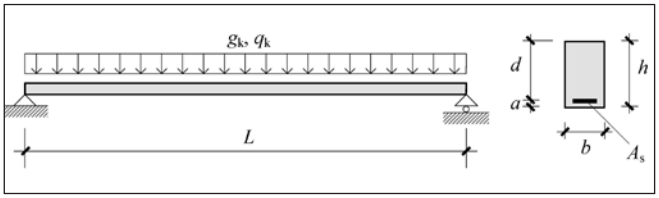

Fig. 2: Notations used in the numerical example

Characteristic values of actions (defined as mean values; see *Sec. 2.2*): permanent load (including self-weight): g_k; live load: q_k.

Cross-sectional data: width: *b*; height: *h*; span: *L*; distance between tension reinforcement and extreme tension fibre (including unfavourable deviation of reinforcement): *a*.

Table 1: *Partial factors of the EC2 and the respective coefficients of variation*

Design variable	Partial Factor	Coefficient of variation (COV) based on	
		partial factors[1)]	on-site measurements[3)]
Actions			
unfavourable permanent action	γ_g=1.15 (=0,85×1,35)	ν_g=0.091	ν_{gf}, ν_{qf}, ν_{Lf1}
favourable permanent action	γ_g=1.35	ν_g=0.213	
traffic loads	γ_q=1.35	ν_q=0.213	
variable actions (other than traffic loads)	γ_q=1.50	ν_q=0.304	
Resistances			
concrete compressive strength	γ_c=1.5	ν_c=0.166[2)]	ν_{cf}, ν_{sf},ν_{Lf2}
reinforcing and prestressing steel strength	γ_s=1.15	ν_s=0.066[2)]	

Notes:
[1)] COV values deduced from partial factors of the EC
[2)] as an example, the ν_{cf} and ν_{sf} components of the ν_c and ν_s (resulting) COV values were statistically determined on standardized samples taken from existing structures as ν_{cf}=0.158 and ν_s=0.061.
[3)] For investigations of existing structures, the determination of COV components, which statistically characterize the distribution of design variables, can be based on on-site measurements. Here, for a typical concrete girder, ν_{gf}, ν_{qf}, ν_{Lf}, ν_{cf} and ν_{sf} represents the COV value of permanent action (i.e. ν_{gf1}, $\nu_{gf2,}$ ... etc. for more permanent actions), variable action (i.e. ν_{qf1}, ν_{qf2}, ... etc.), geometrical data (ν_{Lf1} is associated with geometrical data influencing the actions (e.g. main longitudinal sizes of the girder), and ν_{Lf2} is associated with geometrical sizes influencing the resistance data (e.g. cross-sectional data)), concrete strength and (reinforcing or prestressing) steel strength, respectively. See the numerical example based on deduced COV values in *Sec. 3.2.1* and on COV values obtained from on-site measurements in *Sec. 3.2.2*.

Cross-sectional area of reinforcement (reinforcing steel): A_s.

Strengths: concrete compressive strength: f_{ck} (mean value: f_{cm}); reinforcing steel strength: f_{yk} (mean value: f_{ym}).

According to the partial safety factor method adopted by the EC, the recommended values of the relevant partial factors are γ_g=1,35 and ξ=0,85 for the unfavourable permanent actions; γ_q=1,5 for live loads; γ_c=1,5 for concrete and γ_s=1,15 for reinforcing steel as summarized in *Tab. 1*. Combination factor for live load: ψ_0.

3.2.1 Verification of bending capacity during design

This section applies to newly-built structures by introducing the global safety factor format as a design tool alternative to the widely recommended partial safety factor format.

At the time of design, neither the statistical properties of distribution nor the other uncertainties of the related design variables are known, therefore the designer has no choice but to apply COV values deduced from the respective partial safety factors given by the relevant standard. For the EC, these deduced values can be found in *Tab. 1*.

For the sake of simplicity, the nominal values of all geometrical data are taken as design values (see *Sec. 2.2*) by supposing no uncertainty and respective COV values equal to zero. Consequently, the geometrical data are not treated as random variables in the following procedure; however, the unfavourable deviation of reinforcement from its intended position, which influences the structural depth $d=h-a$, is considered in a in the same way as for the partial safety factor method.

In using *Eq.(3)* for the bending verification of the beam shown in *Fig. 2*, the mean value of both the resistance-side (M_{Rm}) and the action-side (M_{Em}) can be calculated as follows:
Mean value of the ultimate bending capacity:

$$M_{\mathrm{Rm}}\left(f_{\mathrm{ym}},f_{\mathrm{cm}}\right)=A_{\mathrm{s}}f_{\mathrm{ym}}\left(d-\frac{A_{\mathrm{s}}f_{\mathrm{ym}}}{2bf_{\mathrm{cm}}}\right) \tag{27}$$

Mean value of the bending moment at midspan:

$$M_{\mathrm{Em}}\left(g_{\mathrm{k}},q_{\mathrm{k}}\right)=\frac{\left(g_{\mathrm{k}}+q_{\mathrm{k}}\right)L^2}{8} \tag{28}$$

The expression of the resulting standard deviation for the multi-variant
resistance-side:

$$s_{\mathrm{R}}=\sqrt{\left[\left(\frac{\mathrm{d}}{\mathrm{d}f_{\mathrm{ym}}}M_{\mathrm{Rm}}\left(f_{\mathrm{ym}},f_{\mathrm{cm}}\right)\right)\nu_{\mathrm{s}}f_{\mathrm{ym}}\right]^2+\left[\left(\frac{\mathrm{d}}{\mathrm{d}f_{\mathrm{cm}}}M_{\mathrm{Rm}}\left(f_{\mathrm{ym}},f_{\mathrm{cm}}\right)\right)\nu_{\mathrm{c}}f_{\mathrm{cm}}\right]^2} \tag{29}$$

action-side:

$$s_{\mathrm{E}}=\sqrt{\left[\left(\frac{\mathrm{d}}{\mathrm{d}g_{\mathrm{k}}}M_{\mathrm{Em}}\left(g_{\mathrm{k}},q_{\mathrm{k}}\right)\right)\nu_{\mathrm{g}}g_{\mathrm{k}}\right]^2+\left[\left(\frac{\mathrm{d}}{\mathrm{d}q_{\mathrm{k}}}M_{\mathrm{Em}}\left(g_{\mathrm{k}},q_{\mathrm{k}}\right)\right)\nu_{\mathrm{q}}q_{\mathrm{k}}\right]^2} \tag{30}$$

and the resulting COV value for
the resistance-side:

$$\nu_{\mathrm{R}}=\frac{s_{\mathrm{R}}}{M_{\mathrm{Rm}}\left(f_{\mathrm{ym}},f_{\mathrm{cm}}\right)} \tag{31}$$

the action-side:

$$\nu_{\mathrm{E}}=\frac{s_{\mathrm{E}}}{M_{\mathrm{Em}}\left(g_{\mathrm{k}},q_{\mathrm{k}}\right)}. \tag{32}$$

In accordance with the above, the applied COV values for actions (ν_g and ν_q) and materials (ν_s and ν_c) are deduced from the relevant partial factors and summarized in *Tab. 1*. Here, ν_g=0.091 belonging to $\xi\gamma_g$=0.85×1.35 was taken because, on the basis of the current permanent/variable load ratio, the second alternative combination in *Eq.(4)* provided higher

action effect. In closely following the design process of the EC, the mean compressive strength of concrete f_{cm} was taken from the relevant EC2 formula ($f_{cm}=f_{ck}+8$ N/mm^2) based on constant SD instead of calculating it from the characteristic (5%-quantile) value f_{ck} with constant COV (v_{cf}) according to *Sec. 2.3.2*. Because no formula for the mean strength of steel (f_{ym}) was given in the EC2, it was calculated from f_{yk} using constant v_{sf} according to *Sec. 2.3.3*.

After calculating v_R and v_E by *Eq.(31)* and *Eq.(32)* and using the reliability index of $\beta=3.8$ specified by the EC according to *Sec. 2*, the global safety factor can be calculated in iterative way from *Eq.(2)*. The applied sensitivity factors α_R and α_E have to fulfil the $\alpha_R^2+\alpha_E^2=1.0$ condition in each iteration step. The procedure starts with $\alpha_R=0.7$ and $\alpha_E=-0{,}7$ ($\alpha_R^2+\alpha_E^2=0.98\approx1.0$), which corresponds to equal partial risks ($p_R=p_E$) at both sides of *Eq.(1)*, then they are refined in each step until γ_{RE} remains unchanged compared to the previous step. The value of γ_{RE} converges very quickly. The bending capacity is adequate if γ_{RE} of the last step fulfils *Eq.(3)*. The numerical results of the full procedure can be found in *Tab. 3*.

Instead of the above iteration procedure, a safe-side approximation of γ_{RE3}, which corresponds to identical reliability level ($\beta=3.8$), may be determined by the use of the recommended values of α_R and α_E as discussed in *Sec. 2*. These γ_{RE} factors may be chosen from *Tab. 2* as function of the above v_R and v_E.

Note that the values of sensitivity factors in the last iteration step ($\alpha_{E3}=-0.844$ and $\alpha_{R3}=0.536$) significantly differ from their initial values ($\alpha_{E1}=-0.7$ and $\alpha_{R1}=0.7$) as well as from that recommended by the EC ($\alpha_E=-0.7$ and $\alpha_{R3}=0.8$), see. *Sec. 2*). This supports the fact that the introduced global safety factor method is able to take the current variability of action- and resistance-sides into account and to divide the design risk p_{RE} between them accordingly instead of applying previously recommended, constant partial risks p_E and p_R.

3.2.2 Verification of bending capacity for existing structures

This section applies the design procedure introduced for newly-built structures in *Sec. 3.2.1* to existing structures on the basis of the assumption that the necessary statistical properties (i.e. COV values) of the relevant design variables (i.e. load intensities, geometrical properties and strength data) are available from extensive on-site measurements.

Since standardized strength properties without any conversion may be determined only from standardized test specimens, therefore, in taking concrete test specimens (generally cylinders) with sizes differing from standardized ones cut out of an existing structure, attention should be paid to appropriate strength conversion. *Tab. 4* contains conversion factors between concrete cylinders having different height/diameter ratios. As an example, strengths values measured on

Table 3: *Verification of bending capacity with the global safety factor format during design*

Geometry (see *Fig. 2*): L=13.4 m; b=250 mm; h=700 mm; a=30 mm; effective depth: $d = h-a$ = 700-30 = 670 mm;	
Actions and action effects (see *Fig. 2* and *Tab. 1*): g_k = 6 kN/m; q_k = 5 kN/m; v_g=0.091 (γ_g=0.85×1,35=1.15); v_q=0.304 (γ_q=1.5); ψ_0 = 0.7; $M_{Em}(g_k, q_k)$=247 kNm; s_E=36.3 kNm; v_E=0.147.	

Resistance (see *Fig. 2* and *Tab. 1*): A_s=1257 mm^2 (4ϕ20);
concrete: C30/37, f_{ck}=30 N/mm^2, f_{cm}=38 N/mm^2, v_c=0.166;
steel: S500B, f_{yk}=500 N/mm^2, v_{sf}=0.05, f_{ym}=545 N/mm^2, v_s=0.066;
$M_{Rm}(f_{ym}, f_{cm})$=434 kNm; s_R=27.3 kNm, v_R=0.063.	

Iterative adjustment of γ_{RE} by refining α_E and α_R in each step (β=3.8)	
1st step: $\alpha_{E1}=-0.7$; $\alpha_{R1}=0.7$; $\alpha_{E1}^2+\alpha_{R1}^2=0.98\approx1.0$; $\gamma_{RE1}=\exp\left(\beta\alpha_{R1}^{(+)}v_R\right)\left(1-\beta\alpha_{E1}^{(-)}v_E\right)$	γ_{RE1}=1.644
2nd step: $R_{d1}=M_{Em}(g_k,q_k)\left(1-\beta\alpha_{E1}^{(-)}v_E\right)$ $\kappa_1=\sqrt{\left(R_{d1}v_R\right)^2+\left(M_{Em}(g_k,q_k)v_E\right)^2}$ $\alpha_{E2}=-M_{Em}(g_k,q_k)\frac{v_E}{\kappa_1};\ \alpha_{R2}=R_{d1}\frac{v_R}{\kappa_1}$ $\gamma_{RE2}=\exp\left(\beta\alpha_{R2}^{(+)}v_R\right)\left(1-\beta\alpha_{E2}^{(-)}v_E\right)$	R_{d1}=343 kNm κ_1=42.2 kNm $\alpha_{E2}=-0.859$; α_{R2}=0.512 **γ_{RE2}=1.672**
3rd step: $R_{d2}=M_{Em}(g_k,q_k)\left(1-\beta\alpha_{E2}^{(-)}v_E\right)$ $\kappa_2=\sqrt{\left(R_{d2}v_R\right)^2+\left(M_{Em}(g_k,q_k)v_E\right)^2}$ $\alpha_{E3}=-M_{Em}(g_k,q_k)\frac{v_E}{\kappa_2};\ \alpha_{R3}=R_{d2}\frac{v_R}{\kappa_2}$ $\gamma_{RE3}=\exp\left(\beta\alpha_{R3}^{(+)}v_R\right)\left(1-\beta\alpha_{E3}^{(-)}v_E\right)$	R_{d2}=365 kNm κ_2=42.9 kNm $\alpha_{E3}=-0.844$; α_{R3}=0.536 **γ_{RE3}=1.672**
Verification of bending capacity $\gamma_{RE3}\,M_{Em}(g_k, q_k)$ = 1.672×247 = **413 kNm** < $M_{Rm}(f_{ym}, f_{cm})$ = **434 kNm OK**	

Table 4: Conversion factors for concrete cylinders (Szalai, 1998)

Conversion between cylinders with constant height/diameter ratio (α_{g2})		Conversion between cylinders with different height/diameter ratio (α_{g3})	
cylinder diameter [mm]	Standardized cylinder diameter: 150 mm	height/diameter ratio	standardized height/diameter ratio: 2.0
200	**1.05**	6/2	1.1
150	1.00	5/2	1.05
100	0.925	4/2	1.00
80	0.875	3/2	0.95
70	0.850	**2/2**	**0.85**
		1/2	0.65

a concrete test cylinder with height of 200 mm and diameter of 200 mm can be converted into strength values belonging to standard test cylinders with height/diameter ratio of 300/150 by multiplying the measured strength values with $\alpha_{g2}\times\alpha_{g3}$ where $\alpha_{g2}=1.05$ and $\alpha_{g3}=0.85$ according to *Tab. 4*.

It was assumed that previous on-site measurements on concrete beam shown in *Fig. 2* were carried out regarding load intensities, geometrical data (related to actions and resistances) and strengths properties from which their main statistical characteristics (mean values and COV values) were deduced.

The *mean values* obtained from on-site measurements were assumed to be equal to the respective characteristic values for loading data ($g_m=g_k$; $q_m=q_k$), to the respective nominal values for geometrical data ($L_m=L$; $h_m=h$, $b_m=b$; $a_m=a$, $A_{sm}=A_s$) and to values slightly higher than the respective standardized mean values (see *Sec. 3.2.1*) (f_{cm}; f_{ym}). Accounting for the considerations discussed in *Sec. 2.3.1-2.3.3* and *Sec. 2.4*, the respective *COV values* were assumed as follows:

Loading data:
permanent load: $v_{gf}=0.07$ ($< v_g=0.091$ ($\gamma_g=1.15$) in *Tab 1*);
live load: $v_{qf}=0.24$ ($< v_q=0.304$ ($\gamma_q=1.5$) in *Tab 1*);
Geometrical data:
span: $v_{Lf}=0.01$;
cross-sectional height: $v_{hf}=0.02$ ($> v_{Lf}$);
cross-sectional width: $v_{bf}=0.02$ ($= v_{hf}$);
reinforcement position: $v_{af}=0.3$ (accounting for unfavourable deviation);
area of reinforcement: $v_{Asf}=0.01$;

Resistance data
concrete strength: $v_c=0.17$
($> v_{cf}=0.15$ (incl. γ_{cG2}) based on *Sec. 2.3.2*);
steel strength: $v_s=0.06$
($> v_{sf}=0.05$ (incl. γ_{sG2}) based on *Sec. 2.3.3*).
As shown from the above list, in contrast to *Sec. 3.2.1*, here all geometrical data are considered fully as random variables with known mean values and COV values.
Expressions *Eq.(27)-Eq.(32)* used in *Sec. 3.2.1* change accordingly as follows:
Mean value of the ultimate bending capacity:

$$M_{\mathrm{Rm}}\left(f_{\mathrm{ym}},f_{\mathrm{cm}},h_{\mathrm{m}},b_{\mathrm{m}},a_{\mathrm{m}},A_{\mathrm{sm}}\right)=A_{\mathrm{sm}}f_{\mathrm{ym}}\left(h_{\mathrm{m}}-a_{\mathrm{m}}-\frac{A_{\mathrm{sm}}f_{\mathrm{ym}}}{2b_{\mathrm{m}}f_{\mathrm{cm}}}\right) \quad (33)$$

Mean value of the bending moment at midspan:

$$M_{\mathrm{Em}}\left(g_{\mathrm{k}},q_{\mathrm{k}},L_{\mathrm{m}}\right)=\frac{\left(g_{\mathrm{k}}+q_{\mathrm{k}}\right)L_{\mathrm{m}}^2}{8} \quad (34)$$

The expression of the resulting standard deviation for the multi-variant
resistance-side:

$$s_{\mathrm{R}}=\sqrt{\begin{aligned}&\left[\left(\frac{\mathrm{d}}{\mathrm{d}f_{\mathrm{ym}}}M_{\mathrm{Rm}}\left(f_{\mathrm{ym}},f_{\mathrm{cm}},h_{\mathrm{m}},b_{\mathrm{m}},a_{\mathrm{m}},A_{\mathrm{sm}}\right)\right)v_{\mathrm{s}}f_{\mathrm{ym}}\right]^2+\\&+\left[\left(\frac{\mathrm{d}}{\mathrm{d}f_{\mathrm{cm}}}M_{\mathrm{Rm}}\left(f_{\mathrm{ym}},f_{\mathrm{cm}},h_{\mathrm{m}},b_{\mathrm{m}},a_{\mathrm{m}},A_{\mathrm{sm}}\right)\right)v_{\mathrm{c}}f_{\mathrm{cm}}\right]^2+\\&+\left[\left(\frac{\mathrm{d}}{\mathrm{d}h_{\mathrm{m}}}M_{\mathrm{Rm}}\left(f_{\mathrm{ym}},f_{\mathrm{cm}},h_{\mathrm{m}},b_{\mathrm{m}},a_{\mathrm{m}},A_{\mathrm{sm}}\right)\right)v_{\mathrm{hf}}h_{\mathrm{m}}\right]^2+\\&+\left[\left(\frac{\mathrm{d}}{\mathrm{d}b_{\mathrm{m}}}M_{\mathrm{Rm}}\left(f_{\mathrm{ym}},f_{\mathrm{cm}},h_{\mathrm{m}},b_{\mathrm{m}},a_{\mathrm{m}},A_{\mathrm{sm}}\right)\right)v_{\mathrm{bf}}b_{\mathrm{m}}\right]^2+\\&+\left[\left(\frac{\mathrm{d}}{\mathrm{d}a_{\mathrm{m}}}M_{\mathrm{Rm}}\left(f_{\mathrm{ym}},f_{\mathrm{cm}},h_{\mathrm{m}},b_{\mathrm{m}},a_{\mathrm{m}},A_{\mathrm{sm}}\right)\right)v_{\mathrm{af}}a_{\mathrm{m}}\right]^2+\\&+\left[\left(\frac{\mathrm{d}}{\mathrm{d}A_{\mathrm{sm}}}M_{\mathrm{Rm}}\left(f_{\mathrm{ym}},f_{\mathrm{cm}},h_{\mathrm{m}},b_{\mathrm{m}},a_{\mathrm{m}},A_{\mathrm{sm}}\right)\right)v_{\mathrm{Asf}}A_{\mathrm{sm}}\right]^2\end{aligned}} \quad (35)$$

action-side:

$$s_{\mathrm{E}}=\sqrt{\left[\left(\frac{\mathrm{d}}{\mathrm{d}g_{\mathrm{k}}}M_{\mathrm{Em}}\left(g_{\mathrm{k}},q_{\mathrm{k}},L_{\mathrm{m}}\right)\right)v_{\mathrm{gf}}g_{\mathrm{k}}\right]^2+\left[\left(\frac{\mathrm{d}}{\mathrm{d}q_{\mathrm{k}}}M_{\mathrm{Em}}\left(g_{\mathrm{k}},q_{\mathrm{k}},L_{\mathrm{m}}\right)\right)v_{\mathrm{qf}}q_{\mathrm{k}}\right]^2+\left[\left(\frac{\mathrm{d}}{\mathrm{d}L_{\mathrm{m}}}M_{\mathrm{Em}}\left(g_{\mathrm{k}},q_{\mathrm{k}},L_{\mathrm{m}}\right)\right)v_{\mathrm{Lf}}L_{\mathrm{m}}\right]^2} \quad (36)$$

and the resulting COV value for
the resistance-side:

$$v_{\mathrm{R}}=\frac{s_{\mathrm{R}}}{M_{\mathrm{Rm}}\left(f_{\mathrm{ym}},f_{\mathrm{cm}},h_{\mathrm{m}},b_{\mathrm{m}},a_{\mathrm{m}},A_{\mathrm{sm}}\right)} \quad (37)$$

the action-side:

$$v_{\mathrm{E}}=\frac{s_{\mathrm{E}}}{M_{\mathrm{Em}}\left(g_{\mathrm{k}},q_{\mathrm{k}},L_{\mathrm{m}}\right)}. \quad (38)$$

The calculation procedure is identical to that in *Sec. 3.2.1*. The numerical results can be found in *Tab. 5*.

Regarding the final values of sensitivity factors α_{E3} and α_{R3}, the same, which was concluded in *Sec. 3.2.1*, applies.

4. CONCLUSIONS

The paper introduced the application of the global safety factor format for the verification of bending capacity of a simply-supported beam. The benefits of this verification format against the partial safety factor format were discussed for existing structures. The application of this format was introduced on the basis of standardized safety elements and also of on-site-measured data. The biggest advantage of this format is that, in each design situation, the total risk specified (e.g. by the EC) can be divided between the action-side and the resistance-side of the design requirement by taking the current variability of

Table 5: *Verification of bending capacity with the global safety factor format for existing structuresHere a safe-side approximation of γ_{RE3} may also be chosen from Tab. 2 as function of ν_R and ν_E instead of the above iteration procedure. Another simplification for cases when statistical properties of loading data are not available is the substitution of ν_{gf} and ν_{qf} with ν_g and ν_q being in Tab. 1 and not treating L as random variable similarly to that in Sec.3.2.1.*

Geometry (see *Fig. 2*): L_m=13.4 m, ν_{Lf}=0.01; b_m=250 mm, ν_{bf}=0.02; h_m=700 mm, ν_{hf}=0.02; a_m=30 mm, ν_{af}=0.3; effective depth: $d_m(h_m, a_m) = h_m - a_m$ = 700-30 = 670 mm;	
Actions and action effects (see *Fig. 2*): $g_m=g_k$=6 kN/m; $q_m=q_k$=5 kN/m; ν_{gf}=0.07; ν_{qf}=0.24; ψ_0 = 0.7; $M_{Em}(g_m, q_m, L_m)$=247 kNm; s_E=29.0 kNm; ν_E=0.117.	

Resistance (see *Fig. 2* and *Tab. 1*): A_s=1257 mm^2 (4ϕ20);
concrete: C30/37, f_{ck}=30 N/mm^2, f_{cm}=40 N/mm^2, ν_c=0.17;
steel: S500B, f_{yk}=500 N/mm^2, f_{ym}=550 N/mm^2, ν_s=0.06;
$M_{Rm}(f_{ym}, f_{cm}, h_m, b_m, a_m, A_{sm})$=439 kNm; s_R=28.1 kNm, ν_R=0.064.	

Iterative adjustment of γ_{RE} by refining α_E and α_R in each step (β=3.8)	
1st step: α_{E1}=-0.7; α_{R1}=0.7; $\alpha_{E1}^2 + \alpha_{R1}^2$=0.98≈1.0; $\gamma_{RE1} = \exp\left(\beta\alpha_{R1}^{(+)}\nu_R\right)\left(1-\beta\alpha_{E1}^{(-)}\nu_E\right)$	γ_{RE1}=1.555
2nd step: $R_{d1} = M_{Em}(g_k, q_k)\left(1-\beta\alpha_{E1}^{(-)}\nu_E\right)$ $\kappa_1 = \sqrt{(R_{d1}\nu_R)^2 + (M_{Em}(g_k, q_k)\nu_E)^2}$ $\alpha_{E2} = -M_{Em}(g_k, q_k)\frac{\nu_E}{\kappa_1};\ \alpha_{R2} = R_{d1}\frac{\nu_R}{\kappa_1}$ $\gamma_{RE2} = \exp\left(\beta\alpha_{R2}^{(+)}\nu_R\right)\left(1-\beta\alpha_{E2}^{(-)}\nu_E\right)$	R_{d1}=324 kNm κ_1=35.6 kNm α_{E2}= -0.814; α_{R2}=0.581 **γ_{RE2}=1.569**
3rd step: $R_{d2} = M_{Em}(g_k, q_k)\left(1-\beta\alpha_{E2}^{(-)}\nu_E\right)$ $\kappa_2 = \sqrt{(R_{d2}\nu_R)^2 + (M_{Em}(g_k, q_k)\nu_E)^2}$ $\alpha_{E3} = -M_{Em}(g_k, q_k)\frac{\nu_E}{\kappa_2};\ \alpha_{R3} = R_{d2}\frac{\nu_R}{\kappa_2}$ $\gamma_{RE3} = \exp\left(\beta\alpha_{R3}^{(+)}\nu_R\right)\left(1-\beta\alpha_{E3}^{(-)}\nu_E\right)$	R_{d2}=336 kNm κ_2=36.1 kNm α_{E3}= -0.803; α_{R3}=0.596 **γ_{RE3}=1.569**
Verification of bending capacity $\gamma_{RE3}\, M_{Em}(g_m, q_m, L_m)$=1.569×247=**387 kNm** < $M_{Rm}(f_{ym}, f_{cm}, h_m, b_m, a_m, A_{sm})$=**439 kNm OK**	

both sides into account. This can not be done if constant partial risks are applied as recommended by the partial safety factor method according to the EC.

5. REFERENCES

EN 1990:2002 Eurocode: "*Basis of structural design*" CEN, Bruxelles

EN 1992-1-1:2004 Eurocode 2: "*Design of concrete structures. Part 1-1: General rules and rules for buildings*" CEN, Bruxelles

fib (2010): "*fib Model Code 2010*" fib Bulletin 55-56, *fib*, Lausanne

Kármán, T. (1965): "*On the optimum level of safety of structures*" (in Hungarian) ÉTI, Budapest

Mistéth, E. (2001): "*Design theory*" (in Hungarian) Akadémiai Kiadó, Budapest

Soukov, D., Jungwirt, F. (1997): "*Conformity and safety of concrete according to prEN 206 and Eurocodes"* Leipzig Annual Civil Engineering Report, No. 2, Leipzig

Szalai, K. (1998): "*Reinforced Concrete structures*" (in Hungarian) Műegyetemi Kiadó, Budapest

Kálmán Szalai (1930), civil engineer (1953), DSc (1976), professor emeritus at the Department of Structural Engineering, Budapest University of Technology and Economics. Research fields: Design theory, strength theory, quality control, supervision, strengthening and corrosion protection of concrete structures, high strength and high performance concretes. Member of the Hungarian Group of *fib*.

Tamás Kovács (1974), civil engineer (1997), PhD (2010), assistant professor at the Department of Structural Engineering, Budapest University of Technology and Economics. Research fields: dynamic-based damage assessment of concrete structures, high performance concrete for bridges, strengthening of bridges, concrete pavements, reliability of structures, standardization. Secretary of the Hungarian Group of *fib*.

A POST-TENSIONED CONCRETE SLAB CANTILEVERING 6.50 M


Dezső Hegyi - András Árpád Sipos

We designed a post-tensioned concrete cantilever with a 6.50 m free span supported by columns for a villa near Pécs. The shape and number of the bonded strands were determined to balance the dead load of the structure by the transversal component of the prestressing force. The deflections measured on finished structure are in good agreement with the approximated values of the structural calculation.

Keywords: post tensioning, cantilever

1. INTRODUCTION

We took part as structural engineers in the design works of a villa in the suburbs of Pécs. From the structural point of view the most challenging task was to design a flat cantilevered slab over one of the terraces of the building (*Fig. 1*). In the vision of the architect designers the slab should appear as a heavy, monolithic, but in the same time narrow element. Furthermore, the slab is covered by stone-surfacing in all its sides, reducing the available space of the load bearing structure. Not only the 6.50 m free span made the structural design difficult, but forming supports was challenging too, because the terrace is neighboured by a large, open room allowing only columns to be placed under the slab.

During the preparation of the construction plans the idea of a post-tensioned concrete slab occurred. According to the preliminary calculations 300-350 mm thickness seemed to satisfy both the structural requirements and the architectural expectations. Finally we decided to process this solution in details. The structure was constructed in December 2008 and the deflections measured since then are in good agreement with the calculated values.

2. DESIGN AND STRUCTURAL CALCULATIONS

As a first step we designed a structure of steel beams. To fulfill the requirements both in the serviceability and ultimate limit states HEA400 beams should have been placed in 400 mm distance. This is a rather slender structure for such a cantilever but with the additional stone coatings it was even too thick regarding the architectural vision. Another difficulty of this approach is how to establish the point-like supports. The idea of the post-tensioned structure seemed to be a more appropriate answer in the given situation.

Fig. 1: Bottom view of the cantilever after the formwork had been removed

We carried out the structural calculations according to the prescriptions of the Eurocode 2. Slabs with large span or cantilevering are typically difficult to design in the terms of deflections and crack widths and not in the terms of load bearing capacity. Even in the case of a long cantilever and high loads one can determine a cross-section satisfying the design rules in the Ultimate Limit States (ULS), but due to the increase in the weight of the structure the deflections increase rapidly. Basically, a prestressed concrete structure is not more efficient according to its load bearing capacity compared to a conventionally reinforced concrete structure (Bölcskei and Tassi, 1970). Only the higher concrete class leads to a slightly higher bending resistance. (In the case of unbonded tendons the membrane effect increases the load bearing capacity slightly as well, but this is generally neglected in the calculations.) However, in the case of a cantilever the material constants, especially the terms describing the time-dependent deflections are uncertain.

In the case of post-tensioning typically the application of unbonded tendons is more efficient. In this case leading the tendon along the curve obtained by reflecting the bending moment diagram to the horizontal plane gives a good first approximation for the detailed design (fib, 2005).

In the case of bonded tendons the deformations in the concrete influence the stress in the tendons and the losses due to friction. In the mechanical point of view the structure with bonded tendons cannot lose stability if it is loaded only by the prestress. Although in the case of unbonded tendons losing stability is theoretically possible, the postcritical behaviour is still advantageous.

During the calculation we found that the most efficient way of design is determining the number of the strands and the initial prestress from the assumption that they must balance the characteristic value of the rather high dead-load (approximately q_k=14.00 kN/m^2), i.e. no deflection occurs. To provide resistance against the extra bending moments from the

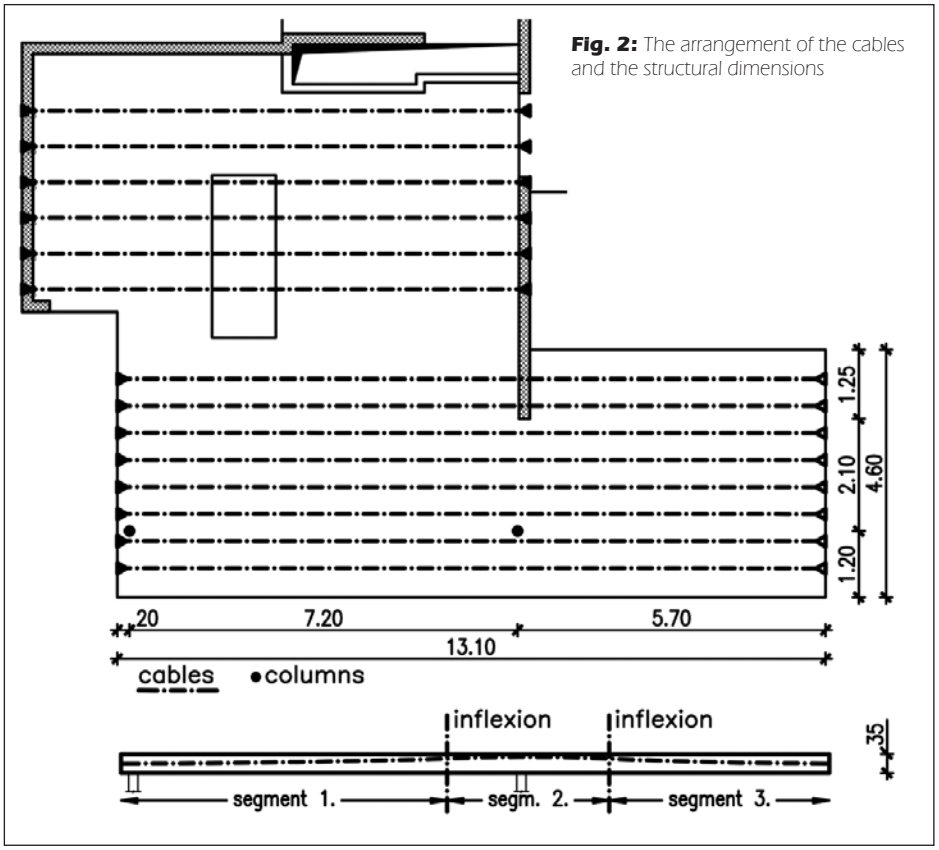

Fig. 2: The arrangement of the cables and the structural dimensions

live loads we placed nonprestressed rebars into the structure. For concrete structures typically the major part of loads is the self weight, thus we aimed a structure which has no deflections under the dead loads long time after construction (i.e the prestress was taken into account with its time dependent losses and the material constants were determined for the infinite time as well). In this case the live loads induce a rather small final deformation of the structure in service. However, one can expect an upward deformation after applying the prestress since generally the highest prestressing force is acting on a concrete which has not reached its designed strength yet (Nilson and Winter, 1987).

The pure application of post-tensioned strands (i.e. by providing such a strand cross section, which fulfil the requirements in the ULS) would result in an upward deflection of the structure even long time after construction due to the high dominancy of the dead loads. The drafted strategy does not only help to avoid this outcome, but it leads to a lower amount of steel usage, too.

As we mentioned above in the ideal case the curve of the tendons follows the reflected bending moment diagram, however, in practice this shape is impossible. For example, above supports the tendon must be led along a curve instead of forming a sharp edge (*Fig. 2*). The tendon is typically placed between the upper and lower layers of reinforcement. As an additional condition on the shape in the case of a cantilever the tendon should be finished at the centreline of the free end and its tangent must be parallel to the plane of the slab to avoid local failure and undesired increments in the deflections (Nilson, 1987).

As a first estimation on the cable layout we determined a curve consisting of more, smoothly connected parabolic segments in such a way, that it is kept between the lower and upper surface of the 350 mm thick slab. Altogether 3 segments were needed to produce the layout of tendons along the slab, the connections of the segments are the inflexion points of the final curve. The determined curve is tangential to the plane of slab at the cantilevered end (*Fig. 2*). Since the segments are parabolic, the transversal component of the prestressing force is constant along one segment (the second derivative of the shape function along one segment is constant). Taking into account the transversal component among the dead loads we determined the needed cross sectional area of the tendons and the number of cables (8 strands each with a 150 mm^2 cross sectional area for a 1.00 m width are placed, they are arranged in 2 cables) and the initial prestress (σ_{p0}=1250 MPa), too. In this arrangement the prestressing completely balances the weight of structure along the cantilever.

As we mentioned above, we approximated the amount of rebars on a simplified model substituting the prestress by its transversal effect. This means that in each parabolic segment the vertical component of the prestressing force is applied as an external load on the structure and the axial load is neglected. Based on the results of the approximation we finished the detailing by a calculation in a FE code where all the loads in the prescribed combinations and the prestressing force with its varying eccentricity along the cables were included.

We found that the simplified model above is rather accurate compared to the FE results in the terms of the amount of the reinforcement. However, in the simplified model the application of the external force alters the resultant load thus the reactions at the supports are underestimated. The cross sections were checked under eccentric compression, including the limitation of stresses in the SLS, which turned out to be crucial in such a highly loaded case.

The design of the anchorage devices requires the highest care. As we mentioned above 4 strands are placed in one cable, the distance between the cables (500 mm) exceeded the prescribed minimum of 400 mm by the manufacturer. Based on the advice of the specialist we chose an anchorage accepting 4 strands. In this case about P_{m0}=750,0 kN force is transferred to the slab at one anchorage at the time of application of prestressing. To avoid splitting a dense (Ø10/60) reinforcement and a beamlike longitudinal reinforcement were applied.

3. CONSTRUCTION

The construction started in autumn, the cantilever was constructed in December. The formwork and the reinforcement were placed by the building contractor but the anchorages and the cables were placed (*Fig. 3*) by the specialist (Pannon-Freyssinet Ltd.). It is crucial to place the cables along the prescribed curves since according to the above explanation a slight difference from the prescribed (parabolic) shape leads to a high error in the transversal load arising from prestress. A special care is needed to avoid the segments with horizontal tangents or small curvatures getting an opposite curvature compared to the designed shape. This leads to an opposite direction of the transverse load. In our case at the ends of the cantilever more modifications were needed to really produce the designed shape.

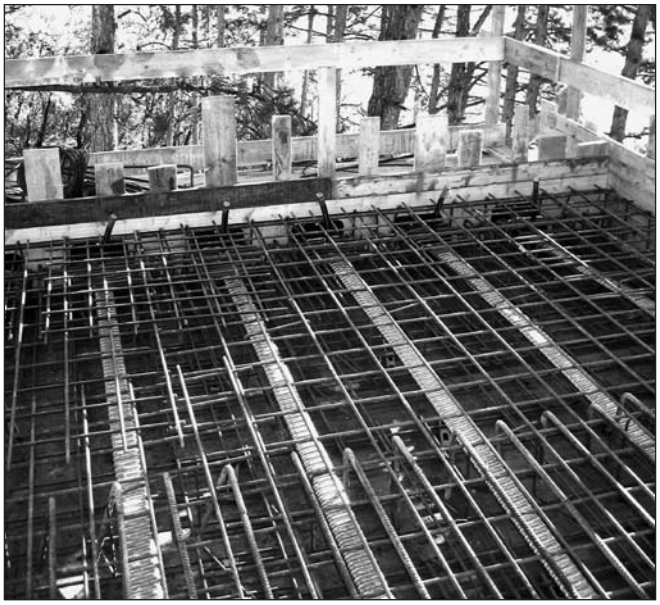

Fig. 3: The cables and the rebars before pouring the concrete

Fig. 4: Side view of the cantilever after the formwork had been removed

We applied a C30/37 classed concrete. In spite of the unfavourable weather the test cubes verified that the designed strength was reached in the construction. The prestressing could be applied just after the prescribed strength of the concrete (23 MPa cylinder strength on specimens) was exceeded. In our case this phase happened about one month after pouring the concrete. After prestressing the protective sheaths were grouted.

Based on the calculations we expected the slab to have a 20 mm upward deflection after prestressing. The upward deflection could not be observed, the slab did not separate from the formwork. A higher concrete class with a higher modulus of elasticity can partially explain this result, however, the main reason is the rather high force needed to balance adhesion and separate the slab and the formwork.

We aimed to measure the deflections after the formwork had been removed to follow the viscose deflections. Unfortunately the construction was stopped after the structural works had been finished so we have no data from the most interesting first six months. What we know is that at the time of removing the formwork there were no observable movements downwards and after 10 month of prestressing the measured deflection is slightly below 20 mm which is 1/650 of the effective span. Applying a dynamic load (jumping on the slab) it seems to be very stiff.

4. CONCLUSION

We designed a 6.50 m cantilever applying a post-tensioned reinforced concrete slab. During the design we investigated some other structural possibilities as well and found that the 350 mm thick slab is the most efficient solution for the problem. The final solution is definitely the thinnest compared to the other variants namely the system of steel beams (HEA members, the thickness is 400 mm) or a reinforced concrete slab strengthened by beams (the thickness is at least 550 mm). Comparing the costs the price of the final solutions was about 50% of the steel system and about 150% of the simple RC slab. In *Figure 4* beyond our cantilever another cantilevered slab made of RC beams is visible as well illustrating the huge difference in the slenderness of the two structural systems.

Now about 50-60% of the final loading is presented so we expect the final deflections will still fulfill the requirements of the standard. Due to the higher load the stiffness against dynamical effects will increase as well. It is worthy to mention that the architectural vision of the building is a dynamic appearance by plenty of parallel edges. Due to the inaccuracy of the construction the final location of more edges differs slightly from their designed position. From several viewpoints these kinds of inaccuracies strengthen the deflection of the cantilever slab visually. We hope that with placing the final coverings the inaccuracy can be reduced. However, it also shows that the conservative limits on deflections due to visual reasons in the standard should be handled with care: in some special architectural arrangements an even stricter limit is needed to fulfill the requirements of the users.

5. ACKNOWLEDGEMENTS

The authors thank Csaba Böhm and Dénes Dalmy from the Pannon-Freyssinet Ldt. for their advices and comments on the plan.

6. REFERENCES

Bölcskei E., Tassi G. (1970): "Concrete Structures – Prestressed Structures" (In Hungarian), *Tankönyvkiadó, Budapest*

Nilson A.H., Winter G. (1987): "Design of concrete structures" *McGraw-Hill Book Company, New York*

Nilson A.H. (1987): "Design of prestressed concrete" *John Wiley and Sons, New York*

MSZ EN 1992-1-1:2005 Eurocode 2: "Design and Construction of Reinforced and Prestressed Concrete Structures Part 1-1"

fib Bulletin 31 (2005) "Post-tensioning in buildings", Technical Report, *fib*

Dezső Hegyi (1976) Received his M.Sc. architect degree from the BUTE in 1999. He defended his PhD in 2006 about nonlinear analysis of membrane structures. He is an assistant professor in the Department of Mechanics, Materials and Structures.

András Árpád Sipos (1980) Received his M.Sc. architect degree from the BUTE in 2003. He defended his PhD in 2007 about the computation of spatial deformation of RC rods. He is an assistant professor in the Department of Mechanics, Materials and Structures and the member of the Hungarian Group of ***fib***.

BASICS OF REINFORCED MASONRY


Anita Fódi – István Bódi

Although brick has been used since the earliest times, the knowledge about the behaviour of masonry is almost the least complete today. Academically established relations are applied in case of engineering of steel and reinforced concrete structures, but a significant part of the formulas of designing masonry are founded on experimental or intuitive, empirical causes in most cases. This paper gives a summary about reinforced masonry, in some cases compared to the plain masonry and to the reinforced concrete. In the following lines the short history of reinforced masonry is summarized and then its topicality in Hungary is emphasized. The typical features of masonry are shown and basic knowledge about the compressive, tensile (flexural) and shear strength is summarized. The two main types of bar reinforced masonry, the bed joint reinforced and pocket reinforced, are outlined. For presentation of the practice, examples constructed in Europe are demonstrated. Finally, basic review is given about the micro- and macro-mechanical behaviour of masonry and brick to facilitate the understanding of the modelling directions of masonry.

Keywords: reinforced masonry, masonry modelling, bed joint reinforcement, masonry behaviour, masonry vs. reinforced concrete

1. INTRODUCTION

There are a lot of arguments about the actuality of reinforced masonry. Although bricks belong to the conventional and traditional building materials, reinforced concrete frames are favoured in construction industry nowadays. In that case the masonry is used purely as an infill wall. The load bearing capacity of masonry is only significant for the design of some-storey constructions. In Hungary many middle-tall buildings are built every year, and reinforced masonry could be a good construction course for this sort of buildings.

Unfortunately, the culture of masonry decayed in the last decades. A possible reason of that is that smaller emphasis is laid on masonry than on reinforced concrete or steel structures in university education. However, masonry is an important part of the building industry because private houses of significant number are built from brick today.

The objective of this paper is to summarize the basic knowledge about the reinforced masonry in order to show its benefits and its diversity.

2. HISTORICAL REVIEW

„…They said to one another, `Come, let us make bricks and bake them. They used bricks for stone and bitumen for mortar. Then they said, `Let us build ourselves a city and a tower with its top in the heavens.´"

The quotation comes from the Old Testament of the Holy Bible, Book of Genesis, Chapter XI, Verses 3 and 4, and proves that building with masonry engaged people's attention those days. The early Egyptians, Romans (and Greeks) built lots of monumental structures from masonry such as the pyramid of Cheops in Egypt, the Greet Wall of China, the Pharos of Alexandria etc. The masonry walls of that time were different: Romans built walls from two leaves of masonry and rubble mixed with mortar in the middle. Greeks used mostly natural stone. Chinese built masonry walls mostly from adobe.

According to researchers in the Middle-East, Syria is said to be the birth place of the masonry arches. In the Middle Ages many castles and cathedrals were built using masonry, avoiding the using of metal or wood as a structural support completely.

Reinforced masonry is not much younger than masonry since the ancient Greeks and Romans already had built anchors for reinforcing the wall work. We can recognize the simplest, immature way to increase the load bearing capacity of the walls. The early adobe was reinforced with straw. At that time our fathers built haulm or reed in their cob walls.

Actually reinforced masonry dates back to about 1813 or 1825. In 1813, the French-born Marc Isambard Brunel designed a tall chimney in which reinforcement was already used. Ten years later, during the design of the shafts of the Blackwall Tunnel, he applied reinforcement to strengthen masonry as well. He designed two brick shafts with a diameter of 50 ft (15.24 m). The height of the walls of the shafts amounted to 70 ft (21.34 m) with a thickness of 30 in. (76.20 cm). Wrought iron ties and hoops with a diameter of 1 inch (25.4 mm) were let in the brickwork as reinforcement (Beamish, 1862).

The Church of Jean de Montmartre in Paris was built at the turn of the 19th century, designed by the architect Anatole *de Baudot*. The brick and ceramic tile-faced structure had exterior brick walls with a thickness of 4.5 in. (11.43 cm), which were reinforced vertically in the holes of the brick and horizontally in the mortar joints (Schneider and Dickey, 1994).

The next step in the history of reinforced masonry was taken between 1900 and 1910. The Park Güell in Barcelona, part of the World Heritage, was engineered in accordance with the plans of the Catalan architect, Antoni *Gaudí*. Only during the maintenance and reconstruction of the hanging balconies of the Park Güell turned out that reinforcing bars were put in the holes

of the flower stands (Árva and Sajtos, 2007). After the Second World War the market was wrestling with the huge lack of steel; new building methods were developed, and reinforced concrete became more and more wide-spread. At the time, however, in some countries building with masonry was found cheaper than structural steel or reinforced concrete. Soon they had to face the problem, that the buildings constructed that way, did not ensure adequate safety in areas threatened by earthquakes. Soon the engineers realized that placing reinforcement in concrete and masonry structures is advantageous because it enhances the deformability of the element. The crack propagation is stabilized owing to the reinforcement. Among other things this fact and also the claim to create taller and taller buildings might have led to the use of reinforcement in masonry walls.

At the beginning of the 1950s years a huge amount of construction of reinforced masonry began in the United States, especially in California. The majority of structures built in that time are public buildings such as hospitals, schools, state buildings, warehouses, banks, churches. It is interesting to note that a hospital, constructed with reinforced masonry, survived the 1971 San Fernando earthquake with no considerable structural damage, meanwhile other hospitals built from another materials were seriously damaged (Csák, Hunyadi and Vértes, 1981).

3. EARLIER HUNGARIAN STATUS OF REINFORCED MASONRY

Reinforced masonry was used in the 1950s in Hungary. The standard gave methods to calculate load bearing capacity of reinforced masonry at that time. *Rózsa, 1953* prescribed a minimum mortar and brick strength if the masonry wants to be reinforced. He distinguished horizontal, mesh reinforcement and longitudinal, vertical reinforcement. The horizontal mesh or zig-zag reinforcement was placed into the mortar layer (*Fig. 1 a* and *b*). The maximal distance between the reinforced layers is 3 courses of bricks. *Fig. 1 c* shows the application of reinforcement in masonry column for bed joint and for vertical reinforcement (Rózsa, 1953). *Fig. 1 d* and *e* show the suggestion for concrete and brick composite columns (The possible place for concrete is signed by hatched area). *Andrejev, 1953* suggests applying reinforced masonry for retaining walls and columns. One of the possible construction methods of columns can be seen in *Fig. 1 f*.

In the 1960s emphasis was put rather on reinforced concrete and the building culture of masonry decayed. The Hungarian Standard MSZ 15023-86 only dealt with plain masonry. At the beginning of the 21st century, the issue of the Eurocode 6 in 2006 brought reinforced masonry back into the practice.

4. TYPICAL FEATURES OF MASONRY WALLS

Masonry is inhomogeneous material and consists of two basic components: brick and mortar. The connection between them is an important feature, too. The properties of clay brick and mortar are different separately or joined together; they act in a distinct way. Now let us take the most important characteristics and features of masonry one by one.

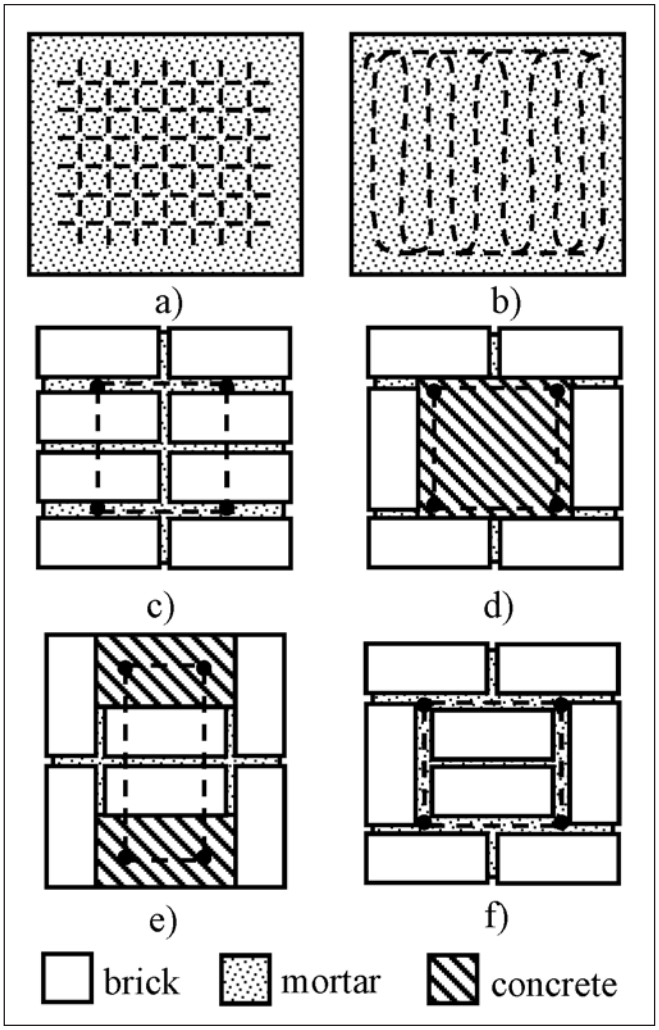

Fig. 1: Suggestions for application of reinforced masonry (Rózsa, 1953 and Andrejev, 1953)

4.1 Compressive strength perpendicular to the bed joint

The compressive strength of masonry depends on the strength and the deformation capacity of bricks and mortar. *Fig. 2* shows the stress-strain diagram of a fired clay brick, mortar and masonry. It shows that the properties of the brick and the masonry are different. It is important to note that the reason of that is not only the mortar, but the bond of bricks.

In case of smaller stress than the compressive strength of mortar the deformation of the masonry is very similar to the deformation of the mortar and the bricks. If the stress from the neighbouring brick is equal to the uniaxial compressive strength of the mortar, the mortar deforms laterally strongly. The stiffer brick tries to prevent lateral deformation of mortar through bond between them. As a result of this strain check, tensile stresses in the bricks and compressive stresses in the mortar occur perpendicularly to the loading direction (*Fig. 3*). In case of adequately strong compression, multiaxial compressive stress condition appears in the mortar bed, while compression-tension condition evolves in the bricks. Due to the strain obstruction the compressive strength of the mortar is higher than real uniaxial compressive strength. The compressive strength of the masonry is smaller than the uniaxial compressive strength of the bricks owing to the additional tensile stresses parallel to the bed joint. It is important to apply adequate mortar stress with the brick stress, as the lower strength of bricks (lower Young's modulus) constructed with higher mortar strength may cause cracks above the head joint. The mortar in the head joints

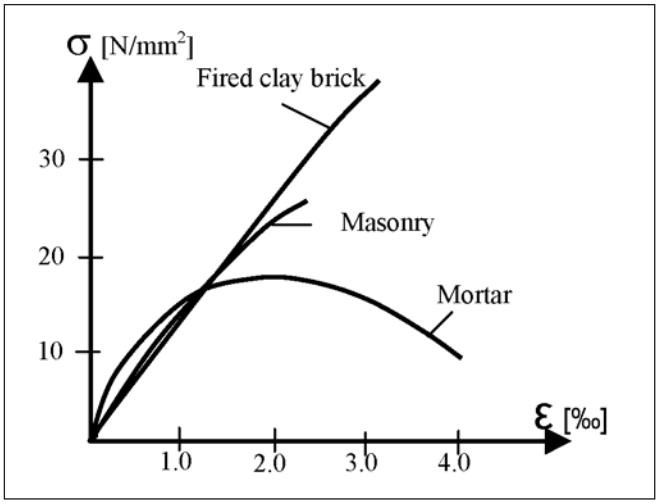

Fig. 2: Stress-strain relationship for fired clay brick, mortar and masonry (Reinhardt, 1989)

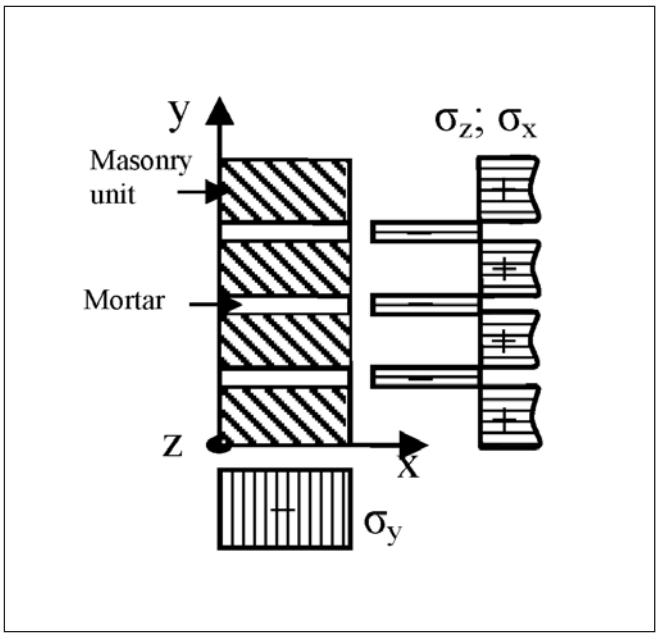

Fig. 3: Stresses of the mortar layers and the bricks due to vertical compression in case of the same horizontal dimensions of bricks

may deform less, and stress concentration occurs. Strength of masonry is also affected by the surface and the size of the bricks, by the thickness of the mortar and by the filling of the joints. It is interesting to note that if no mortar is used between the bricks, the compressive strength of the brickwork is zero according to the Eurocode 6, 2006.

4.2 Tensile and flexural strength

The tensile strength of the brickwork perpendicular to the bed joint can be determined from the cohesion between brick and mortar or from the tensile failure of the bricks; the one that offers the smaller resistance will cause the actual failure mode. The tensile strength may have a significantly different value, and as a consequence the tensile strength of the masonry perpendicular to the bed joint is not considered during the design.

In case of tensile stresses parallel to the bed joint, the failure of the masonry may occur when either the adherence shear stress between the bricks and the mortar disappears or the tensile strength of the bricks exceeds the limit value. In *Fig. 4* the thick line demonstrates the location of the cracks for two different failure modes. The two types of the tensile failure parallel to the bed joint are the stepped cracks through head and bed joint, and the cracks running vertically through the unit and the head joint. The first one is typical if the compressive strength of the mortar is smaller than half of the compressive strength of the unit. In case of the same compressive strength of the unit and the mortar, the bricks are damaged, too (Dulácska, 2000).

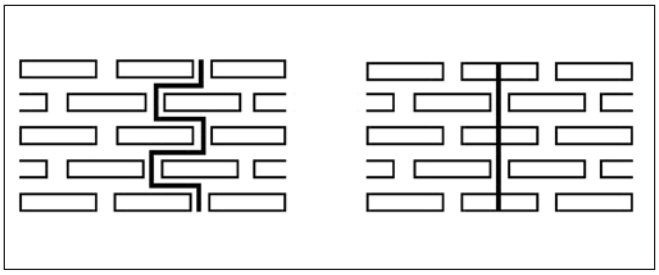

Fig. 4: Possible crack patterns due to tension parallel to the bed joint

There are two different failure modes of the prisms subjected to horizontal forces, depending on the type of the support condition and the bending in terms of the Eurocode 6: the one type is that the plane of the failure is parallel to the bed joint, and the other one is that the plane of the failure is perpendicular to the bed joints (*Fig. 5*).

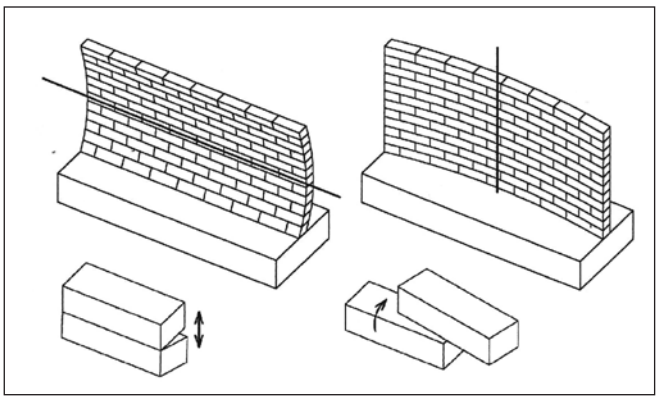

Fig 5: Flexural failures of masonry (Eurocode 6, 2006)

4.3 Shear strength

If a wall is subjected to vertical and horizontal loads in its plane, then skew principal stresses will arise. In the case of wind loading, a biaxial stress condition occurs in the plane of the wall resulting from the normal and shear stresses. The following failure mechanisms can arise from horizontal loads: 1. in case of lower vertical load, the failure occurs in the joints between bricks due to friction (stepped cracking). 2. If the load acting vertically has higher intensity, the bricks will be damaged due to the tensile principal stresses. 3. The highest load intensity will result in compressive failure of the masonry. The Eurocode 6 suggests calculating the shear strength of the brickwork from a shear test. If no test results are available, the shear strength of the masonry can be worked out from the sum of the shear strength without compressive stress and the effect of the compressive stress perpendicular to shear. The characteristic shear strength of the masonry can be calculated as the sum of the initial shear strength of the wall and one part of the compressive stresses perpendicular to shear. The earlier Hungarian Standard MSZ 15023-87 determined an additional 30 % of the compressive stresses to the shear strength. This value from the Eurocode 6 amounts 40 %.

5. ABOUT THE HORIZONTALLY REINFORCED MASONRY

The weaknesses of the masonry could have been seen before: on the one hand, the sensitivity to cracks, and on the other hand the low flexural bearing capacity. Basically, reinforcing in brickwork is applied even for two causes: masonry is a quasi-brittle material and is very sensitive to cracking. Therefore, one part of the cracks can be prevented by using reinforcing bars or mesh embedded in the bed joint, or the size of cracks can be significantly decreased. The flexural (tension) bearing capacity of masonry increases considerably with reinforcing.

Reinforcement can be built in in three ways: either in the bed joints embedded or in the cavities concreted vertically, and in both directions. Using reinforcement to prevent cracks horizontal bed joint reinforcement can be applied in the following cases (Bekaert, 2005): 1. if temperature changes or moisture content variations occur, the bricks may dry out, and cracks will arise as a consequence of shrinkage. 2. Strains resulting from differential settlement (*Fig. 6 a*) or 3. creep can cause big cracks. 4. At the corner of a building and at the cross junction cracks are very common due to the different strain of the differently loaded wall sections. This type of cracks can be decreased with the reinforcing of the junction. In the *Fig. 6 b* the consecutive layers of a T junction can be seen. 5. Infill walls (*Fig. 6 d*) in reinforced concrete frames can suffer damage due to the deflection of the floor. 6. In the place of concentrated load induction (*Fig. 6 c*), tensile stresses occur in the plane perpendicular to loading, which can be handled by the bed joint reinforcement. Increasing the load bearing capacity, the reinforcement improves the stiffness of the masonry, and it distributes the stresses almost uniformly. For example by increasing the capacity of the masonry lintels or beams around openings (*Fig. 6 e, f*), frameworks and steelworks may be prevented. For that purposes, prefabricated reinforcement meshes and lintel hooks are available. 7. If the walls of cellars (*Fig. 6 g*) and retaining walls are unable to carry the loads from the pressure of the soil, it is recommended to use vertical joint reinforcement; however, the implementation is more difficult. The resistance of the walls of silos (*Fig. 6 h*) and shear walls of buildings against horizontal loads (*Fig. 6 i*) can be strengthened in the same way. A detailed description and design of the bed joint reinforced masonry walls can be found in the paper of *Sajtos, 2001 and 2006.*

The behaviour of reinforced masonry towards extreme loads as impact, seismic events, vibration or blasting is more efficient than the behaviour of masonry, as their energy dissipations capacity will increase with the built-in reinforcement owing to the bigger ductility.

In addition, the thermal conductivity of a reinforced masonry beam or lintel is smaller than that of the reinforced concrete; accordingly the thermal insulation presents a far less serious problem than that of a reinforced concrete ring beam.

Moreover reinforced masonry has many architectural and aesthetic benefits. In case of stack bonded walls reinforcement can ensure the better co-operation of bricks, and provided the space in a collar jointed wall between the two leaves is not too big and it is filled with mortar, the two leaves can work together with the reinforcing. Further information can be found in the product identitification of Bekaert, 2005.

A typical precast reinforcement consists of two longitudinal wires which are welded to a continuous zig-zag cross wire to form a lattice truss configuration. If reinforcement mesh or bars are embedded in the bed joint, the bond strength of the brickwork will increase. Another advantage is that the use of separate reinforcing bars is unnecessary, as they may move away from their position during the construction easily, and the bars may be unsatisfactorily covered by mortar.

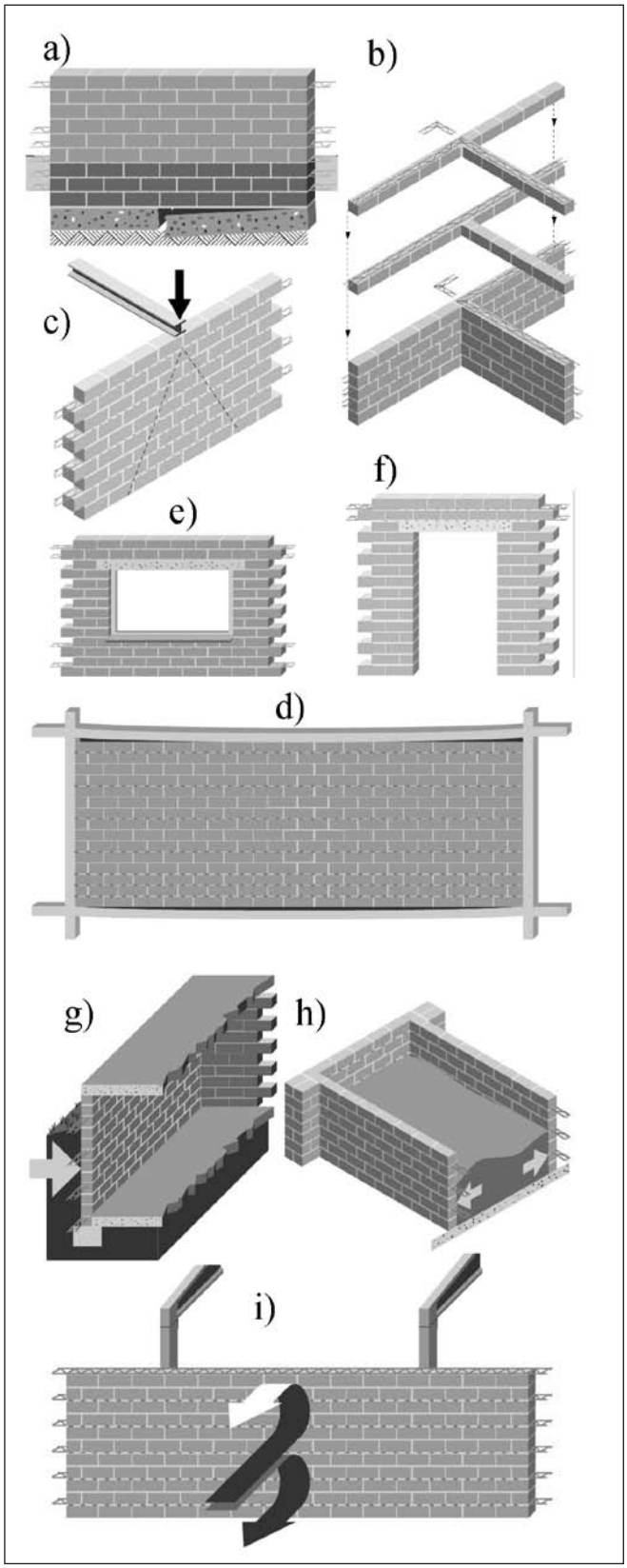

Fig. 6: Applications of bed joint reinforcement (Bekaert, 2005)

The most characteristic construction in Hungary where bed joint reinforced masonry was applied is the „Papp László Sportaréna" in Budapest (*Fig. 7*). The internal walls of the covered stadium are fairly tall, between 4-8 m. Thus the wind load they are subjected to has high intensity, and in case of an emergency they may be overloaded with the escaping people. Using reinforcement, the width of the masonry wall decreased from 30 cm to 20 cm, which resulted reduction in cost and a

Fig. 7: The „Papp László Sportaréna" in Budapest today and during construction

more spectacular sight. The design and the construction were completed by an international corporation of Hungary, France and the UK.

With reinforcement stack bonded (no bonding of bricks) walls can be built, naturally for small non-load bearing walls. In the *Fig. 8 a* one constructed example, an industrial building without overlapping of bricks in Moan can be seen. The other part of the Figure, the *Fig. 8 b* shows a long wall section as a fence. The movement joints are further from each other than usual. According to the directions of the manufacturer movement joints can be 35 m far from each other if the masonry is reinforced in every 200 mm. (If it is not reinforced horizontally, the maximal distance between joints amounts to 20 m.)

Fig. 8: The architectural examples of reinforced masonry: a) stack bonded wall and b) long wall without dilatation

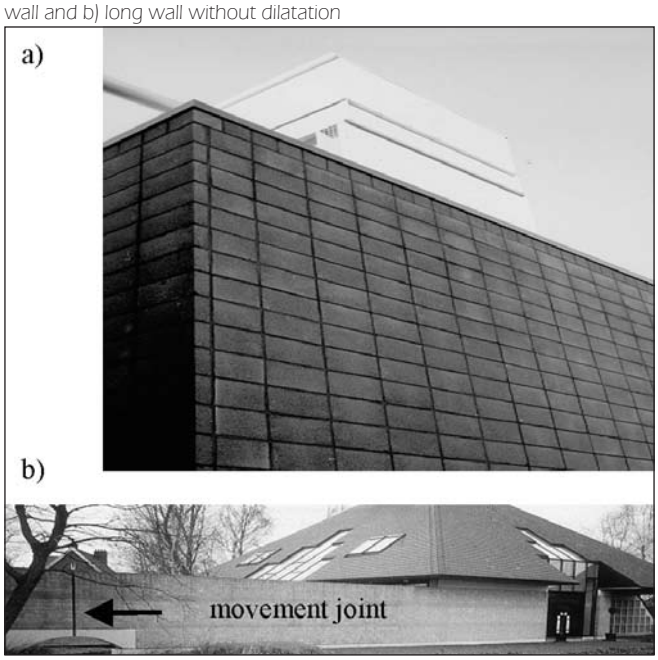

6. THE TYPES OF REINFORCED MASONRY

In Eurocode 6 six types of masonry units are defined: clay units, calcium silicate units, aggregate concrete units, autoclaved aerated concrete units, manufactured stone units and dimensioned natural stone units complied with the relevant European standards EN 771-1 to 6. However, brickwork can be combined from many of the following components: adobe, ashlars, blocks, bricks, bitumen, chalk, cement, lime and mortar. A wide variety of raw materials can be composed in a structure. The reinforcement can dispose of different shape and quality, bar or mesh. The reinforcement can be put in the mortar joint embedded, or placed in the holes and filled out with concrete or grout. Depending on which materials are used, and how they are located, reinforced masonry (RM) walls can be divided into the following classes: confined masonry, reinforced cavity masonry, reinforced solid masonry, reinforced hollow unit masonry, reinforced grouted masonry, and reinforced pocket type walls.

6.1 Confined masonry

According to the paper of the *Engineering Structures Research Centre, 2008* a construction system where plain masonry walls are confined on all four sides by RC members or reinforced masonry is called as confined masonry. The most accurate description of the confined masonry can be read referring to the paper of the *Engineering Structures Research Centre, 2008*: The confining elements are neither intended nor designed to perform as a moment-resisting frame. When such frames are constructed to resist lateral and vertical loads the purpose of the masonry walls is only for space partitioning, and the construction system is called masonry-infilled frames. In the masonry-infilled frames type of housing the reinforced concrete frame structure is constructed first. The masonry is constructed later between the RC members. In the case of confined masonry, the masonry walls are load-bearing and are constructed to carry all of the gravity loads as well as lateral loads. Therefore, both horizontal and vertical ring beams are constructed.

6.2 Reinforced cavity masonry

The cavity wall can be constructed by using bricks, clay tile, concrete blocks. Building two separated leaves is the most significant of their construction (*Fig. 9 a*). Only metal ties or other bonding elements embedded in the bed joint can adjoin the facing and the backing leaves. According to the recommendation of *Schneider and Dickey, 1994* the dimension of the minimum thickness of the wall account for 8 in. (20.32 cm) just in that case if the height of the building does not exceed 35 ft (10.67 m) or three stories. The separating cavity should account for 1-4 in. (2.54-10.16 cm). The referred document attracts the attention to the following: If both of the sides of the wall are subjected to axial forces, each of the leaves must be considered to act independently. This type of the RM can be very effective considering the thermal insulation capacity because of the central cavity.

6.3 Reinforced solid masonry

Solid masonry can be built up from clay brick and concrete blocks that are laid continuously in mortar (*Fig. 9 b*). The following could help to decide which type of the blocks can be applied: The mortar bond to clay bricks is better than to concrete units. The latter could suffer from drying shrinkage

but the previous has a sensibility to moisture content variations. In case of reinforced solid masonry it is recommended to fill all joints as bed, head and wall joints with mortar solidly. The bricks or blocks should be placed staggered, with a required lapping according to the bonding rules of bricks. The masonry could be reinforced with horizontal wires. *Fig. 8* shows a building that was constructed with stack bonding (no overlapping of bricks). Reinforced solid masonry can consist of more leaves. To the better joining of the facing and backing leaves they can be bonded with headers vertically and horizontally. When the backing consists of two leaves this establishment is even more important.

6.4 Reinforced hollow unit masonry

As the name says, to build this type of masonry, hollow units can be applied (*Fig. 9 c*). Both clay and concrete block can be used for the construction. The units are laid with full-face shell mortar beds and the head and bed joints are filled with mortar solidly. The bonding tiles in the courses need to be placed staggered and vertical or horizontal bar reinforcement can be positioned in order to improve the tensile-flexural strength of the wall. This type of construction could be applied in grouted or in not grouted form but the previous is preferred in case of reinforcing.

6.5 Reinforced grouted masonry

It is very similar to the cavity wall; however the spaces are filled out with grout or concrete (*Fig. 9 d*). By the filling the consistence of the grout plays an important role. The grout is able to penetrate small spaces if the aggregate to the grout is well graded, smooth, and consists of small grains. It is important to fill the space around the reinforcing bars thoroughly because of the danger of the corrosion. Grouting the surface of the bricks needs to be decontaminated before. To grout the masonry wall two procedures exist: the low-lift and high lift case. In the first case after the construction of each course the cavity is filled out, in the other case the whole storey is constructed, when the grouting begins.

6.6 Reinforced pocket type wall

Reinforced pocket masonry is a common type of engineered structural masonry. The bricks are placed in so called "quetta bond" in the wall, as can be seen on the *Fig. 9 e*. The bricks are laid like a circle, and the space is filled out with concrete or grout. The vertical reinforcing bars, or stirrups can be positioned in the corner or in the middle of the space. During design the proper anchoring length should be considered. This type of RM is similar to the composing small columns next to each other, and joined together. Horizontal bed joint reinforcement can be placed embedded in the bed joint.

In Hungary those type of reinforced masonry could be applied that contains bed joint reinforcement because the construction is easy. The masonry wall type of *Fig. 9 c* is necessary to build from hollow blocks. These blocks are applied in Hungary and made of concrete, vertical reinforcement is placed in the middle of the element and then they are grouted with concrete. That is the reason why they are designed as concrete members. It is suggested to use other types of reinforced masonry, because units in Hungary are applicable for all types of reinforced masonry walls.

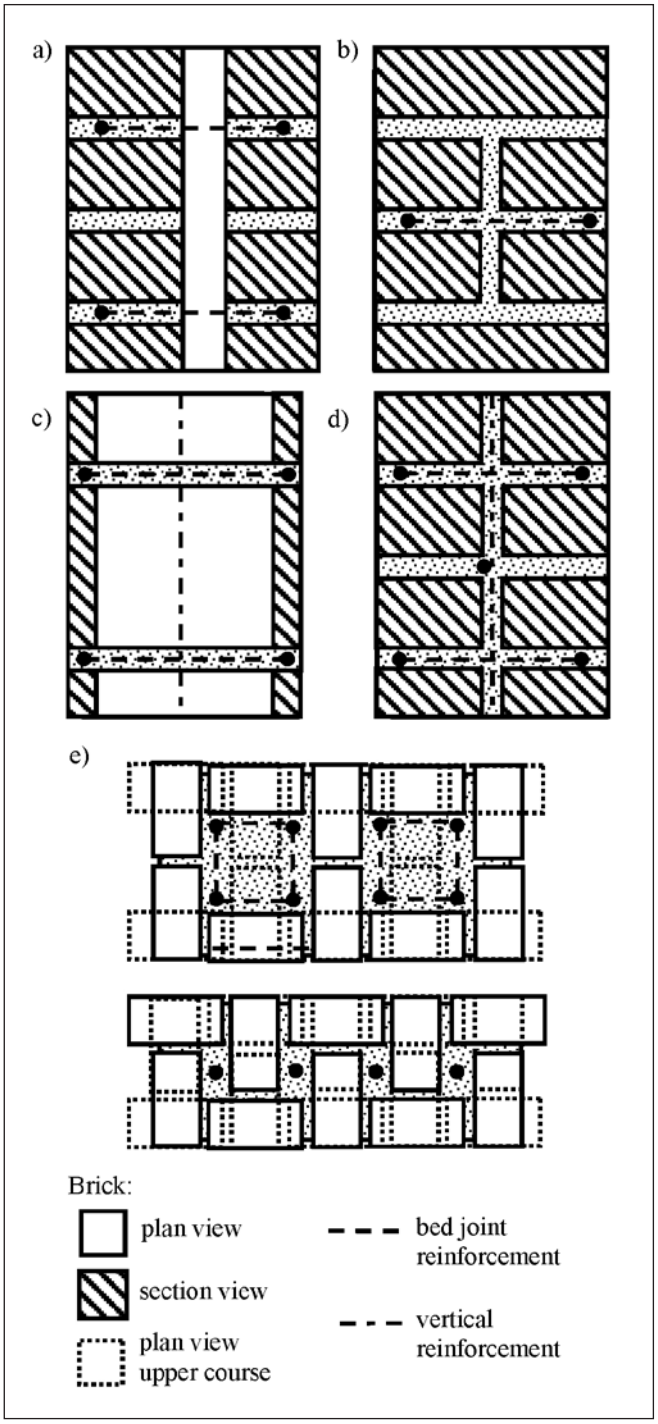

Fig. 9: Construction types of the RM walls: a) Reinforced cavity wall, b) Reinforced solid masonry, c) Reinforced hollow unit masonry, d) Reinforced grouted masonry, e) Reinforced pocket type wall

7. CURRENT METHODS OF MODELLING MASONRY

Two main types of masonry models can be distinguished: the micro- and the macromodelling. The *detailed micromodel* contains the brick and the mortar layer in real sizes. Both are taken into account as continuum elements and the contact between them is the surface where the slip and the cracks occur. This type of modelling allows taking into account all type of failures, even the failures of the units and the mortar. There is a *simplified type of micromodel* containing only brick elements, whose size is increased with the half of the mortar thickness. The surface of the joint represents the mortar and the possible failure plane. In case of *macromodels*, the brick, the mortar and the joint is one homogenous material that represents the behaviour of the masonry.

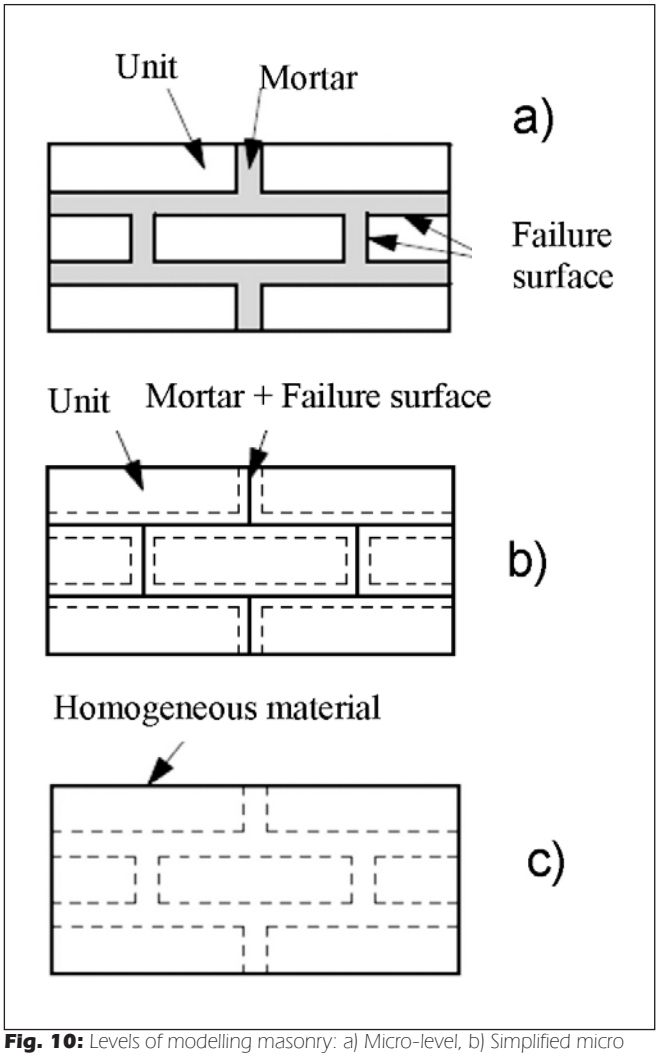

Fig. 10: *Levels of modelling masonry: a) Micro-level, b) Simplified micro level, c) Macro level (Lourenço, 1996)*

Micromodels should be used when local actions need to be analyzed deeply. In case of macromodelling, the global behaviour of the structure is analyzed by a homogeneous material, so the behaviour can be described by the global properties; thus, it is not attempted to make the calculations with local failures. In practice, the modelling mostly represents the analysis on the element level.

7.1 Cracks of ceramics

Brick is a structural type of ceramic products. The brick can be modelled in micro-level and macro-level, too. The micro level is the level of the atoms. Solids are built by primary bonds that form between atoms and that involve the exchanging or sharing of electrons. Ceramics have strong internal covalence or ionic bond. Both of that mean stabile, strong and rigid contact between the atoms. The microstructure of ceramics inclines to realign less, even in case of a little defect the failure of the whole bond system commences abruptly (the atomic bonds are released) due to local defects of the crystal-lattice. In a macro level this effect can lead to the brittle material behaviour. Typically, ceramics are characterized by brittle, cleavage breaks. Due to the strong contact system, their compressive strength and young's modulus are high, but their toughness is much lower than that of metals, and they are especially sensitive to cracking. Increasing toughness is possible by using reinforcement.

The basic stability parameters to characterize the brick are the Young's modulus, the ultimate (limit) stress, and the critical stress intensity factor (limit toughness). Reaching the latter's limit means that the macrocracks of the structure begin to propagate uncontrollably.

Failure of bricks is caused by cracks that are different depending on the type of loading. If the element is loaded by tension, the stress concentration at the crack tip brings first the propagation of microcracks and then the macrocracks into action and if the propagation is unstable, the material stability is lost, a sudden failure occurs. In case of compression the propagation of the microcracks is stable, and the material disaggregates and moulders (*Fig. 11*).

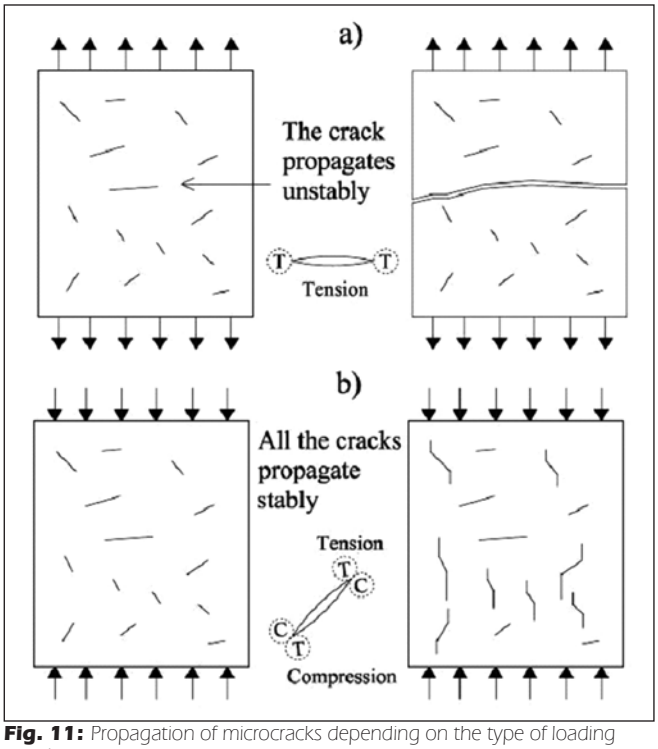

Fig. 11: *Propagation of microcracks depending on the type of loading (Bojtár, 2007)*

The inhomogeneous or reinforced materials are quasi-brittle. In their cases composite types of cracks and fractures occur, which belong to the area of elastic-plastic fracture mechanics. Here the crack tip can not be determined as simply as in case of brittle materials. A bridging zone is formed between the undamaged material and the open crack with a fully stress-free surface. If reinforcement is used in the material, this is the range where reinforcement ensures the connection, and local plastic points may occur. A micro-cracking-zone can develop in the surroundings of the crack top (Anderson, 1995). The stress transmitting rule of this range significantly affects the spread of macrocracks.

7.2 Modelling of materials

Masonry is a heterogeneous material that has different properties in different directions. While analyzing masonry, non-linearity is caused by the material differences, i.e. the fact that there is a limited knowledge of the equations describing the collaborating bonds of bricks, mortar and reinforcement depending on the model and the modelling level chosen. These non linear problems can be solved with computers.

Every type of material can be characterized by a unit whose physical state, stress and strain mark the material. The characteristic unit is called as representative volume element (RVE). It has the dimensions that are big enough to characterize the behaviour of the material and but even little enough to analyze it. This size can amount from a couple of decimetre to even one meter in case of masonry. Continuum mechanics has to be applied if a bigger volume needs to be analyzed than

RVE. If it is smaller than RVE micromechanical model should be constructed. The features of the basic unit can be described with internal variables that are based on microphysics. The micromechanical models have the purpose that the macro attribution of the material can be estimated. The two different levels of the analysis have proper variable systems (stress and strain system). The values at the macro level are the average, counted in some wise, of the micro level's variables. This method is called as homogenisation in the literature and is counted on the RVE. As a masonry wall practically consists of many frequent elements with homologous size, their properties can be observed as periodical in a certain wall section. Using these features, different homogenization techniques are introduced. *Zucchini and Lourenço, 2002* choose a basic unit for masonry as RVE that has adequate boundary conditions and contacts to build the whole wall with reflection and translation (*Fig. 12*). However, it is not applicable for walls that are built in other than running bond.

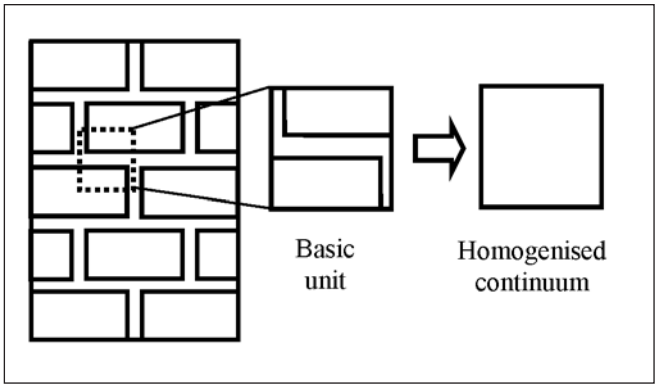

Fig. 12: The basic unit of homogenisation (Zucchini A., Lourenço P. B, 2002)

Continuum damage mechanics is also suitable for modelling of brittle materials. It is assumed that the elements do not collapse, only their material properties change. Continuum damage mechanics says that physical state of material depends on momentary state of microstructure; however, the real material is not continuous. The energy function of the material is described by the damage parameters. These parameters can be attached to the distribution and frequency of the microcracks and they describe the local failure of the material. The connection between stresses and strains is given by them to characterize the loading history. For the analysis of anisotropic masonry with inelastic behaviour, some special models can be found in the literature. A continuum model is shown for masonry in which two internal parameters are represented for the damage in the paper of *Lourenço, Rots and Blaauwendraar, 1998*. The proposed anisotropic model is able to predict the behaviour, the crack pattern and the possible places of the failure of any types of masonry, such as solid and hollow masonry, or clay or concrete masonry. An orthotropic damage model for masonry is developed by *Berto, Saetta, Scotta and Vitaliani, 2002* with the help of four independent internal variables which are controlled by the equivalent stresses.

The continuum mechanics assumes also that the space consists of continuous mass of material points that are infinitely near to each other. Another type of the modelling is the discrete element modelling, which is efficient in the analysis of crack conveyance of masonry. It belongs to the interface models (discontinuum models), which means that the non-linearity is concentrated to the bond surface of the masonry unit and mortar (Bojtár, 2007). The discrete element modelling can describe the whole process of decomposition, and follow the new adjoining elements of materials. Compared to models based on continuum, this method assumes the possibility of system decomposition. The structure is modelled as an aggregation of individual and independent elements. In discrete element modelling, the key problem is defining the properties at the levels of brick and mortar (stiffness, friction parameters etc.) together with examining the interaction between the elements, generally. This happens according to Newton's second law of motion, i.e. the interaction can be determined from the acceleration calculated from the mass of the elements, the forces and motions. The advantage of this modelling is that owing to its time-dependent features it is particularly suitable to analyze cracking patterns occurring along with earthquakes. Determining the exact place and circumstances of the support between is a long and time-consuming project. A discrete element approach can be found for masonry structures by *Chetouane, Dubois, Vinches and Bohatier, 2005*. The authors applied the non-smooth contact dynamics resolution method, and masonry is modelled by assemblage of rigid or deformable elements.

In *Fig. 13* crack patterns of masonry walls can be seen as the results of the experiment and the computational running. The experimental part of the research was carried out at the Budapest University of Technology (Fódi and Bódi, 2010). The discrete element model was built with the program UDEC. In this case the size of the brick was increased by half mortar thickness. Mostly the failure of a masonry wall is caused by the failure of the bond surface of the mortar and the brick. Therefore, in this model, the properties of the mortar and the behaviour of the joint are concentrated into the properties of the joint. Therefore, the model is not able to follow the compressive failure of the mortar. *Fig. 1*3 shows a good agreement between the crack pattern of the model (*Fig. 13 a*) and the experiment

Fig 13: a) and b) The crack pattern of the discrete element model and the experiment

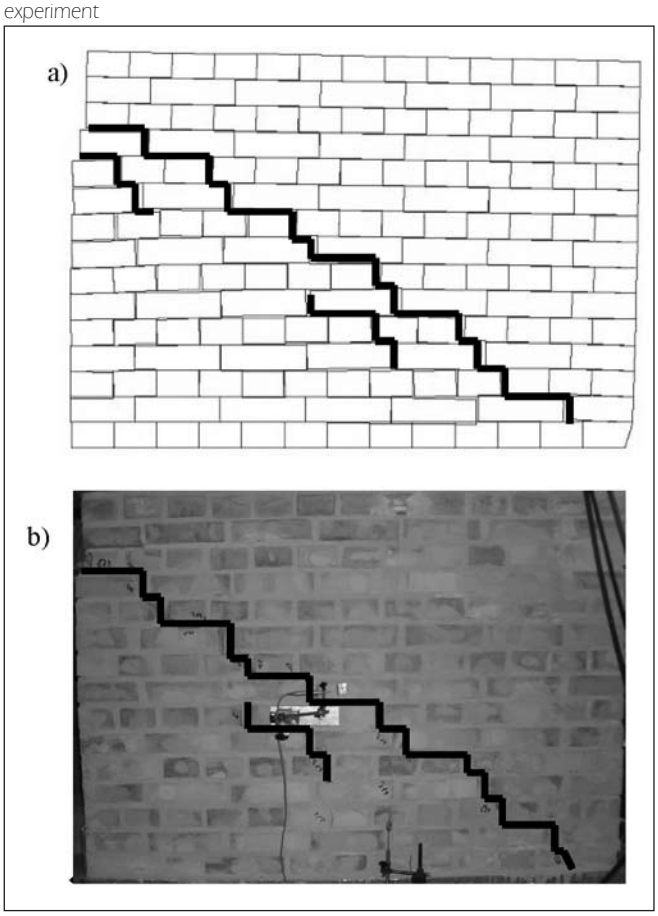

(*Fig. 13 b*). Further information about the model can be found in the paper of *Fódi and Bódi, 2009.* The effect of the vertical reinforcement on the shear capacity is analysed in the paper of *Fódi and Bódi, 2010* inter alia.

8. CONCLUSIONS

In this article the history of reinforced masonry in Europe and in Hungary is shown. Behaviour of masonry is explained in detail for compressive, tensile and shear forces, as well as for bending moments. Different types of reinforced masonry are reviewed and characterized. The practical applications of bed joint reinforced masonry and of the masonry modelling are presented.

The main goal of the present article was to give a general review on reinforced masonry walls in order to highlight its advantages compared to unreinforced masonry. From the summarized behaviours an awakening comparison with reinforced concrete walls can be concluded.

In order to show that reinforced masonry can be a competitor of the cast in situ reinforced concrete structures some important characteristics are compared: the specific weight of reinforced masonry is smaller, the thermal and soniferous conductivity of the masonry is worse and it also has better resistance against fire and chemicals. As formwork is not necessary, the implementation is simpler and cheaper. Last but not least, the wall can be loaded right after finishing the construction. Furthermore an exhaustive list of other advantages of reinforced masonry is shown.

Reinforced masonry is not the most common design and construction method in Hungary, currently. However, it was applied at the beginning of the last century; recently it has gone out of mind. Many middle-tall buildings are built every year and the reinforced masonry could be a good, but in Hungary not well known alternative construction method.

9. REFERENCES

Anderson, T. L., (1995), "Fracture mechanics", *CRC Press*

Andrejev, Sz. A. (1953), *"*Design and calculation of masonry structures*", É.M. Építőipari könyv- és lapkiadó,* Budapest (in Hungarian)

Árva, P., Sajtos, I. (2007), "Determining of the condition of masonry failures with homogenisation), *Abstract of the 10th Hungarian Conference for Mechanics (IUTAM)*, August 27-29, (in Hungarian), 3 p.

Beamish, R. (1862), "Memoir of the life of Sir Marc Isambard Brunel, civil engineer, vice-president of the Royal Society, corresponding member of the Institute of France", *Longman, Green, Longman and Roberts,* London

Bekaert, (2005), "Murfor – Reinforcement for masonry, Product identification, range of applications, installation details, design principles", Editor: Timperman P., *Bekaert*

Berto, L., Saetta, A., Scotta, R., Vitaliani, R. (2002), "An orthotropic damage model for masonry structures", *International Journal for Numerical Methods in Engineering,* pp. 127-157

Bojtár, I. (2007), "Practical approach for fracture mechanics", *Lecture notes, Budapest University of Technology, Department of Structural Mechanics,* (in Hungarian)

Chetouane, B., Dubois, F., Vinches, M., Bohatier, C. (2005), "NSCD Discrete element method for modelling masonry structures", *International Journal for Numerical Methods in Engineering,* Volume 64 Issue 1, pp. 65 – 94

Csák, B., Hunyadi, F., Vértes, Gy. (1981), "The effect of the earthquakes on buildings", *Műszaki Könyvkiadó,* Budapest, (in Hungarian)

Dulácska, E. (2000), "Earthquake hazard, Protection against earthquakes", TT-TS 3, *Logod Bt.,* (in Hungarian)

Engineering Structures Research Centre, City University London (2008), "Low-rise residential construction detailing to resist earthquake, Repair & Strengthening of Brick/Block masonry", http://www.staff.city.ac.uk/earthquakes/Repairstrengthening/index.php, Editor: Virdi, K. S. and Rashkoff, R. D.,04. July, 2008

Fódi A., Bódi I. (2009), "Experimental and numerical investigation of plain and vertically reinforced solid masonry walls subjected to in plain shear", *Proceedings of the Conference ÉPKO 2009,* Csíksomlyó, pp. 144-151 (in Hungarian)

Fódi, A., Bódi, I. (2010), "Comparison of shear behaviour of masonry walls with and without reinforcement", *Pollack Periodica,* Vol. 5, No. 3, pp. 71-82

Lourenço, P. B., Rots, J. G., Blaauwendraar, J. (1998), "Continuum models for masonry: Parameter estimation and validation", *Journal of Structural Engineering, June*, pp. 642-652

Lourenço, P. J. B. B. (1996), "Computational strategies for masonry structures", *Delft University Press*

MSZ 15023-87 (1987), "Design of load bearing masonry structures", 7. December, (in Hungarian)

MSZ EN 1996-1-1:2006 (2006), "Design of masonry structures, Part 1-1: General rules for reinforced and unreinforced masonry structures", p. 41

Reinhardt, H. W. (1989): "Brickwork", Lecture notes, *Universität Stuttgart, Institut für Werkstoffe im Bauwesen* (in German)

Rózsa, M. (1953), "Rules for design of stone-, brick-, reinforced masonry and concrete structures", *Felsőoktatási Jegyzetellátó Vállalat,* Budapest (in Hungarian)

Sajtos, I. (2006), "Reinforced masonry structures – architectural and structural advantages", *Építőmester,* January-February, pp. 24-25 (in Hungarian)

Sajtos, I. (2006), "Reinforced masonry structures", *Építéstechnika,* p. 40 (in Hungarian)

Sajtos, I. (2001), "The Eurocode 6: Design principles and examples" in: Balázs, L. Gy.: Eurocode 6: Masonry Structures, *Építésügyi Minőségellenőrző Közhasznú Társaság,* Budapest, pp. 47-84 (in Hungarian)

Sajtos, I. (2006), "Bed joint reinforced masonry structures", *Építőmester,* May-June, pp. 36-37 (in Hungarian)

Schneider, R. R., Dickey, L. W. (1994), "Reinforced masonry design", Third Edition, *Prentice hall,* Englewood Cliffs, New Jersery

Zucchini, A., Lourenço, P. B. (2002), "A micromechanical model for the homogenisation of masonry" *International Journal of Solids and Structures,* pp. 3233-3255

Anita Fódi (1983) MSc structural engineer, PhD candidate at the Departement of Structural Engineering at the Budapest University of Technology and Economics. During university studies she obtained the Scholarship of the Foundation Gallus Rehm, the Scholarship of the Budapest University of Technology, the Foundation Bizáki Puky Péter and Scholarship of the Hungarian Republic in 2004, in 2005 the DAAD-Scholarship and the Scholarship of the Hungarian Republic, in 2006 the Scholarship of the Hungarian Republic, in 2007 Scholarship of the Budapest University of Technology of First Category and the Scholarship of the Foundation „Scientia et Conscientia". The title of the final thesis was Earthquake analysis of a twelve storey reinforced concrete building. In 2007 she got the degree price of the Foundation Gallus Rehm, and the Hungarian Chamber of Engineers. In 2010 and 2011 she achieved the grant of the Wienerberger GmbH. Her main field of interest is the structural application and design of masonry and reinforced masonry and earthquake design.

Dr. István Bódi (1954) civil engineer, post-graduate engineer in mathematics, PhD, associate professor at the Department of Structural Engineering, Budapest University of Technology and Economics. Research fields: Reconstruction and strengthening of reinforced concrete and conventional structures, modelling of timber structure joints. Has over 80 publications. Member of the ACI (American Concrete Institute) and the ACI Subcommitte#423 „Prestressed Concrete". Editorial member of the Hungarian Version of the journal "Concrete Structures" (Journal of the Hungarian group of ***fib***). Member of the Budapest and Pest County Chamber of Engineers. Former president of the standardization committee Eurocode 5 - MSZ EN 1995 (Timber Structures). Member of the Hungarian Group of ***fib***. Member of the „Schweizerische Arbeitgemeinschaft für das Holz" organisation and the Scientific Association of Hungarian Wood Industry.

EXPERIMENTAL INVESTIGATION OF AN INDIVIDUAL EMBOSSMENT FOR COMPOSITE FLOOR DESIGN


Noémi Seres - László Dunai

The aim of the ongoing research work is to analyze the composite action of the structural elements of composite floors by experimental and numerical studies. The mechanical and frictional interlocks result in a complex behaviour and failure under horizontal shear. This is why the design characteristics can be determined only by standardized experiments. The purpose of the research work (i) is to simplify the experiments and (ii) to develop an advanced numerical model for the simulation based derivation of the constants. The paper has a focus on a novel experimental analysis of the mechanical bond of rolled embossments.

Keywords: Composite floor; interlock; mechanical bond; embossment

1. INTRODUCTION

Composite floor is widely used in the building industry in the last decades. The casting of concrete is carried out on corrugated steel plate (as permanent formwork) which is supported by floor beams. The main advantages of this floor structure, that the profile deck provides the formwork and by this instantly the working area. Besides it supports the upper flange of the floor beams and it works also as reinforcement in the tension zone of the slab.

The force transfer mechanism of composite floors can be characterized by three failure types: (i) flexural failure, (ii) longitudinal shear failure and (iii) vertical shear failure. The longitudinal shear failure is the most common failure type which is affected by the interlock on the steel-concrete interface. The efficiency of the composite slabs then depends on the composite action between the steel and concrete structural members.

The interlock on the contact surface is firstly based on an adhesive rigid bond which is generated by the set of cement on the steel surface. This interlock is lost as soon as interface slip occurs. Then the longitudinal shear is transferred by friction and/or mechanical bonds. A typically applied mechanical bond is the rolled embossment (formed as indentations) on the steel surface (*Fig. 1*, (Crisinel, Marimon, 2004)). Without embossments, the maximum interface interlock strength is related to the rupture of the adhesive bond (Eldib et al. 2009), whereof the magnitude varied between 0.028-0.085 N/mm^2 in case of open ribbed profile; however, the embossments have substantial effect on the shear capacity (Burnet, Oehlers, 2001). Both friction and mechanical bond result in complicated interacting phenomena what can hardly be handled by the classical design methods of shear connectors.

Standards manage horizontal shear strength calculation by using test based design characteristics in the design equations. Two design methods for the verification of composite slabs are given in standards (EN 1994-1-1, 2004): the *m-k* method and the *partial shear connection* method. These methods are based on a test program composed of full scale specimens, which are four point bended, one way slab specimens (Marimuthu et al. 2007). To simplify those tests, small scale specimens are also proposed by push-out and pull-out tests (Crisinel, Marimon, 2004; Mäkeläinen, Sun, 1999). The layout of the full and small scale specimens is shown in *Fig. 2*.

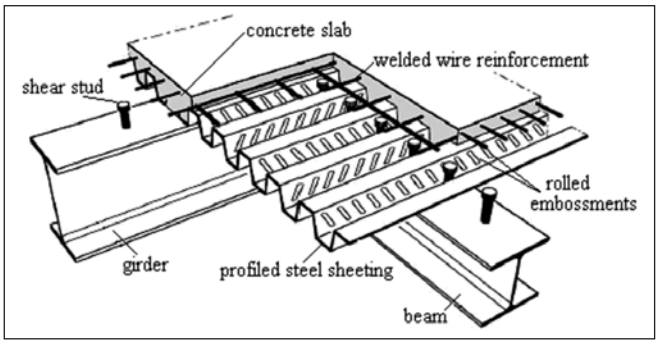

Fig. 1: Composite floor structure (Crisinel, Marimon, 2004)

Both design method consider the mechanical bond as it is smeared all over the interlock surface. The shear resistance is characterized by a fictive friction shear strength, $\tau_{u,Rd}$. In the ongoing research the following strategy is established: the design method is based on a numerical simulation of a full-scale test (global composite model). Submodels are developed for the rolled embossments to follow their behaviour. Based on the results of the submodels a description is to be made, which is to be adopted in the global model. The accuracy of the numerical model is checked by the comparison of the shear resistances from the experiment and from the model.

According to the research strategy, the behaviour of an individual embossment is needed to be followed. Since recent researchers proposed the analysis of more embossments in a specimen through the pull-out tests, a benchmark experimental investigation is planned, which allows the analysis of one separated embossment.

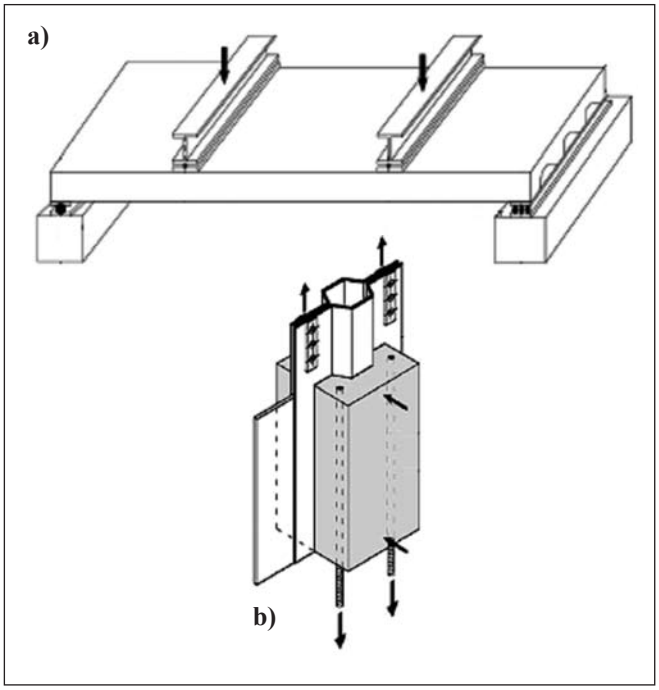

Fig. 2: Standardized test specimens for composite floor design (a) full scale (Marimuthu et al. 2007) and (b) small scale specimens (Crisinel, Marimon, 2004; Mäkeläinen, Sun, 1999)

2. EXPERIMENTAL PROGRAM

2.1 Assumption of the experimental program

The test specimens are made on the basis of traditional pull–out tests (*Fig. 2,b*), with the difference that the steel plate is not a half wave of an open through profile, but such a plate which has one enlarged embossment, as shown in *Fig. 3*. The scope of the enlargement of the embossment is to be able to create the specimen and to follow the phenomenon by strain gauge measurement. In order to keep the original geometric ratio of the embossment, the steel plate thickness is chosen to be thicker than the plate thickness in a regular composite floor. Two plates are placed back-to-back in the middle of one concrete cube. A 6 mm thick spacer plate is installed between the embossed plates. An 80 mm diameter hole is cut on the spacer plate, which leave the area of the embossment without restraint and insures the free deformation of the embossment.

During the design of the specimen the global failure of the concrete block has to be avoided, hence frequently (30 mm) distributed stirrups are put in the concrete block along the plate.

2.2 Materials and measurement technology

The applied concrete material is C25/30 whereof the recipe is designed and used for previous experimental investigation by the author (Seres, 2006). Since the material parameters are previously determined, only the strength of the new mixture is needed to be checked by uniaxial compression tests on cube specimens of 150 mm edge length. The cube specimens are made of the same mixture of concrete as the pull-out specimens. The concrete recipe is detailed in *Table 1*.

Table 1: Concrete recipe

C25/30			kg/m³	l/m³	ρ [g/ml]
Cement	CEM I 42.5 N	DDC	300	97	3.1
Water	v/c	0.55	165	165	1.0
Aggregates	0/4	0.47	903	342	2.64
	4/8	0.25	480	182	2.64
	8/16	0.28	538	204	2.64
Additive	SIKA Viscocrete 5 neu	0.2	0.6	1	1.1
Air	(estimated)		-	10	-
			2387	1000	

Since the pull-out tests were executed at the 15th day after the casting of concrete, the strength of the concrete is determined on the same day. The compression test is executed on three specimens (*Table 2*). It is found that the calculated average compressive strength of the actual concrete mixture is 43.35 N/mm², and the density of the concrete is 2308.68 kg/m³. The density of the actual mixture agreed with the previous material test; however the compressive strength is found 15% higher then the expected value (Seres, 2006).

The reinforcement and the stirrups are made uniformly from 6 mm diameter B38.24 grade steel. The embossed steel plates are made with 340x120x1.5 mm and 340x120x2 mm geometry. The nominal grade of the steel is S355. To obtain exact material data for the steel, additional tests are executed by standardized

Fig. 3: Test specimens (a) plan and (b) after the preparation

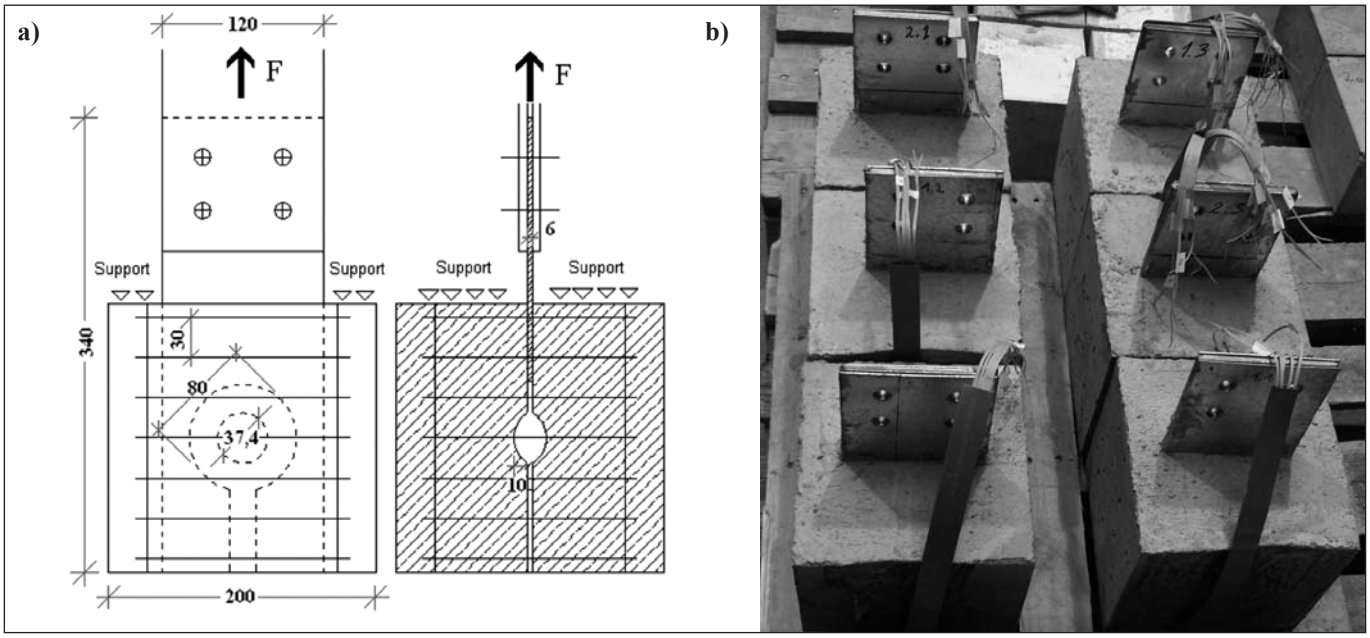

Table 2: Material test for concrete

Geometry	b_1 [mm]	149.5	149.7	149.9
	b_2 [mm]	150.0	152.2	151.8
	h [mm]	150.1	150.0	149.6
Weight [kg]		7.79	7.88	7.85
Force [kN]		987.8	970.6	987.3
Average compressive strength		43.35 N/mm^2		
Average density		2308.68 kg/m^3		

conditions. Tensile tests are made on 6 specimens (3 pieces from each plate thicknesses) to determine the characteristics of the material. The results of the tensile tests are summarized in *Table 3*. Simplified σ–ε relationships are determined for each plate thicknesses. The characteristic points of the stress-strain relationships are calculated from the average of the experimental values.

Table 3: Material test results of steel plate

Sign of the specimen		Geometry	Yield strength	Ultimate strength	Ultimate strain
		Thick/Depth	R_{eH}	R_m	A_{80}
		mm	N/mm^2		%
1.5 mm nominal plate thickness	11	1.53/20.31	450	512	22.5
	12	1.53/20.29	429	513	19.0
	13	1.53/20.12	452	507	22.0
2 mm nominal plate thickness	21	1.92/20.24	457	532	18.5
	22	1.92/20.24	462	536	19.0
	23	1.92/20.40	458	533	19.0

The strains on the steel surface are measured with strain gauges of type KMT-LIAS-06-1.5/350-5E (*Fig. 4*) whereof the active grid length is 1.5 mm and the nominal measurement limit is 10% of strain.

Fig. 4: Applied strain gauge

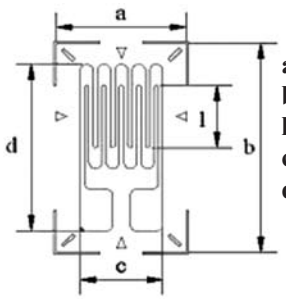

a – depth of grid carrier 2.5 mm
b – length of grid carrier 5.0 mm
l – active grid length 1.5 mm
c – grid depth 1.5 mm
d – full grid length 2.8 mm

Besides the strains, the relative displacement between the steel plate and the concrete cube is also measured with inductive transducers.

2.3 Preparation of the test specimens

The enlarged embossment is pressed by using a 45 mm diameter bearing ball. The embossment's height is 10 mm, its diameter is 37.4 mm.

The strain gauges are glued on the steel surface opposite side of concrete in two arrangements, as shown in *Fig. 5*. Five base gauges are put on all of the embossed plate pairs, and on two of them ten supplementary gauges are put besides. In this way four specimens are made using 5 gauges and two specimens are made using 15 gauges. The positions of the 5 base gauges are placed in the axis of symmetry of the embossment according to the orientation of the load. Gauges #1 and #5 are placed on the plane surface at the bottom edge of the embossment. Gauges #2 and #4 are placed on the opposite side of gauges #1 and #5, respectively on the curved surface. Gauge #3 is put in the middle of the embossment. The role of the other 10 supplementary gauges is to determine the behaviour of the area of the base gauges. Hence, other gauges are placed next to gauges #1, #2, #4 and #5 gauges on the right and left side, and also between the gauges #2 – #3 and #3 – #4 to be able to follow the full longitudinal deformation of the embossment. Six specimens are made, with the data summarized in *Table 4*. The specimens were prepared in the laboratory of the Department of Construction Materials and Engineering Geology.

The pull–out test is executed in a loading frame, where the specimen is hung by loading plates which are fixed on the steel overhang of the specimen and the upper surface of the concrete cube is supported from above, as shown in *Fig. 3/a*. The load is applied through the loading plates. To insure the centric and uniform load transfer, and also to correct the concrete surface's irregularity, ~5 mm thick hard rubber pad is used between the loading frame and the concrete cube's supported surface.

3. TEST RESULTS

3.1 Experimental observations

As the load is introduced, the first mark of the failure appears on the concrete block. When increasing the load, the first crack appears in line with the steel plate at the exterior surface of the concrete block (*Fig. 6*). The first crack appears at the side, where the steel plate is closer to. After, the crack propagates all over the height of the cube and the steel plate slips out of the concrete block, what means the global failure of the specimen. After the specimen is removed from the loading frame, the

Fig. 5: Strain gauge arrangement

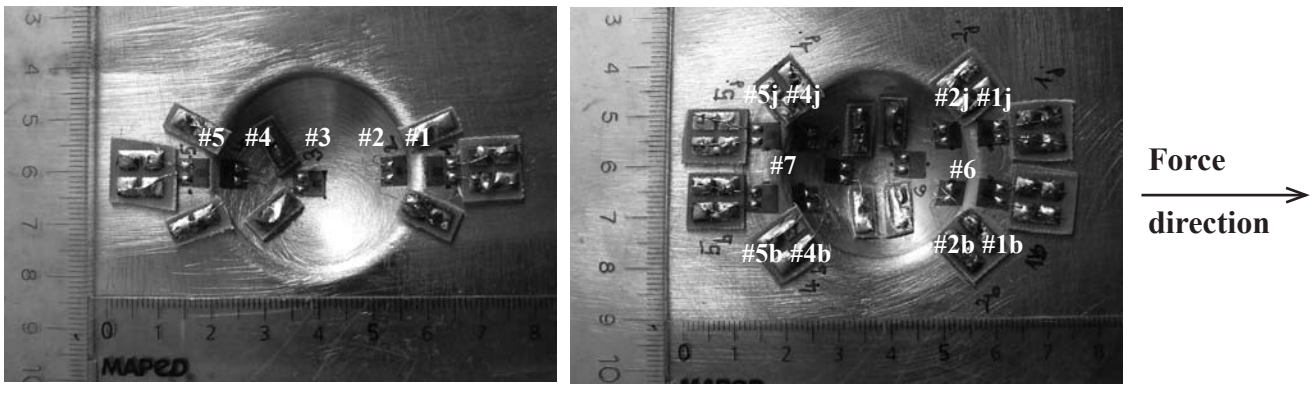

Table 4: Test specimen characteristics

Sign	Sheeting thickness [mm]	Strain gauges [pc]	Concrete cube size [cm]	Steel plate size [mm]	Embossment diameter/ height [mm]	f_y/f_u* of steel [N/mm^2]	f_{ck}** of concrete [N/mm^2]
1.1	1.5	5	20x20x20	340x120	37.4/10	444/510	43.35
1.2	1.5	5	20x20x20	340x120	37.4/10	444/510	43.35
1.3	1.5	15	20x20x20	340x120	37.4/10	444/510	43.35
2.1	2	5	20x20x20	340x120	37.4/10	459/534	43.35
2.2	2	5	20x20x20	340x120	37.4/10	459/534	43.35
2.3	2	15	20x20x20	340x120	37.4/10	459/534	43.35

* yield stress/ultimate stress
** compressive strength

crack pattern on the supported side is analyzed. Two kinds of crack can be identified from the full crack pattern. The first one is parallel with the steel plate and propagates from top to bottom in the concrete cube, and arises also on the supported and the side surfaces. The second one is representative on the supported surface and its near area, and the crack propagates from the edge of the steel plate to the corner of the concrete cube.

The deformation of the steel plate can be analyzed after removing the concrete cover. The concrete cube is completely destroyed, so the inner concrete failure cannot be seen. The ultimate deformation of the embossment is shown in *Fig. 7*.

Fig. 7: Ultimate deformation of the embossment (a) side view (b) top view

3.2 Measurement

Fig. 8 shows two typical load–displacement curves of the specimens made with 1.5 (specimen 1.3) and 2 mm (specimen 2.2) plate thickness, respectively. The response of the specimen is practically rigid for the initial loading (2–3 kN). After, the behaviour changes to be linear. The short linear phase is followed by a nonlinear part, with gradually decreasing slope. By experimental observation, the end of the linear phase can be identified by a micro crack propagation, which leads to the appearance of the first crack on the concrete surface. After the steel plate slips, a small amount of load increase can be observed till failure. The identification of the characteristic curve points are summarized in *Table 5*.

A significant decrease in the slope can be seen on the curves (**Fig. 8**) after the slip of the plate (it indicates the start of the failure mechanism) at an almost uniform value of displacement of 8–9 mm on every specimen. However the global failure occurs at a value of displacement of 30–40 mm. On this

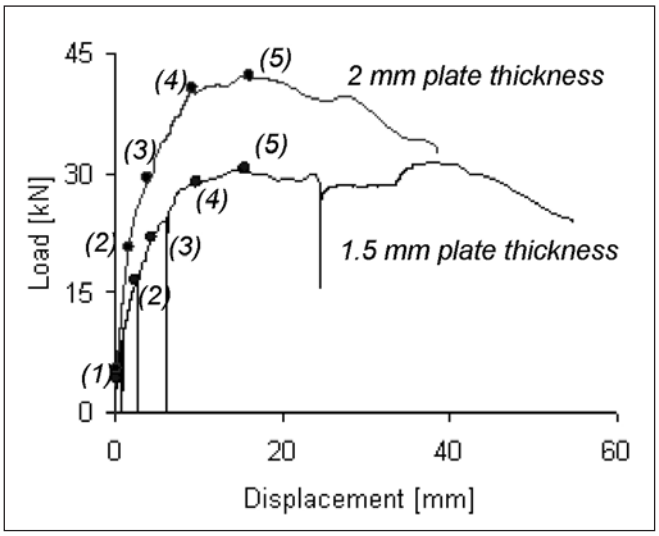

Fig. 8: Force - displacement curves of 2 and 1.5 mm plate thicknesses

basis the connection is ductile, because it has a significant deformation capacity. On the specimen 1.3 three back-loading and reloading are performed which produced three quasi vertical lines on its load-displacement curve.

In accordance with the expectations, the value of initial

Fig. 6: Crack pattern (a) first crack on the side (b) crack propagation on the top surface

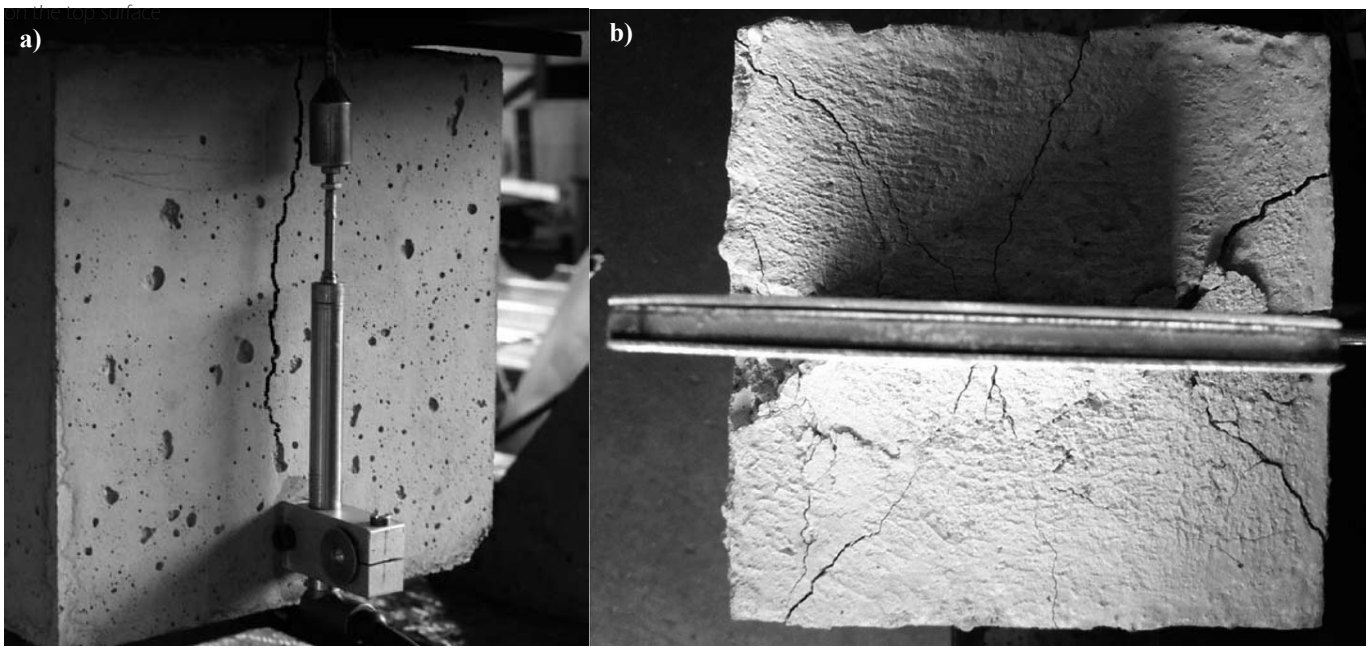

Table 5: Test results

Sign	(1) 1st yielding on steel plate [kN]	(2) End of linear phase [kN]	(3) 1st crack [kN]	(4) Slip of plate [kN]	(5) Ultimate load [kN]
1.3	4.39	16.4	21.9	28.8	31.6
2.2	5.62	20.6	29.3	40.6	42.2

stiffness and the load carrying capacity is higher on the specimens with 2 mm thick steel plate than those with 1.5 mm thick steel plate. According to previous experimental studies these two parameters are influenced by the plate thickness (Mäkeläinen, Sun, 1999). Despite the stiffness and the load carrying capacity is higher with 2 mm thick plate, the character of the load-displacement curve remains the same and the appearance of the characteristic curve points follow the same order, only they belong to higher load levels. So the global behaviour of the specimens does not change by changing the plate thickness. The design related characteristics are given in *Table 6*, as the average of the measured values. The initial stiffness is defined as the slope of the straight line which connects the point of the end of the linear phase and the origin of the curve.

Table 6: Average design characteristics

Plate thickness [mm]	Initial stiffness [N/mm]	Load carrying capacity [kN]
1.5	5 722	34.33
2	11 637	42.2

The strain gauges show same tendency of behaviour by position and by specimen type. For further numerical model verification, the load level is marked at the strain gauges when the strain reaches the value of the yielding limit (2080 and 2300 μm/m in case of 1.5 and 2 mm plate thickness, respectively). By the evaluation of the strain results it is found, that the yielding of the steel plate appears at very low load level (5–10 kN, as shown in *Fig. 8*) at the bottom of the embossment on the loaded

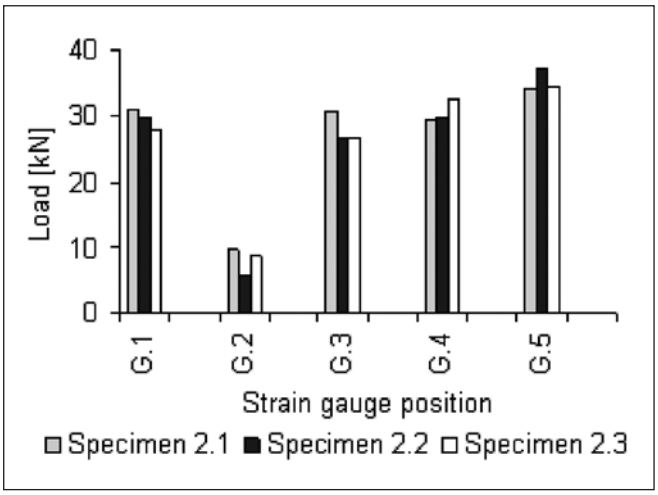

Fig. 9: Yielding at the gauges

side (at gauge #2 position, *Fig. 5*). The appearance of yielding by strain gauges under tension or compression is detailed in *Fig. 9*. The corresponding load levels are given in the case of the specimens made with 2 mm plate thickness.

A typical result of the strain measurement can be seen in *Fig. 10* (specimens with 2 mm plate thickness, gauge #3). The curve shows the relationship of the load and the strain in the centre of the embossment. The appearance of yielding is marked on the curves with asterisk. The character of the curves is the same

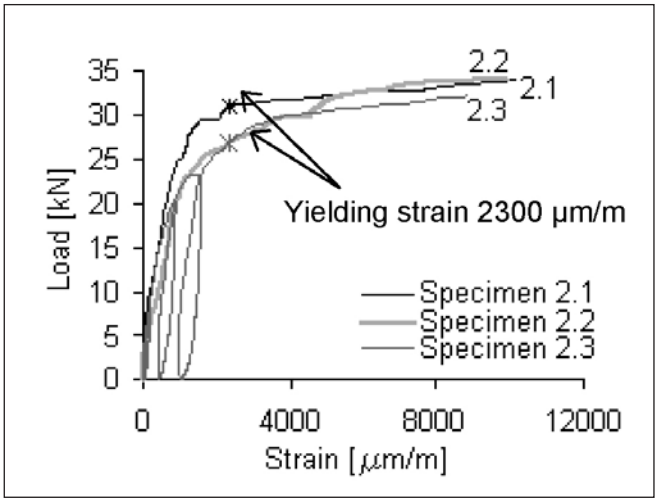

Fig. 10: Strain distribution in the middle of the embossment

on the specimens made with 1.5 mm plate thickness, only the load level is smaller with those specimens.

Supplementary gauges are put in the specimen to follow the longitudinal deformation at the nearby points of the base gauges. The #2j and #2b gauges are put in equal distance on the left and right hand side from #2 gauge as shown in *Fig. 5*. *Fig. 11* shows the measured strains in specimen 1.3 at #2 gauge at the bottom of the embossment on the loaded side, where the first yielding is observed. The supplementary gauges showed similar behaviour with the base gauge, placed in the same cross section of the embossment. The minimal deviation between the #2j and #2b is assumed as the reason of (i) not

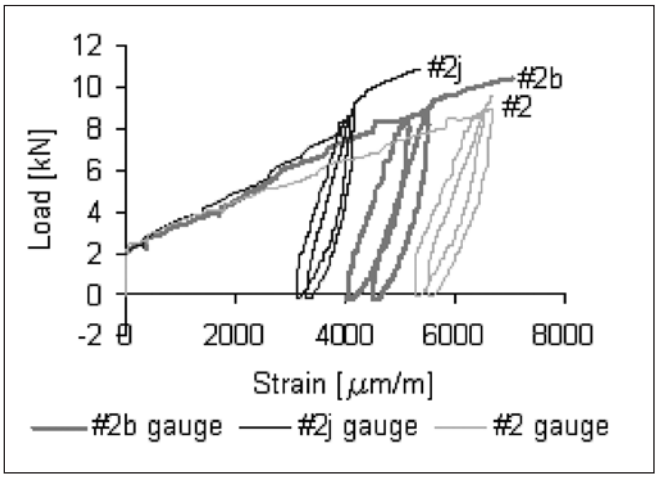

Fig. 11: Comparison of the supplementary gauges and the base gauge results on specimen 1.3

exactly centric loading or (ii) not perfect positioning or (iii) asymmetric buckling of the embossment (keeping in mind that the deformation of the embossment is plastic and irreversible in this case).

4. CONCRETE BEHAVIOUR AND ANALYSIS

In the experiment the global concrete failure is avoided by stirrups which aim to fix the concrete block around the plate. The first visible mark of the failure, however, appears on the concrete part of the specimen. Furthermore, recent experimental investigations showed that the embossment type interaction can unpredictably and exclusively fail from the concrete part as it is shown in *Fig. 12* (Freire, 2009). The specimens of the above mentioned pullout test were made from normal grade of steel

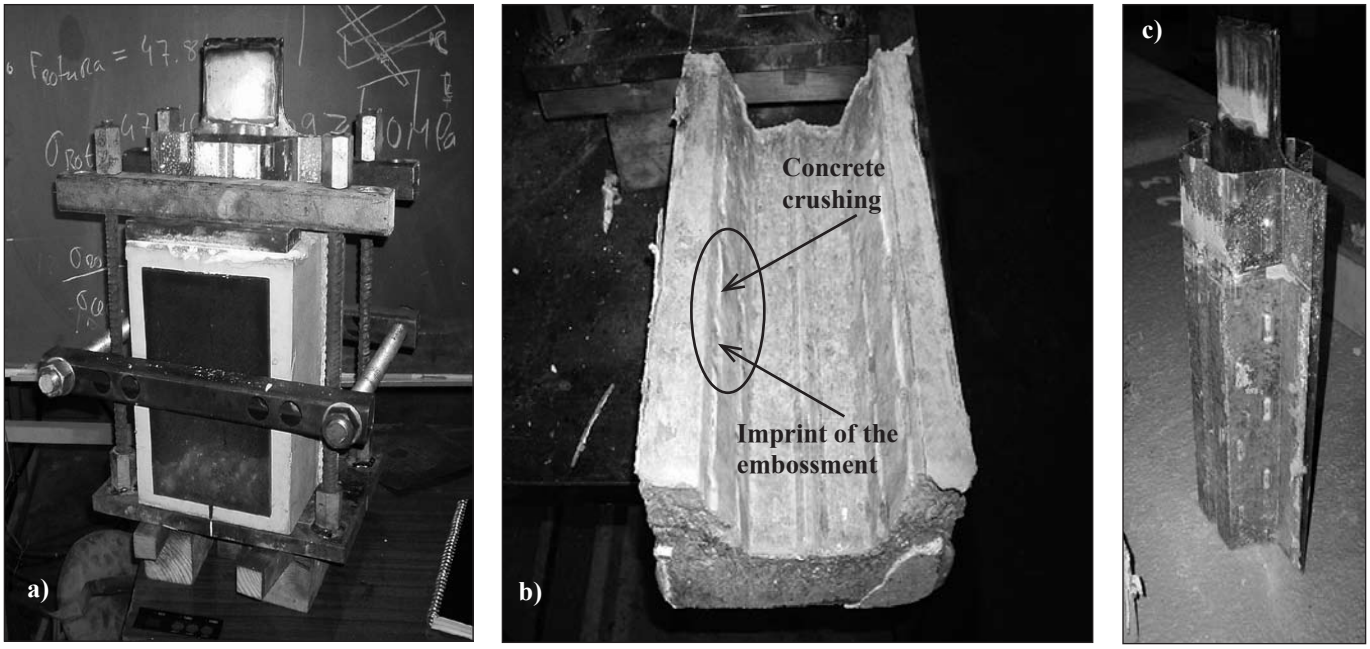

Fig. 12: *Pull-out test of Freire (2009) (a) test specimen (b) concrete part and (c) steel part after the failure of the specimen*

and concrete (f_{sy} / f_{su} =464 / 565 MPa and f_{cm}=38 MPa). It means that we cannot forecast whether the steel embossment whether the surrounding concrete fails first due to loading. In spite that in the actual test the failure mechanism is governed by the failure of the steel part, the analysis of the concrete behaviour is also important and part of the research. The behaviour of reinforced concrete is already analysed by finite element models by the authors (Seres, 2008). The numerical models are developed by ANSYS® v10.0 finite element program. Two models are analysed (i) a reinforced beam model and (ii) the local model of a fictive rolled embossment. It is found that the applied homogenous continuum material model is adequate for the simulation of an entire structure like a beam or a slab, but the internal structure of the material should be considered in local analysis, where the scale of the problem is smaller then the materials representative volume element (RVE). Since the nonlinear behaviour of the concrete is related to the initiation and the propagation of microcracks, the required scale on the model is the mesoscale, where concrete is modelled by the coarse aggregates, the surrounding mortar matrix and by the interface elements on the aggregate-matrix boundary. A finite element mesoscale material model is developed by Caballero et al. (2006) and Ciancio et al. (2007). Good agreement is found in 2D and 3D by comparing it with uniaxial tensile tests, as well as in uniaxial, biaxial and triaxial compression. Since the scale of the material model is proved to be appropriate to capture the local failure in concrete, a similar model is to be used for the further local finite element models.

5. CONCLUSIONS

In the paper an experimental investigation of an individual embossed mechanical bond is detailed. A new test specimen is introduced to analyze the local behaviour of embossments contrary to traditional experimental methods, which take smeared mechanical bond into consideration. The basic behaviour modes are observed from the tests and the results are evaluated quantitatively.

It is found that the failure is a complex phenomenon and the ultimate behaviour is conducted by steel embossment failure due to the yielding extension and the appearance of the yielding mechanism. It is found that the connection is ductile, the failure occurs after large deformation of the embossment. The change of the plate thickness has direct effect on the initial stiffness and the load carrying capacity, but it does not affect the global behaviour. The longitudinal behaviour of the embossment is followed with strain gauge measurement. Early yielding appears on the plate at ~14% of the ultimate load at the bottom of the embossment on the loaded side. The results are used for the validation of the developed finite element model for the embossment's behaviour.

Since the concrete cover is destroyed when removed, the inner concrete failure around the embossment cannot be followed, but the outer crack propagation is well captured on the specimen. Further numerical investigation is planned on concrete cracking, especially to follow the local concrete cracking and crushing around the embossment. The size of the problem requires a mesoscale material model, where the internal structure of the material is considered in the simulation.

6. ACKNOWLEDGEMENT

The authors gratefully acknowledge the helps of the Laboratory of the Department of Construction Materials and Engineering Geology and of the Structural Laboratory of the Department of Structural Engineering in the preparation of the specimens and in the execution of the tests.

In addition the authors wish to thank to the BVM Ltd. and the Lindab Ltd. for the provided reinforcements and steel plates.

7. REFERENCES

ANSYS® v10.0, Canonsburg, Pennsylvania, USA.

Burnet M.J., Oehlers D.J. (2001): „Rib shear connectors in composite profiled slabs", *Journal of Constructional Steel Research*, Vol. 57, 1267-1287.

Caballero, A., Lopez, C.M., Carol, I. (2006): „3D meso-structural analysis of concrete specimens under uniaxial tension", *Computer Methods in Applied Mechanics and Engineering*, vol. 195, pp. 7182–7195.

Ciancio, D., Carol, I., Cuomo, M. (2007): „Crack opening conditions at 'corner nodes' in FE analysis with cracking along mesh lines. Consistent tangent formulation for 3D interface modelling of cracking/fracture in quasi-brittle materials", *Engineering Fracture Mechanics*, vol. 74, pp. 1963–1982.

Crisinel, M., Marimon, F. (2004), „A new simplified method for the design of composite slabs”, *Journal of Constructional Steel Research*, Vol. 60, pp. 491-471.
Eldib, M.E. A-H, Maaly, H.M., Beshay, A.W., Tolba, M.T. (2009), „Modelling and analysis of two-way composite slabs”, *Journal of Constructional Steel Research*, Vol. 65, 1236-1248.
EN 1994-1-1 (2004), „Design of composite steel and concrete structures”, Part 1.1 :General rules and rules for buildings.
Freire, J. (2009), „Analysis on the behaviour of composite slabs under concentrated loads. Experimental tests and numerical simulations”, MSc Thesis, Department of Civil Engineering and Architecture, Higher Technical Institute (IST), TU Lisbon, Portugal (in Portugal).
Marimuthu, V., Seetharaman, S., Jayachandran, A.A., Chellappan, A., Banndyopadhyay, T.K., Dutta, D. (2007), „Experimental studies on composite deck slabs to determine the shear-bond characteristic (m-k) values of the embossed profiled sheet”, *Journal of Constructional Steel Research*, Vol. 63, pp. 791-803.
Mäkeläinen, P., Sun, Y. (1999), „The longitudinal shear behaviour of a new steel sheeting profile for composite floor slabs”, *Journal of Constructional Steel Research*, Vol. 49, pp. 117-128.
Seres, N. (2006): „Analysis on the composite action of composite floors built with profile deck”, MSc Thesis, Department of Civil Engineering, Budapest University of Technology and Economics, Budapest, Hungary 145 p (in Hungarian).
Seres, N. (2008), „Numerical modelling of shear connection between concrete slab and sheeting deck”, 7th fib PhD Symposium in Civil Engineering, Stuttgart, Germany, 11-13 September, p. 10 (CD Rom, paper 13.8, pp. 77-86).

Noémi Seres (1980) Dipl. Engineer (2007).Graduated in 2007 at the Department of Structural Engineering of BME. Started scientific work in 2005 in the topic of composite floors. Since 2007, PhD student under the guidance of Prof. László Dunai in the topic of development of a numerical simulation based design method for composite floors.

Dr. László Dunai (1958) Dipl. Engineer (1986), Dipl. Eng. Mathematics (1986), Dr. Univ (1987), Candidate of Technical Science (1995), Ph.D (1996), Dr. habil. (2002), MTA doctor (2008), Professor and Head of the Department at Structural Engineering BME. Major fields of research: steel- and steel-concrete composite structures, thin-walled structures, stability and fatigue of bridges, numerical modelling of structures. Member of several (Hungarian and international) scientific committees.